UNIVERSITÀ
DEGLI STUDI
DI TRIESTE

UNIVERSITÀ DEGLI STUDI DI TRIESTE
e
UNIVERSITÀ CA' FOSCARI DI VENEZIA

XXXV CICLO DEL DOTTORATO DI RICERCA IN CHIMICA

SUSTAINABLE IMMOBILIZED BIOCATALYSTS FOR INDUSTRIAL PROCESSES

Settore scientifico-disciplinare: CHIM/06 CHIMICA ORGANICA

DOTTORANDO / A
CHIARA DANIELLI

COORDINATORE
PROF. ENZO ALESSIO

SUPERVISORE DI TESI
PROF. LUCIA GARDOSSI

SUPERVISORE DI TESI
DR. LUUK VAN LANGEN

ANNO ACCADEMICO 2022/2023

This project has received funding from the European Union's Horizon 2020 research and innovation programme under the Marie Skłodowska-Curie grant agreement No 860414

INTERfaces

Table of Contents

Disclaimer

This research is part of the European project, EU-ITN INTERfaces project - Heterogeneous biocatalytic reaction cascades training network (Horizon 2020, Grant agreement No 860414), which was focused on the assembly of biocatalysts into reaction sequences and the extension of this concept to multi-step clean reactions catalyzed by enzymes in immobilized form.[1] The present work was carried out in the Laboratory of Applied and Computational Biocatalysis (LACB) of the University of Trieste, Italy and in the laboratory of ViaZym B.V., Delft (The Netherlands). The work and the use of the results are regulated by a Consortium Agreement and a Secondment Agreement signed by the parties. As a consequence of such agreements, some data obtained from this project were not included in the present document since they have potential commercial relevance.

Abstract

The present thesis had the aim to explore new immobilization routes for enzymes of industrial interest, in order to increase the environmental and economic sustainability of the overall immobilization process.

Chapter 3 explores the use of 2,5-diformylfuran (DFF) as bifunctional crosslinking agent for covalent immobilization of enzymes. This bio-based dialdehyde is obtained from the partial oxidation of 2-(hydroxymethyl)furfural (HMF, deriving from sugar dehydration). The final aim of the investigation was to replace glutaraldehyde (GA), the most commonly employed reagent for protein crosslinking, which is causing wide concerns due to its extensively documented toxicity. DFF was studied in terms of its reactivity in water, eco-toxicity and finally it was systematically compared with glutaraldehyde for the covalent immobilization of glucoamylase from *Aspergillus niger*. In water, DFF displayed a much simpler reactivity than glutaraldehyde, as it cannot form enol derivatives and therefore cannot oligomerize. Moreover, only the mono-hydrated form was observed. Notably, DFF is much less volatile than glutaraldehyde, making its handling easier and less hazardous for health. Concerning the eco-toxicity, both glutaraldehyde and DFF showed similar effects in the chosen assay. Most importantly, DFF and glutaraldehyde had very similar efficiency when used for the immobilization of glucoamylase on amino functionalized poly(methyl methacrylate) carrier, even when reaching a low amount of 0.2 μmol of aldehyde used per gram of carrier. The immobilized enzyme was successfully tested in the hydrolysis of maltose both in batch and in a continuous flow assay, where it remained active during the whole period of analysis (13 days). Therefore, results demonstrate the potential of DFF as a bio-based protein crosslinker with low chemical hazard. Some possible biocatalytic routes for its synthesis were tested in the frame of this thesis. However, its employment at industrial scale would require specific efforts and investments for the optimization of economically viable synthetic processes.

Chapter 4 analyses two lipase formulations obtained from the physical immobilization of lipase from *Thermomyces lanuginosus* (TLL) on rice husk, an agricultural byproduct available globally at a scale >120 M ton/year and at cost < 90€ ton. The aim was to explore their performance as potential replacer of the commercial formulation Lipozyme TL IM physically immobilized on silica particles forming granules. Both types of formulations contain water soluble binders and they undergo the leaching of the enzyme when exposed to aqueous media. The granules constituting the commercial preparation also undergo disaggregation whereas the rice-husk based formulation does not, since enzyme is attached on distinct solid fragments. In order to prevent leaching of the TLL immobilized on rice husk, crosslinking with DFF was attempted but unsuccessfully, most probably because the enzyme molecules are spread to a wide surface and they are too far apart to form covalent interlinks. Interestingly, when the crosslinking was carried out in organic solvent the TLL demonstrated higher activity, suggesting the positive effect of the hydrophobic solvent in promoting the interfacial activation of the lipase. The different rice-husk based TLL formulations were all tested in the interesterification of triolein and tristearin, a process employed in industry at a > 10.000 ton/year scale globally to obtain cocoa butter analogues. The formulations that were previously treated according to the crosslinking protocol showed good performances, leading to complete conversion of tristearin within 24 and without

significant production of hydrolytic products. Most probably that was a consequence of the washing and drying steps applied at the end of the crosslinking protocols that removed the residual water more efficiently. The results indicate that TLL physically immobilized on rice husk can be applied in low-water environment, especially in interesterification processes, representing a potential economically and environmentally sustainable replacer of commercial formulations. Further perspectives in the study of these TLL preparations can be the performance of recycling studies together with DSC analysis to have insight on the kinetic of the reaction.

Chapter 5 concerns the systematic investigation of rice husk as a renewable carrier for the covalent immobilization of glucoamylase and lipases. Rice husk was milled, then used as-is (raw) or after delignification. Both the raw and delignified rice husks were characterized by spectroscopic and microscopy techniques that evidenced that the delignification process was efficient without altering the tridimensional morphology of the material. Both rice husk batches were oxidized by (1) chemical oxidation with $NaIO_4$ or (2) enzymatic oxidation with a laccase and TEMPO mediator. The oxidation process has the aim of introducing aldehyde groups suitable to covalently bind the enzyme to rice husk. Two enzymes were used for the immobilization: glucoamylase from *Aspergillus niger* and TLL. Several procedures for the covalent immobilization of glucoamylase were attempted; unfortunately, none of these procedures was successful, suggesting that in the case of glucoamylase the immobilization is determined by additional factors other than the interaction of the enzyme with the lignocellulosic material. Therefore, the chemical or enzymatic functionalization of rice husk for the covalent immobilization of different enzymes appears a difficult route for developing generally applicable protocols. Despite the positive results previously reported with lipases CALB and TLL, similar protocols resulted unsuccessful when the very hydrophilic and glycosylated glucoamylase was employed. Moreover, also in the case of TLL the simple change of batch for the native enzyme led to much lower yields. These variations in the observed results might be also ascribable to stabilizers (e.g. glycerol, salts, etc.) present in different percentage in the commercial native enzymes.

Chapter 6 explores the immobilization of TLL, CaLB and glucoamylase on rice husk using a two-step approach involving adsorption and then crosslinking in the presence of a difunctional agent. Again, the experiments for glucoamylase were unsuccessful, confirming the low affinity of this enzyme for the rice husk. TLL and CaLB were successfully immobilized on rice husk using the bio-based DFF as a crosslinking agent. Notably, the best results were obtained for TLL when immobilized in the presence of hexane (15% of recovered activity). The results confirm that the presence of a hydrophobic phase is crucial for the efficient immobilization of those lipases that undergo interfacial activation. On the other hand, the immobilization of CaLB is not affected by hexane since the enzyme maintain the conformation both in aqueous and hydrophobic media.

Abstract

La presente tesi ha lo scopo di esplorare nuove procedure di immobilizzazione per enzimi di rilevanza industriale, in modo da aumentare la sostenibilità ambientale ed economica del processo di immobilizzazione.

Il capitolo 3 esplora l'uso del 2,5-diformilfurano (DFF) come agente crosslinkante difunzionale per l'immobilizzazione covalente di enzimi. Questa dialdeide *bio-based* viene ottenuta dalla parziale ossidazione del 2-idrossimetil furfurale (HMF, a sua volta derivante dalla disidratazione degli zuccheri). Lo scopo finale della ricerca era quello di rimpiazzare la glutaraldeide (GA), il reagente più ampiamente utilizzato per il crosslinkaggio di proteine, che causa ampie preoccupazioni a causa della sua ben documentata tossicità. Il DFF è stato studiato in termini della sua reattività in acqua, della sua eco-tossicità e infine è stato confrontato sistematicamente con la glutaraldeide per l'immobilizzazione covalente della glucoamilasi da *Aspergillus niger*. In acqua, il DFF mostra una reattività molto più semplice della glutaraldeide, in quanto non può formare derivati enolici e, quindi, non può oligomerizzare. Inoltre, solo la forma mono-idratata del DFF è stata osservata in acqua. È importante sottolineare che il DFF è molto meno volatile della glutaraldeide, il che rende il suo uso più semplice e meno dannoso per la salute. Riguardo all'eco-tossicità, sia la glutaraldeide che il DFF hanno mostrato effetti simili nei saggi selezionati. DFF e glutaraldeide hanno mostrato efficacia simile quando usati per l'immobilizzazione della glucoamilasi su carrier metacrilico ammino-funzionalizzato, anche a basse concentrazioni (0.2 μmol di aldeide utilizzata per grammo di carrier). L'enzima immobilizzato è stato impiegato con successo nell'idrolisi del maltosio sia in batch che in flusso continuo; è rimasto attivo in flusso continuo per l'intero periodo dell'analisi (13 giorni). Di conseguenza, i risultati dimostrano il potenziale del DFF come crosslinker per proteine *bio-based* e con basso rischio chimico. Sempre nell'ambito di questa tesi sono state testate alcune possibili vie biocatalitiche per la sintesi di DFF. Il suo impiego su scala industriale richiederebbe sforzi specifici ed investimenti per l'ottimizzazione di processi sintetici economicamente attuabili.

Il capitolo 4 analizza due formulazioni di lipasi ottenute dall'immobilizzazione fisica della lipasi da *Thermomyces lanuginosus* (TLL) su lolla di riso, un sottoprodotto dell'industria agricola disponibile globalmente su una scala di >120 Mton/anno e con un costo di <90 €/ton. Lo scopo era quello di analizzare la loro performance come potenziali sostituti della formulazione commerciale Lipozyme TL IM, fisicamente immobilizzata su particelle di silica in forma di granuli. Entrambe le formulazioni contengono *binder* solubili in acqua, e di conseguenza subiscono leaching dell'enzima quando esposti ad ambienti acquosi. I granuli della preparazione commerciale vanno anche incontro ad un processo di disgregamento in acqua, mentre la formulazione basata su lolla di riso non lo fa in quanto l'enzima è immobilizzato su singoli frammenti solidi di lolla. Per impedire il leaching della TLL immobilizzata su lolla di riso, è stato tentato il crosslinking con DFF, che però non ha avuto successo, probabilmente perché le singole molecole di enzima sono disperse su una superficie ampia e troppo lontane l'una dall'altra per formare legami covalenti. È interessante notare che, quando il crosslinking è stato effettuato in solvente organico, la TLL ha mostrato attività maggiore che dopo crosslinking in ambiente acquoso, suggerendo un effetto positivo da parte del solvente idrofobico nel promuovere l'attivazione interfacciale della lipasi stessa. Le diverse formulazioni di TLL su lolla di riso sono state anche testate nell'interesterificazione di

trioleina e tristearina, un processo impiegato industrialmente su scala globale di >10,000 ton/anno per ottenere analoghi del burro di cacao. Le formulazioni precedentemente trattate con l'agente crosslinkante hanno mostrato buoni risultati, portando alla completa conversione della tristearina in 24 ore senza produzione significativa di prodotti di idrolisi. Probabilmente questo fenomeno è una conseguenza dei passaggi di lavaggio con solvente organico e asciugatura condotti alla fine del protocollo di crosslinking, che hanno portato ad una più efficace rimozione dell'acqua residua. I risultati indicano che la TLL fisicamente immobilizzata su lolla di riso può essere applicata con successo in ambiente a basso contenuto d'acqua, soprattutto in processi di interesterificazione; di conseguenza, rappresenta un potenziale sostituto, sostenibile sia dal punto di vista ambientale che economicamente, delle preparazioni commercialmente disponibili. Ulteriori prospettive nello studio di queste preparazioni di TLL possono essere condurre esperimenti di riciclo del biocatalizzatore, oltre ad analisi calorimetriche (DSC) per avere informazioni sulla cinetica di reazione.

Il capitolo 5 riguarda l'analisi sistematica della lolla di riso come carrier rinnovabile per l'immobilizzazione covalente di glucoamilasi e lipasi. La lolla di riso è stata prima macinata, poi usata tal quale oppure dopo delignificazione. Sia la lolla tal quale che quella delignificata sono state caratterizzate con tecniche spettroscopiche e di microscopia, le quali hanno evidenziato come il processo di delignificazione sia stato efficace senza però causare cambiamenti nella morfologia tridimensionale del materiale. Entrambe le forme di lolla di riso sono state ossidate tramite (1) ossidazione chimica con $NaIO_4$ oppure (2) ossidazione enzimatica con una laccasi e il mediatore TEMPO; l'ossidazione ha lo scopo di introdurre gruppi aldeidici tali da consentire l'immobilizzazione covalente dell'enzima alla lolla di riso. Due enzimi sono stati usati per l'immobilizzazione su lolla di riso: la glucoamilasi da *Aspergillus niger* e la TLL. Per l'immobilizzazione covalente della glucoamilasi sono state tentate numerose procedure; nessuna di queste ha avuto success, suggerendo che, nel caso della glucoamilasi, l'immobilizzazione covalente è determinata da ulteriori fattori oltre che dall'interazione superficiale dell'enzima con il materiale lignocellulosico. Di conseguenza, la funzionalizzazione chimica o enzimatica della lolla di riso per l'immobilizzazione covalente di enzimi diversi sembra essere una procedura che difficilmente può portare allo sviluppo di protocolli di applicazione generale. Nonostante i risultati positivi riportati precedentemente per le lipasi CaLB e TLL, protocolli analoghi si sono dimostrati fallimentari nell'immobilizzazione della glucoamilasi, altamente idrofilica e glicosilata. Inoltre, anche nel caso della TLL, il semplice cambio di lotto della soluzione di enzima nativo utilizzato nell'immobilizzazione ha portato a rese notevolmente inferiori. Queste variazioni nei risultati osservati potrebbero anche essere dovute alla presenza di stabilizzanti (es. glicerolo, sali, ecc.) presenti in diverse percentuali nei diversi lotti commerciali di enzima nativo.

Il capitolo 6 esplora l'immobilizzazione di TLL, CaLB e glucoamilasi su lolla di riso usando un approccio in due step, cioè l'adsorbimento e il consecutivo crosslinking in presenza di un agente difunzionale. Ancora una volta, gli esperimenti per l'immobilizzazione di glucoamilasi non hanno avuto successo, confermando la scarsa affinità di questo enzima per la lolla di riso. TLL e CaLB sono stati immobilizzati con successo su lolla di riso usando DFF come agente crosslinkante. I risultati migliori sono stati ottenuti per la TLL quando immobilizzata in presenza di esano (15% di attività recuperata). I risultati confermano che la presenza di una fase idrofobica è cruciale per l'efficace immobilizzazione di lipasi che presentano attivazione interfacciale. D'altra parte, l'immobilizzazione di CaLB non è influenzata dall'esano, dal momento che l'enzima mantiene la stessa conformazione sia in ambiente acquoso che in ambiente idrofobico.

List of Abbreviations

AAOx	aryl alcohol oxidase
ABTS	2,2'-azino-bis(3-ethylbenzothiazoline-6-sulfonic acid)
AOx	alcohol oxidase
Arg	arginine
Asn	asparagine
Asp	aspartic acid / aspartate
ATR-IR	Attenuated Total Reflectance – Infrared spectroscopy
BHMF	2,5-bis(hydroxymethyl)furan
BOD	Biochemical Oxygen Demand
BSA	Bovine Serum Albumin
CaLB	Lipase B from *Candida antarctica*
CBEs	Cocoa Butter Equivalents
CBRs	Cocoa Butter Replacements
CBSs	Cocoa Butter Substitutes
CLEs	Cross-Linked Enzymes
CLEAs	Cross-Linked Enzyme Aggregates
CLECs	Cross-Linked Enzyme Crystals
CLSD	Cross-Linked Spray Dried enzymes
Cys	cysteine
DAF	2,5-di(aminomethyl)furan
DCM	dichloromethane
DFF	2,5-diformylfuran / 2,5-furandicarboxaldehyde
DMSO	dimethylsulfoxide
DSC	Differential Scanning Calorimetry
EIE	enzymatic interesterification

ESI	ElectroSpray Ionization
ESR	Early Stage Researcher
EtOH	ethanol
Et_2O	diethyl ether
EXSY	EXchange SpectroscopY
FDCA	furandicarboxylic acid
FFCA	5-formyl-2-furancarboxylilc acid
GA	glutaraldehyde
GaOx	galactose oxidase
Glu	glutamic acid / glutamate
GOx	glucose oxidase
HEC	hydroxyethylcellulose
HMDA	hexamethylenediamine
HMF	2-(hydroxymethyl)furfural
HMFCA	5-hydroxymethyl-2-furancarboxylic acid
HPLC	High Performance Liquid Chromatography
HRP	peroxidase from horse radish
IPA	isopropyl alcohol
KPi	potassium phosphate
Lac	laccase
LCA	Life Cycle Analysis
Leu	Leucine
LMS	laccase mediator system
Lys	lysine
MS	mass spectrometry
MSCA	Marie Skłodowska-Curie Actions

NMR	Nuclear Magnetic Resonance
OOO	triolein
OOS	1,2-oleoyl-3-stearoyl glycerol
OOX	1,2-dioleoyl glycerol diolein
OSO	1,3-oleoyl-2-stearoyl glycerol
OSS	1-oleoyl-2,3-stearoyl glycerol
PDB	Protein Data Bank
PEG	polyethylene glycol
PEI	poly(ethylene imine)
PMMA	poly(methylmethacrylate)
POP	1,3-palmitoyl-2-oleoyl glycerol
POS	1-palmitoyl-2-oleoyl-3-stearoyl glycerol
PVP	polyvinylpirrolidone
RH	rice husk
ROS	Reactive Oxygen Species
SD	Standard Deviation
SEM	Scanning Electron Microscopy
Ser	serine
SOO	1-stearoyl-2,3-oleoyl glycerol
SOS	1,3-stearoyl-2-oleoyl glycerol
SOX	1-stearoyl-2-oleoyl glycerol
SSO	1,2-stearoyl-3-oleoyl glycerol
SSS	tristearin
SSX	1,2-stearoyl glycerol
SVHC	Substance of Very High Concern
TAG	triglyceride (triacylglycerol)

TEMPO	2,2,6,6-Tetramethyl-1-piperidinyloxy, free radical
Thr	threonine
TLC	thin layer chromatography
TLL	Lipase from *Thermomyces lanuginosus*
TRIS	tris(hydroxymethyl)aminomethane
TRP	tryptophan
UNITS	Università di Trieste
UV-Vis	Ultra-Violet Visible spectroscopy
WP	work package
XOX	2-oleoyl glycerol
XSX	2-stearoyl glycerol

1 Introduction

1.1 The INTERfaces project: background and objectives

Industrial-scale production of added value chemicals, with the current processes and technologies, involves a series of intensive steps, particularly considering the material consumption, the energy requirements, and other factors. These steps, which frequently involve the isolation and purification of reaction intermediates, as well as of the final product, cause significant waste generation.[2] For this reason, new, innovative, cleaner processes can be developed by integrating production steps according to sustainability criteria.[3]

This PhD project is part of the INTERfaces MSCA project (grant agreement no. 860414), which aims at the design and technical implementation of heterogeneous enzymatic cascades. The INTERfaces project explores new methods to implement cell-free enzymatic cascades with high productivity for the sustainable manufacture of novel polymers from bio-based molecules, integrating expertise in material science, surface chemistry, protein engineering, biocatalysis and process engineering. To achieve efficient *in vitro* biocatalytic reactions, the biocatalysts employed need to be robust and resistant to the required process conditions, which can be rather extreme for the chosen enzyme. Moreover, the chosen enzyme has to be efficiently recycled, and in the case of multi-enzyme cascades, must allow for compartmentalization, therefore immobilization is key for the process.[4] Finally, for the manufacture of commodities on a large scale, the cost impact of the immobilized biocatalyst must be minimized, therefore the development of new immobilization techniques to reduce the cost of the enzyme preparation is highly important.

To achieve its objectives, INTERfaces was divided in three specific work packages (WPs). WP1 focuses on tailor-made support materials and protein designs, WP2 concerns the systematic assembly of heterogeneous (bio)catalysts and WP3 is focused on process engineering and up-scaling. These WPs worked synergistically to develop, analyze, and validate robust heterogeneous biocatalytic cascades starting from selected bio-based building blocks. In particular, the efforts of the consortium focused on ferulic acid and hydroxystyrene derivative, as well as HMF, as bio-based and highly functionalized model substrates.[5,6]

This thesis project was part of INTERfaces WP3, and its intended objectives were the following:

1. Development of renewable enzyme carriers starting from inexpensive and readily available natural composite materials, as substitutes for fossil-based and expensive methacrylic/polystyrene immobilization carriers, *via* chemical, enzymatic and physical modification of lignocellulosic matrixes.
2. Development of new methodologies to immobilize industrially relevant enzymes by using innovative bio-based cross-linking agents.
3. Analysis of the efficiency of the sustainable immobilized biocatalysts under industrially relevant conditions (e.g. organic solvents, solvent-free or high substrate loadings)
4. Life cycle inventory, technical and economic assessment of the synthesis and the use of the newly developed biobased carrier.

The development of renewable enzyme carriers was tackled by the study and functionalization of rice husk, and the immobilization on the lignocellulosic matrix of several different enzymes (Chapter 5 and Chapter 6). New methodologies for the immobilization of industrially relevant enzymes were achieved by employing DFF for support activation (Chapter 3). The efficiency of the sustainably immobilized biocatalysts was analyzed both for DFF-immobilized glucoamylase (Chapter 3) and for TLL physically immobilized on rice husk (Chapter 4). Finally, the sustainability of the immobilized enzyme preparations was explored with toxicology assays on DFF (Chapter 3) and studying the marine biodegradability of rice husk, compared with that of a methacrylic carrier (Chapter 4). A preliminary evaluation of the cost, reusability and recyclability of carriers made of rice husk was also accomplished.

1.1.1 Project structure and secondments

The INTERfaces project required each ESR to spend ≥50% of the total project time in secondment by the industrial partner. Thus, during every year of the project, the months between July and December were spent in the Netherlands by the laboratories of ViaZym B.V., under the supervision of Dr. Luuk van Langen, while the months between January and June were spent in the laboratories of Prof. Gardossi at the University of Trieste. The activities conducted at ViaZym involved mainly (i) the synthesis of DFF from HMF, (ii) the immobilization of glucoamylase on a methacrylic carrier using DFF for the carrier activation and (iii) the study of the stability of the enzyme preparations under industrially relevant (continuous flow) conditions. The activities conducted at UNITS were (i) the investigation of the reactivity of DFF; (ii) the study of the structural features of the enzyme by means of molecular modeling; (iii) the study and functionalization of rice husk as an enzyme carrier, (iv) the study of rice husk-immobilized enzymes under industrially relevant conditions and (v) the ecotoxicology and biodegradation assays on the supports and crosslinkers.

1.2 Biocatalysis

The use of natural catalysts, such as isolated enzymes or whole microorganisms, to achieve chemical transformations is defined as biocatalysis. By nature, biocatalysis is a multidisciplinary science, which involves disciplines such as molecular biology, biochemistry, organic chemistry, engineering and others.[7] The use of enzymatic reactions has been part of the human history for millennia (for example, for beer and cheese production), but a huge impact on biocatalysis was made by the development of recombinant DNA technology, which allowed for the commercialization of enzymes with the desired characteristics.[8] Nowadays, biocatalytic processes are employed in many different fields, for example for the production of fine chemicals and pharmaceuticals, or for the large-scale production of food commodities[9].

There are several advantages derived from the use of enzymes as catalysts. Firstly, they are biodegradable,[10] and they have low environmental impact. Moreover, they allow to work in relatively mild temperature and pressure conditions,[11,12] which is advantageous in terms of energy consumption of the overall process. They also allow to avoid the use of metal catalysts and organic solvents, and often allow to operate at high substrate concentration or solvent-free conditions. Enzymes also present high substrate specificity,[12] and high chemo-, regio- and stereoselectivity.[13] In some cases, such as the production of high-fructose syrup from the

isomerization of glucose, the enzymatic reaction is the only available efficient technology for the industrial process .[14]

It is important to underline that there are also drawbacks to the use of enzymes as biocatalysts. Despite recombinant DNA technology having increased dramatically the number of enzymes available on the market, many of them still do not have a sufficient stability for the intended application,[15] for example losing activity due to temperature, mechanical stress or pH conditions. Moreover, the process development and optimization remain quite complex, and not all reactions can be catalyzed by known enzymes. Several enzymes require the use of often costly cofactors, that need to be regenerated by another reaction.[12,16] Finally, despite not being toxic, enzymes can still trigger allergic reactions,[17,18] therefore it is important to avoid protein contamination in the final product.

1.3 Industrial scale use of biocatalysts

To be able to use biocatalysts, especially isolated enzymes, at an industrial scale, several conditions have to be taken into consideration. Compared to whole cells biocatalysis, isolated enzymes have higher costs, linked also to lower stability when out of the original organism. The stability can be improved by immobilizing the enzyme, but the cost further increases due to the contribution of the carrier and immobilization process. To ensure scalable sustainable biocatalytic processes, it is important to improve both the concentration of product obtained and the stability of the enzyme under the desired industrial conditions.[19]

It is important to ensure a sufficient amount of product enters the downstream process. This is because a low concentration implies the use of large amounts of solvents, that in enzymatic processes is usually (but not always) water. To ensure the sustainability of the catalytic process, it must be considered the cost of removal of said solvents, as well as the impact of the solvent on the *E*-factor, which is far higher in processes with low product concentration. For low-priced products (<5 $/kg), concentrations over 100 g/L are required; for high-priced products (>100 $/kg), concentrations between 10 and 50 g/L are required. However, in many cases it is not possible to use enzymes as-is in the presence of high concentrations of product due to inhibitory effects. Therefore, process engineering is important to ensure the stability and applicability of the biocatalyst.[19]

As hinted above, another fundamental aspect for industrial biocatalysis is the stability of the enzyme in the operational conditions. In synthetic reaction, the presence of substrate and product at high concentrations over prolonged periods of time, as well as temperature and other operational conditions, influence the biocatalyst stability, that is how much of the initial enzyme activity is maintained over prolonged periods of time. To ensure competitive and sustainable biocatalytic processes, the stability of the biocatalyst needs to be optimized. This can be addressed both by engineering the biocatalyst itself (e.g. by protein engineering and immobilization), or by optimizing the whole synthetic procedure (process engineering).[19]

1.4 Immobilization methods

Immobilized enzymes present a wide range of applications, from the synthesis of pharmaceutical compounds and fine chemicals,[20] to food and cosmetic products.[8,10] There are several advantages in the use of immobilized enzymes instead of their native counterparts. Immobilized enzymes are heterogeneous, insoluble biocatalysts; this translates in easier purification of the product and recycling of the enzyme, while in turn avoiding product contamination. Moreover, the immobilization process often improves the stability of the biocatalyst,[11] which can in turn be used in conditions of temperature or mechanical stress that would inactivate the native enzyme. Finally, the immobilized enzyme allows to conduct reactions both in batch and in continuous flow settings.[13]

There are also limitations related to the immobilization process. For example, the immobilization procedure can be overall very costly, making large-scale applications in industrial settings not economically viable, especially in the case of production of commodities.[15] Moreover, several immobilization techniques cause a reduction of the catalytic activity due to conformational or covalent modification of the protein structure.[21] Finally, there are diffusion and mass transfer limitations which affect the accessibility of the immobilized enzyme, therefore influencing the kinetic of the reaction.[13]

Table 1: Attributes of immobilized biocatalysts (from Di Cosimo et al., 2013)[13]

Advantages	**Disadvantages**
Amenable to continuous and batch formats	Loss of enzyme activity upon immobilization
Reuse over multiple cycles possible	Unfavorable alterations in kinetic properties
Improved stability over soluble enzyme forms	Cost of carrier and fixing agents
Favorable alterations in pH and temperature optima	Cost of immobilization process
Sequester enzyme from product stream	Mass transfer limitation
Co-immobilization with other enzymes possible	Subject to fouling

Despite their advantages, immobilized enzymes are not widely used in industrial processes. This is due to the fact that the cost of a non-immobilized, non-recyclable form of the biocatalyst is only a minor component of the overall economics of a large-scale application; for the immobilization to be advantageous, the immobilized enzyme must be produced at affordable costs.[13,14]

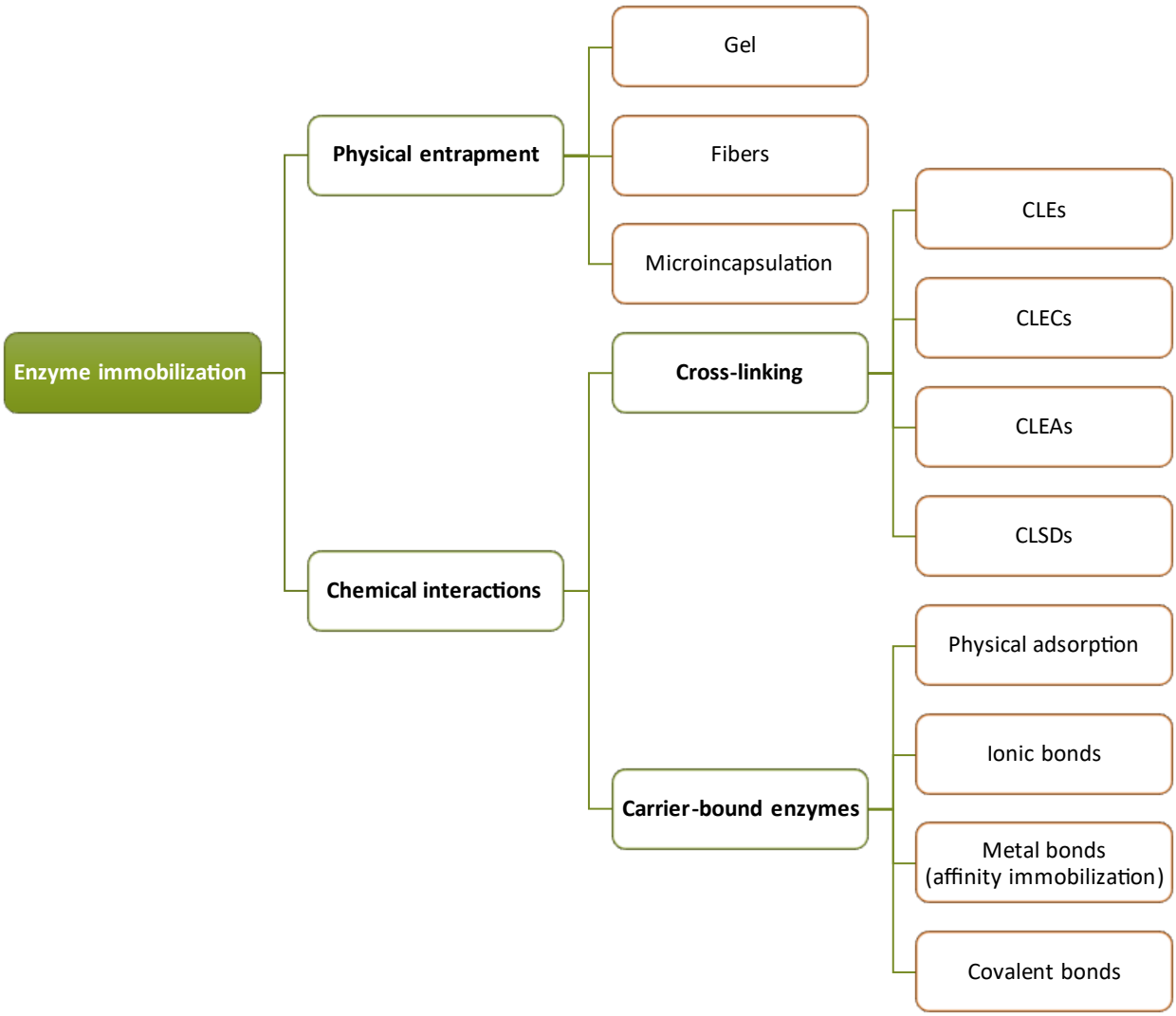

Figure 1: Common enzyme immobilization techniques. CLEs: Cross-Linked Enzymes; CLECs: Cross-Linked Enzyme Crystals; CLEAs: Cross-Linked Enzyme Aggregates; CLSD: Cross-Linked Spray Dried enzymes.

In general, the design of an immobilization procedure is a compromise between the enzymatic activity recovered and the technological advantages that result from the new enzymatic preparation. There are several possible immobilization techniques described in literature, which can be classified according to the nature of the interaction between the enzyme and the solid support. A general overview of immobilization techniques is displayed in Figure 1.

Firstly, the immobilization can be achieved by physical entrapment of the biocatalyst in a gel or a polymeric fiber, or by physical confinement in a membrane device such as a microcapsule.[20] This approach does not cause the formation of a direct bond between the enzyme and a carrier or another enzyme molecule; therefore, in theory there is only a minimal conformational stress on the protein structure. However, the substrate and products must be able to freely diffuse through the matrix, while the biocatalyst should not migrate to the bulk reaction medium; for this reason, physical entrapment is often limited to the immobilization of whole cells.[23]

Another approach is the immobilization *via* interaction of the enzyme with a solid support. These interactions can be of various nature. Surface interactions between the carrier and the enzyme surface can be exploited for the immobilization through adsorption,[11] which is notably used for the production of the CaLB preparation Novozym 435.[24] Immobilization through adsorption can be achieved by straightforward protocols, but a major disadvantage is the ease of leaching of the enzyme from the carrier in aqueous media. Glycosylated enzymes, and more broadly enzymes which present largely hydrophilic surfaces, can also be immobilized on hydrophilic carriers *via* hydrogen bonds. Further examples of non-covalent enzyme immobilization are the exploitation of ionic interactions between ion-exchange resins[25] and the use of metal ions for the affinity immobilization of His-tag engineered enzymes.[26]

Covalent immobilization occurs when there is the formation of a covalent bond between functional groups of the support and amino-acid side chain exposed on the surface of the protein; most commonly, this involves the reaction of terminal amine functionalities of Lys side-chains.[11] The protein generally forms multiple covalent bonds with the carrier, stabilizing the immobilized preparation. Compared to non-covalent immobilization, this presents the advantage of preventing leaching of the protein to the reaction medium, but imposes conformational constraints to its structure thus lowering the recovered activity.

Finally, there are enzyme immobilization techniques which do not involve the use of a solid support, but the cross-linking of enzyme molecules with bifunctional agents. These cross-linked enzyme formulations are furtherly divided into CLEs (Cross-Linked Enzymes), CLECs (Cross-Linked Enzyme Crystals), CLEAs (Cross-Linked Enzyme Aggregates) and finally CLSDs (Cross-Linked Spray Dried enzymes).[27]

CLEs are obtained by cross-linking of a solubilized enzyme with a bifunctional chemical agent, such as glutaraldehyde. This formulation presents several drawbacks, including poor reproducibility and low mechanical stability. In the case of CLECs, the enzyme undergoes a crystallization step before the crosslinking.[28] These preparations have better stability than their non cross-linked counterparts;[27] however, large-scale applications are not advantageous due to the difficulty and cost of the crystallization stage.[12] CLEAs preparation involves firstly the modification of the properties of the protein solution, in order to form physical aggregates of the enzyme; subsequently, these aggregates are cross-linked to obtain the final preparation.[29] The resulting CLEA presents comparable activity and stability to CLECs,[30] without requiring the crystallization step. Nevertheless, the stability of the enzyme preparation remains a crucial problem for cross-linked enzymes.[31,32] Finally, some procedures involve the cross-linking of spray-dried enzyme powders, to form CLSDs. However, this approach has rarely been exploited due to the fact that the spray drying process causes a loss of activity of the enzyme.[27]

1.5 Environmental and economical sustainability of the immobilization process

Environmental factors and stringent regulations are becoming of paramount importance in determining the overall viability of biocatalytic processes.

In the case of immobilized enzymes, one of the critical factors is the use of "ready-to-use" carriers, such as fossil based resins with functional groups to allow for the covalent binding of the enzyme. Life Cycle Analysis (LCA) studies on immobilized enzymes have evidenced that the support production accounts for about 31% to 67% of the energy consumption of the enzyme production process; moreover, it is the primary greenhouse gas emission source, accounting for 51% to 83% of the total for the process.[33]

Also from an economical point of view, the immobilization on fossil-based carriers is impactful on the overall process. For example, the cost of carriers for adsorption immobilization, meaning without reactive chemical groups on the surface, is around 50 €/kg.[34] The cost of more specialized and functionalized carriers can reach 100-300 €/kg. Considering that, for bulk products, the allowable cost contribution of immobilized enzymes should be around 0.05€/kg product,[34] it is evident how cheaper, more sustainable carriers are necessary to be developed.

1.6 Immobilization on biomass

According to the U.S. Biomass Research and Development Act of 2000, the term 'biomass' means any organic matter that is available on a renewable or recurring basis, including agricultural crops and trees, wood and wood wastes and residues, plants (including aquatic plants), grasses, residues, fibers, and animal wastes, municipal wastes, and other waste materials.[35]

Lignocellulose is the most abundant biomass on Earth, with an estimated annual production of 181.5 billion tons. Of these, only 8.2 billion tons are currently used; 7 billion tons derive from dedicated cultures, while 1.2 billion tons come from agricultural by-products.[36] Despite the small amount valorized, agricultural residues represent more than 90% of the total lignocellulosic materials produced.[37] During the years, several applications have been suggested for the valorization of lignocellulosic biomass, including the use of these wastes as fermentation media for enzyme production,[38,39] substrate for the production of sugars,[40] pollutant adsorbent for wastewater treatments,[41,42] or supports for the immobilization of industrially relevant enzymes.[43–46]

Several lignocellulosic biomasses have been exploited for enzyme immobilization, for example green coconut fibers,[47] sugar cane bagasse,[48] corn cobs,[49] soy bean hulls,[50] spent coffee grounds,[51] bamboo powder,[52] and rice husk.[15,53] The interest for lignocellulosic biomasses as enzyme carrier has steadily grown in recent years; for example, the number of papers dealing with lipase immobilization on biomass went from 3 papers in 2000-2005 to 30 in 2018-2021.[46]

Rice husk (RH) is an agricultural byproduct with a production amounting to ≥120 million tons per year, of which only around 20 million tons are currently used. This leaves 100 million tons unexploited, which can be used for valorization in the context of circular economy. Its physical characteristics are interesting, because it

is a low density yet highly robust composite material, formed by about 20% SiO_2, about 5% of organic oxides and 70-80% organic components, of which the majority are cellulose, hemicellulose and lignin.[15] There are several examples of enzymes immobilized on rice husk, which exploit a range of immobilization techniques, summarized in the following table.

Table 2: Examples of conditions for the immobilization of several lipases on rice husk. From Girelli et al., 2023.[46]

Lipase Source	**Immobilization technique**	**Immobilization conditions**	**Source**
C. kikuchii	Adsorption	PEG, 1 h, 25 °C	Costa Silva et al., 2015[54]
G. candidum	Adsorption	Phenyl-silica activation, then lipase pH 7, 12 h, 25 °C	Santos et al., 2021[55]
T. lanuginosus	Adsorption	n-hexane, 2 h and then lipase pH 7, 2 h, 4 °C	de S. Lira et al., 2021[48]
B. cepacia	Covalent	GLU activation, then lipase for 20 min	Abdulla et al., 2017[56]
C. antarctica	Covalent	GLU activation and then lipase pH 7, 5 h, 25 °C	Ulker et al., 2016[57]
C. antarctica	Covalent	$NaIO_4$ and HMDA activation and then lipase pH 8, 24 h, 25 °C	Cespugli et al., 2018[53]
C. rugosa	Covalent	GLU activation, PEG	Costa-Silva et al., 2018[58]
C. kikuchii	Covalent	GLU or $NaIO_4$ or epichlorohydrin activation, PEG and then lipase pH 7, 25 °C	Costa-Silva et al., 2021[59]
C. kikuchii	Covalent	GLU activation, then lipase pH 6.5, PEG, 1 h, 25 °C	Costa-Silva et al., 2016[60]
T. lanuginosus	Covalent	GLU activation, then lipase pH 7, 48 h, 25 °C	Lima et al., 2018[61]
T. lanuginosus *R. oryzae* *C. antarctica*	Covalent	NaIO4 or TEMPO/Laccase oxidation, then lipase, pH8, 24 h, 25 °C	Spennato et al., 2021[62]

2 Objectives of the Thesis

The present thesis aims at finding new, sustainable methodologies to immobilize industrially relevant enzymes. To do so, we decided to tackle the problem from two points of view.

Firstly, the covalent linkage of enzyme molecules to one another or to a solid carrier is usually achieved by using a difunctional molecule, also known as crosslinker. Several crosslinkers have been used in literature, but by far the most widely used is glutaraldehyde, a fossil-based, volatile dialdehyde that readily reacts with amine groups of lysine side chains with mechanisms still not clear. On top of being fossil based, glutaraldehyde also displays acute toxicity, ecotoxicity, and can cause long-term health effects such as skin and lung sensitization. For this reason, we will explore the use of other dialdehydes for enzyme immobilization, in order to (1) find a greener, non-fossil based alternative and (2) find a less hazardous, more manageable chemical for enzyme immobilization.

The other aspects to be improved is the enzyme carrier. Fossil-based resins, either used for adsorption or functionalized for covalent binding, are commonly used for the immobilization of enzymes. However, they present several drawbacks, for example (1) the majority of CO_2 emissions connected to the enzyme immobilization process is linked to the production of the polymeric carrier, (2) the waste management of the spent enzyme after the reaction, since the carrier is in the form of microplastics and (3) the high costs associated with the immobilization, which makes the employment of these immobilized enzyme on industrial scale not cost-effective. For this reason, we will explore the possibility of immobilizing industrially relevant enzymes on renewable lignocellulosic materials, in order to (1) valorize a waste material, such as rice husk (2) simplify waste management of the spent immobilized enzyme (3) find an inexpensive alternative to the costly polymer carriers and (4) find a renewable alternative to the non-renewable, fossil-based carriers.

3 2,5-Furandicarboxaldehyde as a bio-based crosslinking agent replacing glutaraldehyde for covalent enzyme immobilization

3.1 Background

3.1.1 Bifunctional and crosslinking agents for enzyme immobilization

As explained in the introduction, the immobilization of enzymes can be achieved with various techniques, that exploit either non-covalent or covalent interactions. Several of these techniques exploit the reaction of amino acid side chains of the enzyme with other reactive groups.[11] For example, the formation of crosslinked protein conglomerates (CLECs, CLEAs) involves the reaction of a bi- or multifunctional crosslinker with reactive groups on the surface of different protein molecules. In the case of immobilization of solid support, there is the reaction of amino acid residues of the enzyme with reactive groups on the surface of the carrier. In some cases, these reactive groups are introduced on the surface of the polymer during the formulation stage, while in other cases the pre-activation of the carrier with a bifunctional reagent is required.

Numerous examples of such bifunctional and coupling agents have been reported in literature,[63] including bifunctional isothiocyanates,[64,65] bis-dimethyladipimidate,[66] dimethyl suberimidate,[67] 1-ethyl-3-(3-dimethylamino propyl)carbodiimide,[67] terephtalaldehyde,[68] 1,4-phenylene diisocyanate,[69] *p*-benzoquinone,[70] carbohydrate derived dialdehydes,[71] or even polyaldehydes such as dextran polyaldehyde.[72] However, the most used bifunctional agent used for protein immobilization is glultaraldehyde.[73]

3.1.2 Glutaraldehyde

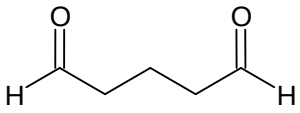

Figure 2: Glutaraldehyde

Glutaraldehyde is a short chained aliphatic dialdehyde, and its ready reactivity with amine groups has been long exploited for enzyme immobilization. In addition to enzyme immobilization, it has several industrial applications including its uses as disinfectant, fixative in tanning, biocide in water treatment, preservative in industrial oils, and several others. Its market revenue was valued at US$ 450 million in 2021, and it is expected to reach US$ 786 million in 2032.[74]

However, its use has several drawbacks. Firstly, it is toxic for humans and hazardous for the environment,[75] and its use is regulated by several governmental agencies. Products containing more than 0.1% of glutaraldehyde are labeled as hazardous.[76] Its use on an industrial scale raises several concerns due to its well documented toxicity,[77,78] and it has been classified as a candidate Substance of Very High Concern by the European Chemicals agency.[79] It is regarded fatal if inhaled, toxic if swallowed, and toxic to aquatic life; moreover, it causes severe long term effects such as skin and respiratory sensitization.[79]

Despite it being widely used in enzyme immobilization, the chemical nature of the bond it forms with enzymes and carriers is not fully understood.[80] In fact, glutaraldehyde displays a very complex behaviour in solution; thirteen different forms, either hydrated, cyclic, oligomeric or polymeric have been identified, and it is still unclear which of these reacts in enzyme immobilization. In many papers, imine bonds are depicted to form between the enzyme and glutaraldehyde, which are labile at acidic pH. However, practice shows that the protein crosslinking obtained with glutaraldehyde is irreversible. Therefore, several alternative mechanisms for enzyme immobilization have been hypothesized, such as Michael addition.

3.1.3 HMF, importance, derivatives

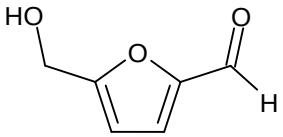

Figure 3: 5-hydroxymethylfurfural (HMF)

5-Hydroxymethylfurfural (HMF) is a bio-based furanic compound produced from the dehydration of sugars.[81–84] Its structure presents one furan aromatic ring, and aldehyde functionality and an alcohol functionality; this makes it a good starting material for the production of several other molecules with various applications. Due to its versatility and potential applications, it was included in the "Top 10 + 4" list of biobased chemicals by the U.S. Department of Energy (DOE).[85] Several different strategies can be employed to convert it into added value products, but the most widely exploited is the oxidation or reduction of its reactive groups.

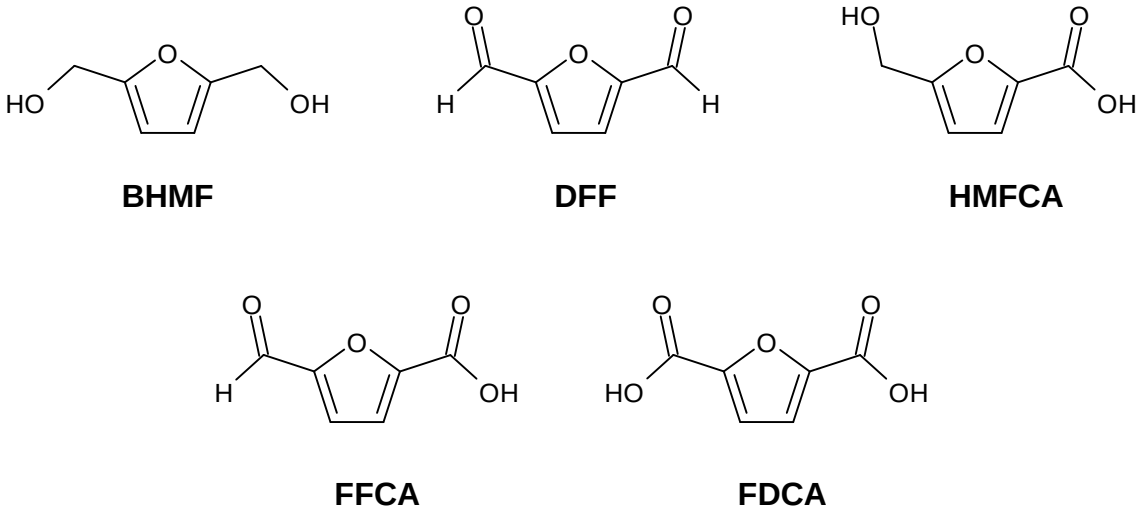

Figure 4: Examples of reduction and oxidation derivatives of HMF

Many derivatives of HMF have been reported in literature. For example, 2,5-bis(hydroxymethyl)furan (BHMF) is a diol that can be obtained by reduction of the aldehyde group; it has applications as monomer for the synthesis of polyesters, polyurethanes and polycarbonates.[86] 5-hydroxymethyl-2-furancarboxylic acid (HMFCA) derives from the oxidation of the aldehyde group of HMF to carboxylic acid; it can be used for the production of interleukin inhibitors, fibers, plastics and as platform molecule for pharmaceutical products.[87]

5-formyl-2-furancarboxylic acid (FFCA) is obtained by oxidation of the aldehyde group to carboxyl group and of the hydroxyl group to aldehyde; it is used as an intermediate for the synthesis of surfactants, biofuels and resins.[87,88] 2,5-furandicarboxylic acid (FDCA) is one of the most important derivatives of HMF, and is obtained by oxidation of both functional groups of HMF to carboxylic acid. It has been listed, together with HMF, in the "Top 10 + 4" list of biobased chemicals,[85] and is the monomer for the synthesis of poly(2,5-furandicarboxylate), a bio-based alternative to poly(ethylene terephthalate).[87]

Finally, the selective oxidation of the alcohol functionality of HMF to aldehyde group leads to the formation of 2,5-diformylfuran (DFF).

3.1.4 DFF, use, synthesis methods and toxicity

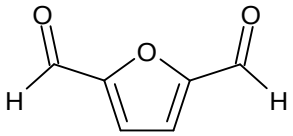

Figure 5: 2,5-diformylfuran (DFF)

2,5-diformylfuran (or 2,5-furandicarboxaldehyde) is the dialdehyde derivative of HMF. It has many interesting potential applications, such as intermediate for the synthesis of pharmaceuticals[89] and fungicides,[90,91] macrocyclic ligands,[92] furan based polymers[93] and resins[94], or novel fluorescent materials.[95] It can also be used to obtain 2,5-di(aminomethyl)furan (DAF), which is a relevant building block for the pharmaceutical industry and an interesting monomer for polymer synthesis.[96]

DFF can be obtained from HMF by selective oxidation of the alcohol functionality. This reaction is not trivial: it is necessary to oxidize the alcohol group without activating and oxidizing the more reactive aldehyde functionality. There is ample literature concerning methods for this oxidation. Several papers report the use of metal catalysts, for example Fe_3O_4@SiO_2–TEMPO,[97] gold nanoparticles supported on MnO_2,[98] Mn/Fe mixed oxides,[99] ruthenium-containing catalysts,[100–102] or vanadium oxide microspheres.[103] Other report the use of classical oxidants such as $NaNO_2$,[104] or $KMnO_4$,[103] or the use of NaBr or KBr in DMSO.[105] Finally, more recent publications concern the use of enzymatic oxidation[106–108] or even whole cell oxidation[109] to convert HMF to DFF.

3.1.4.1 DFF toxicity

The potential use of DFF for larger-scale applications imposes to take into consideration its toxicity. To the best of our knowledge, only three papers address this issue.

In 2014, Frade at al.[110] analyzed the toxicity of HMF and 20 of its derivatives, including DFF, on human skin fibroblast cells of line CRL-1502, a non-tumor cell line chosen for its resemblance with human healthy skin. The cells were incubated with 100-500 μM of the tested compound, in order to establish toxicity curves; a compound is considered toxic when it produces a 50% reduction in cell viability, at a concentration of 500 μM, after 72 hours of exposure. Among the tested compounds, DFF resulted to be the second most toxic, giving a

cell viability of 32 ± 2% compared to the initial after the first 72 hours. On the other hand, HMF can be considered non-toxic in respect to the assayed cell line: cell viability after 72 hours was 94 ± 3 %.

The study also examined the ability of the molecules to generate reactive oxygen species (ROS) and evaluate whether their presence was connected to the principal cytotoxicity mechanism. This appeared not to be the case; DFF, highly cytotoxic, gave an increase in ROS comparable to that of HMF, which was considered non toxic on the selected cell line.

Table 3: Percentage of cell viability and ROS determined for the treated CRL-1502 cells. Cell viability is expressed residual % of the initial viability. From Frade et al., 2014.[110]

Compound	Cell Viability (%)	ROS (%)
HMF	94 ± 3	106 ± 7
DFF	32 ± 2	113 ± 12

Another study from the same research group[111] examined the toxicity of various platform chemicals derived from biomass towards aquatic organisms. The study analyzed 16 compounds derived from carbohydrates, 14 of which are furanic compounds (including HMF and DFF). In this case, a Microtox assay was performed, following the decrease in luminescence of the marine bacterium *Vibrio fischeri*, after exposure to different concentrations of each compound at 15°C for 5, 15 and 30 minutes. The EC_{50} was then calculated for each compound.

Table 4: Median effective concentration (EC_{50}) values, in mg/L, obtained with Vibrio fischeri (Microtox) after 5, 15 and 30 minutes of exposure to different furans and derivatives. From Ventura et al., 2016[111]

Compound	EC_{50} at 5 min (mg/L)	EC_{50} at 15 min (mg/L)	EC_{50} at 30 min (mg/L)
HMF	407	385	389
DFF	39.2	21.3	22.8

For most of the analyzed compounds, the time of exposure did not influence significantly the resulting EC_{50}; an exception is DFF, for which the EC_{50} halved (in other words, toxicity doubled) going from 5 to 30 minutes of exposure. Among the analyzed compounds, the authors regarded DFF as moderately toxic (EC_{50} = 100 – 10 mg/L), while HMF was practically harmless (EC_{50} = 1000 – 100 mg/L). As a general observation, replacing one aldehyde group with a $–CH_2OH$ gives a reduction in the compound toxicity.

Lastly, DFF toxicity was briefly mentioned in a work by Martins et al.,[112] which examines toxicity of HMF and some of its derivatives towards *Aspergillus nidulans*. In this paper, the IC_{50} is calculated as the concentration of compound that can inhibit of 50% the growth of *A. nidulans*. Interestingly, in this study DFF results less toxic (higher IC_{50}) than HMF, unlike what observed in the previous studies.

Table 5: IC_{50} values obtained for HMF and DFF. From Martins et al., 2020.[112]

Compound	IC_{50} (mg/mL)	IC_{50} (mM)
HMF	0.19	1.51
DFF	0.62	4.99

3.1.5 Analysis of the 3D structure of glucoamylase from *A. niger* by molecular modeling

One of the enzymes investigated in this thesis is glucoamylase from *Aspergillus niger*. Glucoamylases (EC: 3.2.1.3) are enzymes of the family glycoside hydrolase 15, which catalyze the cleavage of α-1,4- and β-1,6-glycosidic bonds, starting from the non-reducing end of the polysaccharide chain.[113,114] Their mechanism involves inversion of configuration, releasing β-glucose as a product (Scheme 1).[115] Structurally, they are composed by an N-terminal catalytic domain, highly conserved between different organisms, and a smaller, C-terminal starch-binding domain; the two domains are linked by a highly flexible linker region.[114,116] Even when isolated, the catalytic domain can hydrolyze oligosaccharides, but the starch binding domain is fundamental for the processing of starch, an insoluble polymeric substrate.[116]

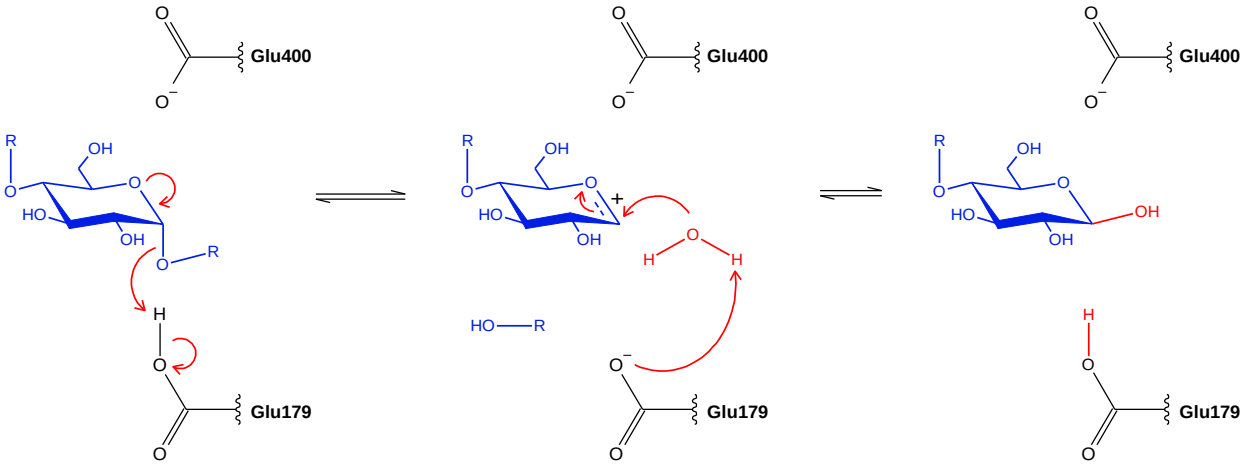

Scheme 1: Catalytic mechanism of glucoamylase[117,118]

In literature there are no crystallographic structures of the whole *A. niger* glucoamylase, due to the breaking of the flexible linker region when undergoing the crystallization process. There are, however, several crystallographic structures of the catalytic domain (isolated or with the linker portion) and of the isolated starch binding domain.

Crystallographic studies[114] comparing the complete structure of different glucoamylases from fungi, together with considerations regarding the characteristics of the linker region (which is highly flexible and presents extremely variable lengths among glucoamylases from different organisms), suggest that the relative position of catalytic and starch-binding domain is not important for the overall enzyme activity. For this reason, the following considerations are based on the isolated structures of the two main protein domains.

3.1.5.1 Catalytic domain

The following study was made on protein tridimensional models obtained with the Chimera software.[119]

The catalytic domain of glucoamylase from *A. niger* has a globular structure; it is formed mainly by α-helixes, 13 in total, 12 of which are arranged as a $(\alpha/\alpha)_6$-barrel (tubular structure with 5 internal helixes and 6 external helixes).[113] This tridimensional structure is shown in Figure 6.

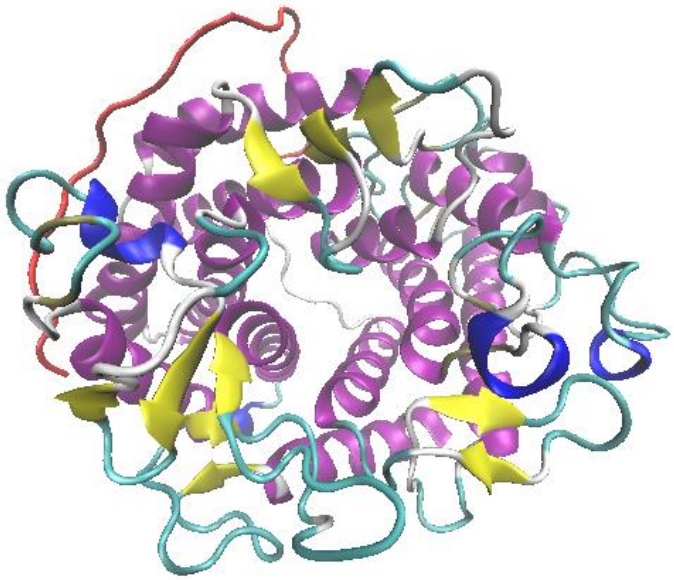

Figure 6: Model of the tridimensional structure of the catalytic domain. In purple are shown the a-helix segments, while in red is shown the C-terminal linker. (PDB ID: 3EQA)

The active site is located in the center of the $(\alpha/\alpha)_6$-barrel, at the end of a tunnel on the protein surface. It presents six conserved amino acid residues that bind the substrate (Arg78, Asp79, Leu201, Trp202, Glu204 e Arg329), and the catalytic residues Glu203 (protonated) and Glu424 (deprotonated). The entrance to the active site is highlighted in red in Figure 7B.

It is important to observe the amount and position of lysine residues, which are generally responsible for the formation of covalent bonds with the carrier,[120] are highlighted in yellow in Figure 7**.** As evident, there are lysin residues both in proximity of the catalytic site entrance and away from it (one residue, on the opposite side of the protein surface, is not visible in the picture). A lysine residue is located exactly at the entrance of the catalytic site, and it could theoretically cause a decrease in recovered enzymatic activity after covalent immobilization.

A) **B)**

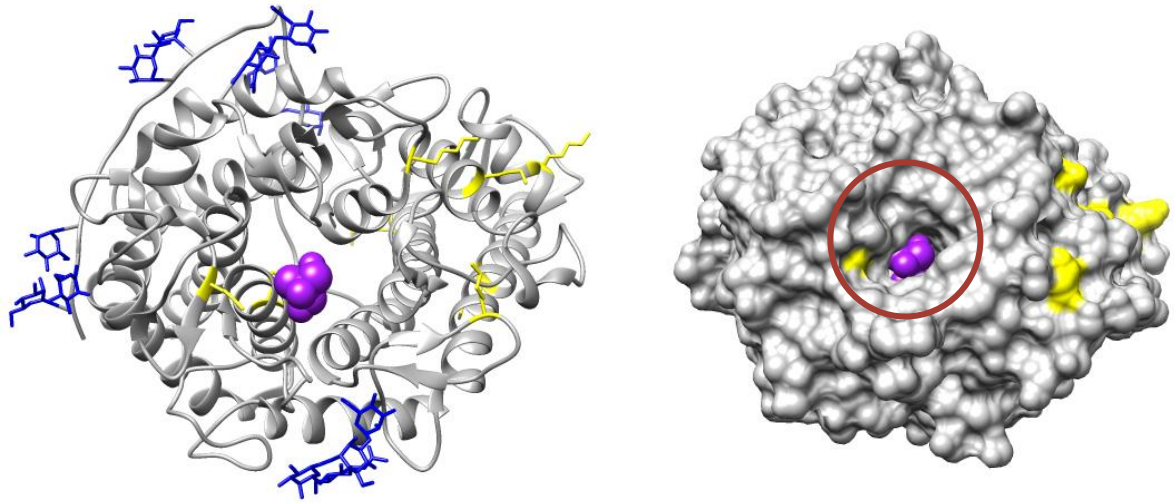

Figure 7: Tridimensional model of the structure of the catalytic domain. ***A)*** *In yellow, lysine residues; in blue, glycosylation sites; in purple, TRIS inhibitor inside the catalytic site.* ***B)*** *Representation of the protein surface, with highlighted in yellow superficial lysine residues and in purple TRIS inhibitor inside the catalytic site. It is also present (not visible in the picture) a residue of Lys on surface opposite to the entrance of the catalytic site (PDB ID: 3EQA)*

As apparent from Figure 8, the surface of the catalytic domain is manly hydrophilic (blue areas of the surface).

Moreover, as can be seen in Figure 7A, the catalytic domain is highly glycosylated; fragments of the glycans still attached to the enzyme after crystallization are highlighted in blue in the figure. In particular, there are nine glycosylation sites, of which seven are O-glycosylation sites (Ser467, Ser468, Thr476, Ser477, Ser483, Ser484 and Thr486) and two are N-glycosylation sites (Asn195 and Asn419). The O-glycosylation sites are mainly located in the flexible, C-terminal linker portion.

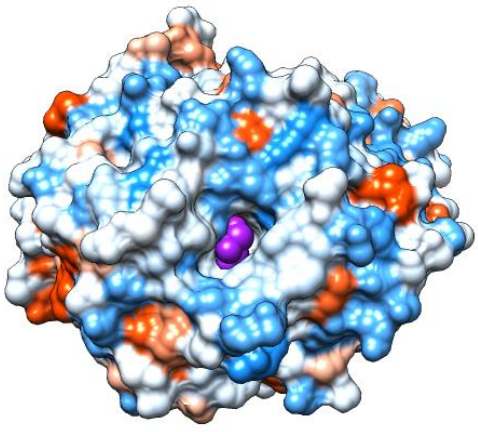

Figure 8: Model of the surface of the catalytic domain, in which are highlighted hydrophobic (red) and hydrophilic (blue) areas. (PDB ID: 3EQA)

3.1.5.2 Starch-binding domain

Figure 9 reports the structure of the starch-binding domain of glucoamylase from *A. niger*. This domain consists of a short portion of protein, mainly formed by β secondary structures (seven in total, in yellow in Figure 9A); in particular, there is a characteristic structure of β-sheet sandwich. Two cysteine residues, Cys 509 (N-terminal of the crystallographic structure) and Cys604, are involved in the formation of a disulfide bond.

Only two lysine residues are present in this portion of the protein, and are highlighted in yellow in Figure 9B; as the ones in the catalytic domain, these residues are potentially responsible of the immobilization on the carrier.

A) **B)**

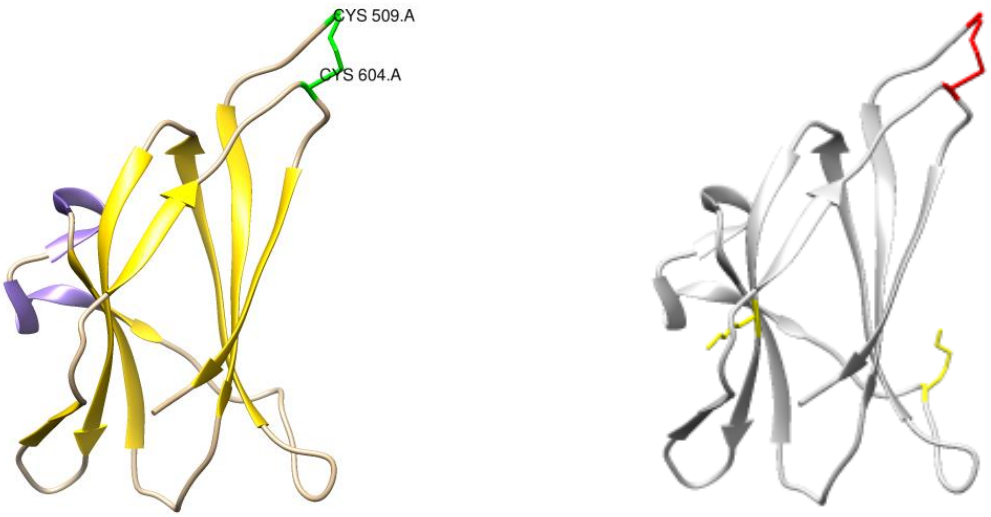

Figure 9: Tridimensional representation of the structure of the starch-binding domain of glucoamylase from A. niger. ***A)*** *In yellow are highlighted β structures, in α-helix portions. Cys residues involved in the formation of a S-S bond are highlighted in green.* ***B)*** *In red is highlighted the disulfide bond, in yellow Lys residues potentially responsible of the covalent immobilization (PDB ID: 5GHL)*

As evidenced in Figure 10, the starch-binding domain is mainly hydrophilic (blue areas in the figure), even if it has a mainly hydrophobic portion (in red) on one of the sides of the surface (Figure 10B).

The crystallographic structure used for this analysis does not present information about glycosylation of the starch-binding domain; for this reason, it was decided to conduct an analysis of the possible glycosylation sites of the protein.

A) B)

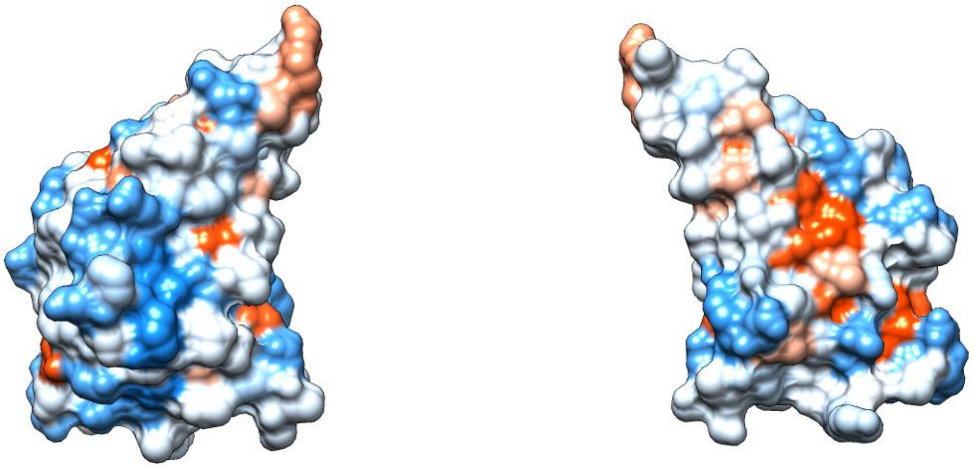

Figure 10: Model of the surface of the starch-binding domain. Hydrophilic areas (in blue) and hydrophobic areas (in red) are highlighter (PDB ID: 5GHL)

3.1.5.3 Analysis of the protein glycosylation sites

The analysis of possible N-glycosylation sites was conducted using the server NetNGlyc[121], while the analysis of possible O-glycosylation sites was conducted using the server NetOGlyc.[122] The primary sequence used, pertaining to the entire protein, has the Uniprot code P69328.

In the case of the N-glycosylation sites, the analysis showed as glycosylated the positions that also resulted glycosylated in the crystallographic structure used for the protein modelling.

Concerning the O-glycosylation sites, the analysis identified 44 possible O-glycosylation positions. Of these, seven matched with the O-glycosylation sites displayed in the crystallographic structure in Figure 7A; the majority of the remaining possible O-glycosylation sites is located in the starch binding domain of the protein.

In general, it can be said that glucoamylase from *Aspergillus niger* is a highly glycosylated protein, in addition to displaying mainly hydrophilic amino acids on its surface. Therefore, the protein can be regarded as highly hydrophilic.

3.2 Objectives of the chapter

In this chapter, we aim to demonstrate that DFF can be used as a replacement for glutaraldehyde in the field of enzyme immobilization. Replacing glutaraldehyde was deemed necessary due to (i) its acute and long-term toxicity, both in humans and from an environmental point of view and (ii) to find a bio-based alternative to this fossil-based crosslinker.

First of all, the possibility of a biocatalytic production of DFF starting from its precursor HMF will be explored. Then, the properties of DFF for enzyme immobilization will be studied by (i) studying its behaviour in aqueous environment, (ii) studying its reactivity with amine groups, (iii) comparing its toxicity in marine environment with that of glutaraldehyde, (iv) systematically comparing it with glutaraldehyde in the immobilization of glucoamylase on an amino functionalized methacrylic carrier, (v) testing the stability of the resulting enzyme preparation in a continuous flow setting.

3.3 Results and discussion

3.3.1 Synthesis of DFF

2,5-diformylfuran (DFF) was synthesized from 2-(hydroxymethyl)furfural (HMF) via oxidation, to be used as a reference compound and tested as a crosslinker for enzyme immobilization. DFF was obtained via Swern oxidation, using DMSO and KBr. The final yield after product purification was 50%. The purified product was characterized via ^{1}HNMR, ^{13}CNMR and UV-Vis spectroscopy.

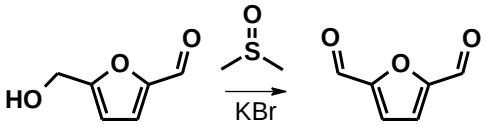

Scheme 2: Swern oxidation of HMF to DFF

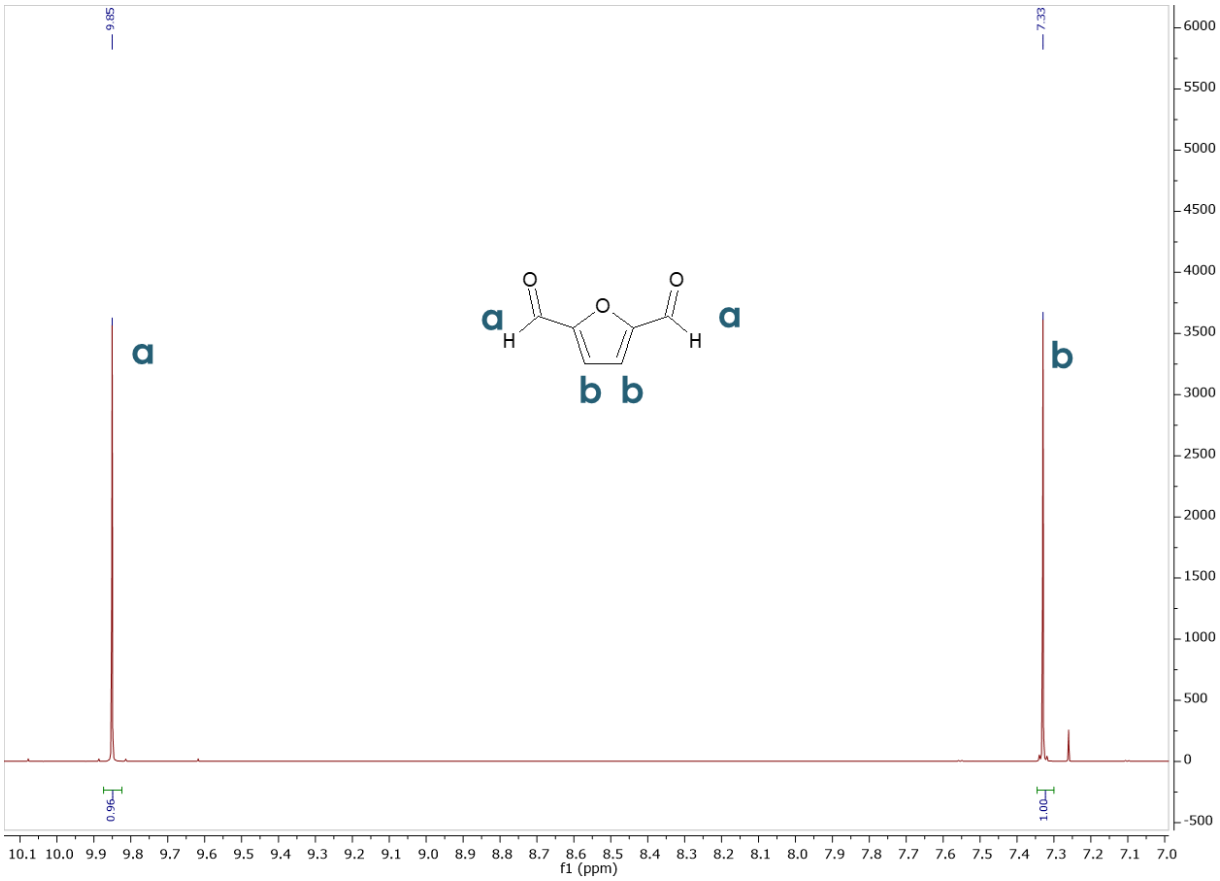

Figure 11: ^{1}H NMR spectrum of DFF obtained by chemical oxidation of HMF. ^{1}H NMR (400 MHz, $CDCl_3$) δ 9.85 (s, 2H), 7.33 (s, 2H)

The NMR spectrum in chloroform evidenced the purity of the resulting product; no signals of residual HMF were identified. The obtained DFF was deemed suitable for use in enzyme immobilization, as well as for further characterization experiments to clarify its reactivity.

3.3.1.1 Enzyme screening for the oxidation of 2-(hydroxymethyl)furfural to 2,5-diformylfuran

In order to explore the possibility of using a greener procedure for HMF oxidation, several enzymes were screened using HMF as a substrate. The enzymes were identified in literature[106] as suitable to oxidize HMF; however, it is important to select an enzyme that does not cause overoxidation of HMF to the corresponding diacid FDCA.

The reaction conditions are detailed in the Materials and Methods section for this chapter. A general reaction scheme for the oxidation of HMF to DFF is reported in Scheme 3.

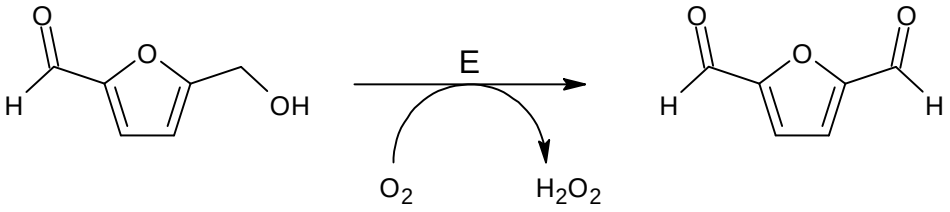

Scheme 3: Enzymatic oxidation of HMF to DFF

In the case of galactose oxidase and alcohol oxidase, the reaction required the addition of catalase to the reaction mixture in order to remove H_2O_2, that forms as a by-product of the oxidation process and causes the inactivation of the oxidative enzyme (Scheme 4). Both enzymes yielded DFF as the oxidation product.

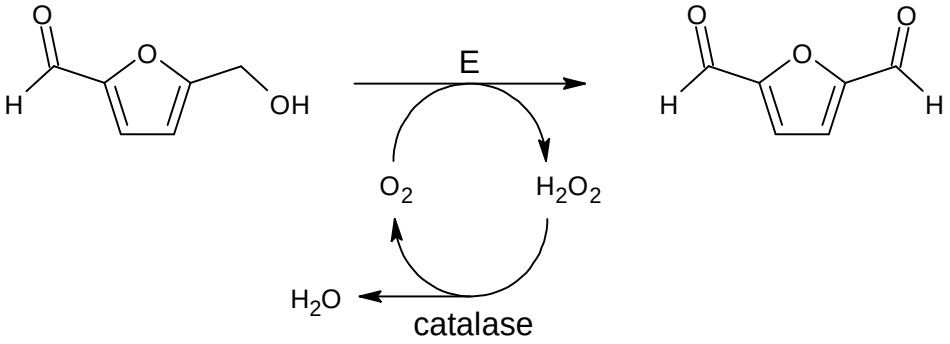

Scheme 4: Oxidation of HMF to DFF in the presence of catalase. E = galactose oxidase or alcohol oxidase.

Laccase, a fungal oxidative enzyme, was tested with and without the presence of a mediator, 2,2,6,6-Tetramethyl-1-piperidinyloxyl (TEMPO). The mediator is a small molecule which is oxidized by the laccase, and in turn oxidizes the substrate; its presence is often required when working with laccases, as the enzyme by itself has a relatively low redox potential (350-800 mV)[123] and cannot oxidize many non-natural substrates. In the case of the oxidation of HMF, no reaction was observed without the mediator. In the presence of TEMPO (20 mol% of the substrate), there is the formation of DFF, but only as a reaction intermediate/byproduct: the reaction ultimately leads to the overoxidation of HMF to FDCA (Figure 12), whose presence was verified by TLC analysis. Notably, in this preliminary screening the problem of TEMPO recycling has not been addressed. However, regeneration of the mediator has been observed, catalyzed for example by the enzyme itself,[62] by a metal catalyst,[124] or by electrochemical means.[125,126]

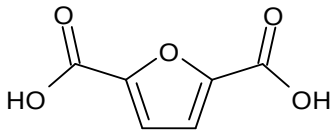

Figure 12: Furandicarboxylic acid

Finally, unlike the other enzymes tested, horseradish peroxidase uses hydrogen peroxide as an oxidant, reducing it to H_2O while oxidizing the substrate (Scheme 5). For this reason, when using HRP for the reaction, H_2O_2 (0.5 eq) was added to the reaction mixture.

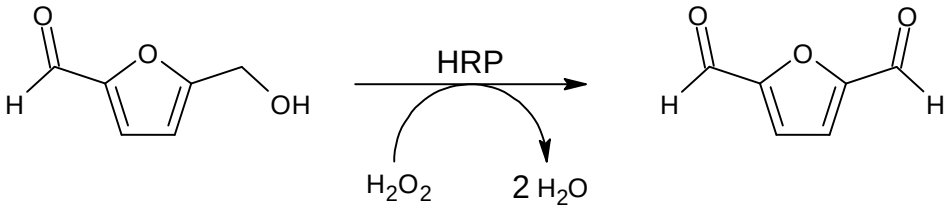

Scheme 5: Oxidation of HMF to DFF using horseradish peroxidase

The screening reactions were solely monitored via TLC, comparing the reaction mixtures with pure HMF and pure DFF, to verify the formation of DFF as well as the presence of other products. This study was a preliminary qualitative screening aiming only at detecting the formation of the desired product. Therefore, product isolation was not performed. The following table summarizes the screened enzymes and the results of the screening.

Table 6: Enzyme screening for the oxidation of HMF to DFF

Reaction	**Enzyme**	**pH**	**DFF Formation**	**Notes**
1	Galactose oxidase from *D. dendroides*	6.0	YES	Added catalase
2	Laccase from *T. versicolor*	6.0	NO	
3	Aryl alcohol oxidase	6.0	YES	
4	Peroxidase from horse radish	6.0	NO	Added 0.5 eq H_2O_2
5	Alcohol oxidase from *P. pastoris*	7.5	YES	Added catalase
6	Laccase from *T. versicolor*	5	YES*	Added mediator (TEMPO), 20 mol%

Among the tested enzymes, those that gave the formation of DFF as the only product of the reaction were galactose oxidase, aryl alcohol oxidase and alcohol oxidase.

3.3.1.2 Biocatalytic oxidation of HMF with Pichia pastoris whole cells

Among the enzymes screened previously for the selective oxidation of HMF to DFF, alcohol oxidase (AOx) from *Picha pastoris* is the most likely candidate for further biocatalytic oxidation reactions, as it does not show over-oxidation of HMF to FDCA. Moreover, it has the advantage of being less expensive and more readily commercially available than the other two enzymes with similar characteristics, galactose oxidase and aryl alcohol oxidase. A downside of this enzyme is that it requires the presence of a catalase, to neutralize hydrogen peroxide produced in the oxidation reaction which can inactivate the AOx.

Alcohol oxidase and catalase are both simultaneously expressed by *Pichia pastoris* in cellular vesicles called peroxisomes, when the yeast is grown in cellular cultures using methanol as the sole source of carbon.[127,128] Due to the presence of both enzymes simultaneously in the cells, it was decided to explore the oxidation of HMF to DFF with *Pichia pastoris* whole cells.

A suitable *Pichia pastoris* strain was identified among those commercially available. Engineered *P. pastoris* strains often exploit the methanol-growth mechanism of the yeast to produce exogenous enzymes, which replace either alcohol oxidase or catalase in the organism genome. Thus, the selected *P. pastoris* strain needed to be a wild type. Among those commercially available, the X-33 strain (ThermoFischer) was selected due to its commercial availability.

As mentioned above, the alcohol oxidase is expressed when the yeast is fermented in methanol. For this reason, a specific fermentation protocol by Rennig et al. was selected.[129] The fermentation process was interrupted at the beginning of the stationary phase of cell growth; cells were then lyophilized for long-term storage and stored at 4°C. The fermentation and lyophilization process was performed by Biosphere S.r.l.

Alcohol oxidase activity of *Pichia pastoris* whole cells

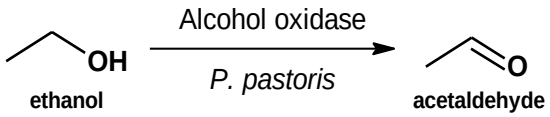

Scheme 6: Biocatalysed oxidation of ethanol to acetaldehyde

Once the lyophilized *P. pastoris* whole cells were obtained, they were first used in the oxidation of ethanol to acetaldehyde, to verify if alcohol oxidase activity was still present after the lyophilization process. This reaction, catalyzed by *P. pastoris* whole cells, is reported in the literature.[130] *Pichia pastoris* lyophilized cells (100 mg) were resuspended in 4.75 mL of 0.1 M, pH 7 potassium phosphate aqueous buffer. Then, 0.25 mL of ethanol were added to the mixture, to a final volume of 5 mL. The final concentration of biomass is 20 g/L, while the final concentration of methanol is 40 g/L. The mixture was shaken on the orbital shaker at 25°C for 24 hours.

The concentration of acetaldehyde after 24 hours was determined using a commercial acetaldehyde assay kit (Megazyme K-ACHYD). For the analysis, 0.2 mL of the reaction mixture were centrifuged to separate suspended cells from the supernatant. Then, 50 µL of the supernatant were diluted 20 times with distilled water. The diluted sample was then analyzed following the procedure of the commercial assay. The measured

concentration of acetaldehyde in the sample after 24 hours was 11.13 g/L; the presence of acetaldehyde confirmed that the *Pichia pastoris* whole cells retained alcohol oxidase activity after the lyophilization process.

It is important to note that the oxidation of ethanol to acetaldehyde was not studied in detail nor followed for longer reaction times. The reason is that studying this reaction in detail was beyond the aim of the project, as it was only used to verify the presence of alcohol oxidase activity in the lyophilized cells.

Reference reaction with isolated alcohol oxidase

The enzymatic oxidation of HMF to DFF with isolated commercial alcohol oxidase and catalase was repeated to confirm the characterization of the reaction product, as the previous reaction was only followed by TLC for screening purposes.

The raw reaction product was analyzed by ^{1}HNMR. The resulting spectrum (Figure 13) confirmed that the product detected via TLC analysis was indeed DFF. The ratio between HMF and DFF, calculated using the signals of the non-labile aromatic protons, is HMF:DFF = 61:39.

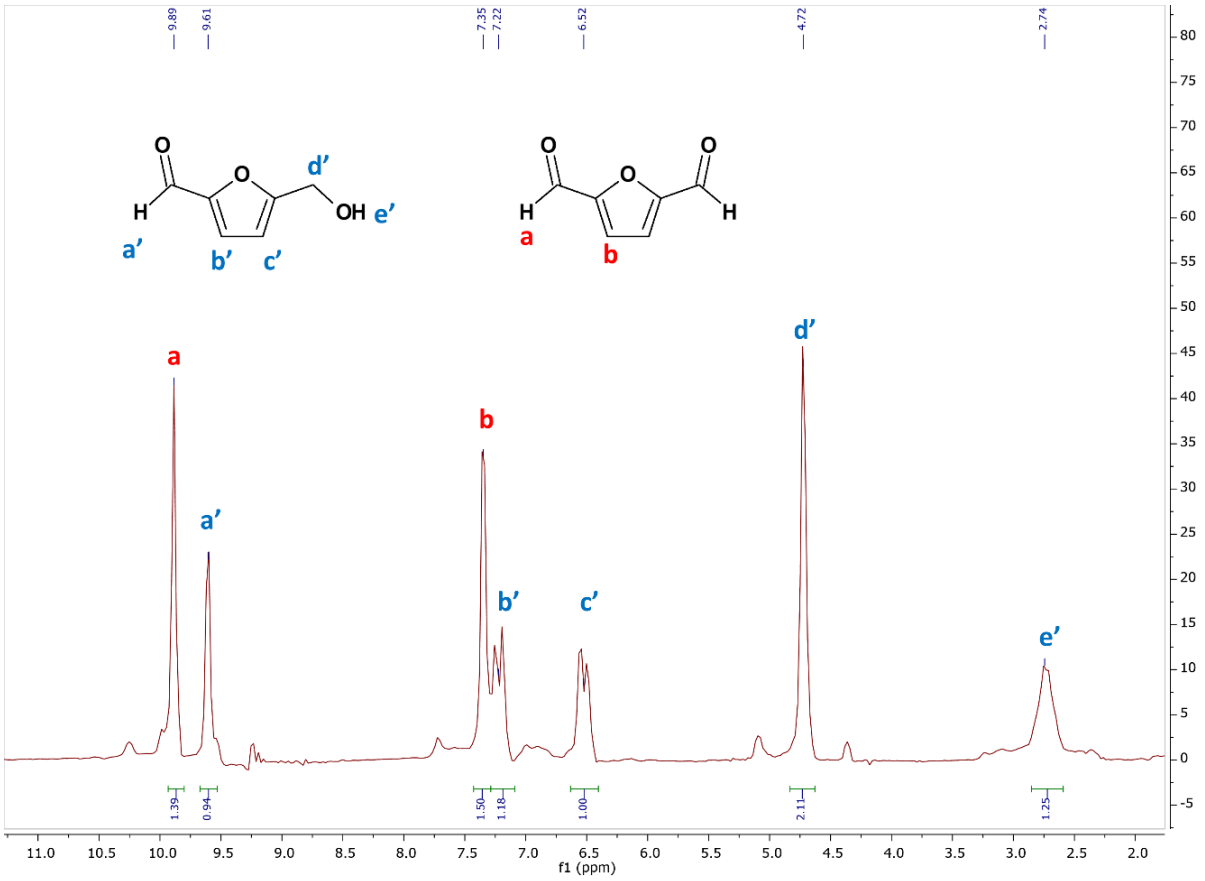

Figure 13: ^{1}HNMR of the raw reaction product of the enzymatic oxidation of HMF to DFF. ^{1}HNMR (60 MHz, $CDCl_3$): δ 9.89, 9.61, 7.35, 7.22, 6.52, 4.72, 2.74

Table 7: Peak chemical shift and integration of the ^1H NMR spectrum in Figure 13.

Peak	δ (ppm)	Area
a	9.89	1.39
b	7.35	1.50
a'	9.61	0.94
b'	7.25	1.18
c'	6.52	1.00
d'	4.72	2.11
e'	2.44	1.25

Reaction condition screening – *Pichia pastoris* whole cells

Various reaction conditions, based on previous studies reported in the literature,[131,132] were screened for the biocatalytic oxidation of HMF to DFF. Due to issues with the available HPLC column, and due to the low field of the available 60 MHz NMR spectrometer (which does not allow for the analysis of small amount of sample), the screening was purely qualitative.

The biotransformation was conducted in: (a) aqueous KPi (0.1 M, pH 7) (b) biphasic systems, with different cosolvents and compositions. The lyophilized cell concentration used for all experiments was 5 mg/mL; HMF concentration was also 5 mg/mL. All reactions were followed for 48 hours using TLC analyses, to verify the formation of DFF formation. TLC analysis was conducted by using as eluent pure Et_2O, using pure DFF and pure HMF as reference.

Screening in monophasic aqueous system

Two different conditions were screened for the biotransformation in aqueous medium. In one case, the *Pichia pastoris* cells were resuspended in the aqueous buffer and directly used in the biotransformation. In the other case, the resuspended cells were sonicated for 5 minutes before the reaction, to verify if disruption of the cell wall would have an effect on DFF production due to increased mass transfer.

Table 8: Screening of reaction conditions for the oxidation of HMF to DFF with Pichia pastoris whole cells. For both reactions, V = 10 mL. The samples incubated at 30°C for 48 hours, with a shaking speed of 300 rpm.

	Buffer	Cell conc. (mg/mL)	[HMF] (mg/mL)	Sonicated	T (°C)	DFF formation
1	KPi, 0.1 M, pH 7	5	5	No	30	YES
2	KPi, 0.1 M, pH 7	5	5	Yes	30	YES

In both cases, DFF formation was observed. The TLC analysis did not show any visible increase of DFF formation with the sonicated *Pichia* cells, but of course a quantitative analysis would be necessary for the determination of the species concentration in solution.

Screening in biphasic system

P. pastoris whole cells have been reported to catalyse biotransformation of aromatic aldehydes in biphasic reaction systems.[132] The use of a biphasic system has the potential advantage of promoting the partition of the product in the organic solvent, thus facilitating its extraction and reducing product inhibition of the enzyme.

Three different organic solvents were used for the screening: (1) toluene, (2) ethyl acetate and (3) isopropyl ether; in all cases, the aqueous phase was KPi, 0.1 M, pH 7. For each solvent, two different reaction mixture compositions were tested: (a) solvent/KPi 50:50 (b) solvent/KPi 95:5. Reaction volume is 1 mL. The solvents used for the reaction, as well as the solvent/KPi rations, were derived from literature.[131,133–135] All samples were incubated in the thermomixer (30°C, 800 rpm) for 2 days; the formation of DFF was followed by analysing both the aqueous and the organic phase via TLC. The following table summarizes the experiments.

Table 9: Screening of reaction conditions for the oxidation of HMF to DFF with Pichia pastoris whole cells in biphasic reaction systems.

	Cosolvent	Cosolvent/KPi ratio	Cell conc. (mg/mL)	[HMF] (mg/mL)	DFF formation
1	Toluene	95:5	5	5	No
2	Toluene	50:50	5	5	Yes
3	Isopropyl ether	95:5	5	5	No
4	Isopropyl ether	50:50	5	5	Yes
5	Ethyl acetate	95:5	5	5	No
6	Ethyl acetate	50:50	5	5	No

Only reaction conditions 2 and 4 lead to the formation of DFF; again, a quantitative analysis would be necessary to determine the final product concentration.

It must be underlined that the screening reactions reported above were conducted in order to verify the possibility to explore in the future different synthetic routes for an economically viable production of DFF at industrial scale, given the positive results obtained in the immobilization processes and the current absence of convenient large-scale production of this dialdehyde. However, due to the fact that the main objective of the thesis was the development of novel immobilization methods, the optimization of the different synthetic routes was not attempted, since they would have required excessive investment of time and efforts. More importantly, another PhD student involved in WP3 of the INTERfaces project invested most of her thesis work on the study of the biocatalysed synthesis of DFF starting from HMF, so that we decided to avoid duplication but rather we looked for synergic collaborations.

3.3.2 DFF characterization

Glutaraldehyde, which is widely used as crosslinking agent for enzyme immobilization, has a very complex behaviour in aqueous solution (Figure 14). Thirteen different forms, either hydrated, cyclic, oligomeric or polymeric have been identified,[80] and it is still unclear which form reacts with lysine residues in enzyme immobilization.

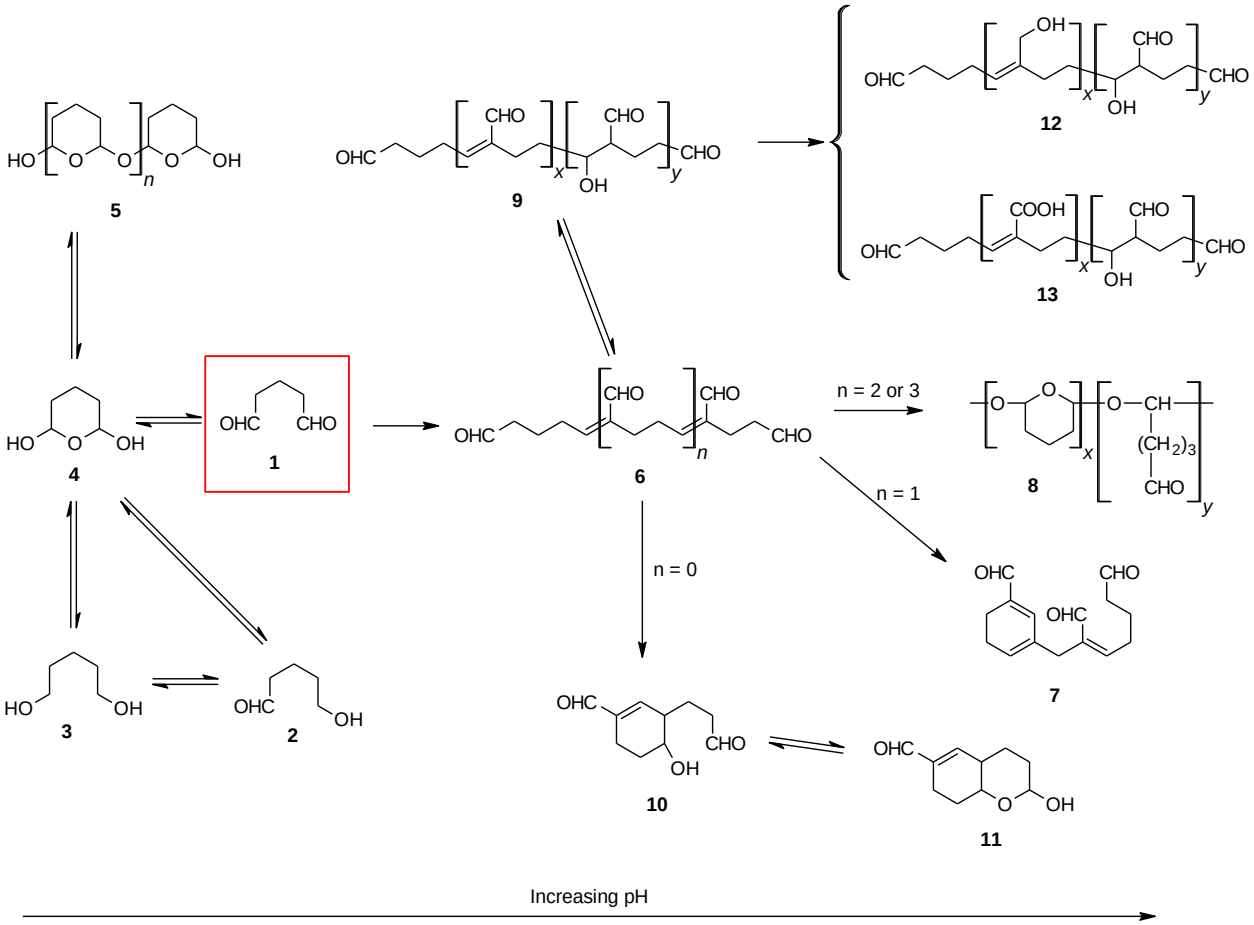

Figure 14: Identified forms of glutaraldehyde in aqueous solution. Adapted from Migneault et al.[80]

Since DFF is being studied as a substitute of glutaraldehyde, a more thorough characterization has been conducted in order to clarify its behaviour in aqueous environment, and to compare it with that of glutaraldehyde. The DFF used in the analysis was chemically synthesized by oxidation of HMF following a literature procedure.[105]

A first characterization of DFF was the acquisition of the ^{1}H NMR spectrum in D_2O, in order to assess its behaviour in aqueous environment and to compare it with that of glutaraldehyde. Two series of peaks can be seen in the spectrum: two signals (a and b in Figure 16) correspond to DFF, as expected, while four peaks (1 to 4 in the Figure 16) belong to its monohydrated diol. Interestingly, only one of the two aldehyde groups is hydrated to diol, as there are no signals from a hypothetic di-hydrated form (Figure 15).

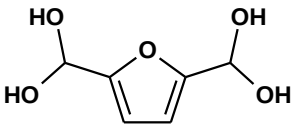

Figure 15: Dihydrated DFF derivative

The assignations were confirmed by comparison with literature.[88] NMR spectra in different, non-aqueous solvents, namely $CDCl_3$ (Figure 17), only presented signals from DFF, confirming that no impurities were present in the starting sample.

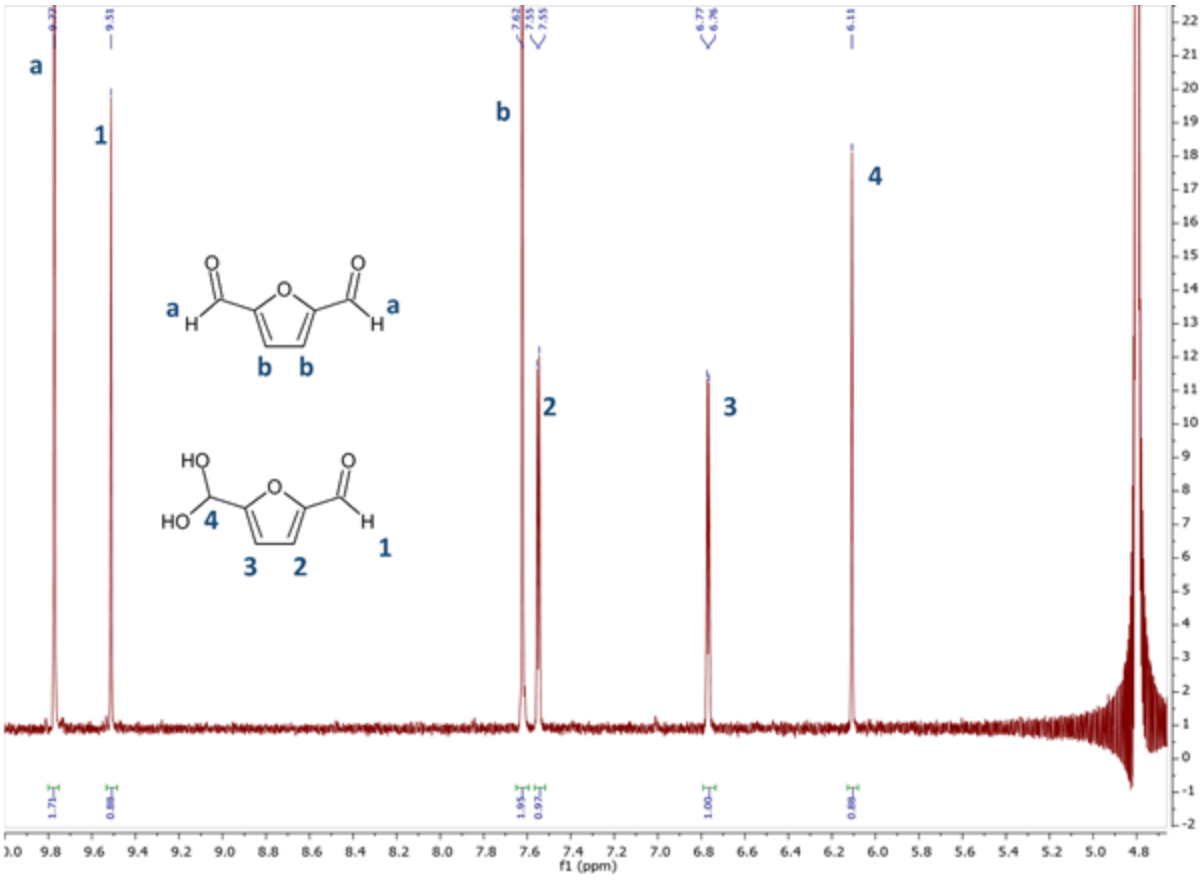

Figure 16: ^{1}H NMR spectrum of DFF in D_2O. ^{1}H NMR (400 MHz, D_2O) δ 9.77 (s, 2H), 9.51 (s, 1H), 7.62 (s, 2H), 7.55 (d, J = 3.6 Hz, 1H), 6.77 (d, J = 3.7 Hz, 1H), 6.11 (s, 1H).

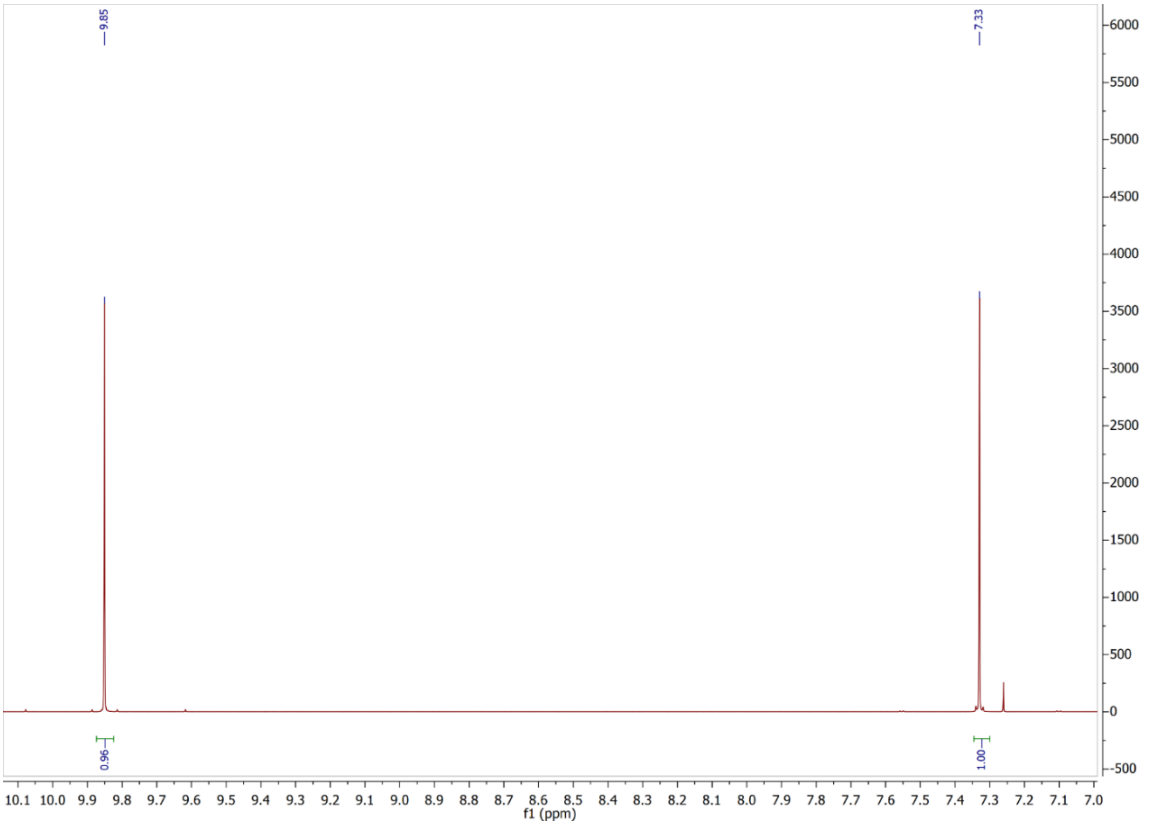

Figure 17: ¹H NMR spectrum of DFF in $CDCl_3$. ¹H NMR (400 MHz, $CDCl_3$) δ 9.85 (s, 2H), 7.33 (s, 2H).

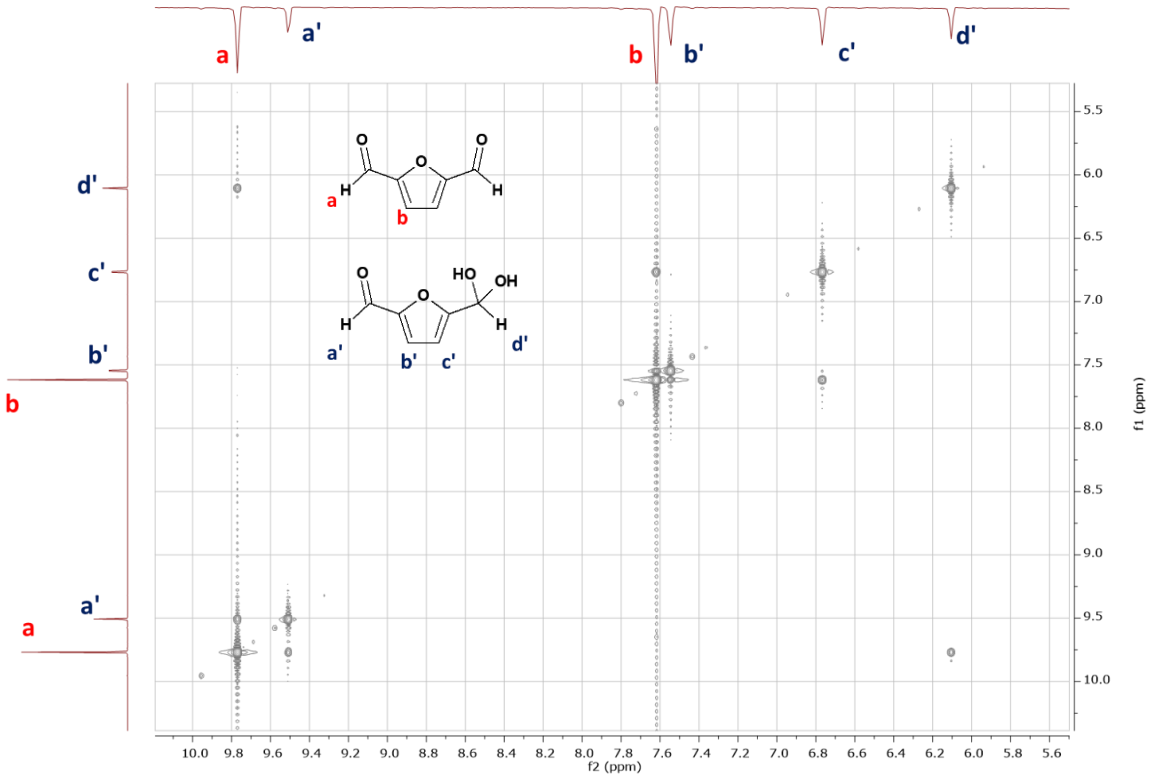

Figure 18: EXSY NMR spectrum (400 MHz, D_2O) of DFF and its mono-hydrated form.

Further NMR analysis, by means of an EXSY experiment (Figure 18) confirmed that the two forms are in equilibrium with each other (Scheme 7). UV-Vis spectroscopy experiments were not able to illustrate the equilibrium kinetics, suggesting that is reached very quickly.

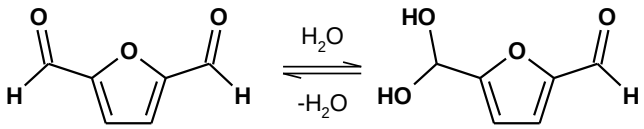

Scheme 7: Equilibrium between DFF and the mono-hydrated diol derivative

3.3.3 DFF characterization: model reaction with *n*-butylamine

The NMR spectra of DFF in D_2O evidence the presence of DFF and its mono-hydrate diolic form at equilibrium; however, no symmetric diolic form is present in solution, suggesting that DFF reactivity is asymmetrical in these conditions. Thus, it was necessary to investigate whether the reaction of DFF with amine functionalities, responsible for the covalent binding of an enzyme to an amino-functionalized carrier, can happen in a symmetrical way.

The first model reaction selected for this analysis was that of DFF with *n*-butylamine (Scheme 8), which models the lysine side chains of the protein (Figure 19), responsible of the covalent enzyme immobilization on the solid support. The conditions selected for the reaction reproduced the previously used for enzyme immobilization: potassium phosphate aqueous buffer, 0.1 M, pH 7.

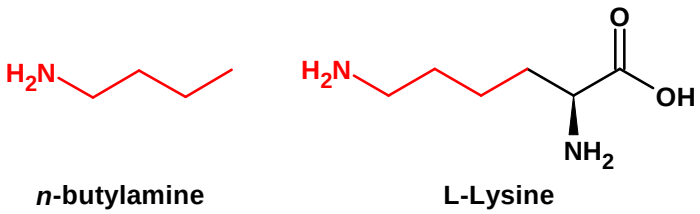

Figure 19: Chemical structures of n-butylamine and L-Lysine

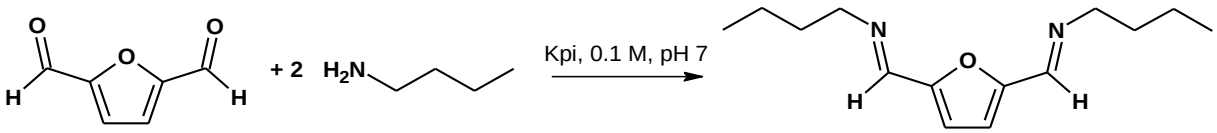

Scheme 8: Reaction between DFF and n-butylamine

In these conditions, the reaction happened almost immediately, and the formation of an oily product was observed; the product separated *in situ* from the aqueous reaction medium. The product was isolated and characterized *via* ^{1}H NMR and ^{13}C NMR (Figure 20 and Figure 21), which confirmed that the isolate product is the di-imine; the formation of a di-adduct suggests that DFF can be employed for the covalent immobilization of enzymes on a solid support.

However, the separation of the product from the reaction did not allow for the reaction to be studied over longer periods of time, and to determine whether the equilibrium was shifted towards the di-imine merely because of the precipitation of the product.

Of course, the results here reported were observed in the presence of an excess of water. As a matter of fact, DFF has a very low solubility in water (5-10 mg/mL); the solution analyzed was saturated with DFF, in order to reach conditions as close as possible to those employed for the immobilization of enzymes.

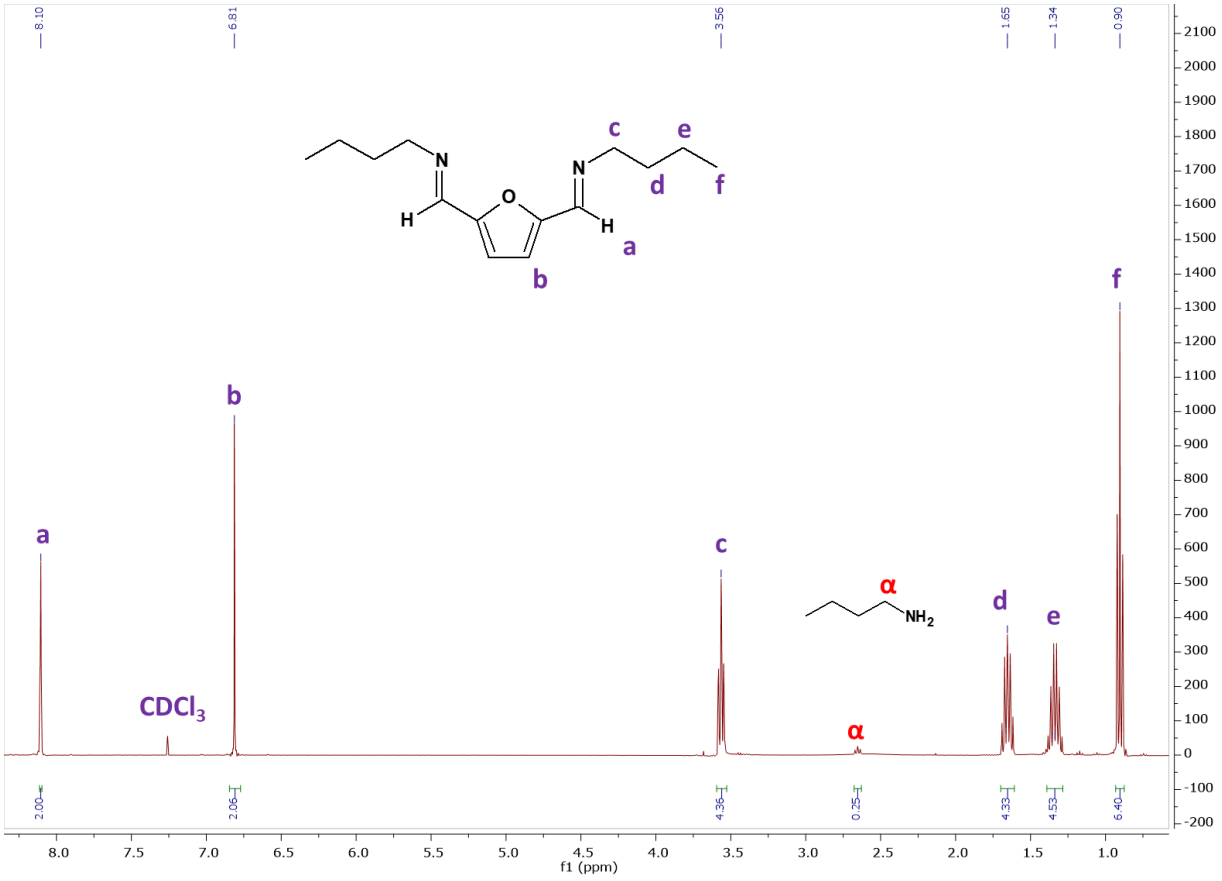

Figure 20: ^{1}H NMR spectrum of the product of reaction between DFF and n-butylamine. ^{1}H NMR (400 MHz, $CDCl_3$) δ 8.10 (d, J = 0.7 Hz, 2H), 6.81 (d, J = 0.7 Hz, 2H), 3.56 (t, J = 6.8 Hz, 4H), 1.70 – 1.61 (m, 4H), 1.34 (h, J = 7.4 Hz, 4H), 0.90 (t, J = 7.4 Hz, 6H).

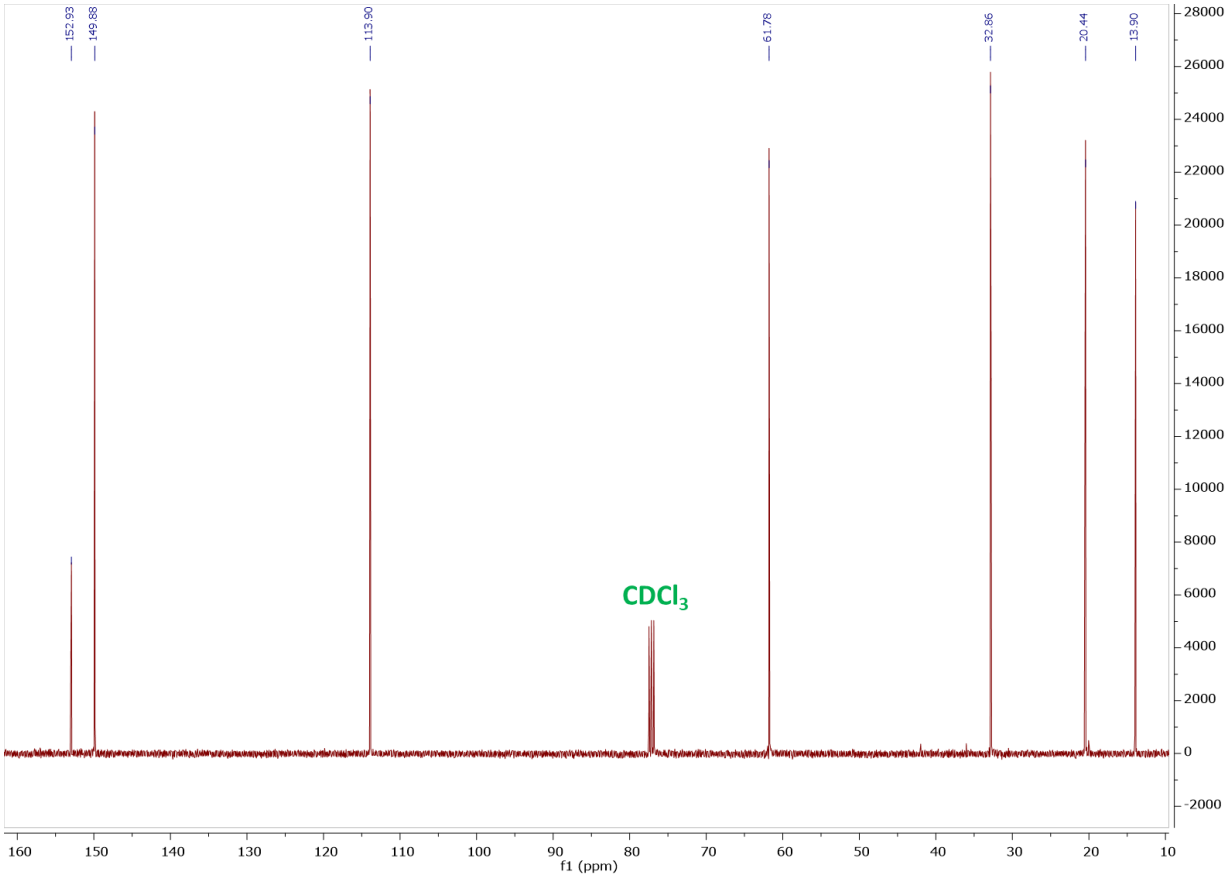

Figure 21: ^{13}C NMR spectrum of the product of reaction between DFF and n-butylamine. ^{13}C NMR (101 MHz, cdcl3) δ 152.93, 149.88, 113.90, 61.78, 32.86, 20.44, 13.90.

3.3.4 DFF characterization: reaction with isopropylamine

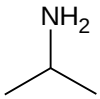

Figure 22: Isopropylamine

Studying the reactivity of DFF with amines over long reaction times is important to determine the stability of an enzyme preparation immobilized with this dialdehyde. For this reason, a new model reaction was studied, selecting isopropylamine as the model amine (Figure 22), because it forms a soluble reaction product with DFF. This allowed to monitor the reaction in solution for longer times. The reaction was conducted in potassium phosphate buffer diluted with deuterated water, in order to follow the reaction via ^{1}H NMR. The reaction was conducted in 0.1 M, pH 7 buffer, and ^{1}H NMR spectra were acquired after 1 hour, 1 day, 3 days and 1 week (see Annex for spectra).

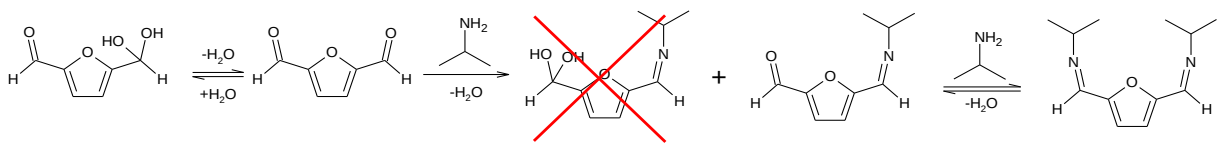

Scheme 9: Reaction of DFF with isopropylamine

After 1 hour, the reaction had already reached equilibrium, as evident by the ^{1}H NMR spectra; the spectrum acquired after 1 week of reaction is reported in Figure 23; the ratio between the mono- and di-imine is 1.22 : 1. Interestingly, the hypothetical hydrated monoimine is not present, indicating that the formation of an imine bond on one aldehyde group shifts the equilibrium of the other aldehyde group towards the non-hydrated form.

In the ^{1}H NMR spectrum, three series of peaks can be identified: there are signals from the di-imine derivative and the mono-imine derivative, as well as signals of unreacted isopropylamine (18% of the initial amount of amine is still free in solution) and no signal of residual, unreacted DFF. This shows that: (1) the formation of the products between isopropylamine, a primary amine, and DFF happens within the first hour of reaction, (2) after a long reaction time, at which the equilibrium has been reached, the only products in solution at 22°C are the imine products, (3) the di-imine product shows high stability over long storage times, not displaying the formation of side (oxidation) products.

This suggests that the immobilization of enzymes with DFF, that is conducted in similar conditions at room temperature, only involves the formation of Schiff bases between DFF and the protein, and that the resulting imine bond is stable under immobilization conditions, probably due to the conjugation of the imine bond with the furan ring and the resonance stabilization.

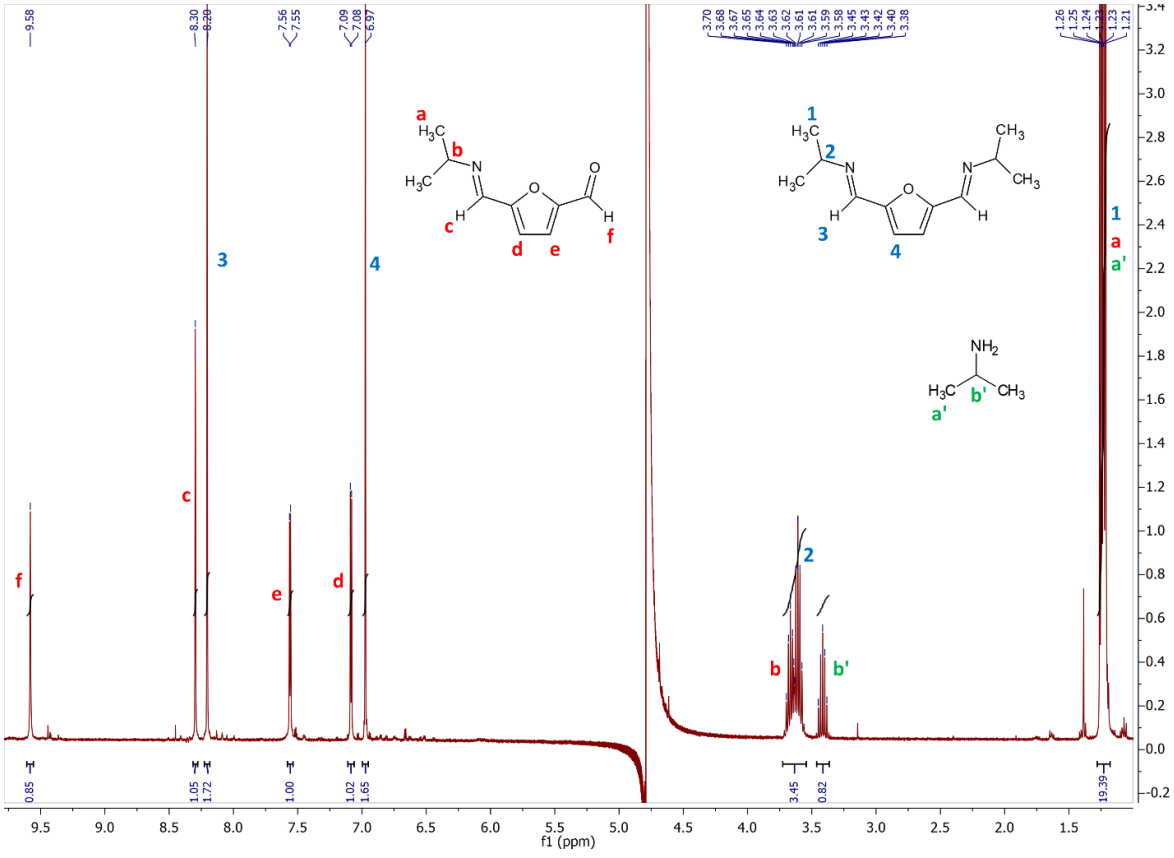

Figure 23: Presaturated ^{1}H NMR spectrum in D_2O of the reaction between DFF and isopropylamine, after 1 week of reaction. ^{1}H NMR (400 MHz, Deuterium Oxide) δ 9,58 (s, CHO), 8.30 (s, CH=N), 8.20 (s, CH=N), 7.56 (d), 7.09 (d), 6.97 (s), 3.70-3.58 (m), 3.36 (p),1.26-1.21 (m, CH_3)

3.3.5 DFF characterization: ecotoxicological studies

As mentioned in the introduction for this chapter, glutaraldehyde toxicity is well documented.[77,78] Of course, the high reported toxicity of glutaraldehyde is a consequence of the prompt reactivity of amino groups with the aldehyde functionalities of the molecule, but also with the other forms of gluraraldehyde present in equilibrium in aqueous solution.

On the contrary, the toxicity of DFF was examined only in a handful of studies.[110–112] For this reason, ecotoxicological studies were conducted to better understand the applicability of DFF in a green context and compare it to that of glutaraldehyde.

The ecotoxicological tests were performed on *Aliivibrio fischeri*, to compare the marine toxicity of DFF with that of glutaraldehyde. Tests conducted with *Aliivibrio fischeri* are highly standardized and repeatable, and for this reason it is widely used to compare the eco-compatibility of different substances.

Ecotoxicological tests were performed on *Aliivibrio fischeri*, in order to compare the marine toxicity of DFF to that of glutaraldehyde. *Aliivibrio fischeri* was chosen for the evaluation since the assay with this organism is highly standardized and repeatable, and it is therefore widely used to evaluate the eco-compatibility of chemicals.[136,137]

Inhibition of the natural bioluminescence at the maximum concentration tested is reported in the following table as a mean value, with the standard deviation expressed in %, of several replicate measures. The results were corrected according to the DMSO natural toxicity at the concentration used to solubilize the substances (0.5% DMSO in 20 g/L NaCl, ultrapure water).

Table 10: Inhibition of natural bioluminescence at the exposure time normalized compared to negative controls.

	15 min		**30 min**	
	Mean (%)	**St. Dev. (%)**	**Mean (%)**	**St. Dev. (%)**
DFF	2.31	1.13	3.76	0.32
Glutaraldehyde	0.41	0.35	4.37	0.33

The results highlighted that the toxicity of DFF is comparable to that of glutaraldehyde at the maximum dose tested of 5 mg/L. The values are close to one another, and both are lower than 5% of bioluminescence inhibition after 30 minutes of exposure (5% inhibition is the significance threshold for the measure). This further suggests that DFF can be used as a substitute for glutaraldehyde, without resulting in a significant increase in the toxicity risks of the overall immobilization process.

3.3.6 Immobilization of glucoamylase on an amino-functionalized PMMA carrier

3.3.6.1 Immobilization with glutaraldehyde

Glucoamylase (Dextrozyme GA) was successfully immobilized on an amino-functionalized PMMA carrier using glutaraldehyde as a crosslinker, using a standard protocol.

The carrier (ReliZyme HA403/M) was first activated by incubation with glutaraldehyde (200 μmol/g_{wet}) in a pH 7 phosphate buffer solution. The resulting activated carrier was washed to remove residual free glutaraldehyde and then incubated overnight with glucoamylase (120 U/g_{wet}) in a pH 7 phosphate buffer solution. The resulting immobilized enzyme preparation was washed with demineralized water and stored in the fridge in a phosphate buffer solution. A detailed procedure is reported in the Materials and Methods section for this chapter.

A preliminary activity assay was performed assessing the enzyme activity in the hydrolysis of maltose. The recovered activity resulted to be 42.3 U/g_{wet}, and the enzymatic preparation retained its activity for at least 3 batch assay cycles.

3.3.6.2 Immobilization with DFF

To verify if DFF could be used as a crosslinker for enzyme immobilization, glucoamylase (Dextrozyme GA) was immobilized on an amino-functionalized PMMA carrier using the same protocol described in the previous paragraph, but replacing glutaraldehyde with DFF.

The carrier (ReliZyme HA403/M) was incubated with DFF (200 μmol/g_{wet}) in a pH 7 phosphate buffer solution. The resulting activated carrier was washed to remove residual free DFF, and then incubated overnight with glucoamylase (120 U/g_{wet}) in a pH 7 phosphate buffer solution. The resulting preparation was analyzed with the standard glucoamylase activity assay, to determine if the enzyme was successfully immobilized on the carrier.

The resulting activity of the preparation was of 43.6 U/g_{wet}, and retained its activity for at least three hydrolytic assay cycles. These results are comparable with that obtained in the immobilization with glutaraldehyde as a difunctional agent, and are summarized in Table 11.

Table 11: Results of the proof of concept immobilization experiments of glucoamylase on PMMA carrier

Crosslinker	Crosslinker amount (μmol/g_{wet})	Enzyme loading (U/g_{wet})	Recovered activity (U/g_{wet})
Glutaraldehyde	200	120	42.3
DFF	200	120	43.6

These encouraging results pointed to the viability of DFF as a difunctional agent for covalent enzyme immobilization. Given these preliminary data, a systematic comparison of the two immobilization protocols (with glutaraldehyde and with DFF) was planned. This involved: (a) the determination of the concentration of

aldehyde groups on the activated carrier and (b) a systematic comparison of the stability of the enzymatic preparation with different amounts of crosslinker used in the carrier activation step.

3.3.7 Comparison of DFF and glutaraldehyde –Decrease in crosslinker amount

To further compare the behaviour of the two dialdehydes, four different concentrations of each dialdehyde were used for enzyme immobilization. To do this, the amino-functionalized PMMA carrier ReliZyme HA403/M was firstly incubated with different concentrations of each dialdehyde (0.2, 2, 20 and 200 $\mu mol_{aldehyde}/g_{wet\ carrier}$). The resulting activated carriers were then incubated with the same amount of enzyme (120 $U/g_{wet\ carrier}$), and the resulting enzymatic preparations were analyzed by measuring the recovered glucoamylase activity. A scheme of the experiment is reported in the Annex section for this chapter.

These experiments are meant as confirmation of the crucial data concerning the direct comparison of glutaraldehyde and DFF as cross-linkers, using a more extended analytical procedure. The recovered activity measures were performed over four batch activity assay cycles, in order to confirm a constant specific activity eliminating the contribution of leachable enzyme. The following table summarizes the recovered activity for all samples, as well as the aldehyde concentration used in the activation step.

Table 12: Measured recovered activity for glucoamylase covalently immobilized on a PMMA carrier using decreasing concentrations of DFF and glutaraldehyde in the carrier activation step.

Crosslinker amount	**Glutaraldehyde**		**DFF**	
(μmol/g carrier)	**Assay cycle**	**Activity (U/g_{dry})**	**Assay cycle**	**Activity (U/g_{dry})**
200	**1**	105.37	**1**	136.92
	2	89.69	**2**	106.78
	3	86.01	**3**	107.08
	4	87.46	**4**	107.39
20	**1**	213.75	**1**	124.15
	2	120.80	**2**	89.59
	3	107.38	**3**	82.62
	4	89.59	**4**	79.51
2	**1**	169.52	**1**	118.48
	2	119.83	**2**	96.49
	3	76.64	**3**	69.68
	4	76.38	**4**	65.73
0.2	**1**	112.92	**1**	118.94
	2	84.05	**2**	94.64
	3	76.74	**3**	77.35
	4	75.34	**4**	72.83

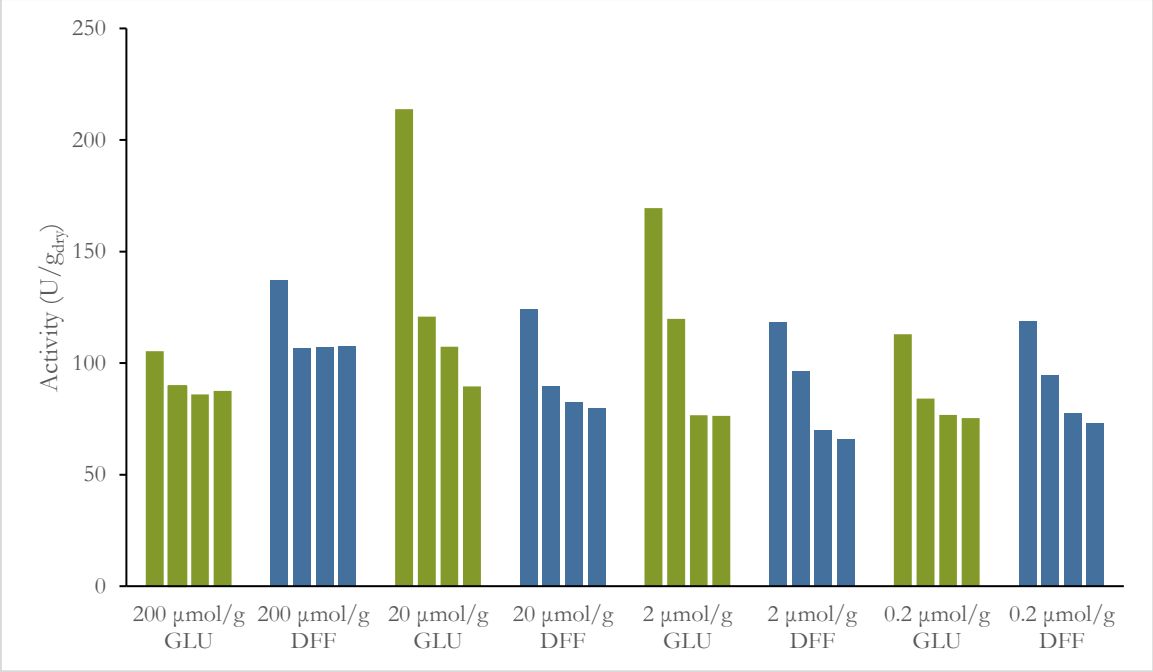

Figure 24: Measured recovered activity for glucoamylase covalently immobilized on a PMMA carrier using decreasing concentrations of DFF and glutaraldehyde in the carrier activation step for four consecutive cycles

As stated above, the activity was measured over four consecutive cycles, performed during 2 hours at a temperature of 25°C. More importantly, the enzyme was washed by resuspending the preparation in demineralized water and shaking it over the course of 10 minutes, in order to remove residual glucose on the surface of the polymeric beads. Therefore, the enzyme was subject to a certain stress, but still remained active in the assay conditions.

From the results, it is evident that the immobilized activity remains similar throughout a wide range of cross-linker concentration, ranging from 200 to 0.2 µmol/$g_{carrier}$. Moreover, the immobilized activities are very similar for the two tested crosslinkers, glutaraldehyde and DFF. These observations confirm the conclusions in the previous two quarterly reports:

1. The efficiency of each crosslinker remains very similar throughout all the samples, as decreasing the crosslinker amount does not give a remarkable decrease in the measured recovered activity.
2. The behavior of the two crosslinking agents for the covalent immobilization of glucoamylase is very similar.

3.3.8 Application of the DFF-immobilized glucoamylase preparations in a continuous flow setting

The operational stability of glucoamylase immobilized on a PMMA carrier using either DFF or glutaraldehyde was analyzed in a continuous flow experiment, over the course of 10 days. The enzyme samples used for the experiment are those immobilized with 0.2 µmol$_{aldehyde}$/$g_{wet\ carrier}$.

150 mg of immobilized enzyme sample were introduced in a 10 mL glass column. During the course of the experiment, a constant flow of substrate solution was pumped through the column at a rate of 0.15 mL/minute. The substrate solution is a 25% maltose in 10 mM citrate buffer (pH 4.5); maltose is hydrolyzed to glucose by the enzyme, as shown in Scheme 10.

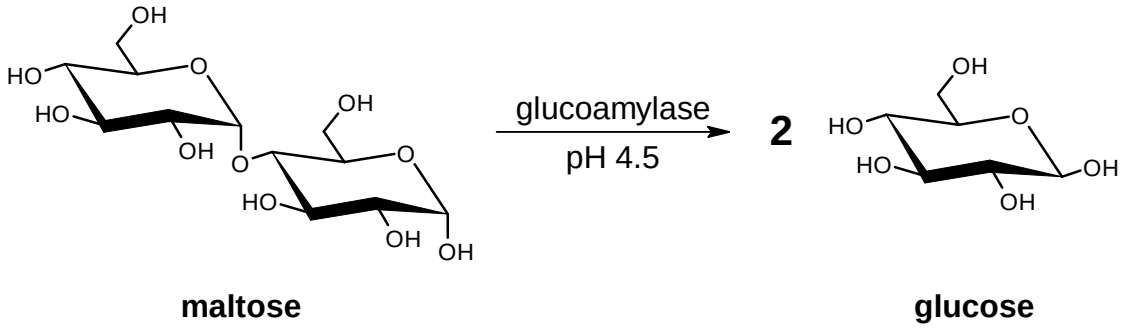

Scheme 10: Hydrolysis of maltose catalyzed by glucoamylase

The reaction was monitored for 14 days at 25°C, collecting samples of the effluent. At the end of the experiment, the effluent samples were analyzed to determine:

- Glucose concentration, determined with an enzymatic colorimetric assay
- Enzyme leaching, evaluated by using a highly sensitive enzymatic activity assay.

After the experiment, the enzymatic preparation was recovered and dried under high vacuum to express all results relating to dry enzyme preparation weight.

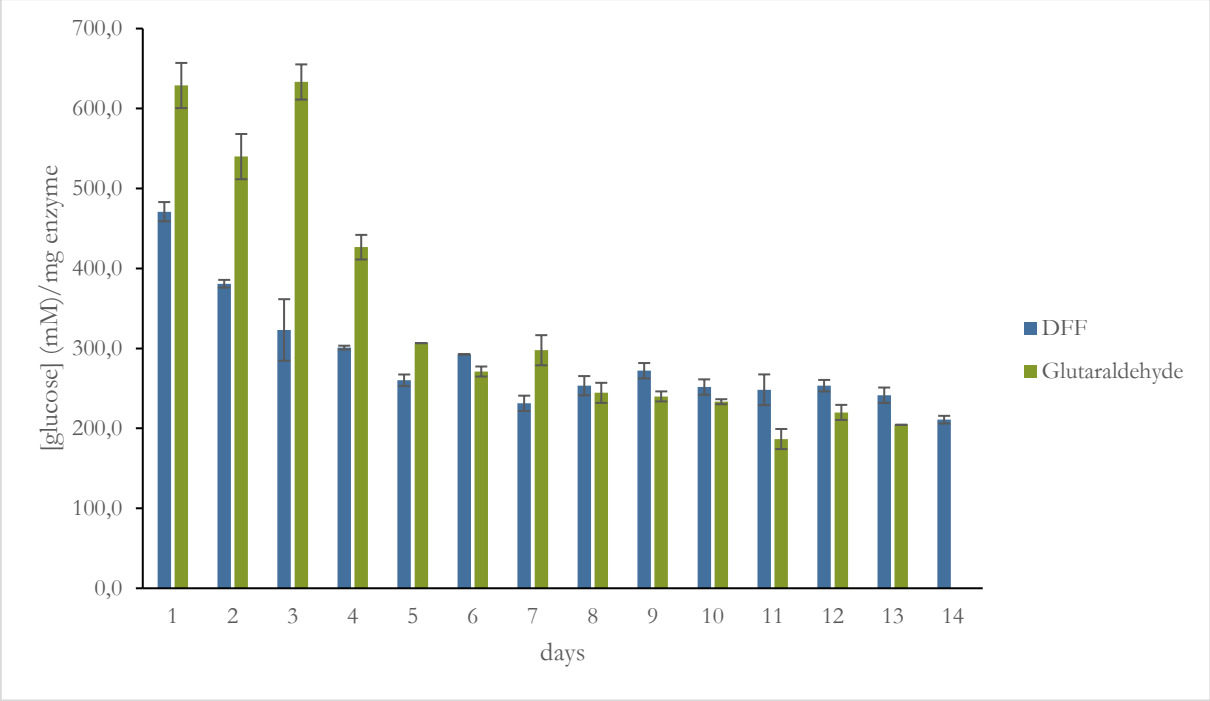

Figure 25: Glucose concentration per mg of dry enzyme preparation in the effluent of the continuous flow column experiment for glucoamylase immobilized with 0.2 µmol/$g_{carrier}$ of glutaraldehyde (in green) and DFF (in blue).

As can be seen in Figure 25, the glucose concentration in the effluent decreases in the first 4 days, stabilizing for later measurement days. This trend is comparable between the samples immobilized with the two crosslinkers, and is confirmed by the leaching measures (Figure 26), which show enzyme leaching in the first four days of the continuous assay column.

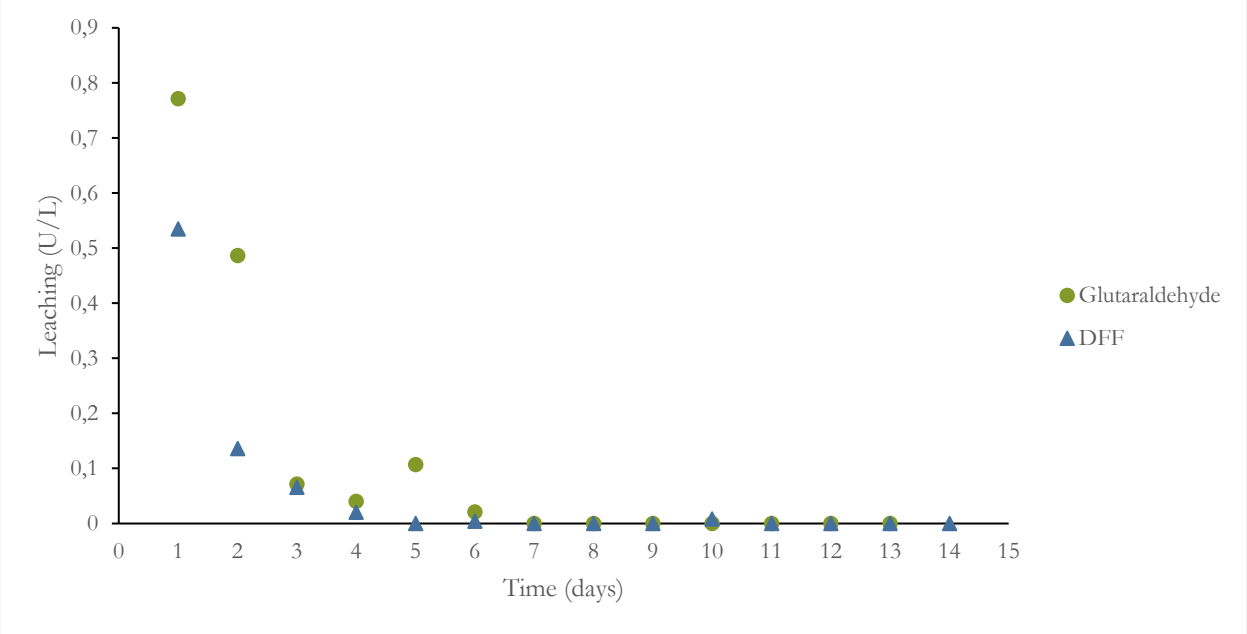

Figure 26: Protein leaching in the effluent of the continuous flow column experiment for glucoamylase immobilized with 0.2 µmol/$g_{carrier}$ of glutaraldehyde (in green circles) and DFF (in blue triangles)

The data obtained with the continuous flow experiment further confirm a similar behaviour between glutaraldehyde and DFF for the covalent immobilization of glucoamylase on the selected PMMA carrier.

3.4 Conclusions

Chapter 3 reports the investigations towards the properties of DFF as a potential "greener" alternative for glutaraldehyde. In order to be considered a suitable replacer, DFF should (a) have a similar performance to glutaraldehyde in the intended applications, (b) be safer to handle, (c) have production routes which adhere to the principles of green chemistry, (d) have a sufficiently low cost, to make the intended application economically sustainable, and (e) comply to regulations.

Paragraphs 3.3.6, 3.3.7 and 3.3.8 clearly show that DFF has similar performances as glutaraldehyde when used for the immobilization of enzymes on amino-functionalized polymeric carriers. The performance is confirmed even when using a very low concentration of dialdehyde for the immobilization. Moreover, the continuous flow experiment described in paragraph 3.3.8 shows that both crosslinkers gave stable biocatalysts, which did not display the leaching of the enzyme from the solid support. Therefore, it can be assumed that DFF can be considered as a viable alternative to glutaraldehyde also for other applications, such as the fixation of tissue material.[138]

At the present moment, it is difficult to define the safety of handling DFF as compared to glutaraldehyde. This is simply because the amount of data concerning DFF toxicity are very limited when compared to glutaraldehyde, which has a long history of large-scale use. The marine ecotoxicity study described in paragraph 3.3.5 evidenced no relevant toxicity, but it was only a preliminary study. Moreover, no long-term toxicity study is available at the time of writing this thesis.

However, it is important to underline that glutaraldehyde has a well documented environmental and occupational toxicity. Its detrimental effects are strictly linked to its high volatility, which makes it easily inhaled; the inhalation causes severe respiratory sensitization. There are a plethora of detrimental effects correlated with glutaraldehyde exposure.[77] On the other hand, DFF is solid at room temperature, therefore it has a smaller presence in the environment when used at larger scale, such as in an industrial setting.

Concerning the production of DFF, it can be considered greener because it is obtainable from biomass, and more specifically from HMF oxidation. Looking for sustainable biocatalysed oxidation processes, screening work showed that several biocatalysts, either isolated enzymes or whole cells, were able to selectively oxidize HMF to DFF without over-oxidation to FDCA. This proof of concept forms a solid basis for further development of a green oxidation process of HMF.

Currently, DFF is an expensive compound, as it is only available on a small scale for research purposes. The same applies to HMF, which is expensive when purified. Crude HMF, as obtained by heating a sugar solution under pressure in the presence of a catalyst, is not available on the market as it is directly further processed to FDCA. Further studies for the development of an industrial-scale, low-cost synthesis of HMF and DFF are needed, and the biocatalytic route briefly explored in paragraph 3.3.1 is definitely an attractive one. However, the development of such a synthesis technology is beyond the scope of this thesis.

It should be noted that an industrial use of DFF on large scale (> 1 ton/year in the EU) can only be possible if it is properly registered according to REACH regulations. The cost related to the toxicity testing required for the registration must be justified by the envisioned use. For moderate use, e.g. as an industrial enzyme crosslinker, the annual demand might be below these thresholds, so its production and use could be considered with reduced regulatory demands.

In conclusion, DFF was demonstrated to be a technical equivalent to glutaraldehyde for enzyme immobilization. DFF was shown to have a simpler chemical behaviour in water than glutaraldehyde, enabling a better understanding of the chemical nature of the enzyme immobilization.

Finally, preliminary toxicity data do not indicate that DFF has an unexpectedly high toxicity compared to glutaraldehyde, and its low volatility might make this compound much less harmful for the human respiratory system at long term exposure.

3.5 Materials and methods

3.5.1 Materials

2,2,6,6-tetramethyl-1-piperidinyloxy, free radical (TEMPO), (CAS: 2564-83-2), **2,2'-azino-bis(3-ethylbezothiazoline-6-sulfonic acid) (ABTS)** (CAS: 28752-68-3), **5-(hydroxymethyl)furfural (HMF)**, ≥99%, food grade (CAS: 67-47-0), **D-glucose**, (CAS 500-99-7), **ethanol** (absolute, ≥99.8%) (CAS: 64-17-5), **glutaraldehyde**, 25% w/w solution in water (CAS: 111-30-8), **hydrogen peroxide 30% solution**, (CAS: 7777-84-1), **HCl**, 37% in water (CAS: 7647-01-0), **isopropyl ether** (CAS: 108-20-3), **KH_2PO_4** (CAS 7778-77-0), **K_2HPO_4** (CAS: 7758-11-4), **NaCl** (CAS 7647-14-5), **NaOH** (CAS: 7757-82-6), ***p*-nitrophenol** (CAS: 100-02-7), ***p*-nitrophenyl-α-D-glucopyranoside** (CAS: 2492-87-7), **potassium permanganate** (CAS: 7722-64-7), **sodium sulfate (anhydrous)** (CAS: 7757-82-6) and **toluene** (CAS: 108-88-3) were purchased from Sigma Aldrich.

Citric acid (CAS 77-92-9) was purchased from Fischer Scientific.

D-maltose monohydrate (CAS 6363-53-7) and **dimethylsulfoxide (DMSO)** >99.0% (CAS: 67-68-5) were purchased from TCI Europe.

Diethyl ether (CAS 60-29-7), **ethyl acetate** (CAS: 141-78-6) and **petroleum ether 40-60** (CAS 8032-32-4) were purchased from VWR Chemicals International.

KBr (CAS 7758-02-3) and ***n*-butylamine** (CAS: 109-73-9) were purchased from JT Baker.

K_2CO_3 (CAS 584-08-7) was purchased from Carl Roth.

3.5.2 Biocatalysts

Alcohol oxidase from *Pichia pastoris*, buffered aqueous solution, (activity: 32 U/mg protein; protein concentration: 47 mg/mL) was purchased from Sigma Aldrich. **Aryl alcohol oxidase** was an internal reagent, kindly donated by ViaZym B.V. **Catalase from *Micrococcus lysodeikticus***, liquid (declared activity: 16600 U/mL) was purchased from Sigma Aldrich. **Galactose oxidase from *Dactylium dendroides***, lyophilized powder (declared activity: 23950 U/g solid) was purchased from Sigma Aldrich **Glucoamylase from *Aspergillus niger***, liquid solution (Dextrozyme GA, activity according to the assay presented later: 240 U/g, protein content: 83 mg/mL) was from Novozymes (Denmark). **Laccase from *Trametes versicolor*,** lyophilized powder (declared activity: 12 U/g) was purchased from Sigma Aldrich. **Peroxidase from Horse Radish**, type II, essentially salt free, lyophilized powder (declared activity: 199 U/mg solid) was purchased from Sigma Aldrich. **Wild-type *Pichia pastoris*** whole cells (strain X-33) were purchased from ThermoFisher and fermented by Biosphere S.r.l.

3.5.3 Carriers

Relizyme HA403/M was purchased from Resindion (Binasco, Milano); Lot IP18-061. Product features as from the producer: matrix poly(methylmethacrylate); functional group hexamethyleneamino; ion exchange

capacity min 600 μmol/g_{wet}; median pore diameter 40-60 nm; water retention 60-70%; particle size range 200-500 μm.

3.5.4 NMR Characterization

NMR Spectra were acquired with a JEOL 60 MHz MY-NMR spectrometer, a Varian 400 (400 MHz) and a Varian 500 (500 MHz). Deuterated solvents, $CDCl_3$, DMSO-d_6 and D_2O, were purchased from Eurisotop and Sigma Aldrich.

3.5.5 Other equipment

Roti-Spin Mini-10 columns were purchased from Carl Roth. Samples were centrifuged in a Heraeus Biofuge 13 centrifuge. UV-Vis spectra were acquired with a PerkinElmer Lambda 2 UV/Vis Spectrophotometer, connected to a data acquisition/switch unit Agilent 34972A, and a Shimadzu UV-2450. pH measures were conducted with a Metrohm 632 pH-meter, equipped with a VWR SJ225 pH electrode. Continuous flow experiments were conducted using a Supelco C3794 glass column (Luer Lock, Non-jacketed, bed volume 8 mL, I.D. × L 1.0 cm × 10 cm) connected to a Metrohm 665 Dosimat pump. The commercial kit for the concentration of acetaldehyde was the K-ACHYD Acetaldehyde Assay Kit from Megazyme.

3.5.6 Chemical oxidation of HMF to DFF

5 g of HMF were solubilized in 80 mL of DMSO. After complete solubilization, 1.42 g of KBr were added to the reaction mixture. The mixture was heated at 150°C in an oil bath for 6 hours. The course of the reaction was monitored *via* TLC analysis (eluent: petroleum ether/ethyl acetate 50:50 v/v).

The reaction mixture was cooled down to room temperature, then diluted 1:1 with water. The mixture was subsequently extracted with diethyl ether 6 times. The reunited organic phases were washed with small quantities of brine, then dried on Na_2SO_4. After removal of the sodium sulphate, the organic phase was evaporated under reduced pressure. The product was obtained as a white solid.

3.5.7 Screening for the enzymatic oxidation of HMF to DFF

The reactions were carried out in 5 mL vials, in the presence of 2 mL of the appropriate buffer. In each vial were introduced about 25 mg of substrate (HMF). After dissolving the substrate in the buffer, the corresponding quantity of each enzyme was added to the vial; in some cases, catalase was also added to the mixture in order to remove hydrogen peroxide formed in the reaction, which can inactivate the oxidative enzyme. The procedures are detailed as following and summarized in Table 13.

3.5.7.1 Screening reaction 1 – Galactose oxidase from Dactylium dendroides

25 mg of HMF were dissolved in 2 mL of KPi aqueous buffer (100 mM, pH 6.0). Then, 5.4 mg of galactose oxidase from *D. dendroides*, followed by 10 μL of catalase commercial solution (Sigma Aldrich) were added to the reaction mixture. The reaction mixture was kept under magnetic stirring at 25°C for 60 hours and monitored by TLC analysis (see procedure below).

3.5.7.2 Screening reaction 2 – Laccase from Trametes versicolor

25 mg of HMF were dissolved in 2 mL of KPi aqueous buffer (100 mM, pH 6.0). Then, 50 mg of laccase were added to the reaction mixture. The reaction mixture was kept under magnetic stirring at 25°C for 60 hours and monitored by TLC analysis (see procedure below).

3.5.7.3 Screening reaction 3 – Aryl Alcohol Oxidase

25 mg of HMF were dissolved in 2 mL of KPi aqueous buffer (100 mM, pH 6.0). Then, 50 µL of aryl alcohol oxidase preparation were added to the reaction mixture. The reaction mixture was kept under magnetic stirring at 25°C for 60 hours and monitored by TLC analysis (see procedure below).

3.5.7.4 Screening reaction 4 – Peroxidase from horse radish

25 mg of HMF were dissolved in 2 mL of KPi aqueous buffer (100 mM, pH 6.0). Then, 10 mg of peroxidase powder were added to the mixture, together with 0.1 mmol of H_2O_2. The reaction mixture was kept under magnetic stirring at 25°C for 60 hours and monitored by TLC analysis (see procedure below).

3.5.7.5 Screening reaction 5 – Alcohol oxidase from Pichia pastoris

25 mg of HMF were dissolved in 2 mL of KPi aqueous buffer (100 mM, pH 7.5). Then, 50 µL of alcohol oxidase commercial preparation were added to the reaction mixture, together with 10 µL of catalase. The reaction mixture was kept under magnetic stirring at 25°C for 70 hours and monitored by TLC analysis (see procedure below).

3.5.7.6 Screening reaction 6 – Laccase from Trametes versicolor with mediator (TEMPO)

25 mg of HMF were dissolved in 2 mL of sodium citrate aqueous buffer (50 mM, pH 5.0). Then, 50 mg of laccase were added to the reaction mixture, together with 5 mg of TEMPO mediator. The reaction mixture was kept under magnetic stirring at 25°C for 76 hours and monitored by TLC analysis (see procedure below).

3.5.7.7 TLC analysis of the screening enzymatic reactions

The reactions were followed by TLC analysis (eluent: diethyl ether 100%, stain: potassium permanganate acid solution), comparing the samples with reference solutions of HMF and DFF in diethyl ether.

TLC sample preparation: 100 µL of reaction mixture were transferred in an Eppendorf vial and extracted with 300 µL of diethyl ether. After extraction, the samples were centrifuged for 2 minutes at 1000 rpm to properly separate the two phases. The supernatant organic phase was then spotted on the TLC plates for the analysis.

Table 13: Summary of the reaction condition for the screening of the biocatalytic oxidation of HMF to DFF

Reaction	Enzyme	pH	Buffer	[buffer] (mM)	Enzyme quantity	Catalase	H_2O_2	TEMPO	Time (h)
1	GaOx	6.0	Phosphate	100	5.4 mg	10 µL	–	–	60
2	Lac	6.0	Phosphate	100	50 mg	–	–	–	60
3	AAOx	6.0	Phosphate	100	50 µL	–	–	–	60
4	HRP	6.0	Phosphate	100	10 mg	–	0.1 mmol	–	60
5	AOx	7.5	Phosphate	100	50 µL	10 µL	–	–	70
6	Lac	5.0	Citrate	50	50 mg	–	–	5 mg	76

3.5.8 Oxidation of HMF to DFF with alcohol oxidase – Reference reaction

50 mg of HMF were dissolved in 4 mL of potassium phosphate aqueous buffer (0.1 M, pH 7). Then, 50 µL of AOx solution (82 U) and 10 µL of catalase solution (166 U) were added to the system. The reaction was left shaking at 25°C for 48 h and followed by with TLC (eluent: diethyl ether 100%, stain: potassium permanganate acid solution).

The mixture was then extracted with Et_2O until no more product or reactant were detected in the aqueous phase (TLC). The reunited organic phases were evaporated under reduced pressure, and the raw product was analyzed by ^{1}HNMR.

3.5.9 Biocatalytic oxidation of ethanol with *Pichia pastoris* whole cells

100 mg of *Pichia pastoris* lyophilized cells were suspended in 4.75 mL of KPi (0.1 M, pH 7), to a final concentration of cells of 20 g/L.[135] Then, 0.25 mL of ethanol were added to the reaction system. The reaction was left shaking on the orbital shaker (350 rpm) for 24 hours at 25°C. At the end of the reaction, the mixture was centrifuged (7000 rpm, 10 minutes) to separate the cells and stop the reaction. The supernatant was analyzed with a commercial acetaldehyde concentration assay (Megazymes) to determine the product concentration.

3.5.10 Biocatalytic oxidation of HMF to DFF with *Pichia pastoris* whole cells

3.5.10.1 Without cell lysis

500 mg of *Pichia pastoris* lyophilized cells were suspended in 25 mL of KPi (0.1 M, pH 7), to a final cell concentration of 20 g/L. Then, 125 mg of HMF were added to the reaction mixture, to a concentration of 5 g/L. The flask was covered with a cotton plug, to prevent spilling of the solution and at the same time allow oxygen circulation. The flask was then shaken in an incubator at 30°C, 150 rpm for 72 hours. The reaction was followed by TLC analysis (eluent: 100% Et_2O) to detect the formation of the product, DFF.

3.5.10.2 With cell lysis

80 mg of *Pichia pastoris* lyophilized cells were suspended in 4 mL of KPi (0.1 M, pH 7), to a concentration of 20 g/L. The cells were then sonicated for 5 minutes.

Then, 20 mg of HMF were added to the reaction mixture, to a concentration of 5 g/L. The mixture was then shaken in an incubator at 30°C, 150 rpm for 72 hours. The reaction was followed by TLC analysis (eluent: 100% Et_2O) to detect the formation of the product, DFF.

3.5.10.3 In biphasic reaction system – Solvent/KPi ratio 50:50

50 mg of HMF were dissolved in 5 mL of KPi (0.1 M, pH 7). For each reaction, 125 µL of HMF aqueous solution were introduced in a 1.5 mL Eppendorf vial; then, 1.25 mg of lyophilized *Pichia pastoris* whole cells were added to the vial. Finally, 125 µL of organic cosolvent (toluene, isopropyl ether, or ethyl acetate) were added to the mixture. The final volume is 250 µL, the final cell concentration is 5 g/L and the final substrate concentration is 5 g/L.

The reaction mixtures were incubated in a thermomixer at 30°C, 800 rpm and followed by TLC analysis for 72 hours. For the TLC, a sample of both the organic and aqueous phase was spotted on the plate. The eluent was 100% Et_2O.

3.5.10.4 In biphasic reaction system – Solvent/KPi ratio 95:5

50 mg of HMF were dissolved in 0.5 mL of KPi (0.1 M, pH 7). For each reaction, 12.5 µL of HMF aqueous solution were introduced in a 1.5 mL Eppendorf vial; then 1.25 mg of lyophilized *Pichia pastoris* whole cells were added to the vial. Finally, 237.5 µL of organic cosolvent (toluene, isopropyl ether, or ethyl acetate) were added to the mixture. The final volume is 250 µL, the final cell concentration is 5 g/L and the final substrate concentration is 5 g/L.

The reaction mixtures were incubated in a thermomixer at 30°C, 800 rpm and followed by TLC analysis for 72 hours. For the TLC, a sample of both the organic and aqueous phase was spotted on the plate. The eluent was 100% Et_2O.

Table 14: Summary of the reaction condition for the screening of the biocatalytic transformation of HMF to DFF with Pichia pastoris whole cells in biphasic reaction system. Shaking speed: 350 rpm.

	Cosolvent	Cosolvent/KPi ratio	V HMF solution (µL)	V cosolvent (µL)	mg cells	Cell conc. (g/L)	[HMF] (g/L)
1	Toluene	95:5	12.5	237.5	1.25	5	5
2	Toluene	50:50	125	125	1.25	5	5
3	Isopropyl ether	95:5	12.5	237.5	1.25	5	5
4	Isopropyl ether	50:50	125	125	1.25	5	5
5	Ethyl acetate	95:5	12.5	237.5	1.25	5	5
6	Ethyl acetate	50:50	125	125	1.25	5	5

3.5.11 Reaction of DFF with *n*-butylamine

6.2 mg of DFF (0.05 mmol) were dissolved in 1 mL of potassium phosphate buffer (0.1 M, pH 7.0). Then, 10 µL of *n*-butylamine were added to the reaction mixture. The reaction solution was stirred at 22°C for 24 hours. The formation of an oily orange precipitate was observed.

The aqueous phase was extracted with 4 × 2 mL of diethyl ether. The reunited organic phases were dried over anhydrous Na_2SO_4, then evaporated. The precipitate was dried under vacuum and analyzed *via* ^1H NMR in $CDCl_3$.

3.5.12 Reaction of DFF with isopropylamine

6.2 mg of DFF (0.05 mmol) were dissolved in 0.1 mL of potassium phosphate buffer (1 M, pH 7.0) and 0.9 mL of D_2O. The final buffer concentration is 0.1 M. Then, 8.6 µL (5.9 mg, 0.1 mmol) of isopropylamine were added to the solution. The reaction solution was stirred at 22°C for 3 days. The reaction was directly monitored by ^1H NMR after 1 hour, 5 hours, 1 day and 3 days.

3.5.13 Ecotoxicological studies

Ecotoxicological tests were performed on *Aliivibrio fischeri* (bacteria, UNI EN ISO 11348-1:2019), based on normalized methods following standardized conditions and positive controls reported by the cited methods. Tests on bacteria were performed using MICROTOX® instrument (Modern Water) and internal cultured bacterial stocks. Responses obtained in tested solutions are set respect to natural bioluminescence of tested bacteria. A solution of DMSO (0.5%) added to an aqueous NaCl solution in ultrapure water (20 g L^{-1}) was used as solvent for hydrophobic substances and tested to evaluate the natural toxicity of the solubilizing solution. Results are considered as negative control and used for the normalization of obtained results on the molecules of interest solubilized using DMSO. Scalar dilutions starting from the maximum concentration of 5 mg L^{-1} were tested. Both solubilized DFF and glutaraldehyde were tested after 15 and 30 minutes of exposure and results were normalized by the natural toxicity of DMSO-made negative controls. Natural toxicity of DMSO-made negative controls were always below 5% of bioluminescence inhibition after 30 min of exposure. To evaluate bacterial activity and responsiveness to the exposure, both negative controls (NaCl 20 g L^{-1} solution in ultrapure water) and positive controls were also performed, using 3,5-dichlorophenol at the standard concentration of 4.5 mg L^{-1}. Obtained responses on positive controls (71.3%, SD 0.5%) were included within the range of acceptability for the performed test (20–80%).

3.5.14 Immobilization of glucoamylase on PMMA carrier

10 g of carrier ReliZyme HA403/M are suspended in 16 mL of potassium phosphate buffer (25 mM, pH 7, 1.6 mL/$g_{carrier}$). Then, 200 µmol$_{dialdehyde}$/$g_{carrier}$) are added to the mixture. The mixture is shaken at 25°C for 2 hours. The supernatant is then removed, and the activated carrier is washed 3 times with 20 mL of demineralized water.

The activated carrier is resuspended in 16 mL of potassium phosphate buffer (25 mM, pH 7, 1.6 mL/$g_{carrier}$). 5 g of Dextrozyme GA (commercial glucoamylase solution; 120 U/$g_{carrier}$ referred to the initial carrier amount)

are added to the reaction mixture. The mixture is kept shaking at 25°C for 24 hours. The supernatant is then removed and tested for residual enzyme activity. The immobilized enzyme is washed 3 times with 20 mL of demineralized water.

The immobilized enzyme is stored at 4°C in potassium phosphate buffer (25 mM, pH 7).

3.5.15 Glucoamylase activity assay

The applied glucoamylase activity assay is based on the enzymatic hydrolysis of maltose to two units of glucose:

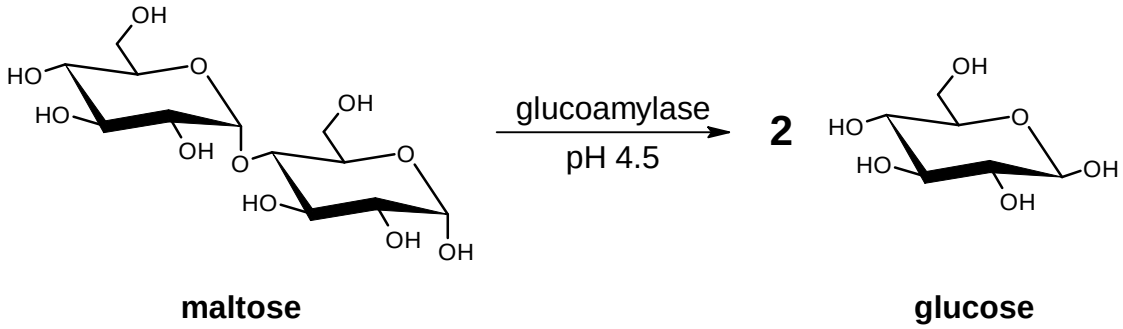

Scheme 11: Enzymatic hydrolysis of maltose to glucose

One Immobilized Glucoamylase Unit (IGU) is defined as the amount of enzyme that hydrolyses one µmol of maltose at the following conditions: 25% maltose in 10 mM citrate buffer, pH 4.5, at room temperature (20°C).

The maltose solution used in the assay is obtained by dissolving 26.3 g of D-maltose monohydrate and 0.19 g of citric acid in about 70 mL of demineralized water; the pH is then adjusted to 4.5 using 1M NaOH, and water is added to a final volume of 100 mL.

For the assay, 50 mg of immobilized glucoamylase are suspended in 5 mL of the maltose solution; the mixture is shaken at room temperature for 1 hour. Every 10 minutes, a sample (50 µL) of the supernatant is taken and diluted 10 times with 0.1 M HCl before glucose analysis.

3.5.15.1 Glucose concentration measures

The glucose concentration in the samples is measured using an enzymatic glucose assay. The glucose assay solution is obtained by dissolving 55 mg of ABTS in 50 mL of 25 mM KPi (potassium phosphate buffer); then, to the solution are added 0.2 mL of a glucose oxidase aqueous solution (1 mg/mL) and 0.2 mL of a horse radish peroxidase aqueous solution.

50 µL of the 10× diluted sample are added, in a 4 mL UV-Vis cuvette, to 2.95 mL of the glucose assay solution. The cuvette is mixed by inversion, and the absorbance at 405 nm is monitored for 5 minutes. The increase in absorbance over time is compared to that of a reference solution of 5 mM D-glucose in water. The glucose concentration in each sample is obtained by:

$$[glucose](mM) = \frac{\Delta A_{405,sample}\ (min^{-1})}{\Delta A_{405,ref}\ (min^{-1})} \times \frac{[glucose]_{ref}\ (mM)\ \times\ V_{ref}\ (mL)}{V_{sample}(mL)} \times df$$

Where:

- $\Delta A_{405,sample}$ and $\Delta A_{405,ref}$ are the variations in absorbance, in **min^{-1}**, of the sample and the reference solution, respectively.
- $[glucose]_{ref}$ is the glucose concentration of the reference solution in **mM**, here 5 mM.
- V_{ref} is the volume of reference solution used in **mL**, here 0.05 mL.
- V_{sample} is the volume of the glucoamylase solution sample in **mL**, here 0.05 mL.
- df is the dilution factor, here 10.

A negative measure is also performed by introducing 50 µL of 10× diluted maltose assay solution to 2.95 mL of the glucose assay solution and analysing it in the same way as the collected samples. The glucose concentration in the negative is then subtracted from that of all measured samples.

The glucose concentration data is then plotted in a [glucose] *vs* time graph. Using the difference in glucose concentration over time, the glucoamylase activity is calculated by:

$$Activity\ (U\ g^{-1}) = \frac{\frac{\Delta[glucose]\ (mM\ min^{-1})}{2} \times V_{assay}\ (L) \times 1000}{g_{sample}}$$

Where:

- $\frac{\Delta[glucose]\ (mM\ min^{-1})}{2}$ is the rate of maltose hydrolysis in **mM min^{-1}**.
  - $\Delta[glucose]\ (mM\ min^{-1})$ is the rate of glucose formation, which is the slope of the [glucose] vs time curve.
- $V_{assay}\ (L)$ is the volume of the assay, here 0.005 L.
- 1000 is the conversion factor from mmol to µmol.
- g_{sample} is the weight of anhydrous immobilized enzyme, in grams, used for the assay.

3.5.16 Determination of anhydrous immobilized enzyme

After the last activity assay cycle, the supernatant maltose solution is removed by decanting, and the immobilized enzyme sample is rinsed with 3×10 mL H_2O. The water is then removed, and the enzyme preparation is dried in the vacuum oven (100°C, 6 h). The weight of the anhydrous immobilized enzyme is used for the activity calculations.

3.5.17 Continuous flow experiment

150 mg of wet weight immobilized enzyme were introduced in a 10 mL glass column. The column was filled with a 25% maltose solution in 10 mM citrate buffer, pH 4.5. A continuous flow of maltose solution was supplied to the column at a rate of 0.15 mL/min over the course of 13 days. Every day, a sample (3-4 mL) of effluent was collected. Of this sample, 50 µL were immediately diluted 10 times with HCl 0.1 M, to be used for glucose concentration analysis; the rest was used for glucoamylase leaching evaluation.

At the end of the experiment, the effluent samples were analysed to determine: (1) Glucose concentration (see previous paragraph) (2) Enzyme leaching (see following paragraph). After the experiment, the enzymatic

preparation was recovered and dried under high vacuum to express all results relating to dry enzyme preparation weight.

For glucose concentration, a negative measure was performed on 50 µL of 10 times diluted maltose assay solution. The glucose concentration in the negative is subtracted from that of all measured samples.

3.5.18 Glucoamylase leaching evaluation – *p*-nitrophenyl-α-D-glucopyranoside assay

The assay used for the determination of protein leaching in the continuous flow experiment is based on the hydrolysis of *p*-nitrophenyl-α-D-glucopyranoside to glucose and *p*-nitrophenol, represented in the following figure.

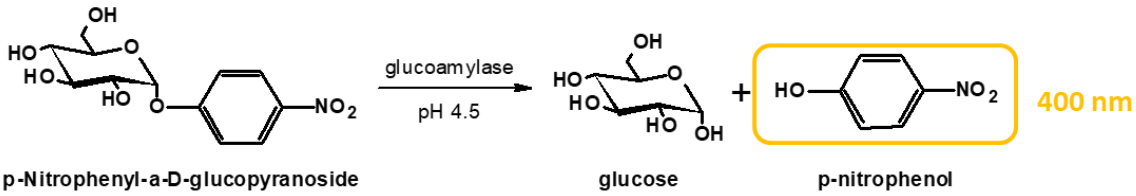

Figure 27: Hydrolysis of p-nitrophenyl-L-D-glucopyranoside to glucose and p-nitrophenol by glucoamylase

The formation of *p*-nitrophenol in the samples can be monitored by measuring the absorbance of the solution at 400 nm.

For the assay, 600 µL of effluent from the continuous flow column are concentrated to about 60 µL by placing a Roti-Spin Mini-10 column (Carl Roth) in a centrifuge at 7000 rpm for about 10 minutes. 20 µL of the concentrated sample are then mixed with 500 µL of a 1 mg/mL solution of *p*-nitrophenyl-L-D-glucopyranoside in sodium citrate buffer (0.1M, pH 4.5); the mixture is then incubated at 56°C for 4h. After incubation, 500 µL of a 0.5M potassium carbonate solution are added to the mixture. The absorbance of the final mixture at 400 nm is directly measured and compared with a *p*-nitrophenol calibration curve, to calculate the product concentration in the samples

3.5.18.1 p-nitrophenol calibration curve

A *p*-nitrophenol (Sigma-Aldrich) calibration curve was set up by measuring the absorbance at 400 nm (A_{400}) of *p*-nitrophenol standards with concentrations ranging from 0.02-0.14 mM. The different components added to each standard solution, to a total volume of 1020 µL, can be seen in the following table.

Table 15: p-nitrophenol calibration curve solutions

[4-nitrophenol] (mM)	1 mM 4-nitrophenol stock (µL)	0.5M carbonate solution (µL)	0.1M acetate buffer pH 4.5 (µL)
0.02	20.4	500	499.6
0.04	40.8	500	479.2
0.06	61.2	500	458.8
0.08	81.6	500	438.4
0.10	102.0	500	418.0
0.14	142.8	500	377.2

The measured absorbance values at 400 nm are plotted in a A_{400} *vs* [*p*-nitrophenol] (mM) graph. The slope of the graph can be used to extrapolate the *p*-nitrophenol concentration in the analyzed samples.

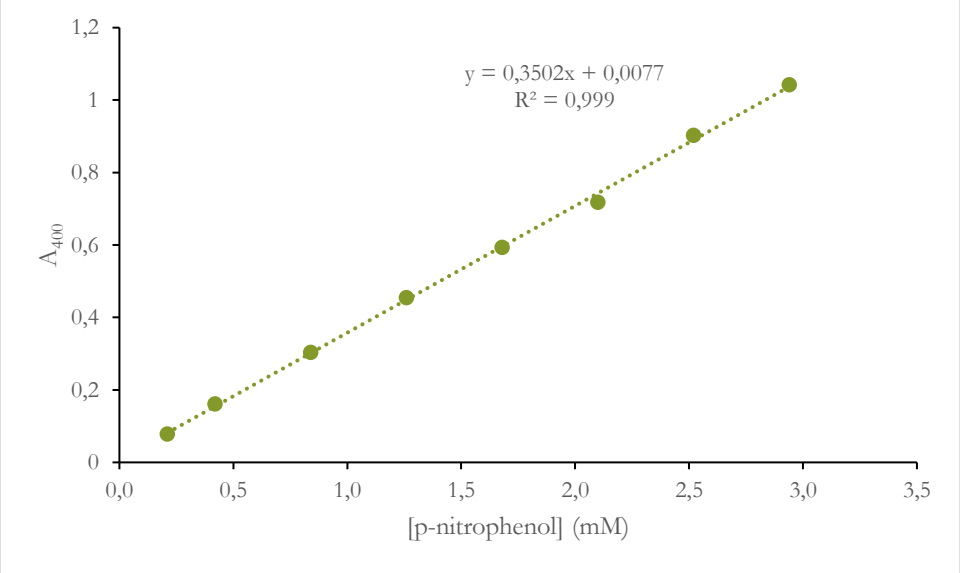

Figure 28: p-nitrophenol calibration curve

3.6 Annex

3.6.1 Glycosylation site analysis

```
Name:  Sequence          Length:  640
MSFRSLLALSGLVCTGLANVISKRATLDSWLSNEATVARTAILNNIGADGAWVSGADSGIVVASPSTDNPDYFYTWTRDS      80
GLVLKTLVDLFRNGDTSLLSTIENYISAQAIVQGISNPSGDLSSGAGLGEPKFNVDETAYTGSWGRPQRDGPALRATAMI     160
GFGQWLLDNGYTSTATDIVWPLVRNDLSYVAQYWNQTGYDLWEEVNGSSFFTIAVQHRALVEGSAFATAVGSSCSWCDSQ     240
APEILCYLQSFWTGSFILANFDSSRSGKDANTLLGSIHTFDPEAACDDSTFQPCSPRALANHKEVVDSFRSIYTLNDGLS     320
DSEAVAVGRYPEDTYYNGNPWFLCTLAAAEQLYDALYQWDKQGSLEVTDVSLDFFKALYSDAATGTYSSSSSTYSSIVDA     400
VKTFADGFVSIVETHAASNGSMSEQYDKSDGEQLSARDLTWSYAALLTANNRRNSVVPASWGETSASSVPGTCAATSAIG     480
TYSSVTVTSWPSIVATGGTTTTATPTGSGSVTSTSKTTATASKTSTSTSSTSCTTPTAVAVTFDLTATTTYGENIYLVGS     560
ISQLGDWETSDGIALSADKYTSSDPLWYVTVTLPAGESFEYKFIRIESDDSVEWESDPNREYTVPQACGTSTATVTDTWR     640
.................................................................................      80
.....................................N.........................................     160
....................................N.....N.....................................     240
.................................................................................     320
.................................................................................     400
..................N..............................................................     480
.................................................................................     560
.................................................................................     640

(Threshold=0.5)
--------------------------------------------------------------------------------
SeqName      Position  Potential    Jury    N-Glyc
                                  agreement result
--------------------------------------------------------------------------------
Sequence     117 NPSG   0.6798     (7/9)    +    WARNING: PRO-X1.
Sequence     195 NQTG   0.7102     (9/9)    ++
Sequence     206 NGSS   0.7647     (9/9)    +++
Sequence     419 NGSM   0.5491     (5/9)    +
--------------------------------------------------------------------------------
```

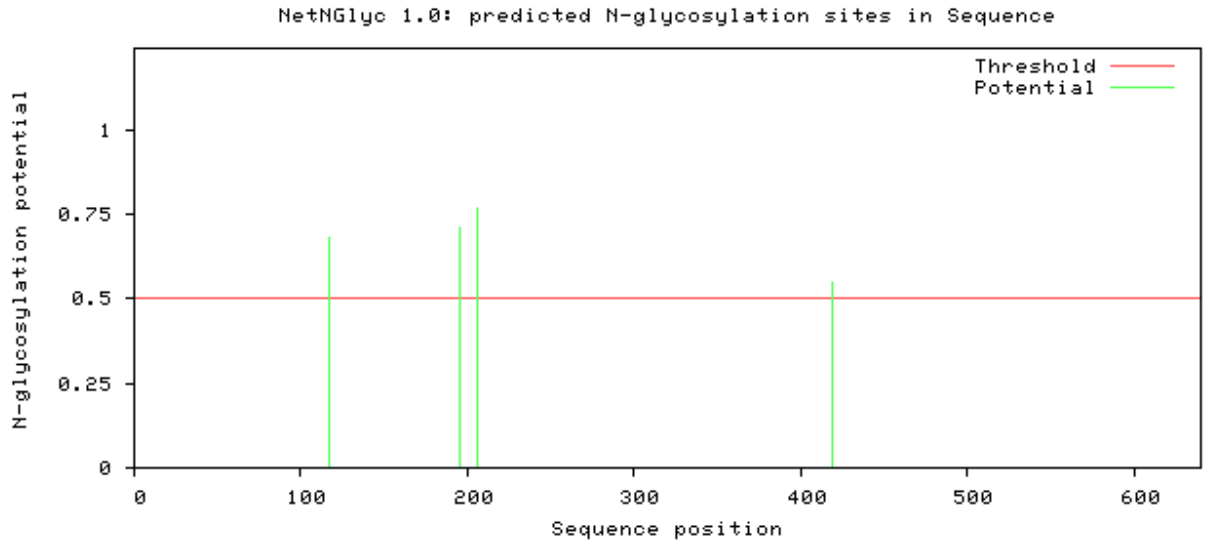

Figure 29: Analysis of the possible N-glycosylation sites in glucoamylase from A. niger. The identified N-glycosylation sites are confirmed by the crystallographic structure reported in Figure 7A.

```
##gff-version 2
##source-version NetOGlyc 4.0.0.13
##date 21-3-2
##Type Protein
#seqname        source  feature start   end     score   strand  frame   comment
SEQUENCE        netOGlyc-4.0.0.13       CARBOHYD        2       2       0.0497717       .       .
SEQUENCE        netOGlyc-4.0.0.13       CARBOHYD        5       5       0.0610398       .       .
SEQUENCE        netOGlyc-4.0.0.13       CARBOHYD        10      10      0.0448418       .       .
SEQUENCE        netOGlyc-4.0.0.13       CARBOHYD        15      15      0.189139        .       .
SEQUENCE        netOGlyc-4.0.0.13       CARBOHYD        22      22      0.452708        .       .
SEQUENCE        netOGlyc-4.0.0.13       CARBOHYD        26      26      0.259396        .       .
SEQUENCE        netOGlyc-4.0.0.13       CARBOHYD        29      29      0.194924        .       .
SEQUENCE        netOGlyc-4.0.0.13       CARBOHYD        32      32      0.291853        .       .
SEQUENCE        netOGlyc-4.0.0.13       CARBOHYD        36      36      0.222524        .       .
SEQUENCE        netOGlyc-4.0.0.13       CARBOHYD        40      40      0.0810226       .       .
SEQUENCE        netOGlyc-4.0.0.13       CARBOHYD        54      54      0.0580388       .       .
SEQUENCE        netOGlyc-4.0.0.13       CARBOHYD        58      58      0.081787        .       .
SEQUENCE        netOGlyc-4.0.0.13       CARBOHYD        64      64      0.207234        .       .
SEQUENCE        netOGlyc-4.0.0.13       CARBOHYD        66      66      0.075947        .       .
SEQUENCE        netOGlyc-4.0.0.13       CARBOHYD        67      67      0.102353        .       .
SEQUENCE        netOGlyc-4.0.0.13       CARBOHYD        75      75      0.00770886      .       .
SEQUENCE        netOGlyc-4.0.0.13       CARBOHYD        77      77      0.0063052       .       .
SEQUENCE        netOGlyc-4.0.0.13       CARBOHYD        80      80      0.0118261       .       .
SEQUENCE        netOGlyc-4.0.0.13       CARBOHYD        86      86      0.0562815       .       .
SEQUENCE        netOGlyc-4.0.0.13       CARBOHYD        96      96      0.0378854       .       .
SEQUENCE        netOGlyc-4.0.0.13       CARBOHYD        97      97      0.0744493       .       .
SEQUENCE        netOGlyc-4.0.0.13       CARBOHYD        100     100     0.0263688       .       .
SEQUENCE        netOGlyc-4.0.0.13       CARBOHYD        101     101     0.0197502       .       .
SEQUENCE        netOGlyc-4.0.0.13       CARBOHYD        107     107     0.19316 .       .
SEQUENCE        netOGlyc-4.0.0.13       CARBOHYD        116     116     0.306975        .       .
SEQUENCE        netOGlyc-4.0.0.13       CARBOHYD        119     119     0.112435        .       .
SEQUENCE        netOGlyc-4.0.0.13       CARBOHYD        123     123     0.0984065       .       .
SEQUENCE        netOGlyc-4.0.0.13       CARBOHYD        124     124     0.163494        .       .
SEQUENCE        netOGlyc-4.0.0.13       CARBOHYD        138     138     0.131561        .       .
SEQUENCE        netOGlyc-4.0.0.13       CARBOHYD        141     141     0.293712        .       .
SEQUENCE        netOGlyc-4.0.0.13       CARBOHYD        143     143     0.103372        .       .
SEQUENCE        netOGlyc-4.0.0.13       CARBOHYD        157     157     0.0524689       .       .
SEQUENCE        netOGlyc-4.0.0.13       CARBOHYD        172     172     0.058872        .       .
SEQUENCE        netOGlyc-4.0.0.13       CARBOHYD        173     173     0.119033        .       .
SEQUENCE        netOGlyc-4.0.0.13       CARBOHYD        174     174     0.0869305       .       .
SEQUENCE        netOGlyc-4.0.0.13       CARBOHYD        176     176     0.212258        .       .

SEQUENCE        netOGlyc-4.0.0.13       CARBOHYD        188     188     0.0608223       .       .
SEQUENCE        netOGlyc-4.0.0.13       CARBOHYD        197     197     0.0205522       .       .
SEQUENCE        netOGlyc-4.0.0.13       CARBOHYD        208     208     0.0226382       .       .
SEQUENCE        netOGlyc-4.0.0.13       CARBOHYD        209     209     0.0401721       .       .
SEQUENCE        netOGlyc-4.0.0.13       CARBOHYD        212     212     0.087199        .       .
SEQUENCE        netOGlyc-4.0.0.13       CARBOHYD        224     224     0.379123        .       .
SEQUENCE        netOGlyc-4.0.0.13       CARBOHYD        228     228     0.420818        .       .
SEQUENCE        netOGlyc-4.0.0.13       CARBOHYD        232     232     0.0222534       .       .
SEQUENCE        netOGlyc-4.0.0.13       CARBOHYD        233     233     0.105139        .       .
SEQUENCE        netOGlyc-4.0.0.13       CARBOHYD        235     235     0.0526273       .       .
SEQUENCE        netOGlyc-4.0.0.13       CARBOHYD        239     239     0.207133        .       .
SEQUENCE        netOGlyc-4.0.0.13       CARBOHYD        250     250     0.0307423       .       .
SEQUENCE        netOGlyc-4.0.0.13       CARBOHYD        253     253     0.0479019       .       .
SEQUENCE        netOGlyc-4.0.0.13       CARBOHYD        255     255     0.0112417       .       .
SEQUENCE        netOGlyc-4.0.0.13       CARBOHYD        263     263     0.055693        .       .
SEQUENCE        netOGlyc-4.0.0.13       CARBOHYD        264     264     0.0909878       .       .
SEQUENCE        netOGlyc-4.0.0.13       CARBOHYD        266     266     0.0968192       .       .
SEQUENCE        netOGlyc-4.0.0.13       CARBOHYD        272     272     0.223033        .       .
SEQUENCE        netOGlyc-4.0.0.13       CARBOHYD        276     276     0.149954        .       .
SEQUENCE        netOGlyc-4.0.0.13       CARBOHYD        279     279     0.384829        .       .
SEQUENCE        netOGlyc-4.0.0.13       CARBOHYD        289     289     0.0642802       .       .
SEQUENCE        netOGlyc-4.0.0.13       CARBOHYD        290     290     0.056433        .       .
SEQUENCE        netOGlyc-4.0.0.13       CARBOHYD        295     295     0.553132        .       .       #POSITIVE
SEQUENCE        netOGlyc-4.0.0.13       CARBOHYD        308     308     0.123056        .       .
SEQUENCE        netOGlyc-4.0.0.13       CARBOHYD        311     311     0.135411        .       .
SEQUENCE        netOGlyc-4.0.0.13       CARBOHYD        314     314     0.129949        .       .
SEQUENCE        netOGlyc-4.0.0.13       CARBOHYD        320     320     0.0897915       .       .
SEQUENCE        netOGlyc-4.0.0.13       CARBOHYD        322     322     0.107466        .       .
SEQUENCE        netOGlyc-4.0.0.13       CARBOHYD        334     334     0.0174431       .       .
SEQUENCE        netOGlyc-4.0.0.13       CARBOHYD        345     345     0.0153931       .       .
SEQUENCE        netOGlyc-4.0.0.13       CARBOHYD        364     364     0.225336        .       .
SEQUENCE        netOGlyc-4.0.0.13       CARBOHYD        368     368     0.12658 .       .
SEQUENCE        netOGlyc-4.0.0.13       CARBOHYD        371     371     0.178361        .       .
SEQUENCE        netOGlyc-4.0.0.13       CARBOHYD        380     380     0.273538        .       .
SEQUENCE        netOGlyc-4.0.0.13       CARBOHYD        384     384     0.282868        .       .
SEQUENCE        netOGlyc-4.0.0.13       CARBOHYD        386     386     0.310319        .       .
SEQUENCE        netOGlyc-4.0.0.13       CARBOHYD        388     388     0.404647        .       .
SEQUENCE        netOGlyc-4.0.0.13       CARBOHYD        389     389     0.518046        .       .       #POSITIVE
SEQUENCE        netOGlyc-4.0.0.13       CARBOHYD        390     390     0.35701 .       .
SEQUENCE        netOGlyc-4.0.0.13       CARBOHYD        391     391     0.28299 .       .
SEQUENCE        netOGlyc-4.0.0.13       CARBOHYD        392     392     0.574814        .       .       #POSITIVE
SEQUENCE        netOGlyc-4.0.0.13       CARBOHYD        393     393     0.371562        .       .
```

Figure 30: Analysis of the possible O-glycosylation sites in glucoamylase from A. niger.

SEQUENCE	netOGlyc-4.0.0.13	CARBOHYD	395	395	0.277135	.	.	
SEQUENCE	netOGlyc-4.0.0.13	CARBOHYD	396	396	0.342668	.	.	
SEQUENCE	netOGlyc-4.0.0.13	CARBOHYD	403	403	0.0389276	.	.	
SEQUENCE	netOGlyc-4.0.0.13	CARBOHYD	410	410	0.227346	.	.	
SEQUENCE	netOGlyc-4.0.0.13	CARBOHYD	414	414	0.111214	.	.	
SEQUENCE	netOGlyc-4.0.0.13	CARBOHYD	418	418	0.3197	.	.	
SEQUENCE	netOGlyc-4.0.0.13	CARBOHYD	421	421	0.0833272	.	.	
SEQUENCE	netOGlyc-4.0.0.13	CARBOHYD	423	423	0.0374171	.	.	
SEQUENCE	netOGlyc-4.0.0.13	CARBOHYD	429	429	0.0157849	.	.	
SEQUENCE	netOGlyc-4.0.0.13	CARBOHYD	435	435	0.0368818	.	.	
SEQUENCE	netOGlyc-4.0.0.13	CARBOHYD	440	440	0.0407853	.	.	
SEQUENCE	netOGlyc-4.0.0.13	CARBOHYD	442	442	0.183605	.	.	
SEQUENCE	netOGlyc-4.0.0.13	CARBOHYD	448	448	0.0889974	.	.	
SEQUENCE	netOGlyc-4.0.0.13	CARBOHYD	455	455	0.5358	.	.	#POSITIVE
SEQUENCE	netOGlyc-4.0.0.13	CARBOHYD	460	460	0.429805	.	.	
SEQUENCE	netOGlyc-4.0.0.13	CARBOHYD	464	464	0.693643	.	.	#POSITIVE
SEQUENCE	netOGlyc-4.0.0.13	CARBOHYD	465	465	0.618343	.	.	#POSITIVE
SEQUENCE	netOGlyc-4.0.0.13	CARBOHYD	467	467	0.682241	.	.	#POSITIVE
SEQUENCE	netOGlyc-4.0.0.13	CARBOHYD	468	468	0.798299	.	.	#POSITIVE
SEQUENCE	netOGlyc-4.0.0.13	CARBOHYD	472	472	0.534929	.	.	#POSITIVE
SEQUENCE	netOGlyc-4.0.0.13	CARBOHYD	476	476	0.688825	.	.	#POSITIVE
SEQUENCE	netOGlyc-4.0.0.13	CARBOHYD	477	477	0.687779	.	.	#POSITIVE
SEQUENCE	netOGlyc-4.0.0.13	CARBOHYD	481	481	0.263251	.	.	
SEQUENCE	netOGlyc-4.0.0.13	CARBOHYD	483	483	0.416392	.	.	
SEQUENCE	netOGlyc-4.0.0.13	CARBOHYD	484	484	0.565706	.	.	#POSITIVE
SEQUENCE	netOGlyc-4.0.0.13	CARBOHYD	486	486	0.263215	.	.	
SEQUENCE	netOGlyc-4.0.0.13	CARBOHYD	488	488	0.551365	.	.	#POSITIVE
SEQUENCE	netOGlyc-4.0.0.13	CARBOHYD	489	489	0.51314	.	.	#POSITIVE
SEQUENCE	netOGlyc-4.0.0.13	CARBOHYD	492	492	0.790018	.	.	#POSITIVE
SEQUENCE	netOGlyc-4.0.0.13	CARBOHYD	496	496	0.901518	.	.	#POSITIVE
SEQUENCE	netOGlyc-4.0.0.13	CARBOHYD	499	499	0.643041	.	.	#POSITIVE
SEQUENCE	netOGlyc-4.0.0.13	CARBOHYD	500	500	0.926223	.	.	#POSITIVE
SEQUENCE	netOGlyc-4.0.0.13	CARBOHYD	501	501	0.878478	.	.	#POSITIVE
SEQUENCE	netOGlyc-4.0.0.13	CARBOHYD	502	502	0.948394	.	.	#POSITIVE
SEQUENCE	netOGlyc-4.0.0.13	CARBOHYD	504	504	0.853941	.	.	#POSITIVE
SEQUENCE	netOGlyc-4.0.0.13	CARBOHYD	506	506	0.917561	.	.	#POSITIVE
SEQUENCE	netOGlyc-4.0.0.13	CARBOHYD	508	508	0.946344	.	.	#POSITIVE
SEQUENCE	netOGlyc-4.0.0.13	CARBOHYD	510	510	0.89224	.	.	#POSITIVE
SEQUENCE	netOGlyc-4.0.0.13	CARBOHYD	512	512	0.933235	.	.	#POSITIVE
SEQUENCE	netOGlyc-4.0.0.13	CARBOHYD	513	513	0.952957	.	.	#POSITIVE
SEQUENCE	netOGlyc-4.0.0.13	CARBOHYD	514	514	0.96821	.	.	#POSITIVE
SEQUENCE	netOGlyc-4.0.0.13	CARBOHYD	515	515	0.912784	.	.	#POSITIVE
SEQUENCE	netOGlyc-4.0.0.13	CARBOHYD	517	517	0.966162	.	.	#POSITIVE
SEQUENCE	netOGlyc-4.0.0.13	CARBOHYD	518	518	0.92731	.	.	#POSITIVE
SEQUENCE	netOGlyc-4.0.0.13	CARBOHYD	520	520	0.966772	.	.	#POSITIVE
SEQUENCE	netOGlyc-4.0.0.13	CARBOHYD	522	522	0.971225	.	.	#POSITIVE
SEQUENCE	netOGlyc-4.0.0.13	CARBOHYD	524	524	0.918773	.	.	#POSITIVE
SEQUENCE	netOGlyc-4.0.0.13	CARBOHYD	525	525	0.979672	.	.	#POSITIVE
SEQUENCE	netOGlyc-4.0.0.13	CARBOHYD	526	526	0.922856	.	.	#POSITIVE
SEQUENCE	netOGlyc-4.0.0.13	CARBOHYD	527	527	0.971219	.	.	#POSITIVE
SEQUENCE	netOGlyc-4.0.0.13	CARBOHYD	528	528	0.939953	.	.	#POSITIVE
SEQUENCE	netOGlyc-4.0.0.13	CARBOHYD	529	529	0.764988	.	.	#POSITIVE
SEQUENCE	netOGlyc-4.0.0.13	CARBOHYD	530	530	0.942912	.	.	#POSITIVE
SEQUENCE	netOGlyc-4.0.0.13	CARBOHYD	531	531	0.68235	.	.	#POSITIVE
SEQUENCE	netOGlyc-4.0.0.13	CARBOHYD	532	532	0.738914	.	.	#POSITIVE
SEQUENCE	netOGlyc-4.0.0.13	CARBOHYD	534	534	0.741542	.	.	#POSITIVE
SEQUENCE	netOGlyc-4.0.0.13	CARBOHYD	535	535	0.488534	.	.	
SEQUENCE	netOGlyc-4.0.0.13	CARBOHYD	537	537	0.505551	.	.	#POSITIVE
SEQUENCE	netOGlyc-4.0.0.13	CARBOHYD	542	542	0.209674	.	.	
SEQUENCE	netOGlyc-4.0.0.13	CARBOHYD	546	546	0.0171517	.	.	
SEQUENCE	netOGlyc-4.0.0.13	CARBOHYD	548	548	0.0535957	.	.	
SEQUENCE	netOGlyc-4.0.0.13	CARBOHYD	549	549	0.0749523	.	.	
SEQUENCE	netOGlyc-4.0.0.13	CARBOHYD	550	550	0.0234858	.	.	
SEQUENCE	netOGlyc-4.0.0.13	CARBOHYD	560	560	0.0239165	.	.	
SEQUENCE	netOGlyc-4.0.0.13	CARBOHYD	562	562	0.0232685	.	.	
SEQUENCE	netOGlyc-4.0.0.13	CARBOHYD	569	569	0.134763	.	.	
SEQUENCE	netOGlyc-4.0.0.13	CARBOHYD	570	570	0.240768	.	.	
SEQUENCE	netOGlyc-4.0.0.13	CARBOHYD	576	576	0.157512	.	.	
SEQUENCE	netOGlyc-4.0.0.13	CARBOHYD	581	581	0.224589	.	.	
SEQUENCE	netOGlyc-4.0.0.13	CARBOHYD	582	582	0.539142	.	.	#POSITIVE
SEQUENCE	netOGlyc-4.0.0.13	CARBOHYD	583	583	0.114082	.	.	
SEQUENCE	netOGlyc-4.0.0.13	CARBOHYD	590	590	0.0280832	.	.	
SEQUENCE	netOGlyc-4.0.0.13	CARBOHYD	592	592	0.15047	.	.	
SEQUENCE	netOGlyc-4.0.0.13	CARBOHYD	598	598	0.0166481	.	.	
SEQUENCE	netOGlyc-4.0.0.13	CARBOHYD	608	608	0.00595865	.	.	
SEQUENCE	netOGlyc-4.0.0.13	CARBOHYD	611	611	0.00912226	.	.	
SEQUENCE	netOGlyc-4.0.0.13	CARBOHYD	616	616	0.0727347	.	.	
SEQUENCE	netOGlyc-4.0.0.13	CARBOHYD	623	623	0.0556065	.	.	
SEQUENCE	netOGlyc-4.0.0.13	CARBOHYD	630	630	0.126792	.	.	
SEQUENCE	netOGlyc-4.0.0.13	CARBOHYD	631	631	0.276066	.	.	
SEQUENCE	netOGlyc-4.0.0.13	CARBOHYD	632	632	0.107804	.	.	
SEQUENCE	netOGlyc-4.0.0.13	CARBOHYD	634	634	0.0991393	.	.	
SEQUENCE	netOGlyc-4.0.0.13	CARBOHYD	636	636	0.0332672	.	.	
SEQUENCE	netOGlyc-4.0.0.13	CARBOHYD	638	638	0.0374652	.	.	

Figure 31: Analysis of the possible O-glycosylation sites in glucoamylase from A. niger.

3.6.2 NMR Spectra

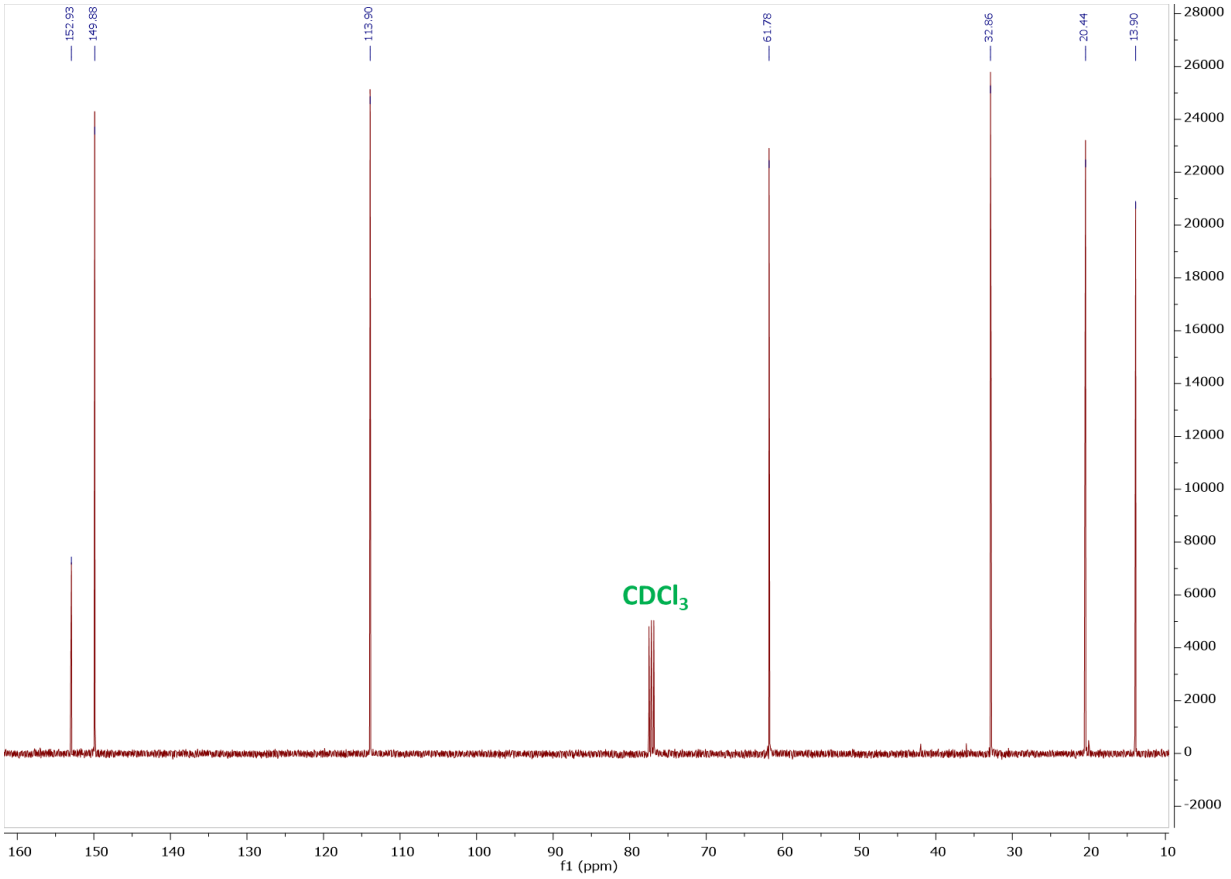

Figure 32: ^{13}C NMR spectrum of the product of reaction between DFF and n-butylamine. ^{13}C NMR (101 MHz, cdcl$_3$) δ 152.93, 149.88, 113.90, 61.78, 32.86, 20.44, 13.90.

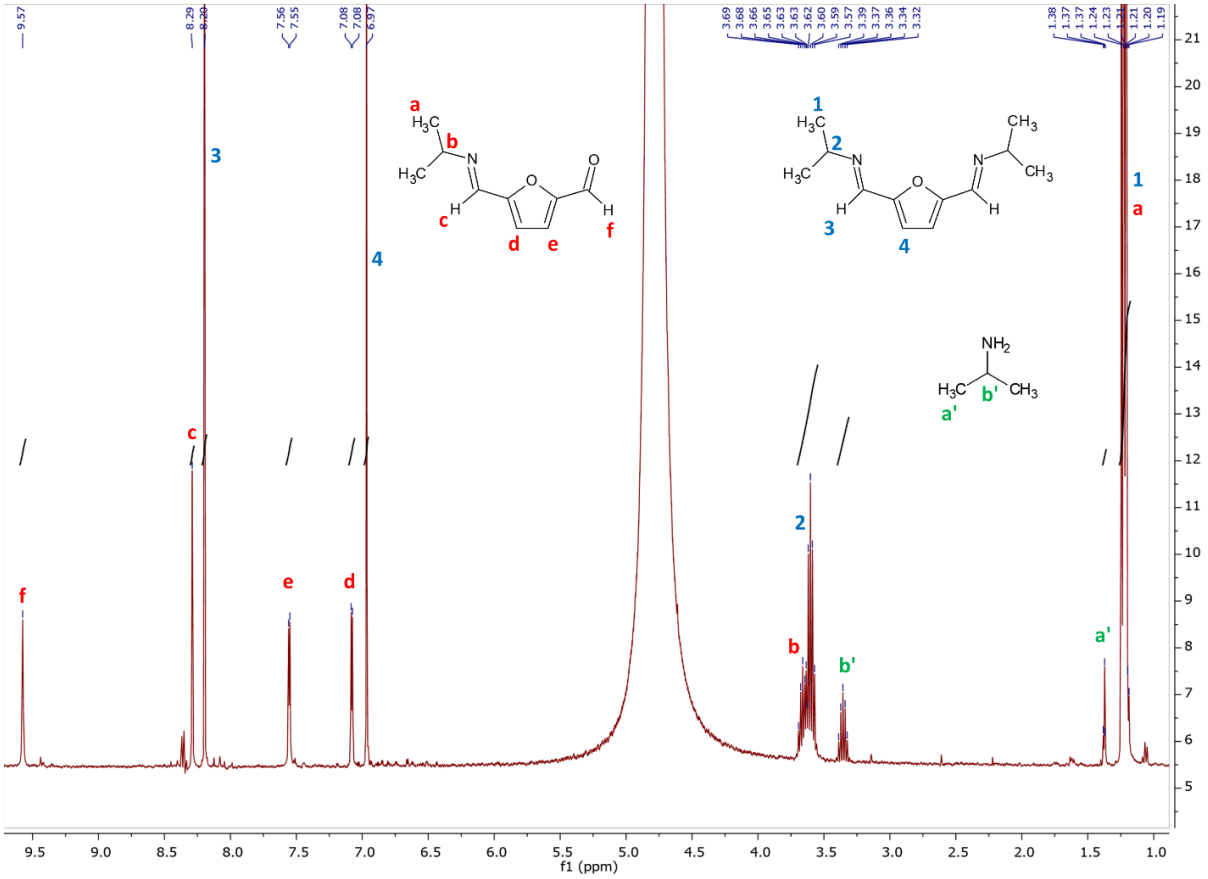

Figure 33: ^{1}H NMR spectrum in D_2O of the reaction between DFF and isopropylamine, after 1 hour of reaction. ^{1}H NMR (400 MHz, Deuterium Oxide) δ 9,57 (s, C<u>H</u>O), 8.29 (s, C<u>H</u>=N), 8.20 (s, C<u>H</u>=N), 7.56 (d), 7.08 (d), 6.97 (s), 3.69-3.57 (m), 3.36 (p), 1.38-1.37 (m), 1.24-1.19 (m, C<u>H$_3$</u>)

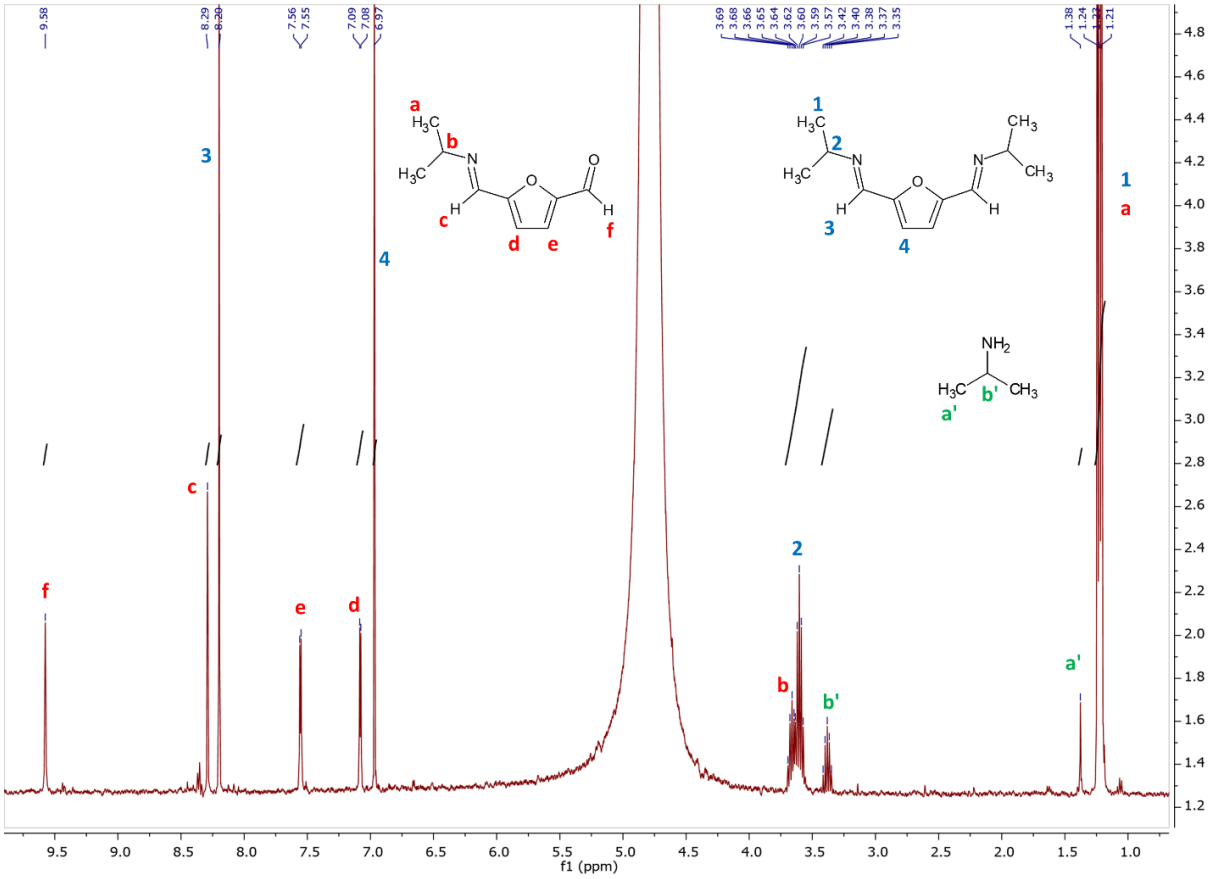

Figure 34: ^{1}H NMR spectrum in D_2O of the reaction between DFF and isopropylamine, after 5 hours of reaction. ^{1}H NMR (400 MHz, Deuterium Oxide) δ 9.58 (s, CHO), 8.29 (s, CH=N), 8.20 (s, CH=N), 7.56 (d), 7.09 (d), 6.97 (s), 3.69-3.57 (m), 3.38 (p), 1.38(s), 1.24-1.21 (m, CH_3)

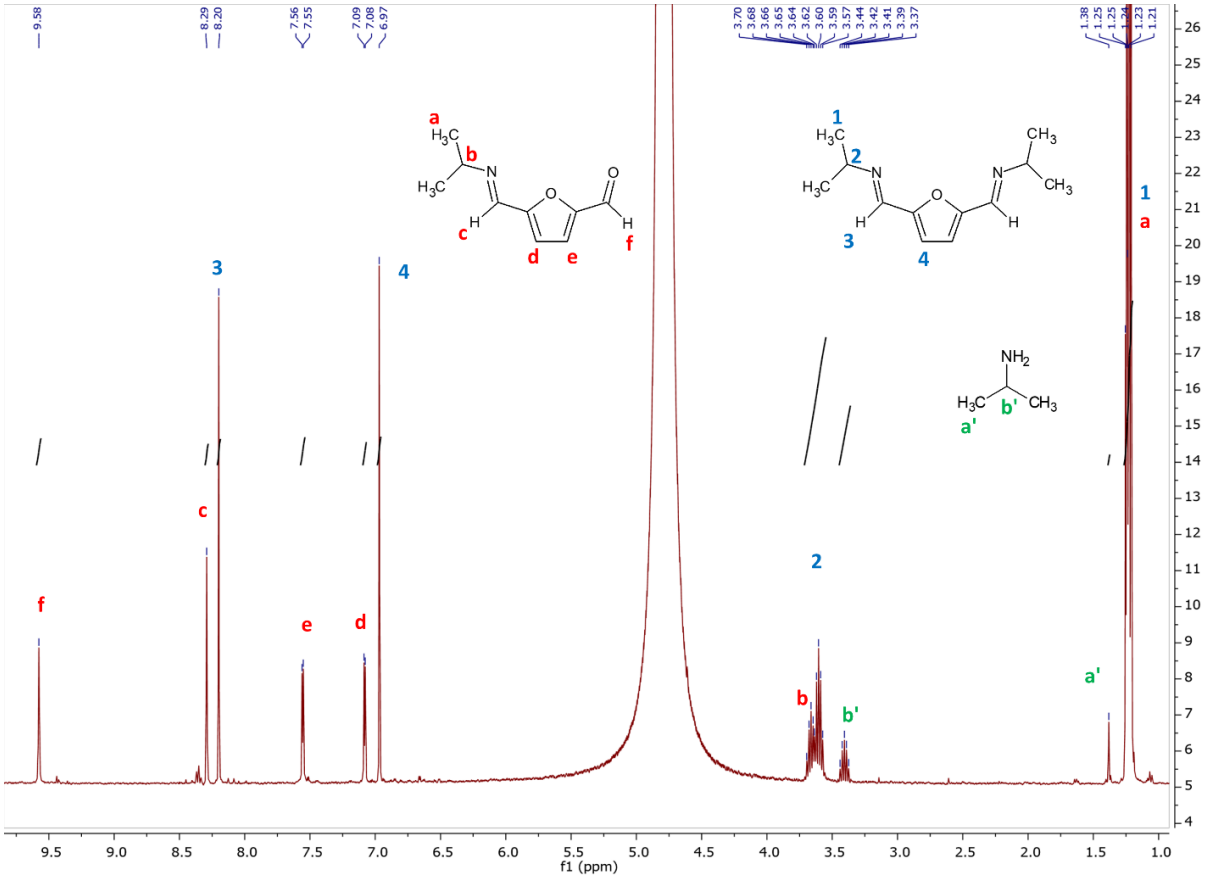

Figure 35: ^{1}H NMR spectrum in D_2O of the reaction between DFF and isopropylamine, after 1 week of reaction. ^{1}H NMR (400 MHz, Deuterium Oxide) δ 9.58 (s, CHO), 8.29 (s, CH=N), 8.20 (s, CH=N), 7.56 (d), 7.09 (d), 6.97 (s), 3.70-3.57 (m), 3.41 (p), 1.38 (s), 1.25-1.21 (m, CH_3)

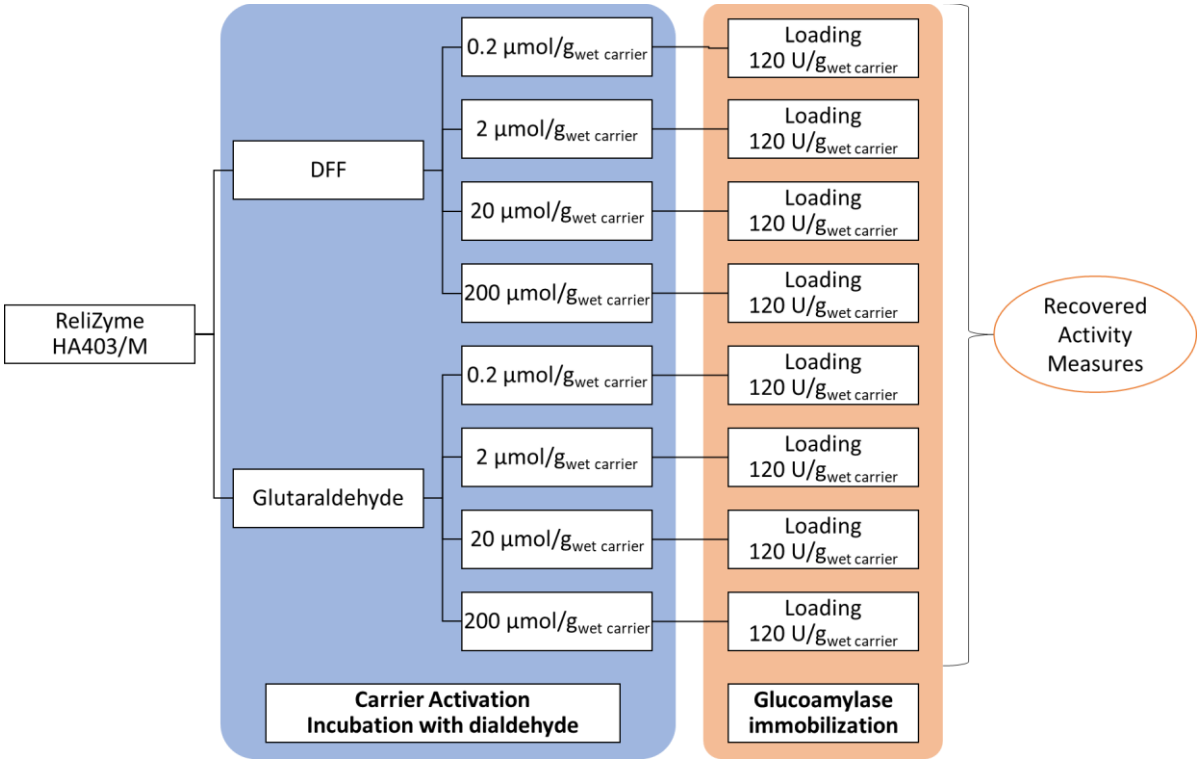

Figure 36: Comparison of DFF and glutaraldehyde – Carrier activation with different amounts of crosslinking agent.

3.6.3 Paper – 2,5-Furandicarboxaldehyde as a bio-based crosslinking agent replacing glutaraldehyde for covalent enzyme immobilization

The work described in the previous chapter resulted in a publication, titled "2,5-dicarboxaldehyde as a bio-based crosslinking agent replacing glutaraldehyde for covalent enzyme immobilization" and published on RSC Advances.

The manuscript is presented in the following pages.

RSC Advances

PAPER

View Article Online
View Journal | View Issue

Cite this: *RSC Adv.*, 2022, **12**, 35676

2,5-Furandicarboxaldehyde as a bio-based crosslinking agent replacing glutaraldehyde for covalent enzyme immobilization†

Chiara Danielli,[ab] Luuk van Langen,[b] Deborah Boes,[bc] Fioretta Asaro,[a] Serena Anselmi,[d] Francesca Provenza,[de] Monia Renzi[e] and Lucia Gardossi*[a]

In the quest for a bio-based and safer substitute for glutaraldehyde, we have investigated 2,5 diformylfuran (DFF) as bifunctional crosslinking agent for the covalent immobilization of glucoamylase on amino-functionalized methacrylic resins. Immobilization experiments and systematic comparison with glutaraldehyde at four different concentrations for the activation step showed that DFF leads to comparable enzymatic activities at all tested concentrations. Continuous flow experiment confirms a similar long term stability of the immobilized formulations obtained with the two crosslinkers. The NMR study of DFF in aqueous solution evidenced a much simpler behaviour as compared to glutaraldehyde, since no enolic forms can form and only a mono-hydrated form was observed. Unlike in the case of glutaraldehyde, DFF reacts covalently with the primary amino groups *via* imine bond formation only. Nevertheless, the stability of the covalent immobilization was confirmed also at acidic pH (4.5), most probably because of the higher stability of the imine bonds formed with the aromatic aldehydes. In terms of toxicity DFF has the advantage of being poorly soluble in water and, more importantly, poorly volatile as compared to glutaraldehyde, which displays severe respiratory toxicity. We have performed preliminary ecotoxicity assays using *Aliivibrio fischeri*, a marine bacterium, evidencing comparable behaviour (below the toxicity threshold) for both dialdehydes at the tested concentrations.

Received 11th November 2022
Accepted 5th December 2022

DOI: 10.1039/d2ra07153c

rsc.li/rsc-advances

Introduction

The use of enzymes as biocatalysts has several advantages: they have high selectivity, perform reactions in mild conditions and often are able to catalyse transformations not viable through conventional chemistry. Immobilized enzymes, which are insoluble enzyme formulations, present advantages such as applicability in low-water media or continuous flow settings.[1–3] For this reason, immobilized enzymes are used in industry in pharmaceutical synthesis, in the food sector, in the cosmetic sector and for the synthesis of fine chemicals.[1–4]

The immobilization of enzymes can be achieved with various techniques, including carrier-free direct cross-linking of protein conglomerates (CLECs, CLEAs), adsorption on solid carriers or covalent binding to solid carriers.[5] In this last case, the enzyme is bound to a carrier through residues on the protein surface, usually amine residues.[5] Likewise, the carrier needs to have active groups to which the enzyme can bind either directly (such as epoxy groups) or after activation using a bifunctional reagent. Amino-functionalized carriers are examples of this latter case. The most common bifunctional reagent is glutaraldehyde, but several alternatives have been proposed, including carbohydrate-derived dialdehydes.[6]

Other industrial applications of glutaraldehyde include its use as disinfectant, hardener in X-ray film processing, fixative in tanning, biocide in water treatment, preservative in industrial oils, biocide in sanitary solutions for aircraft and portable toilets, in small quantities as a disinfectant for air ducts, tissue fixative in electron and light microscopy and in histochemistry and biocide in aquaculture. Conversely, the glutaraldehyde market revenue was valued at US$ 450 million in 2021.[7]

However, the exact behaviour of glutaraldehyde in water, as well as the chemical nature of the bonds it forms with the enzyme and the carrier, is not fully understood.[8] In fact, it displays a very complex behaviour in aqueous solution. Thirteen different forms, either hydrated, cyclic, oligomeric or polymeric have been identified, and it is still unclear which of these react with lysine side chains of the protein in enzyme immobilization. In most scientific papers, imine bonds are depicted as responsible for enzyme immobilization with glutaraldehyde,

[a]*Department of Chemical and Pharmaceutical Sciences, University of Trieste, Via L. Giorgieri 1, 34127 Trieste, Italy. E-mail: gardossi@units.it*

[b]*ViaZym B.V., Molengraaffsingel 10, 2629 JD, Delft, The Netherlands*

[c]*Department of Biotechnology, Delft University of Technology, Van der Maasweg 9, NL-2629 HZ Delft, The Netherlands*

[d]*Bioscience Research Center, Via Aurelia Vecchia, 32, 58015 Orbetello, GR, Italy*

[e]*Department of Life Science (DSV), University of Trieste, Via L. Giorgieri 10, 34127 Trieste, Italy*

† Electronic supplementary information (ESI) available. See DOI: https://doi.org/10.1039/d2ra07153c

but this could raise questions about the expected reversibility of imine bond at acidic pH. In fact, practice shows that glutaraldehyde yields viable, irreversible, protein cross-linking, applicable in a wide range of conditions. In one study a pyridinium ion form was isolated after reaction of glutaraldehyde with amines, and it was hypothesized that this structure could also be formed during enzyme immobilization.[9]

In spite of its wide use, the industrial use of glutaraldehyde raises increasing concerns due to its widely documented toxicity.[10,11] It has been classified as a candidate substance of very high concern (SVHC) by the European Chemicals Agency,[12] and it is regarded fatal if inhaled, toxic if swallowed, and toxic to aquatic life.[13] It can also cause severe long-term effects, such as respiratory and skin sensitization. Its highly toxic and environmentally hazardous nature is anticipated to act as a major restraint for the market growth, since the use of this chemical is highly regulated by the government in respective regions, owing to health risks associated with it. Even a 1% solution of glutaraldehyde is poisonous for humans and animals, and products containing more than 0.1% glutaraldehyde solution are labelled as hazardous. Therefore, market players are focusing to lower dependency on glutaraldehyde and to find suitable substitutes, as high level of precaution is needed to reduce occupational and environmental exposure to glutaraldehyde.

In the general quest for finding greener and safer molecules, we have identified 2,5-diformylfuran (DFF) as a bio-based alternative for glutaraldehyde. DFF is a derivative of 5-hydroxymethylfurfural (HMF), which is obtained from the dehydration of carbohydrates. The oxidation of HMF to DFF can be achieved either by chemical routes[14] or by biotransformations, including the use of isolated enzymes or whole cells.[15,16]

In the present study, we analysed its property as a replacement of glutaraldehyde for enzyme immobilization. We have investigated and directly compared the efficiency of glutaraldehyde and DFF in the covalent immobilization of glucoamylase, an enzyme of large industrial use, on amino-functionalized methacrylic resins. We employed the two di-functional reagents in a wide range of concentrations, up to very low concentrations at which differences in behaviour would be magnified. The resulting immobilized preparations have been compared in a continuous flow experiment, to simulate industrially relevant conditions. The reactivity of DFF towards primary amino groups was investigated by means of NMR spectroscopy, shedding light on the bonds formed in aqueous solution. Moreover, we compared the two crosslinkers in an ecotoxicological study, using marine micro-organisms, since at the present moment only few papers are known dealing with DFF toxicity.[17–19] With this work we intend to pave the way for future studies and potential applications of this bio-based difunctional agent.

Experimental

Materials

Chemicals. 5-(Hydroxymethyl)furfural (HMF, ≥99% food grade, CAS 67-47-0); glutaraldehyde 25% w/w solution (CAS 111-30-8), 2,2′-azino-bis(3-ethylbenzothiazoline-6-sulfonic acid) (ABTS, CAS 30931-67-0), *p*-nitrophenyl-β-D-glucopyranoside (CAS 2492-87-7), D-glucose (CAS 50-99-7), KH_2PO_4 (CAS 7778-77-0), K_2HPO_4 (CAS 7758-11-4), NaOH (CAS 1310-73-2), Na_2SO_4 (CAS 7757-82-6), Bradford reagent (product no. B6916), HCl 37% (CAS 7647-01-0) were from Sigma Aldrich. K_2CO_3 (CAS 584-08-7) was from Carl Roth. *n*-Butylamine 98% (CAS 109-73-9) and KBr were from JT Baker. Ethyl acetate (CAS 141-78-6), diethyl ether (CAS 60-29-7) and petroleum ether 40–60 (CAS 8032-32-4) were from VWR Chemicals International. Dimethyl sulfoxide (DMSO, CAS 67-68-5), D-maltose monohydrate (CAS 6363-53-7) were from TCI Europe. Citric acid (CAS 77-92-9) was from Fisher Scientific.

DFF was chemically synthesized by oxidation of HMF based on a literature procedure.[14] The product was obtained with a 99% purity determined by ^{1}H NMR in $CDCl_3$ (see ESI†).

Carriers. Carrier ReliZyme HA403/M (lot IP18-061) was acquired from Resindion (Binasco, Milano). Product features as from the producer: matrix poly(methacrylate); functional group hexamethylenamino; ion exchange capacity min 600 μmol g_{wet}^{-1}; median pore diameter 40–60 nm; water retention 60–70%; particle size range 200–500 μm.

Enzymes. Glucoamylase from *Aspergillus niger* (EC 3.2.1.3, CAS 9032-08-0, liquid solution, activity according to the here described assay: 240 U g^{-1}, protein content: 83 mg mL^{-1}, commercial name Dextrozyme GA) was purchased from Novozymes (Denmark). Peroxidase from horseradish (HRP, EC 1.11.1.7, CAS 9003-99-0, type II, lyophilized powder, 150–250 U mg^{-1}) and glucose oxidase from *Aspergillus niger* (EC 1.1.3.4, CAS 9001-37-0, type X-S, lyophilized powder, 100 000–250 000 U g^{-1} solid) were purchased from Sigma Aldrich.

NMR characterization. NMR spectra were acquired with a JEOL 60 MHz MY-NMR spectrometer, a Varian 400 (400 MHz) and a Varian 500 (500 MHz). Deuterated solvents, $CDCl_3$, DMSO-d_6 and D_2O, were purchased from Eurisotop and Sigma Aldrich. Tetramethyl silane was purchased from Eurisotop.

Other equipment. Roti-Spin Mini-10 columns were purchased from Carl Roth. Samples were centrifuged in a Heraeus Biofuge 13 centrifuge. UV-Vis spectra were acquired with a PerkinElmer Lambda 2 UV/Vis Spectrophotometer, connected to a data acquisition/switch unit Agilent 34972A, and a Shimadzu UV-2450. pH measures were conducted with a Metrohm 632 pH-meter, equipped with a VWR SJ225 pH electrode.

Methods

Immobilization of glucoamylase on PMMA carrier. 10 g of carrier ReliZyme HA403/M were suspended in 16 mL of potassium phosphate buffer (25 mM, pH 7, 1.6 mL $g_{carrier}^{-1}$). Then, 200 $\mu mol_{dialdehyde}$ $g_{carrier}^{-1}$ were added to the mixture. The mixture was shaken at 25 °C for 2 hours. The supernatant was then removed, and the activated carrier was rinsed 3 times with 20 mL of demineralized water.

The activated carrier was resuspended in 16 mL of potassium phosphate buffer (25 mM, pH 7, 1.6 mL $g_{carrier}^{-1}$). 5 g of Dextrozyme GA (commercial glucoamylase solution; 120 U $g_{carrier}^{-1}$ referred to the amount of wet carrier as provided by the manufacturer) were added to the reaction mixture. The mixture

was kept shaking at 25 °C for 24 hours. The supernatant was then removed and tested for residual enzyme activity. The immobilized enzyme was rinsed 3 times with 20 mL of demineralized water.

The immobilized enzyme was stored at 4 °C in potassium phosphate buffer (25 mM, pH 7).

Glucoamylase activity assay. One Immobilized Glucoamylase Unit (IGU) is defined as the amount of enzyme that hydrolyses one μmol of maltose at the following conditions: 25% maltose in 10 mM citrate buffer, pH 4.5, at room temperature (20 °C).

For the assay, 100 mg of immobilized glucoamylase were suspended in 10 mL of the maltose solution; the mixture was shaken at room temperature for 1 hour. Every 10 minutes, a sample (50 μL) of the supernatant was taken and diluted 10 times with 0.1 M HCl before glucose analysis.

Glucose concentration assay. The glucose assay solution was obtained by dissolving 55 mg of ABTS in 50 mL of 25 mM potassium phosphate buffer pH 7; then, to the solution were added 0.2 mL of a glucose oxidase aqueous solution (1 mg mL^{-1}) and 0.2 mL of a horse radish peroxidase aqueous solution (1.5 mg mL^{-1}).

50 μL of the 10× diluted glucoamylase assay sample were mixed with 2.95 mL of the glucose assay solution in a 4 mL UV-Vis cuvette. The cuvette was mixed by inversion, and the absorbance at 405 nm was monitored for 5 minutes. The variation in absorbance over time was compared to that of a reference solution of 5 mM D-glucose in water. The glucose concentration in each sample was obtained by:

$$[\mathrm{Glu}]\ (\mathrm{mM}) = \frac{\Delta A_{405,\mathrm{sample}}\ (\mathrm{min}^{-1})}{\Delta A_{405,\mathrm{ref}}\ (\mathrm{min}^{-1})} \times \frac{[\mathrm{glu}]_{\mathrm{ref}}\ (\mathrm{mM}) \times V_{\mathrm{ref}}\ (\mathrm{mL})}{V_{\mathrm{sample}}\ (\mathrm{mL})} \times \mathrm{df}$$

where $\Delta A_{405,\mathrm{sample}}$ and $\Delta A_{405,\mathrm{ref}}$ are the variations in absorbance of the sample and the reference solution, respectively; $[\mathrm{glu}]_{\mathrm{ref}}$ is the glucose concentration of the reference solution; V_{ref} is the volume of reference solution; V_{sample} is the volume of the glucoamylase solution sample; df is the dilution factor.

Activity calculation. The glucose concentration data were plotted in a [glucose] *vs.* time graph. Glucoamylase activity was calculated by:

$$\mathrm{Activity}\ (\mathrm{U\ g^{-1}}) = \frac{\frac{\Delta[\mathrm{glucose}]\ (\mathrm{mM\ min^{-1}})}{2} \times V_{\mathrm{assay}}\ (\mathrm{L}) \times 1000}{g_{\mathrm{sample}}}$$

where: Δ[glucose]/2 is the rate of maltose hydrolysis; V_{assay} is the volume of the assay; 1000 is the conversion factor from mmol to μmol; g_{sample} is the weight of dried immobilized enzyme used for the assay.

After the last activity assay cycle, the supernatant maltose solution was removed by decanting, and the immobilized enzyme sample was rinsed with 3 × 10 mL H_2O. The water was then removed, and the enzyme preparation was dried in the vacuum oven (100 °C, 6 h). The weight of the anhydrous immobilized enzyme was used for the activity calculations.

Continuous flow activity assay. 150 mg of wet weight immobilized enzyme were introduced in a 10 mL glass column. The column was filled with a 25% maltose solution in 10 mM citrate buffer, pH 4.5. A continuous flow of maltose solution was supplied to the column at a rate of 0.15 mL min^{-1} over the course of 13 days. Every day, a sample (3–4 mL) of effluent was collected. Of this sample, 50 μL were immediately diluted 10 times with HCl 0.1 M, to be used for glucose concentration analysis; the rest was used for glucoamylase leaching evaluation.

At the end of the experiment, the effluent samples were analysed to determine: (1) glucose concentration (see previous section), (2) enzyme leaching (see following section). After the experiment, the enzymatic preparation was recovered and dried under high vacuum to express all results relating to dry enzyme preparation weight.

For glucose concentration, a negative measure was performed on 50 μL of 10 times diluted maltose assay solution. The glucose concentration in the negative is subtracted from that of all measured samples.

Glucoamylase leaching evaluation – *p*-nitrophenyl-β-D-glucopyranoside assay. 600 μL of effluent from the continuous flow column were concentrated to about 60 μL using a Roti-Spin Mini-10 column and centrifuging the sample at 7000 rpm for about 10 minutes. 20 μL of the concentrated sample were then mixed with 500 μL of a 1 mg mL^{-1} solution of *p*-nitrophenyl-β-D-glucopyranoside in sodium citrate buffer (0.1 M, pH 4.5); the mixture was then incubated at 56 °C for 4 h. After incubation, 500 μL of a 0.5 M potassium carbonate solution were added to the mixture. The absorbance of the final mixture at 400 nm was directly measured and compared with a *p*-nitrophenol calibration curve, to calculate the product concentration in the samples.

Reaction of DFF with *n*-butylamine. 500 mg of DFF (4.03 mmol) were mixed with 20 mL of potassium phosphate buffer (0.1 M, pH 7.0). The mixture was kept under magnetic stirring. Then, 0.797 mL of *n*-butylamine (free base, 8.06 mmol) were added dropwise to the reaction medium using a syringe. The reaction was stirred at 22 °C for 24 hours. The aqueous phase was extracted 3 times with 20 mL of diethyl ether. The collected organic phases were dried with anhydrous Na_2SO_4. The organic layer was evaporated. The product was analysed with ^{1}H NMR and ^{13}C NMR in $CDCl_3$.

Reaction of DFF with isopropylamine. 6.2 mg of DFF (0.05 mmol) were dissolved in 0.1 mL of potassium phosphate buffer (1 M, pH 7.0) and 0.9 mL of D_2O. The final buffer concentration is 0.1 M. Then, 8.6 μL (5.9 mg, 0.1 mmol) were added to the solution. The reaction solution was stirred at 22 °C for 3 days. The reaction was directly monitored by ^{1}H NMR after 1 hour, 5 hours, 1 day and 3 days.

Protein modelling. The crystallographic structures of glucoamylase from *Aspergillus niger* were obtained from Protein Data Bank (PDB ID: 3EQA, 5GHL). The structures were analysed with the visualization software UCSF Chimera (University of California), and a prediction of glycosylation sites was

conducted with the servers NetOGlyc and NetNGlyc (Technical University of Denmark).

Methods for toxicological studies. Ecotoxicological tests were performed on *Aliivibrio fischeri* (bacteria, UNI EN ISO 11348-1:2019), based on normalized methods following standardized conditions and positive controls reported by the cited methods. Tests on bacteria were performed using MICROTOX® instrument (Modern Water) and internal cultured bacterial stocks. Responses obtained in tested solutions are set respect to natural bioluminescence of tested bacteria. A solution of DMSO (0.5%) added to an aqueous NaCl solution in ultrapure water (20 g L^{-1}) was used as solvent for hydrophobic substances and tested to evaluate the natural toxicity of the solubilizing solution. Results are considered as negative control and used for the normalization of obtained results on the molecules of interest solubilized using DMSO. Scalar dilutions starting from the maximum concentration of 5 mg L^{-1} were tested. Both solubilized DFF and glutaraldehyde were tested after 15 and 30 minutes of exposure and results were normalized by the natural toxicity of DMSO-made negative controls. Natural toxicity of DMSO-made negative controls were always below 5% of bioluminescence inhibition after 30 min of exposure. To evaluate bacterial activity and responsiveness to the exposure, both negative controls (NaCl 20 g L^{-1} solution in ultrapure water) and positive controls were also performed, using 3,5-dichlorophenol at the standard concentration of 4.5 mg L^{-1}. Obtained responses on positive controls (71.3%, SD 0.5%) were included within the range of acceptability for the performed test (20–80%).

Results and discussion

Behaviour and reactivity of DFF in aqueous solution

In sharp contrast with glutaraldehyde, which has a very complex behaviour in aqueous environment, the behaviour of DFF in water appears to be very simple. DFF has no alpha hydrogen on the aldehyde functions, thus avoiding the formation of enols, whereas GA undergoes aldol-reactions giving rise to aldol-form intermediates leading to different reactivity and contributing to toxic effects.[20]

As evident from the ^{1}H NMR spectrum in D_2O (Fig. 1), only two forms are present in aqueous solution. There are two series of signals: two peaks (a and b) correspond to DFF, as expected, while four peaks (1 to 4) belong to its monohydrated diol. Interestingly, only one of the two aldehyde groups is hydrated to diol, as there are no signals from a hypothetic di-hydrated form. The assignations were confirmed by comparison with literature.[21]

The NMR spectrum in $CDCl_3$ (see ESI†) presents signals only from DFF, confirming that no impurities were present in the starting sample.

On the light of the NMR evidence that the hydration equilibrium is asymmetric and that only one of the two aldehyde groups is hydrated to diol, it was necessary to investigate whether the reaction of DFF with primary amine groups occurs in a symmetrical way. That is the prerequisite for achieving the covalent binding of superficial lysine residues of an enzyme to an amino-functionalized carrier.[22]

The amine selected for the reaction was *n*-butylamine (Scheme 1a), which models the Lys side chains of the amino acid residues. The conditions of the model reaction reproduce the protocols typically used for enzyme immobilization: potassium phosphate aqueous buffer, 0.1 M, pH 7; an oily product started forming almost immediately, and the reaction was let to continue for an additional 24 hours. The precipitation of the imine product has similarities with the behaviour of the bond between the enzyme and the solid carrier, which does not participate in the equilibrium of the chemical species in solution. It must be underlined that previous studies found that the thermodynamic equilibrium of chemical reactions can significantly change in favour of the synthetic product when a soluble compound binds to molecules linked to a solid support. That is the case of the formation of amide bonds in solid phase synthesis of peptides catalysed by proteases.[23]

In these conditions the di-imine derivative (pictured in Scheme 1a), which separated from the solution, was isolated and characterized *via* ^{1}H NMR (in $CDCl_3$) and ^{13}C NMR (in $CDCl_3$) (see ESI†). The spectra proved that the di-imine structure is symmetrical, further confirming the applicability of DFF as an enzyme crosslinker.

In addition, isopropylamine was chosen as another model amine, because it forms a water-soluble product with DFF. This allows to monitor the reaction in solution for longer times, in contrast to the *n*-butylamine product that directly separates from the solution. The reaction was conducted in potassium phosphate buffer diluted with deuterated water, in order to follow the reaction *via* ^{1}H NMR.

After 1 hour, the reaction reached the equilibrium. The ^{1}H NMR spectrum (see ESI†) indicates that the ratio between the mono- and di-imine is 1.2 : 1.0. Interestingly, the hypothetical hydrated mono-imine is not present, indicating that the formation of an imine bond shifts the equilibrium of the other aldehyde group towards the non-hydrated form. The spectrum did not change during the following 30 days (see ESI†), reporting the signals from the di-imine derivative and the mono-imine derivative (pictured in Scheme 1b), residual signals of isopropylamine (18% of the initial amount of amine is still free in solution) and no signal of residual DFF in solution. These observations lead to the following conclusions: (i) the formation of the products between isopropylamine, a primary amine, and DFF happens within the first hour of reaction; (ii) after reaching the equilibrium, the only products present in solution at 22 °C are the imine products, even after 1 week; (iii) the di-imine product shows high stability over long storage times, not displaying the formation of side (oxidation) products.

These findings suggest that the immobilization of enzymes with DFF, that is conducted in similar conditions at room temperature, only involves the formation of Schiff bases between DFF and the protein, and that the resulting imine is stable under immobilization conditions, most probably due to the conjugation of the imine bond with the furan ring and the resonance stabilization. The higher stability of the aromatic imines and the consequent shift of the equilibrium towards the

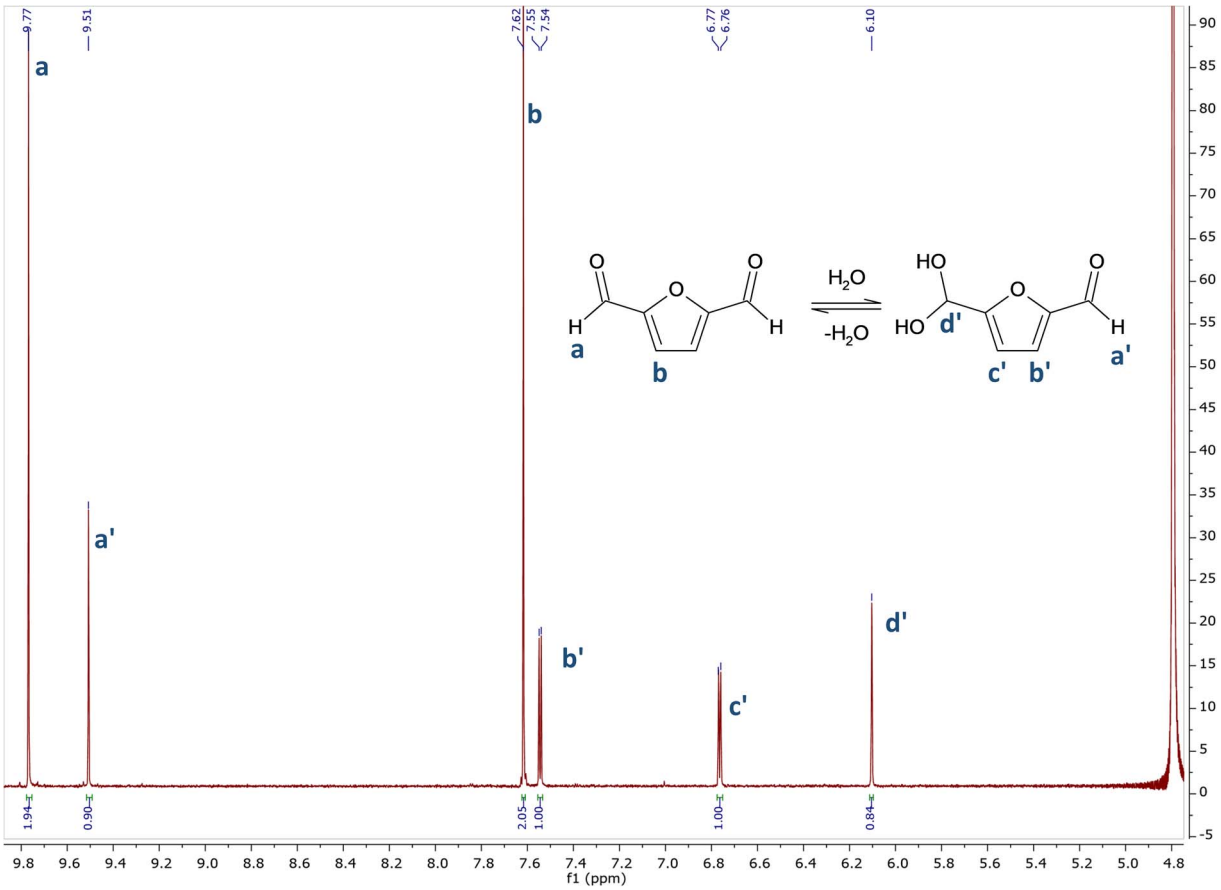

Fig. 1 ^{1}H NMR spectrum of DFF in D_2O. ^{1}H NMR (400 MHz, D_2O) δ 9.77 (s), 9.51 (s), 7.62 (s), 7.55 (d, $J = 3.6$ Hz), 6.77 (d, $J = 3.7$ Hz), 6.11 (s).

imine products have been already investigated and documented.[24] For instance, terephthalaldehyde, has been used as crosslinking agent to form stable gelatine membranes.[20]

Conveniently, the behaviour of DFF in aqueous environment is more predictable than that of glutaraldehyde, facilitating further studies towards the nature of the stable chemical bond. Moreover, the dosage of this crosslinking agent can be easily determined and any excess prevented because the clearer elucidation of the chemistry of the binding process. Finally, the formation of toxic side products can be excluded due to the absence of enolic equilibria, as in the case of glutaraldehyde.

Glucoamylase from *Aspergillus niger*

The immobilization study employed glucoamylase from *Aspergillus niger* as the model enzyme. Glucoamylase belongs to the

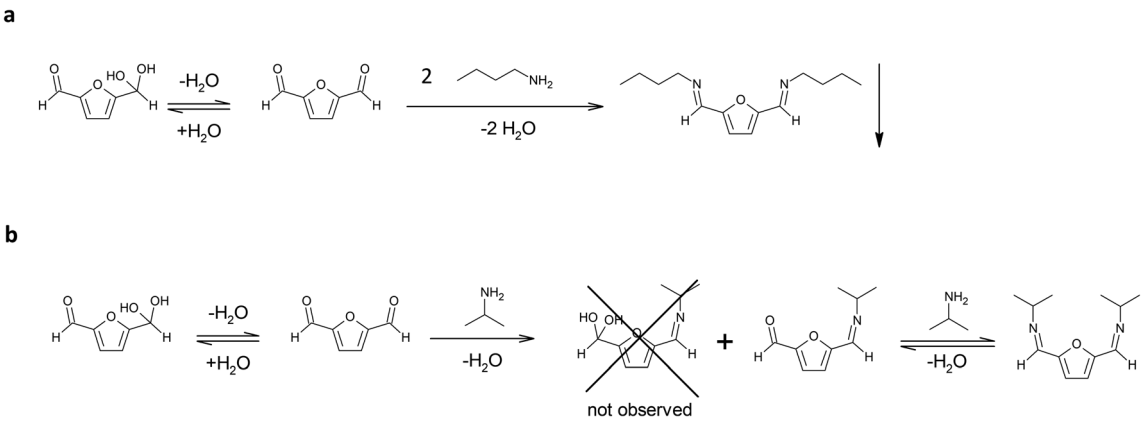

Scheme 1 (a) Reaction between DFF and *n*-butylamine in potassium phosphate buffer, 0.1 M, pH 7. (b) Reaction of DFF with isopropylamine in potassium phosphate buffer, 0.1 M, pH 7.

family of glycoside hydrolases (E.C. 3.2.1.3), which catalyses the cleavage of α-1,4- and β-1,6-glycosidic bonds, starting from the non-reducing end of the polysaccharide chain.[25,26] This enzyme was chosen due to its employment on a large scale in industry,[27] as well as its easy immobilization on methacrylic carriers.

Structurally, glucoamylases are composed by an N-terminal catalytic domain, highly conserved between different organisms, and a smaller, C-terminal starch-binding domain; the two domains are linked by a highly flexible linker region.[28]

The crystallographic structure of glucoamylase from *A. niger* was analysed *in silico*, using existing structures of the catalytic domain (PDB ID: 3EQA) and the starch binding domain (PDB ID: 5GHL), to establish whether covalent binding to the carrier is possible. No structures were found of the whole protein, as the flexible linker portion that connects the two domains breaks during the crystallization process;[26] however, for the present study it was deemed sufficient to analyse the isolated domain structures. The analysis concerned the presence of lysine residues on the enzyme surface; both the catalytic (Fig. 2A) and starch binding domain (Fig. 2B) present superficial Lys residues. It is therefore possible, in principle, to covalently immobilize the protein. In conclusion, glucoamylase from *Aspergillus niger* is suitable for covalent immobilization due to the presence of lysine residues on its surface.

Comparison of DFF and glutaraldehyde: immobilization of glucoamylase on PMMA carrier

Glucoamylase was immobilized on an amino-functionalized poly(methylmethacrylate) carrier, using the following general procedure: (a) activation of the carrier by incubation with the dialdehyde, (b) immobilization by incubation of the activated resin with the enzyme preparation; both steps were carried out in aqueous potassium phosphate buffer (25 mM, pH 7).

The activation step was studied using four different amounts of each dialdehyde (200, 20, 2 and 0.2 μmol $g_{carrier}^{-1}$), in order to directly compare the efficiency of DFF and glutaraldehyde over a wide range of concentrations. The highest concentration of dialdehyde used for the activation step corresponds to one third of the concentration of amine groups of the methacrylic resin (600 μmol g_{resin}^{-1}), as declared by the producer.

The resulting activated carriers were then incubated with a fixed amount of enzyme (120 U $g_{wet\ carrier}^{-1}$). An excess of enzyme was used in the immobilization process, leading to a 20% of residual activity in the supernatant after the procedure (data not shown). Therefore, the observed differences in recovered activity are not ascribable to a shortage of enzyme in the procedure.

The activity of the resulting enzymatic preparations was measured in a standard assay, by recycling the enzyme for four consecutive assays, until a plateau activity value was reached. This plateau value is regarded as the enzymatic activity immobilized on the carrier. The results are presented in Table 1.

The decrease in activity between the first and the following assay cycles can be explained by the presence of adsorbed, non-covalently bound enzyme on the carrier, and it is comparable between the two crosslinkers.

By comparing the plateau values of the last two cycles, we concluded that the binding efficiency of glutaraldehyde and DFF for enzyme immobilization is comparable at all tested concentrations.

Concerning the different crosslinker concentration, the results (Table 1) show how the immobilized activity remains similar throughout the range of tested concentrations, even with a 1000-fold decrease in the dialdehyde concentration. With such a low concentration of crosslinker, and an excess of enzyme, any difference in crosslinker efficiency would be evident. The activity values are very similar between the two different crosslinking agents, glutaraldehyde and DFF. This observation further supports the conclusion that the binding efficiency of the two crosslinkers is comparable.

In order to test the behaviour of the immobilized enzyme preparations for longer times, the operational stability of

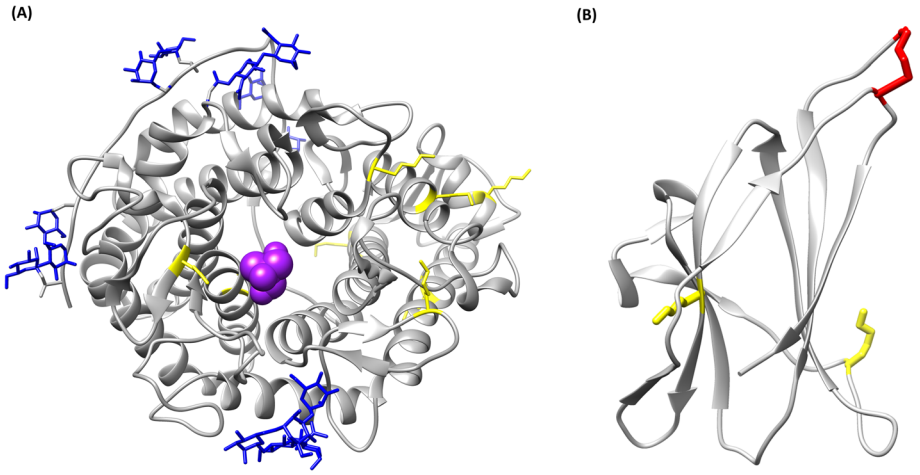

Fig. 2 Tridimensional models of the structure of glucoamylase from *Aspergillus niger*. In yellow, lysine residues; in blue, glycan residues; in purple, TRIS inhibitor in the catalytic pocket; in red, disulfide bonds. (A) Catalytic domain (PDB ID: 3EQA), (B) starch binding domain (PDB ID: 5GHL).

Table 1 Measured recovered activity for glucoamylase covalently immobilized on a PMMA carrier using decreasing concentrations of DFF and glutaraldehyde in the carrier activation step[a]

	Glutaraldehyde		DFF	
Crosslinker amount (μmol $g_{carrier}^{-1}$)	Assay cycle	Activity (U g_{dry}^{-1})	Assay cycle	Activity (U g_{dry}^{-1})
200	1	105	1	137
	2	90	2	107
	3	86	3	107
	4	87	4	107
20	1	214	1	124
	2	121	2	90
	3	107	3	83
	4	90	4	80
2	1	170	1	118
	2	120	2	96
	3	77	3	70
	4	76	4	66
0.2	1	113	1	119
	2	84	2	95
	3	77	3	77
	4	75	4	73

[a] DFF and glutaraldehyde comparison – continuous flow experiment.

glucoamylase immobilized on a PMMA carrier using either DFF or glutaraldehyde was analysed in a continuous flow experiment, over the course of 13 days. The immobilized enzyme was introduced in a glass column, which was filled with a 25% maltose solution in 10 mM citrate buffer, pH 4.5. A continuous flow of solution was supplied to the column at a rate of 0.15 mL min^{-1} over the course of the experiment. The enzyme samples used for the experiment are those immobilized with the lowest amount of crosslinker (0.2 $\mu mol_{aldehyde}$ $g_{wet\ carrier}^{-1}$).

As can be seen in Fig. 3, the productivity of the enzyme decreases significantly in the first three days, stabilizing for later measurements. The trend is comparable in the samples immobilized with both crosslinkers. The cause of this behaviour is elucidated by Fig. 4, which reports the measures of enzymatic activity in the effluent as a consequence of the detachment of some residual non-covalently bound enzyme. Notably, after 2 days of the reaction, no detached enzyme is found in the effluent, and the productivity in glucose remains constant.

In conclusion, the data obtained for long term stability with the continuous flow experiment further demonstrate the efficiency of DFF for the covalent immobilization of glucoamylase on the selected PMMA carrier and confirm its potential use as a more sustainable replacer of glutaraldehyde for this purpose.

Ecotoxicological studies

To the best of our knowledge, the scientific literature reports only three papers dealing with DFF toxicity.[17–19] In 2014, Frade *et al.*[17] analysed the toxicity of HMF and twenty among its derivatives, including DFF, on human skin fibroblast cells of line CRL-1502. This is a non-tumour cell line, chosen for its resemblance with human healthy tissues. The cells were incubated with 100–500 μM of the tested compounds, DFF resulted in a cell viability of 32 ± 2% after 72 hours.

Another study from the same research group[19] examines the toxicity of various *platform chemicals*, including DFF, in a Microtox assay, following the decrease in luminescence of marine bacteria *Aliivibrio fischeri*. The assay consisted in exposing *A. fischeri* to nine different concentrations of the analysed compounds, at a temperature of 15 °C, for 15 and 30 minutes. After the exposure, the luminescence of the sample is analysed, and the EC_{50} is determined as the concentration

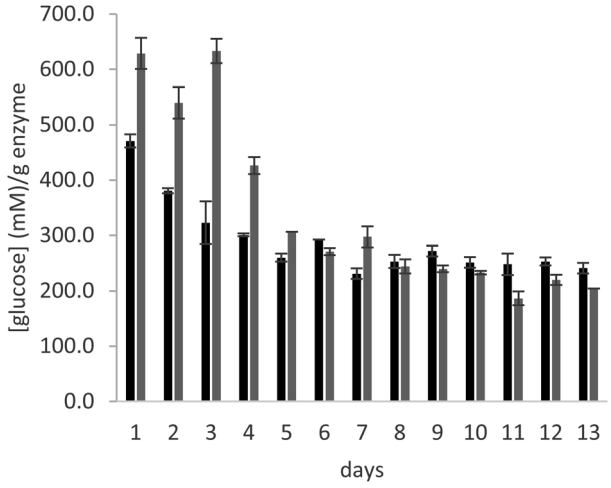

Fig. 3 Glucose concentration per g of dry enzyme preparation in the effluent of the continuous flow column experiment for glucoamylase immobilized with 0.2 μmol $g_{carrier}^{-1}$ of glutaraldehyde (in grey) and DFF (in black). Reaction conditions: 25% maltose solution in 10 mM citrate buffer, pH 4.5, 25 °C.

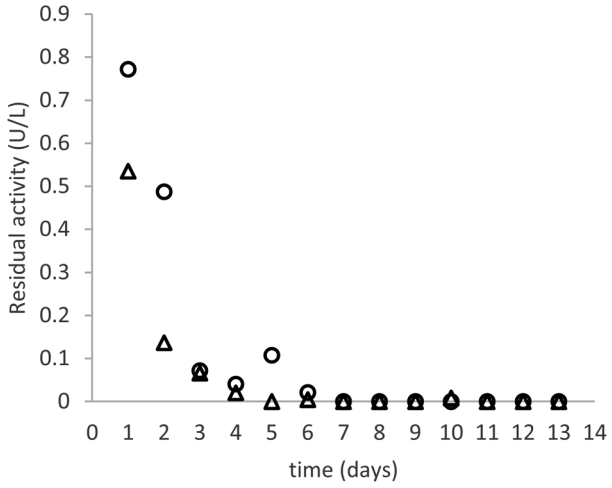

Fig. 4 Residual glucoamylase activity in the effluent of the continuous flow column experiment for glucoamylase immobilized with 0.2 μmol $g_{carrier}^{-1}$ of glutaraldehyde (circles) and DFF (triangles). Reaction conditions: 25% maltose solution in 10 mM citrate buffer, pH 4.5, 25 °C.

Table 2 Inhibition of natural bioluminescence at the exposure time normalized compared to negative controls

	15 min		30 min	
	Mean (%)	SD (%)	Mean (%)	SD (%)
DFF	2.31	1.13	3.76	0.32
Glutaraldehyde	0.41	0.35	4.37	0.33

corresponding to a 50% decrease in luminescence of the bacteria.

For most of the analysed compounds, the time of exposure does not influence significantly the resulting EC_{50}; an exception is DFF, for which EC_{50} halves (in other words, toxicity doubles) going from 5 to 30 minutes of exposure. Among the analysed compounds, the authors regard DFF as moderately toxic (EC_{50} = 100–10 mg L^{-1}).

Lastly, DFF toxicity is briefly mentioned in a work by Martins *et al.*,[18] which examines toxicity of HMF and some of its derivatives towards *Aspergillus nidulans*. In this paper, IC_{50} is calculated as the concentration of compound that can inhibit of 50% the growth of *A. nidulans*, and DFF is briefly mentioned compared to other molecules. Interestingly, in this study it is less toxic (higher IC_{50}) than HMF, unlike what observed in the other papers.

In this paper, we examined the ecotoxicology of DFF, directly comparing it to that of glutaraldehyde. Ecotoxicological tests were performed on *Aliivibrio fischeri*, in order to compare marine toxicity of DFF as compared to that of glutaraldehyde. Inhibition of natural bioluminescence at the maximum concentration tested was reported in Table 2 as mean value (standard deviation, SD) of experimental replicates. Reported results were corrected according to the DMSO natural toxicity at the concentration used to solubilize tested chemicals (0.5% DMSO in 20 g L^{-1} NaCl ultrapure water).

Results highlighted that toxicity of tested chemicals are comparable at the maximum dose tested of 5 mg L^{-1}, closer together and lower of 5% of bioluminescence inhibition after 30 minutes of exposure. Effects lower than 15% are considered not toxic by the Italian law[29] and the specific literature.[30,31] This is an encouraging result as it demonstrates that DFF can be a valid substitute for traditional aldehyde in terms of eco-compatibility. Although bacteria constitute the first link in the trophic web of aquatic ecosystems, the ecotoxicological assay with *A. fischeri* is widely used to evaluate the eco-compatibility of chemicals in both freshwater and marine ecosystems as it is highly standardized and repeatable and largely used to evaluate ecotoxicity of chemicals of possible industrial interest.[32,33] These results are important to highlight that DFF shows an absence of toxicity under tested conditions for the standardized species used (*A. fischeri*).

Overall, in terms of toxicity DFF also has the advantage of being poorly soluble in water (about 5 mg mL^{-1}) which decreases its harmful potential in aqueous environment as compared to the fully miscible glutaraldehyde. More importantly, the high boiling point of DFF (276.8 °C at 760 mmHg) makes this crosslinking agent considerably less harmful for human handling as compared to the volatile glutaraldehyde (boiling point 187 °C) that causes severe respiratory toxicity.

Conclusions

DFF was successfully employed as cross-linker for glucoamylase immobilization on amino-functionalized methacrylic carriers. Immobilization experiments and systematic comparison with glutaraldehyde at four different concentrations show that the efficiency of the two crosslinkers is very similar, giving comparable activities at all tested concentrations, even at very low crosslinker concentration for the activation step. Continuous flow experiment confirms that the glucoamylase immobilized with the two crosslinking agents displays comparable activity and long-term stability, with the leaching of residual adsorbed protein during the first three days of the continuous process and then reaching a plateau for the remaining 9 days.

NMR studies show that the formation of covalent bonds between DFF and primary amino groups occurs *via* imine bond formation only, unlike the case of glutaraldehyde where different mechanisms of reaction are possible.[8] It is widely known that the formation of an imine – from an amine and an aldehyde – is a reversible reaction which operates under thermodynamic control such that the formation of kinetically competitive intermediates are, in the fullness of time, replaced by the thermodynamically most stable product.[34] However, when the glucoamylase was immobilized on DFF activated amino-carriers the stability of the covalent immobilization was confirmed also at acid pH (4.5). The shifting of the equilibrium towards the imine product is probably ascribable to the higher stability of the imine bonds formed with the aromatic aldehydes, as already documented in investigations dealing with terephthalaldehyde.[24] The ecotoxicology study of DFF against *Aliivibrio fischeri* showed a decrease in bioluminescence below the toxicity threshold for both dialdehydes. In terms of toxicity DFF has the advantage of being poorly soluble in water and, more importantly, poorly volatile as compared to glutaraldehyde, which causes severe respiratory toxicity.

The present study paves the way for further investigations aiming at the replacement of glutaraldehyde as crosslinking agent in an array of industrial applications, with the bio-based, less volatile, easy to handle DFF, which has the additional advantage of reacting according to clear and simple reaction mechanisms. The latter feature enables its easier dosage as crosslinking agent while minimizing the chemical routes that might cause toxic effects.

Author contributions

Conceptualization: Chiara Danielli, Luuk van Langen, Lucia Gardossi. Methodology: Chiara Danielli, Luuk van Langen, Deborah Boes, Monia Renzi. Validation: Chiara Danielli, Deborah Boes, Serena Anselmi, Francesca Provenza. Investigation: Chiara Danielli, Deborah Boes, Serena Anselmi, Francesca Provenza, Fioretta Asaro. Writing – original draft preparation: Chiara Danielli, Monia Renzi. Writing – reviewing and editing:

Chiara Danielli, Luuk van Langen, Lucia Gardossi, Fioretta Asaro, Monia Renzi. Supervision: Luuk van Langen, Lucia Gardossi. Funding acquisition: Luuk van Langen, Lucia Gardossi.

Conflicts of interest

The authors declare that they have no known competing financial interests or personal relationships that could have appeared to influence the work reported in this paper.

Acknowledgements

We thank prof. Patrizia Nitti for fruitful discussions. We are grateful to Resindion (Binasco, Milano) for providing the methacrylic carrier. This project has received funding from the European Union's Horizon 2020 research and innovation program under the Marie Skłodowska-Curie grant agreement no. 860414 (INTERfaces project).

Notes and references

1 R. Di Cosimo, J. Mc Auliffe, A. J. Poulose and G. Bohlmann, *Chem. Soc. Rev.*, 2013, **42**, 6437–6474.
2 M. C. R. Franssen, P. Steunenberg, E. L. Scott, H. Zuilhof and J. P. M. Sanders, *Chem. Soc. Rev.*, 2013, **42**, 6491–6533.
3 R. A. Sheldon, *Adv. Synth. Catal.*, 2007, **349**, 1289–1307.
4 A. Basso and S. Serban, *Mol. Catal.*, 2019, **479**, 110607.
5 U. Hanefeld, L. Gardossi and E. Magner, *Chem. Soc. Rev.*, 2009, **38**, 453–468.
6 R. Schoevaart, A. Siebum, F. Van Rantwijk, R. Sheldon and T. Kieboom, *Starch/Staerke*, 2005, **57**, 161–165.
7 *Glutaraldehyde Market Overview*, **https://www.futuremarketinsights.com/reports/glutaraldehyde-market**.
8 I. Migneault, C. Dartiguenave, M. J. Bertrand and K. C. Waldron, *Biotechniques*, 2004, **37**, 790–802.
9 P. M. Hardy, G. J. Hughes and H. N. Rydon, *J. Chem. Soc., Perkin Trans. 1*, 1979, 2282–2288.
10 T. Takigawa and Y. Endo, *J. Occup. Health*, 2006, **48**, 75–87.
11 *Toxicological Profile*, **https://www.atsdr.cdc.gov/sites/peer_review/tox_profile_glutaraldehyde.html**.
12 *Glutaraldehyde ECHA Substance Information*, **https://echa.europa.eu/it/substance-information/-/substanceinfo/100.003.506**.
13 *Glutaraldehyde ECHA Brief Profile*, **https://echa.europa.eu/it/brief-profile/-/briefprofile/100.003.506**.
14 C. Laugel, B. Estrine, J. Le Bras, N. Hoffmann, S. Marinkovic and J. Muzart, *ChemCatChem*, 2014, **6**, 1195–1198.
15 M. M. Cajnko, U. Novak, M. Grilc and B. Likozar, *Biotechnol. Biofuels*, 2020, **13**, 1–12.
16 A. Millán Acosta, C. Cuesta Turull, D. Cosovanu, M. Núria Sala and R. Canela-Garayoa, *ACS Sustain. Chem. Eng.*, 2021, **9**, 14550–14558.
17 R. F. M. Frade, J. A. S. Coelho, S. P. Simeonov and C. A. M. Afonso, *Toxicol. Res.*, 2014, **3**, 311–314.
18 C. Martins, D. O. Hartmann, A. Varela, J. A. S. Coelho, P. Lamosa, C. A. M. Afonso and C. Silva Pereira, *Microb. Biotechnol.*, 2020, **13**, 1983–1996.
19 S. P. M. Ventura, P. De Morais, J. A. S. Coelho, T. Sintra, J. A. P. Coutinho and C. A. M. Afonso, *Green Chem.*, 2016, **18**, 4733–4742.
20 J. Biscarat, B. Galea, J. Sanchez and C. Pochat-Bohatier, *Int. J. Biol. Macromol.*, 2015, **74**, 5–11.
21 J. Carro, P. Ferreira, L. Rodríguez, A. Prieto, A. Serrano, B. Balcells, A. Ardá, J. Jiménez-Barbero, A. Gutiérrez, R. Ullrich, M. Hofrichter and A. T. Martínez, *FEBS J.*, 2015, **282**, 3218–3229.
22 S. Cantone, V. Ferrario, L. Corici, C. Ebert, D. Fattor, P. Spizzo and L. Gardossi, *Chem. Soc. Rev.*, 2013, **42**, 6262–6276.
23 R. V. Ulijn, N. Bisek, P. J. Halling and S. L. Flitsch, *Org. Biomol. Chem.*, 2003, **1**, 1277–1281.
24 E. Kulla and P. Zuman, *J. Phys. Chem. A*, 2007, **111**, 12871–12877.
25 J. Lee and M. Paetzel, *Acta Crystallogr., Sect. F: Struct. Biol. Cryst. Commun.*, 2011, **67**, 188–192.
26 C. Roth, O. V. Moroz, A. Ariza, L. K. Skov, K. Ayabe, G. J. Davies and K. S. Wilson, *Acta Crystallogr., Sect. D: Struct. Biol.*, 2018, **74**, 463–470.
27 P. W. Tardioli, M. F. Vieira, A. M. S. Vieira, G. M. Zanin, L. Betancor, C. Mateo, G. Fernández-Lorente and J. M. Guisán, *Process Biochem.*, 2011, **46**, 409–412.
28 J. Sauer, B. W. Sigurskjold, U. Christensen, T. P. Frandsen, E. Mirgorodskaya, M. Harrison, P. Roepstorff and B. Svensson, *Biochim. Biophys. Acta, Protein Struct. Mol. Enzymol.*, 2000, **1543**, 275–293.
29 *Italian decree by the Ministry for the Environment, D.M 173/2016*, **https://www.gazzettaufficiale.it/eli/id/2016/09/06/16G00184/sg**.
30 A. Broccoli, L. Morroni, A. Valentini, V. Vitiello, M. Renzi, C. Nuccio and D. Pellegrini, *Aquat. Toxicol.*, 2021, **237**, 105905.
31 M. Piccardo, F. Provenza, S. Anselmi, A. Broccoli, A. Terlizzi and M. Renzi, *J. Mar. Sci. Eng.*, 2021, **9**, 1–17.
32 S. Bruzzone, C. Chiappe, S. E. Focardi, C. Pretti and M. Renzi, *Chem. Eng. J.*, 2011, **175**, 17–23.
33 C. Pretti, M. Renzi, S. Ettore Focardi, A. Giovani, G. Monni, B. Melai, S. Rajamani and C. Chiappe, *Ecotoxicol. Environ. Saf.*, 2011, **74**, 748–753.
34 M. E. Belowich and J. F. Stoddart, *Chem. Soc. Rev.*, 2012, **41**, 2003–2024.

4 Application of lipases physically immobilized on rice husk in industrially relevant processes

4.1 Background

4.1.1 Lipases

Lipases (triacylglycerol hydrolases, EC 3.1.1.3) are ubiquitous enzymes which catalyze the hydrolysis of triglycerides to glycerol and fatty acids.[139,140] They are serine hydrolases, which indicates that their catalytic mechanism is based on a "catalytic triad" formed by serine, histidine, and aspartate or glutamate.[139] The hydrolysis mechanism is displayed in Scheme 12. In the catalytic triad, the serine acts as a nucleophile,[141] and it forms with the substrate a tetrahedral intermediate which is stabilized by a so-called oxyanion hole via hydrogen bonds.

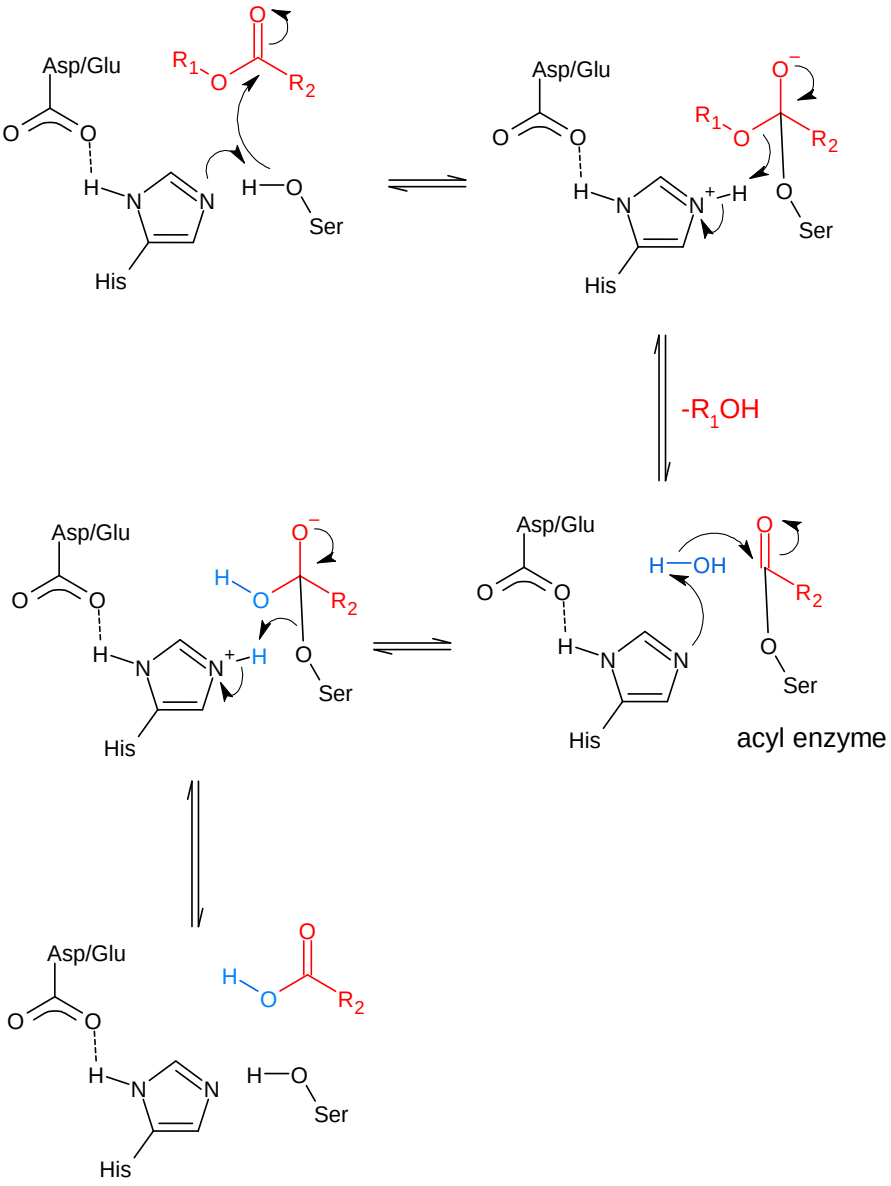

Scheme 12: Hydrolytic mechanism of lipases

A characteristic of lipases is that they act at the lipid-water interface on non-water soluble substrates;[140] for this reason, it is said that they display *interfacial activation*.[142] This is due to a protein structure called *lid*, formed by one or more α-helixes joined to the main protein structure by flexible protein segments.[141] The lid is amphiphilic, presenting an hydrophobic face and a hydrophilic face.[140] In aqueous environment, the hydrophilic face of the lid is exposed to the bulk medium, and the lid blocks the access to the active site; the protein is in the so-called "closed" conformation. In the presence of a lipid-water interface, there is a conformational change to the protein structure, which causes the exposure of the hydrophobic face of the lid to the bulk; the access to the active site is now open, and the protein is in the so-called "open" conformation. Many lipases, such as the one *Rhizomucor miehei*, *Rhizopus oryzae* or *Thermomyces lanuginosus*, present a lid in their structure, while others, most notably the lipase B from *Candida antarctica*, do not.

In addition to the reaction of hydrolysis of triglycerides to fatty acids and glycerol, lipases have been shown to catalyze other reactions in non-aqueous media, such as esterification or transesterification reactions. For this reason, they have found many applications in the industrial sector.

4.1.2 Industrial and commercial relevance of lipases

From an industrial perspective, lipases represent the third most commercialized enzyme; as of 2015, they accounted for more than one fifth of the global enzyme market.[143] Their versatility resides in the ability to catalyze different reaction depending on the nucleophile that intervenes in the catalytic process (Scheme 13). As stated before, physiologically lipases catalyze the hydrolysis of esters (triglycerides) to carboxylic acid (fatty acids) and alcohol (glycerol), using water as a nucleophile. In the presence of limited amounts of water, a lipase can catalyze the inverse reaction of esterification between a carboxylic acid and an alcohol. There are then a series of reactions collectively referred to as "transesterifications", which involve the replacement of the –OR group of the ester with another –OR' functionality. These transesterification reactions can be further divided into: (a) alcoholysis (between an ester and an alcohol), (b) acidolysis (between an ester and a carboxylic acid), (c) aminolysis (between an ester and an amide) and (d) interesterification (between two esters).

Due to this variety of catalyzed reactions, there are numerous industrial applications for lipases, which have been extensively reviewed in literature.[10,13,141,143,144] Some of these applications will be summarized in the following section.

Hydrolysis

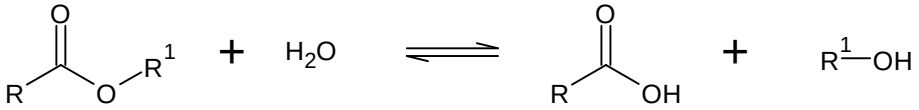

Esterification

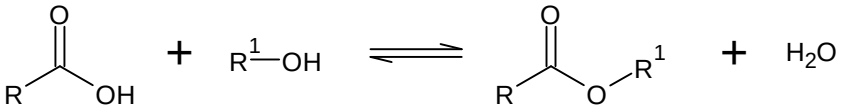

Alcoholysis

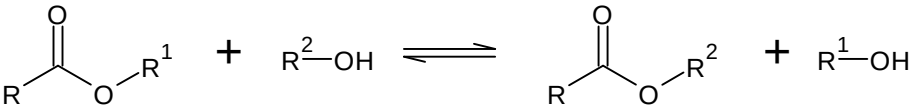

Acidolysis

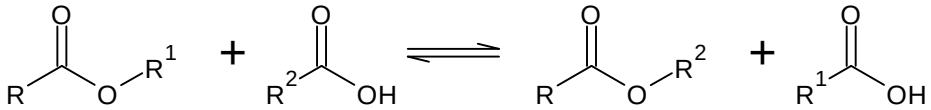

Aminolysis

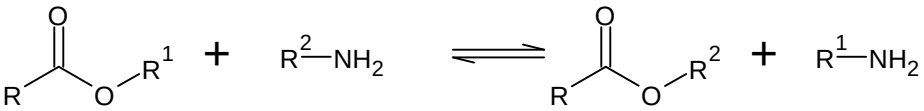

Interesterification

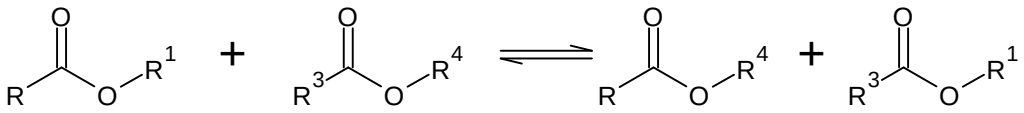

Scheme 13: Examples of reactions catalyzed by lipases[141,143]

4.1.2.1 Detergent industry

One of the first large-scale applications of lipases is as additives in the formulation of detergents, due to their natural ability to degrade triglycerides. They can be used in laundry detergents, to remove fatty stains;[145,146] the first lipase used in this field was lipase from *Thermomyces lanuginosus*, commercialized in 1988 by Novo Nordisk.[147] It has been demonstrated that lipase-enriched detergents are 15-20% more effective, compared to non-lipase-containing detergents, in removing olive oil from cotton fabrics.[148] They have also commercial applications in dishwashing liquids,[149,150] to purify dry-cleaning solvents,[151] or for contact lens cleaning.[152]

4.1.2.2 Food industry

Lipases find widespread applications in the food industry. They are widely employed in the dairy sector. For example, the hydrolysis of triglycerides in milk fat produces free fatty acids, which subsequently react to form other molecules which contribute to the flavor of the final cheese product. [153,154] The use of lipases as additives in cheese production can also reduce ripening times, while improving flavour characteristics.[155,156] Finally, the characteristic aroma of blue cheese is due to lipase from *Penicillium roqueforti*.[157]

Cocoa butter is widely used in the confectionery industry for the production of chocolate and spreadable creams, but it is a costly product and the amount produced yearly is not sufficient to meet the market demand. For this reason, another important application of lipases is the production of cocoa butter equivalents by enzymatic interesterification of cheaper vegetable oils, rich in palmitic, oleic and stearic acid, to reach a product with the desired melting and rheological characteristics.[158,159]

The flavor of processed food can be modified by enzymatic synthesis of esters of short chain fatty acids and alcohols which are known flavour and fragrance compounds;[160] examples of such molecules include the short chain esters of *n*-butanol and geraniol.[161]

Several applications of lipases can be found in the baking industry, to improve the texture of bread and crumb structure,[162] and to prolong the shelf-life[163] and improve the softness and volume of baked goods.[164]

Lipases are also used for the removal of fats from meat and fish, to produce lean meat,[165] to improve texture in wheat-based pasta and noodles,[166] to obtain vegetable oils enriched with ω-3 polyunsaturated fatty acids,[167,168] or to obtain human milk fat substitutes.[169] Finally, the addition of lipases during the tea fermentation process can modify the flavour of the final black tea product, increasing the concentration of desirable flavour compounds.[170]

4.1.2.3 Pulp and paper industry

Lipases find numerous applications in the pulp and paper industry.[171] For example, they are used for the removal of pitch. Pitch is the collective name given to lipophilic extracts of wood and other lignocellulosic materials; these extracts include, among others, triglycerides, and waxes. They tend to accumulate on machinery during the paper making process, causing spots and stains on the final product. Lipases, such as Resinase® A2X (Novozymes), can be used to control the amount of pitch in paper products. This enzymatic pitch-control

technology was initially developed in the 1980s by Nippon Paper Industries in Japan.[172] Another application of lipases is the deinking of paper derived from recycled materials.[173,174]

4.1.2.4 Pharmaceutical industry, medical and diagnostic applications

The use of lipases in the pharmaceutical sector involves their application to obtain enantiomerically pure compounds. For example, they are used in the kinetic resolution of racemic flurbiprofen,[175] a nonsteroidal anti-inflammatory drug used in the treatment of osteoarthritis and rheumatoid arthritis. Another example is the synthesis of baclofen,[176] used for the therapy of pain or as a muscle relaxant. Several commercially available lipases, both immobilized[177–179] and in solution,[180,181] are specifically marketed for use in pharmaceutical synthesis.

On top of being used in the synthesis of pharmaceuticals, lipases also find direct therapeutic applications. For example, they are involved in the activation of Tumor Necrosis factor, and can therefore be used in the treatment of malignant tumors.[182] Moreover, pancreatic lipases are used in enzyme replacement therapy for patients with pancreatic insufficiency.[183]

They can also be used as biosensors to determine the concentration of triglycerides,[184] and levels of lipases in blood serum can be used as a diagnostic tool for detecting conditions such as acute pancreatitis.[185]

4.1.2.5 Other industrial and commercial applications

Lipases have also been used in the cosmetic industry, for example in the production of substances such as isopropyl palmitate and 2-ethylhexyl palmitate, used as emollients in personal care products.[186] Retinoids, which are used in skin-care products, can be synthesized with immobilized lipases.[187] There are also formulations of hair waving preparations containing lipases.[188]

The production of biofuels from vegetable oils can be achieved by the enzymatic transesterification of said vegetable oils with ethanol and methanol.[189–191]

In the leather industry, an important step prior to leather tanning is the removal of fat and protein debris from animal skin. This can be achieved by treating the skin with a mixture of enzymes, including proteases and lipases.[192,193]

Wastewaters containing hydrophobic, fatty components can pose significant environmental issues. The removal of grease, fats and oils from wastewaters from restaurants and households can be achieved through the use of lipases.[194,195]

4.1.3 Industrial Enzymatic Interesterification (EIE)

Interesterification is the redistribution of fatty acid chains on the glycerol backbone by ester-ester exchange.[196] A result of this process is the modification of the triglycerides (TAG) for the production of mixtures with the desired physical and nutritional characteristics.[197]

The interesterification reaction can be chemical or enzymatic. Chemical interesterification requires heat and the use of an alkaline reactant such as sodium methoxide.[196,197] This process randomly rearranges the fatty acid chains on the glycerol backbone of the triglyceride.[198,199] Enzymatic interesterification, on the other hand, is achieved by the use of a lipase. The enzymatic process is receiving more and more attention due to several aspects: it employs milder reaction conditions, does not involve the use of hazardous chemicals, leads to the formation of less by-products and has an easier product recovery process.[198,200] Moreover, the interesterification process can be oriented towards the 1,3 position or the 2 position on the glycerol backbone depending on the specificity of the employed lipase.[201] The use of milder reaction conditions, more specifically lower reaction temperature (40–90°C) compared to that of chemical interesterification (210–260°C), prevents the degradation of bioactive compounds and fatty acids, ensuring a higher quality and better shelf-life of the final reaction product.[198] Several immobilized lipases are commercialized for interesterification purposes, including the *sn*-1,3-specific Lipozyme TL IM and Lipozyme RM IM (Novozymes) and the non-specific Novozym 435 (Novozymes) and Lipase PS-D-I (Amano).[200]

Important products industrially obtained by interesterification are human milk fat substitutes,[202] oils enriched in poly-unsaturated fatty acids,[203] functional 1,3-diglycerides and structured lipids,[204] and cocoa butter substitutes.

4.1.3.1 Cocoa butter alternatives

Cocoa butter is an expensive and relatively scarce produce of the agricultural industry, and for this reason the synthesis of cocoa butter substitutes from cheaper fats and oils is a very important industrial process. The characteristics and melting properties of cocoa butter are associated with (1) high content in 1,3-stearoyl-2-oleoyl glycerol (SOS), 1-palmitoyl-2-oleoyl-3-stearoyl glycerol (POS) and 1,3-palmitoyl-2-oleoyl glycerol (POP), (2) 85% or more oleic acid residues at the sn-2 position of the glycerol backbone, (3) 82% desaturated mono-unsaturated triglycerides on the total triglyceride content and (4) a suitable crystal structure.[205]

Cocoa butter alternatives are categorized as cocoa butter equivalents (CBEs), cocoa butter replacements (CBRs) and cocoa butter substitutes (CBSs). Of these, CBRs and CBSs cannot be mixed with natural cocoa butter, due to the different molecular composition of the contained triglycerides; this leads to sensory defects that prevent the commercial distribution of such products.[206] On the other hand, cocoa butter equivalents have fatty acid distributions compatible with that of cocoa butter, but to obtain reaction products it is necessary to use enzymes in order to have a regiospecific reaction on the original vegetable oil. Microbial lipases used with this aim are, for example, those from *Rhizomucor miehei* and *Thermomyces lanuginosus*, which are *sn*-1,3-specific.

4.1.4 Lipozyme TL IM – Immobilized lipase from *Thermomyces lanuginosus*

At the beginning of the 2000s, Novozymes commercialized an immobilized lipase from *Thermomyces lanuginosus* which would become very popular for trans- and interesterification applications. Lipozyme TL IM was marketed as a robust and cost-effective formulation. Its production combines the use of an inorganic support, in this case porous silica, and an organic binder, Glucidex DE21; the silica is fed into a mechanical granulator, while the binder is dissolved in the aqueous enzyme solution and successively added in the granulator. This

way, the silica aggregates into granules containing the enzyme and held together by the binder. The granules are then dried to obtain particles of size in the range of 300-1000 μm, with a mean of 500-600 μm.[207]

These granules were developed as a cost-effective lipase formulation, suitable for both batch and fixed bed operation. However, as the developers point out, they are not suitable for aqueous processes, since the granules disintegrate in water.[207]

Over the years, several studies have been aimed at investigating the stability of Lipozyme TL IM in industrially relevant processes. The results of these investigations evidence how the stability of the enzyme depends greatly on the tested reaction conditions. Here are reported some examples.

Rønne et al.[208] studied the stability of two immobilized lipases, Lipozyme TL IM and Lipozyme RM IM, in the interesterification of butter fat with rapeseed oil. In particular, the operational stability of Lipozyme TL IM was studied in a continuous packed bed reactor. The lipase activity was deemed by the authors "not very stable" over a 30-day operation period: the activity remained practically constant for the first five days of reaction, then it decreased dramatically until day 15, where it reached a plateau at about 40% of the initial activity level. The reduction in activity was attributed to the reaction system: free butyric acid, a byproduct of the reaction, was observed to lower the activity of the immobilized lipase.

Zhang et al.[209] studied the interesterification of palm stearin with coconut oil for margarine production in 1-kg or 300-kg pilot-scale batch stirred tank reactors. On both tested scales, the authors observed good reusability of the immobilized enzyme over 11 batch reaction cycles, showing a stable relative degree of interesterification.

Yang et al.[210] analyzed the production of structured lipids by *sn*-1,3-specific interesterification of soybean oil with medium-chain triacylglycerol in continuous conditions. They employed Lipozyme TL IM in a packed bed reactor, and analyzed the stability of the immobilized enzyme over 17 consecutive 12-hour reaction batches. The interesterification degree decreased gradually until it was close to 0 in the last cycle.

Osório et al.[211] also analyzed the operational stability of Lipozyme TL IM in a packed bed reactor in solvent free conditions. Two fat blends were analyzed as substrates of the study: (a) palm stearin (55 % wt.), palm kernel oil (25% wt.) and sunflower oil (20% wt.) and (b) palm stearin (66% wt.), palm kernel oil (35% wt.) and EPAX 4510TG (10% wt.). EPAX 4510TG is a commercial triglyceride blend rich in polyunsaturated fatty acids. The bioreactor was kept in continuous operation at 70°C for 580 h (blend a) and 390 h (blend b). The authors observed half-lives of 135 h (blend a) and 77 h (blend b), and attribute the lower stability with blend b to the presence of polyunsaturated fatty acid chains, which are prone to oxidation.

4.2 Summary and objectives

Previous works from prof. Gardossi's research group[62] concerned the physical immobilization of TLL on rice husk; the aim was to obtain a biocatalyst to be used in low-water, hydrophobic media as a potential alternative for Lipozyme TL IM. The resulting biocatalysts, consisting of TLL physically immobilized on rice husk with water-soluble binders, was developed in order to ensure the environmental and economic sustainability of the overall enzymatic process.

In this chapter, these TLL formulations were studied in relation to their ability to catalyze the interesterification of two triglycerides, tristearin and triolein. The interesterification reaction was chosen as industrially relevant for several applications, including the production of cocoa butter equivalents, of zero-*trans* margarine, and of oils enriched in polyunsaturated fatty acids.

The stability in water of the TLL formulations was poor, due to the soluble nature of the binders used in water. An attempt to improve this stability in water was made by cross-linking the enzyme preparations with DFF, whose ability to bind with proteins was demonstrated in the previous chapter. The stability of the resulting crosslinked preparations was analyzed in aqueous environment.

Finally, the TLL preparations were tested for the solvent-free interesterification of triolein and tristearin in solvent-free systems for exploring their applicability in this process of high industrial relevance.

4.3 Results and Discussion

In previous works from prof. Gardossi's research group,[62] TLL had been physically immobilized on milled RH in a fluidized bed in the presence of different water-soluble binders. The resulting preparation is constituted by single RH fragments coated with a layer of immobilized enzyme. The binders employed for the immobilization were polyvinylpyrrolidone (PVP) and hydroxyethyl cellulose (HEC).

Before attempting to employ the physically immobilized TLL for an industrially relevant reaction, the activity of the preparations was tested for tributyrin hydrolysis. The water content of the enzyme preparations was also measured. The results are presented in the following table.

Table 16: Water content and hydrolytic activity (hydrolysis of tributyrin) for two preparations of physically immobilized TLL

	Activity (U/g)	**Water content (%)**
PVP-TLL	5698 ± 869	6.9
HEC-TLL	3472 ± 66	7.8

The stability of the TLL formulations had been previously tested in the hydrolysis of tributyrin in aqueous emulsion.[62] The results are displayed in the following figure.

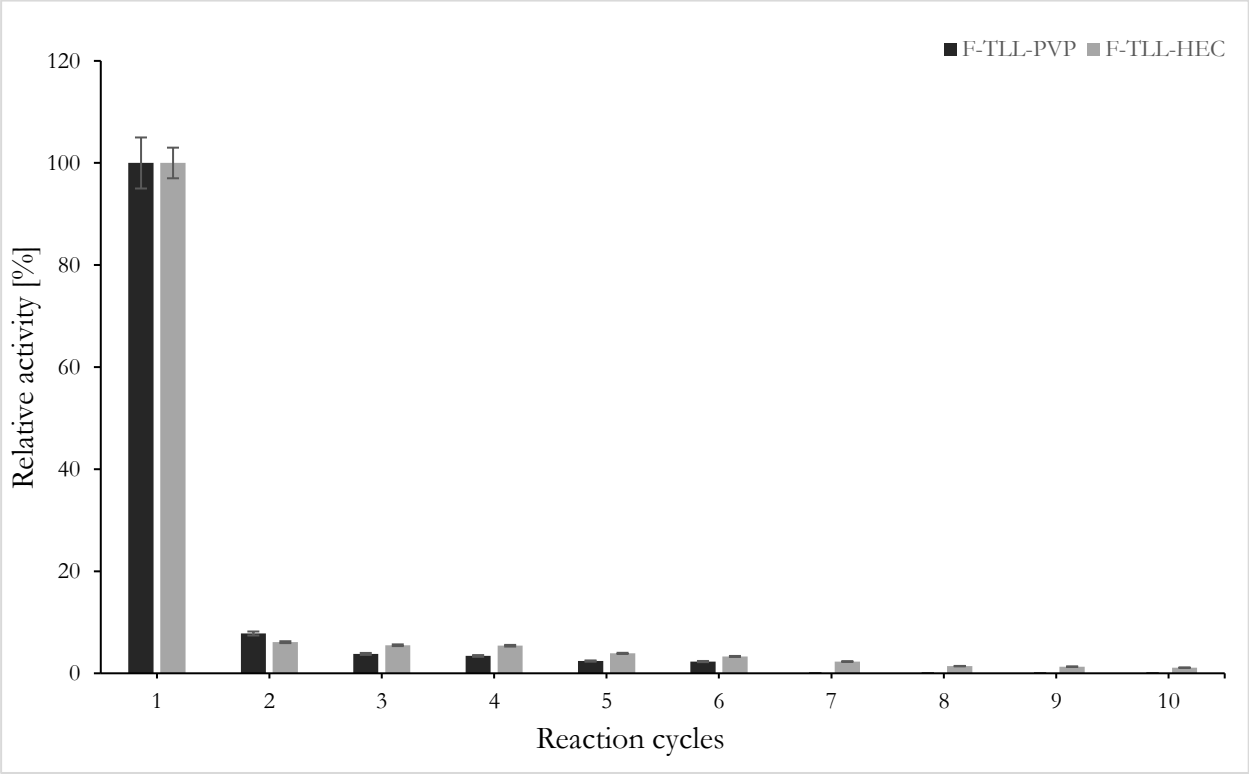

Figure 37: Decrease of hydrolytic activity of the two formulations obtained by adsorbing TLL on rice husk. From Spennato et al., 2021[62]

It is clear that the lipase formulations are not stable in aqueous environment. This is due to the binders used in the formulation: being water-soluble, they dissolve in water, leading to a leaching of the enzyme from the rice husk. In order to improve the stability of the enzyme in these conditions, the stabilization of the enzymatic formulation was explored, by crosslink the enzyme molecules with the bifunctional agent DFF.

4.3.1 Crosslinking of the physically immobilized TLL

4.3.1.1 Crosslinking in aqueous environment

The physically immobilized TLL preparations were crosslinked using DFF as a difunctional agent and different crosslinking protocols based on pre-existing literature.[15] The results are displayed in Table 17, while the crosslinking conditions are detailed in the "Materials and Methods" section.

Table 17: Recovered activity from the experiments of crosslinking of TLL physically immobilized preparations in aqueous environment

Crosslinking Protocol	Solvent	DFF (μmol/g)	Activity (U/g_{dry})	
			PVP	HEC
Reference[a]	–	–	5698 ± 869	3472 ± 66
1	KPi (0.1 M, pH 7)/IPA 1:1	72.5	286 ± 35	352 ± 71
2	NaCl 3M	800	251 ± 17	207 ± 24
3	KPi 0.1 M, pH 7	800	123 ± 23	191 ± 20

[a] Non-crosslinked enzyme preparation

As can be seen in the table, all experiments resulted in a decrease of the specific hydrolytic activity of the enzyme formulations after crosslinking. This decrease in specific activity is presumably due to a detachment of the enzyme from the support. The binders used for the physical immobilization on rice husk are water-soluble, and the crosslinking was attempted in aqueous environment, therefore the enzyme probably leached in solution from the support during the crosslinking process. For this reason, the crosslinking experiments were also attempted in organic solvent.

4.3.1.2 Crosslinking in organic solvent

The solvent chosen for the crosslinking experiments was dichloromethane. The choice of the solvent was due to the low solubility of DFF in the majority of other tested organic solvents. Since Table 17 indicates that the amount of crosslinker does not appreciably influence the recovered activity, it was decided to use a low amount of DFF (80 μmol/g). Two different reaction times were tested, 4 and 24 hours, to determine whether an increase in reaction time would result in a more efficient crosslinking of the protein.

Table 18: Recovered activity from the experiments of crosslinking of TLL physically immobilized preparations in dichloromethane

Crosslinking protocol	V CH_2Cl_2 (mL)	DFF (µmol/g)	Reaction time (h)	Activity (U/g_{dry})	
				PVP	HEC
Reference[a]	–	–	–	5698 ± 869	3472 ± 66
4	2.5	80.5	4	2015 ± 443	2656 ± 367
5	2.5	80.5	24	1284 ± 34	2683 ± 788

[a] Non-crosslinked enzyme preparation

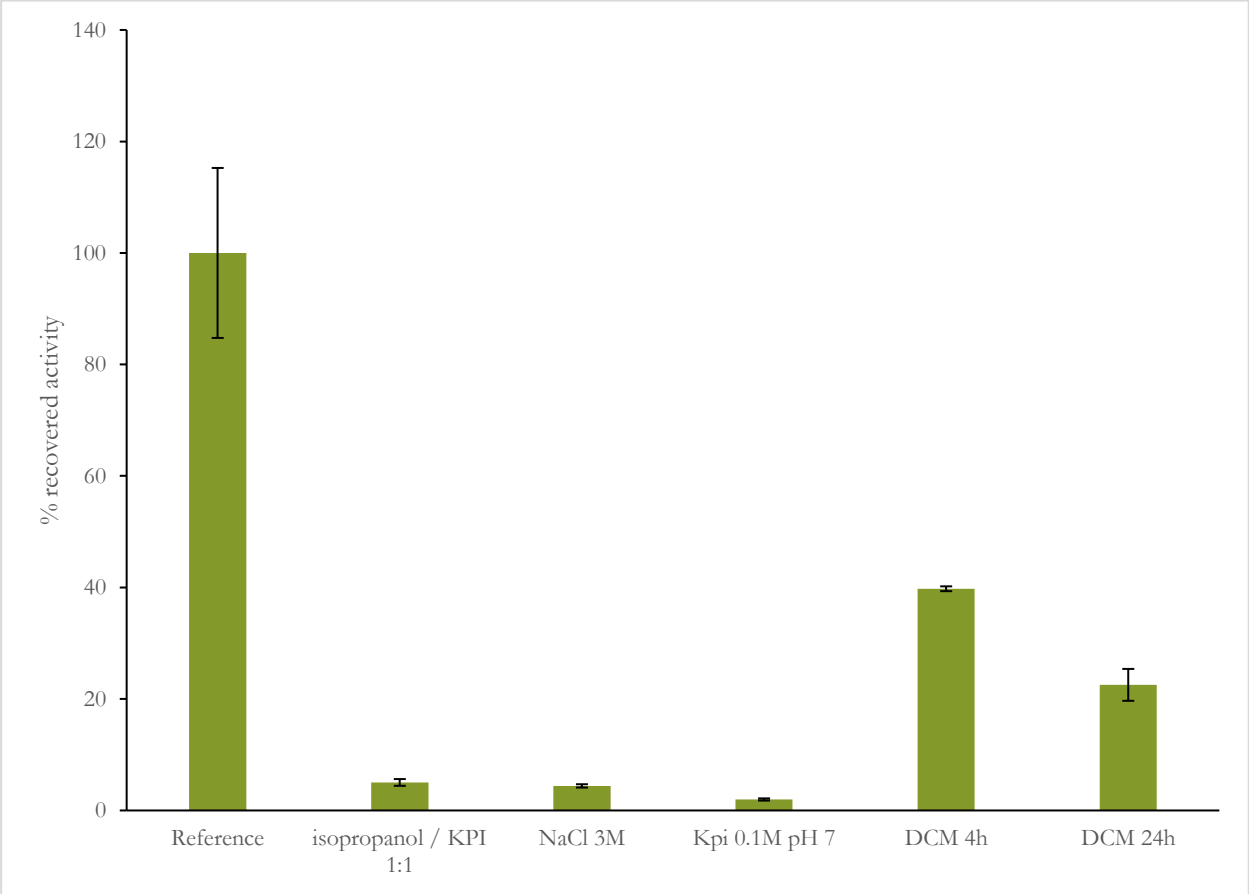

Figure 38: Recovered activity, expressed in % of the non-crosslinked sample activity, of the PVP-TLL crosslinked samples

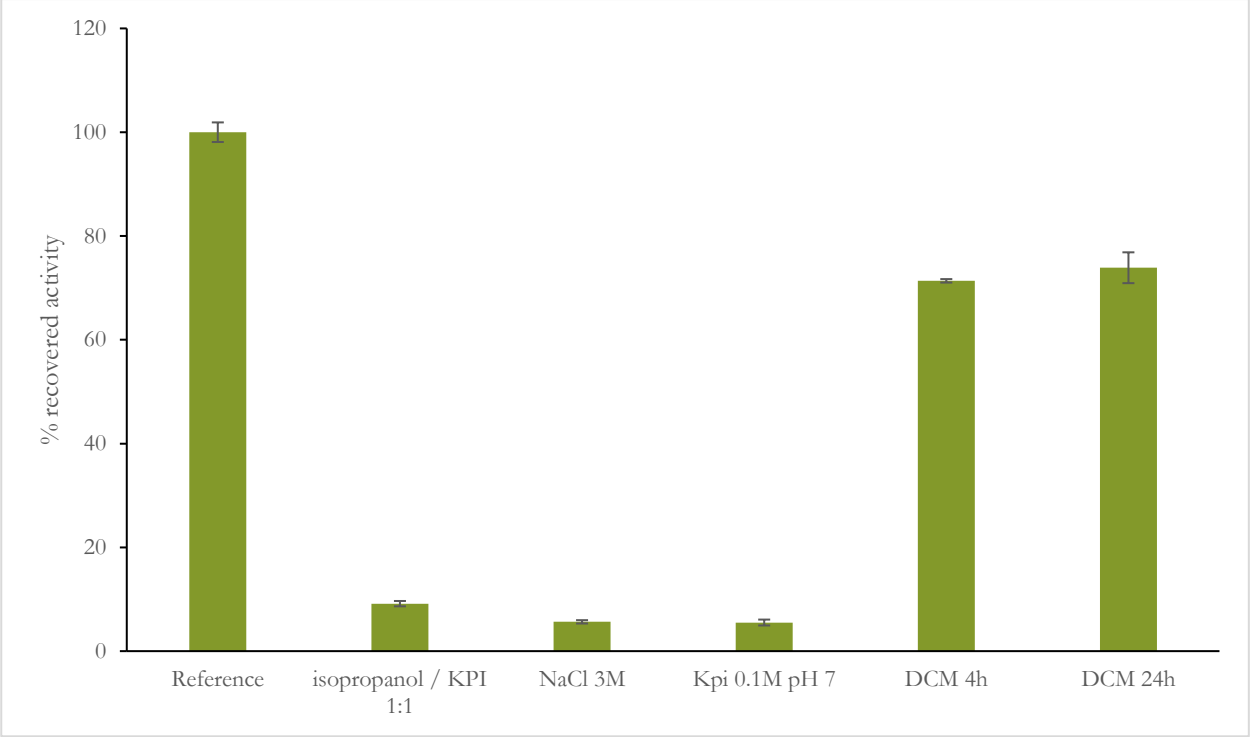

Figure 39: Recovered activity, expressed in % of the non-crosslinked sample activity, of the HEC-TLL crosslinked samples

Table 18, Figure 38 and Figure 39 report the results of the crosslinking experiments, expressed both in specific activity (Table 18) and in % of recovered activity compared to the reference of non-crosslinked enzymatic preparation (Figure 38 and Figure 39).

The results show that, in the case of PVP-TLL formulation, an increase in reaction time from 4 to 24 hours did cause a decrease in recovered activity after the crosslinking. On the other hand, in the case of HEC-TLL formulation, the recovered activities with 4- and 24-hours reaction times are similar.

Moreover, in the case of PVP-TLL formulation, the recovered activity after the crosslinking is about 40% of the initial activity (in the case of the 4 hours reaction). On the other hand, in the case of the HEC-TLL, the recovered activity after crosslinking is about 75% of the initial activity.

The activity of the formulation crosslinked in organic solvent was also tested in recycle batch experiments of tributyrin hydrolysis. The results are reported in Table 19, Figure 40, Figure 41, Figure 42 and Figure 43.

Table 19: Recycle experiments of the TLL enzyme preparations crosslinked in organic solvent

Cycle	Activity (U/g_{dry})			
	PVP CH_2Cl_2 4h	**PVP CH_2Cl_2 24h**	**HEC CH_2Cl_2 4h**	**HEC CH_2Cl_2 24h**
1	1624	1333	3033	3100
2	174	187	146	112
3	110	71	61	63
4	70	52	54	20
5	59	25	21	40

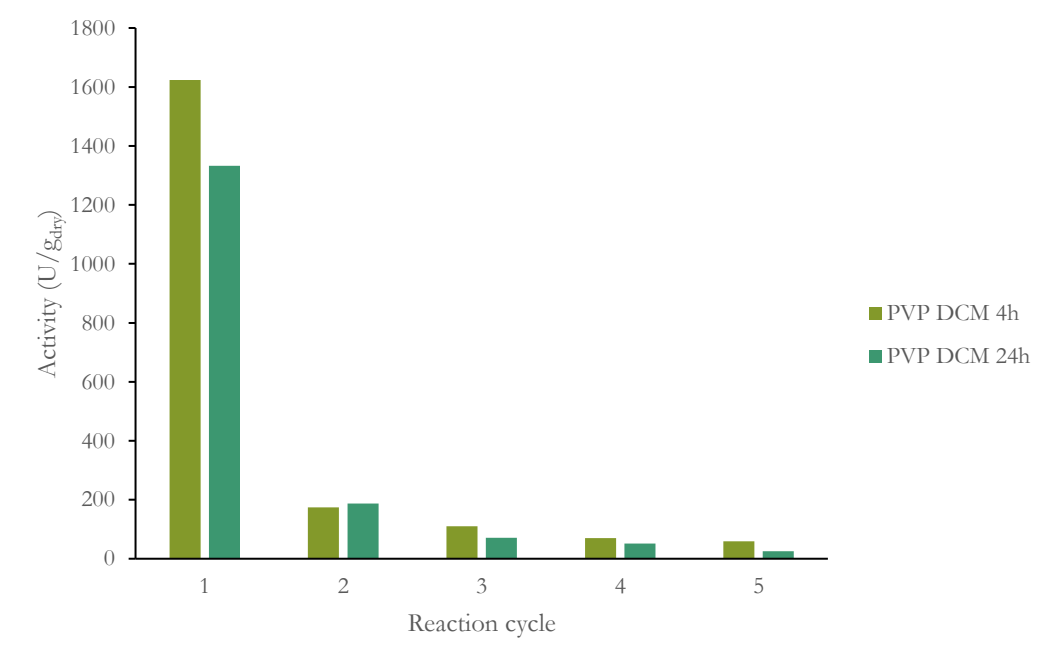

Figure 40: Recycle experiments of PVP-TLL crosslinked in organic solvent

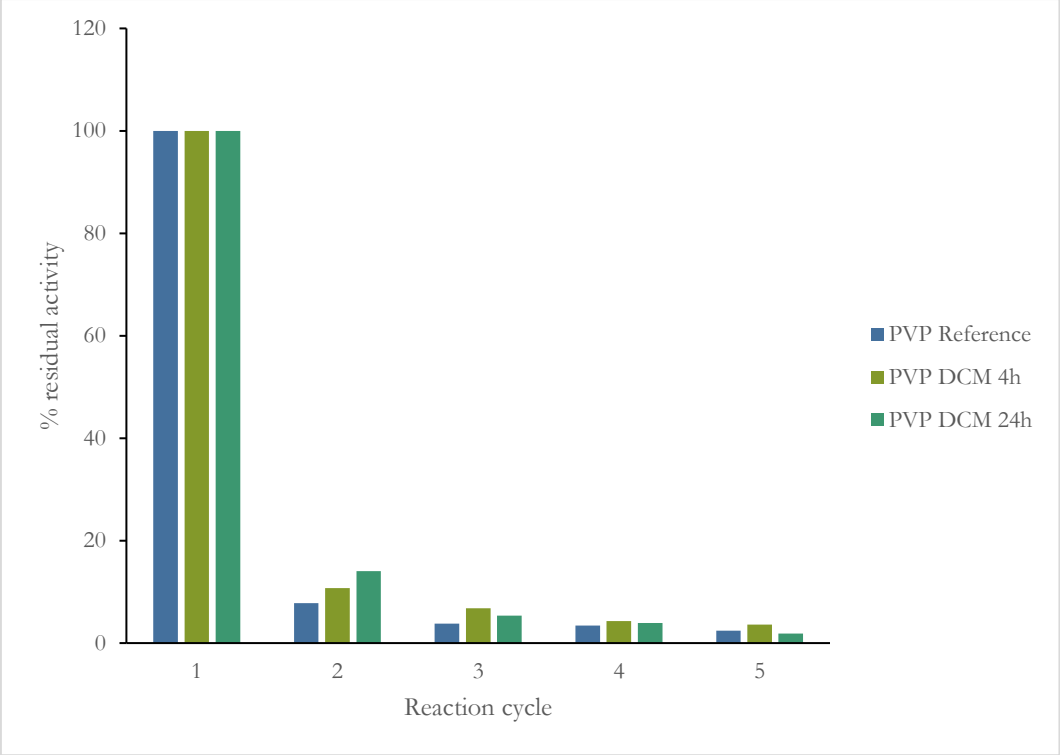

Figure 41: Recycle experiments of PVP-TLL crosslinked in organic solvent – Results expressed in % of the first cycle activity. The reference corresponds to the PVP-TLL preparation before crosslinking. Reference data from Spennato et al., 2021.[62]

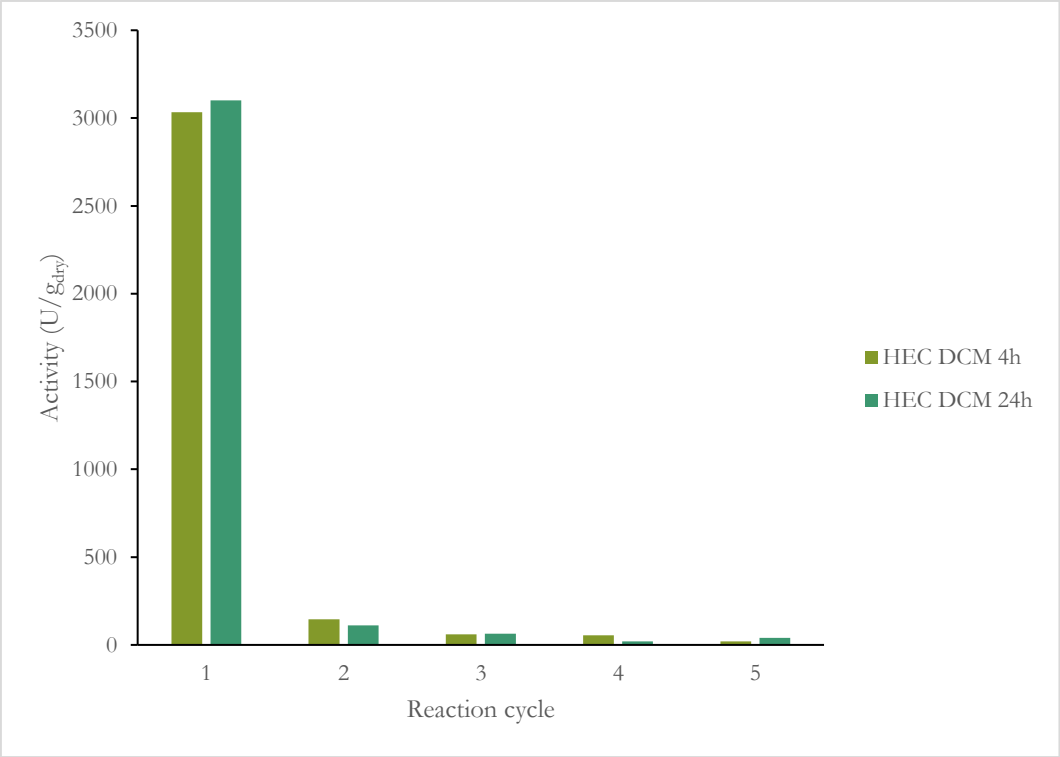

Figure 42: Recycle experiments of HEC-TLL crosslinked in organic solvent

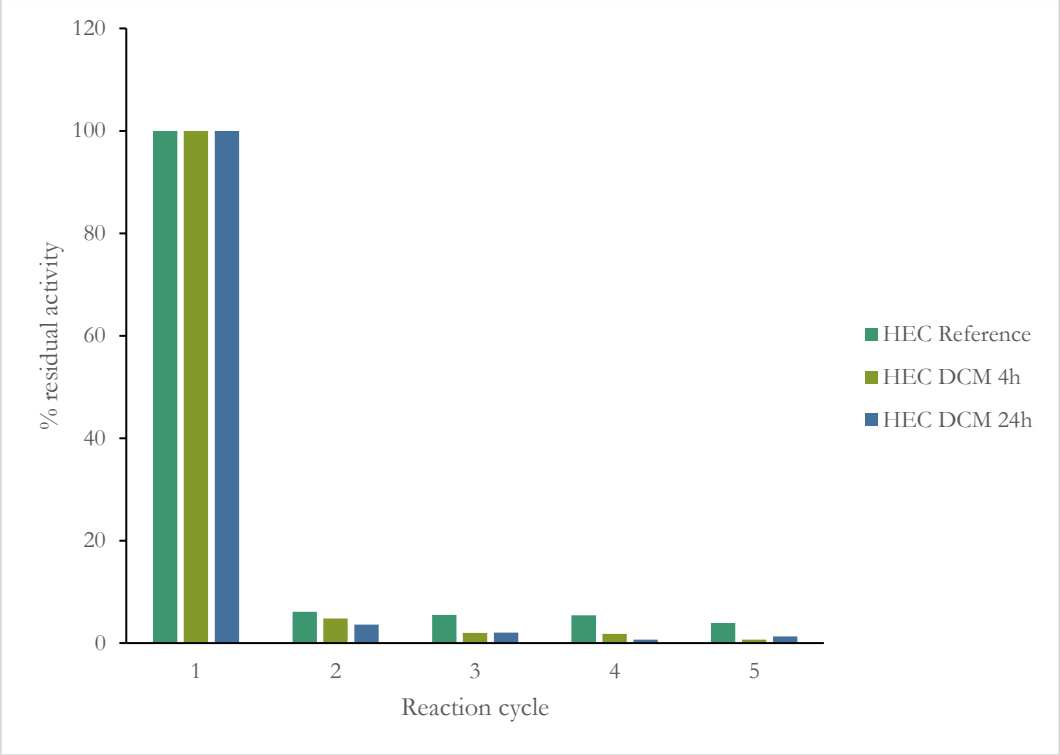

Figure 43: Recycle experiments of HEC-TLL crosslinked in organic solvent – Results expressed in % of the first cycle activity. The reference corresponds to the HEC-TLL preparation before crosslinking. Reference data from Spennato et al., 2021.[62]

In the recycle experiments it is apparent that the recovered activity in the assay cycles after the first is drastically reduced (going to about 10% of the first cycle activity). In the case of PVP-TLL, there is a slight improvement in the residual activity of the preparation after the first cycle compared to the non-crosslinked preparation: the PVP-TLL preparation crosslinked with a reaction time of 24 hours, in the second cycle, has an activity of 14% of that of the first cycle, compared to a 7% in the case of the non-crosslinked preparation.

In conclusion, the use of organic solvent did not lead to a more efficient crosslinking of the proteins but rather had a positive effect on the enzyme activity. This is in agreement with the widely described phenomenon of "interfacial activation" described for TLL.[139,141] The exposure of the physically adsorbed enzyme to the organic solvent offers a hydrophobic interface to the enzyme, which acquire a more favorable open conformation.

4.3.2 Interesterification with non-crosslinked PVP-TLL and HEC-TLL

The formulations were then tested for the interesterification of triolein and tristearin; this reaction was selected due to its industrial importance, as it is used for obtaining cocoa butter analogues in the food industry.

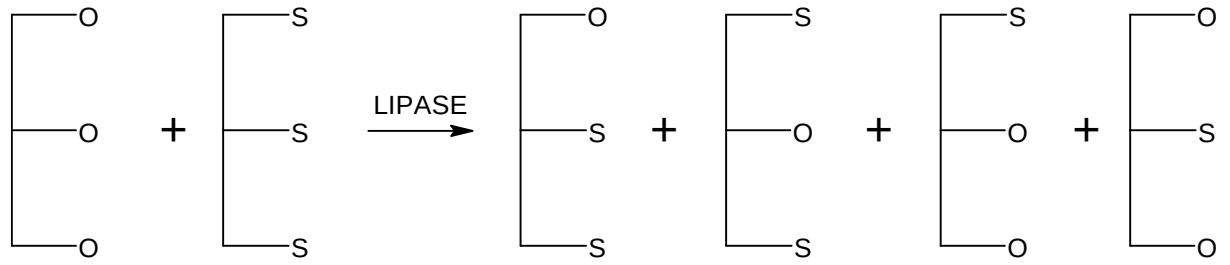

Scheme 14: Enzymatic interesterification of triolein and tristearin. S = Stearic acid, O = Oleic acid

The reaction conditions selected for the preliminary reaction were derived from literature.[207] The reaction substrate was a mixture of tristearin and triolein (27:73 w/w), with an enzyme dosage of 10 wt.%, and no solvent. The mixture was heated to 70°C for 72 hours, and monitored once a day *via* TLC.

Table 20: Enzyme loading for the interesterification assay with PVP-TLL and HEC-TLL

Reaction	Enzyme	Enzyme amount (U)	Enzyme amount ($U/g_{substrate}$)
1	PVP-TLL	285	560
2	HEC-TLL	174	348

Figure 68 in the Annex section reports the TLC obtained on the reaction mixtures after 72 hours. As can be seen, the samples of reaction mixtures show three spots not present in the reference samples, which can be attributed to reaction products. Considering that immobilized TLL is selective towards positions 1 and 3 of the triglyceride,[212] all possible reaction products and their mass have been determined, and are reported in the Annex section for this chapter.

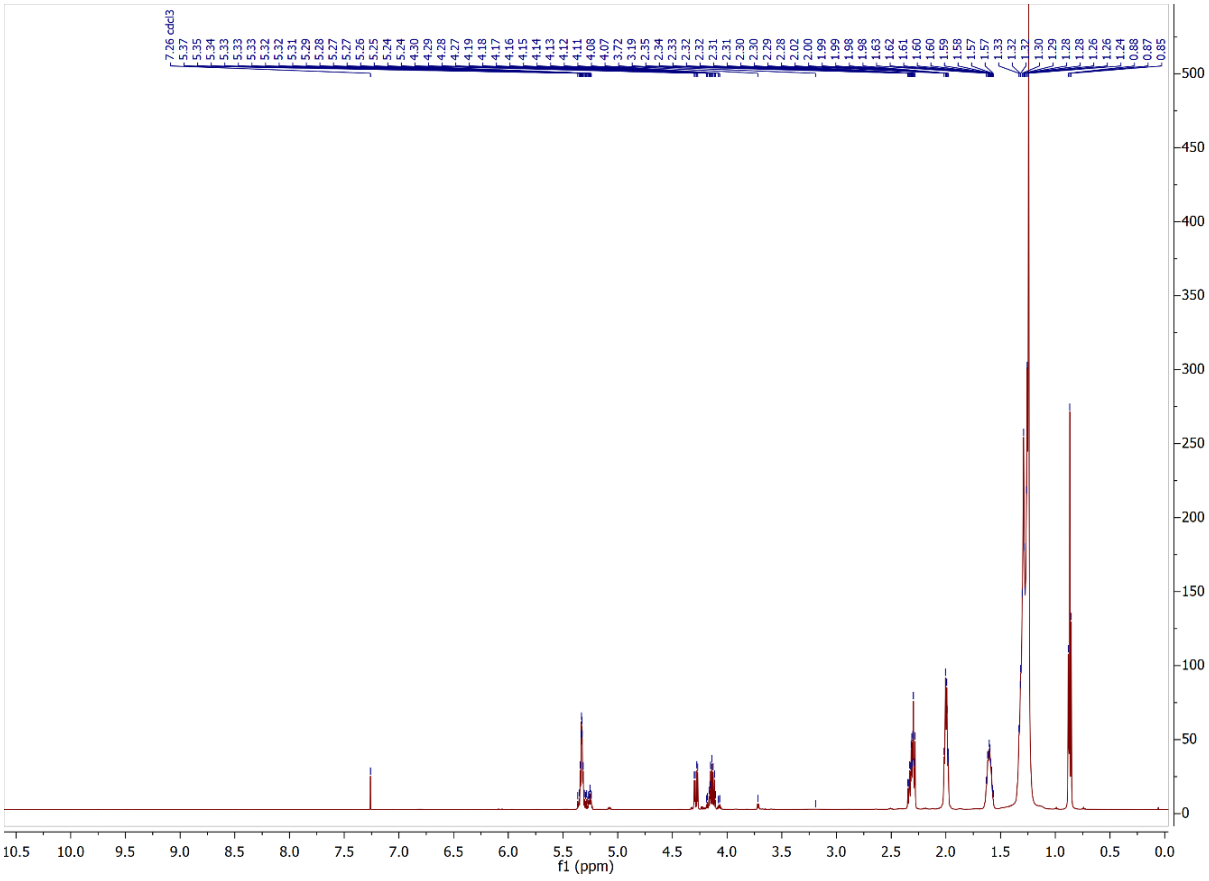

Figure 44: ^{1}H NMR spectrum ($CDCl_3$, 500 MHz) of the interesterification reaction crude after 72 hours

The presence of hydrolysis products in the reaction mixture would have determined the presence of free stearic acid or oleic acid in the mixture. To verify whether these acids were present due to hydrolysis reaction competing with the transesterification reaction, a ^{1}H NMR spectrum in $CDCl_3$ of the reaction mixture was acquired. The spectrum is reported in Figure 44.

As can be seen in the figure, the NMR spectrum presents no signals in the area between 9 and 10.5 ppm. This indicates that, if present, the concentration of hydrolysis products is negligible, and the main reaction in the system is the interesterification.

Finally, ESI-MS spectra were acquired of the two reaction mixtures. The spectra are reported in Figure 45 and Figure 46, while enlargements are reported in Figure 47.

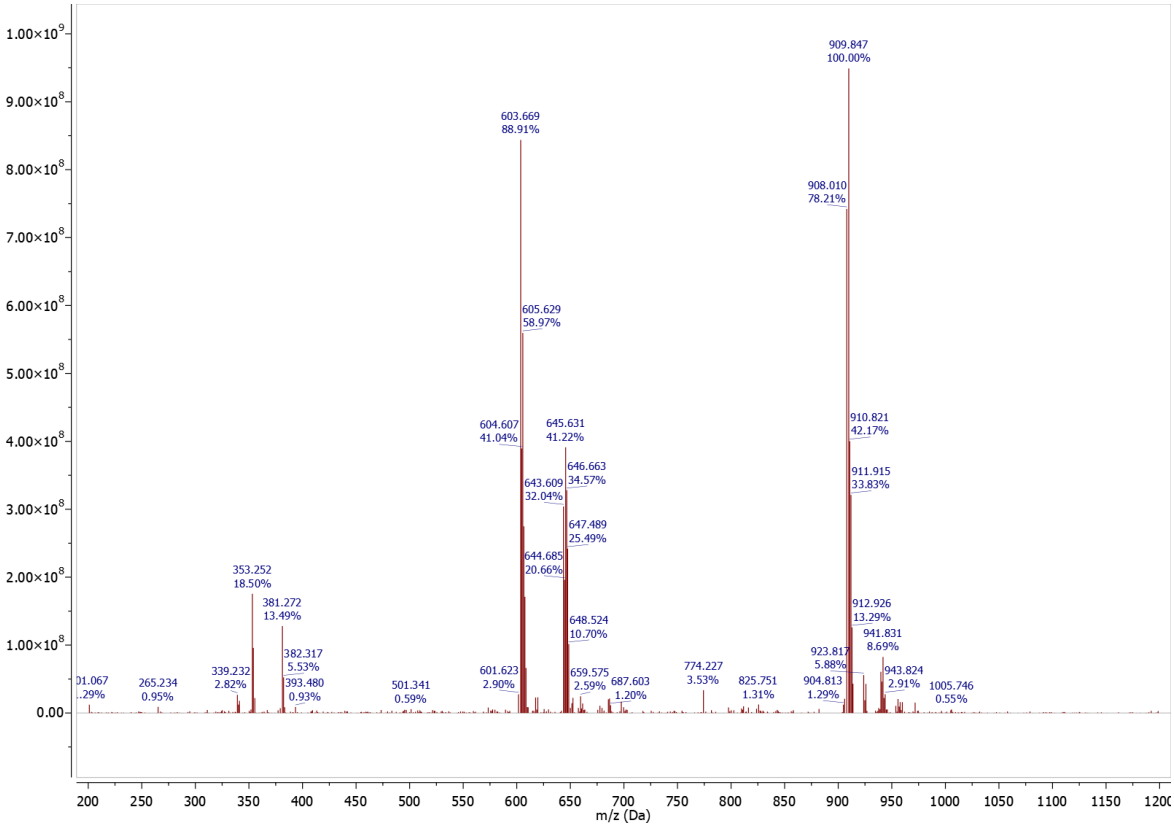

Figure 45: ESI-MS spectrum of the crude of the interesterification catalyzed by PVP-TLL

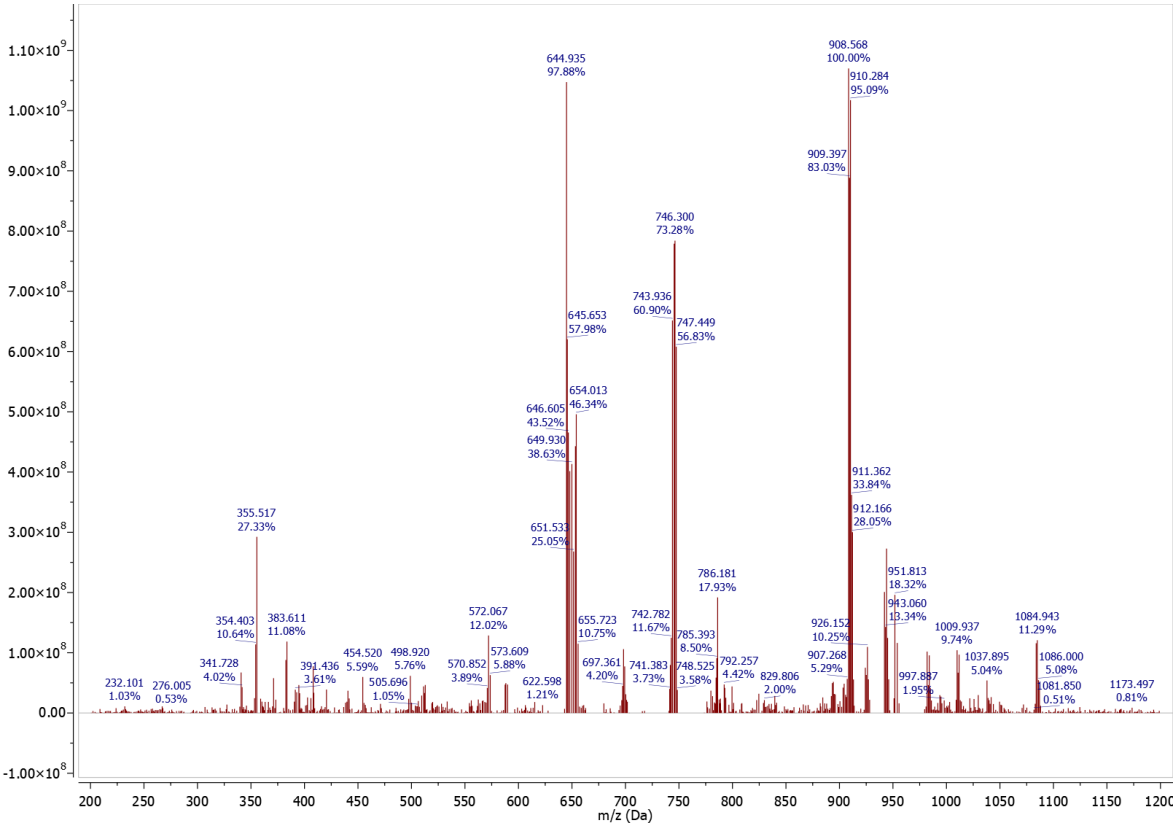

Figure 46: ESI-MS spectrum of the crude of the interesterification catalyzed by HEC-TLL

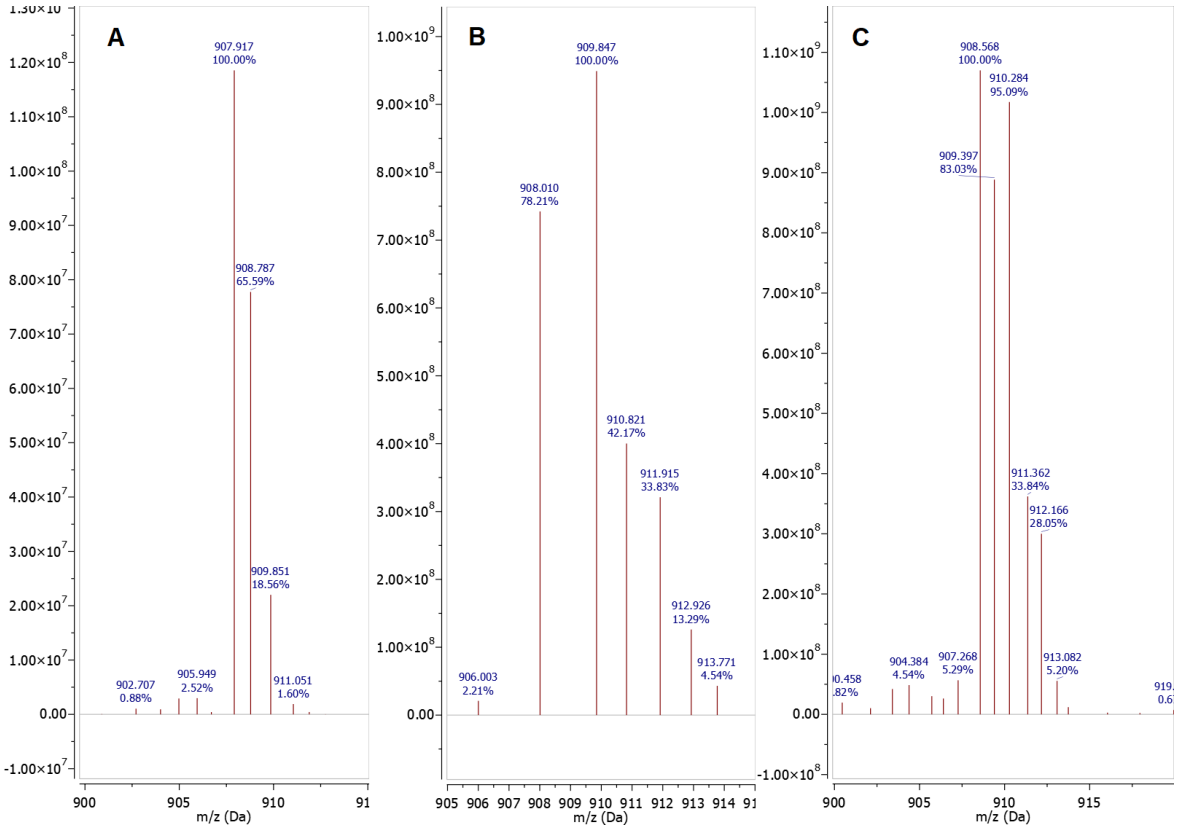

Figure 47: Enlargement of the ESI-MS peaks for the interesterification reaction of triolein and tristearin catalyzed by TLL physically immobilized on rice husk. (A) Reference spectrum of triolein. (B) Crude reaction product of PVP-TLL. (C) Crude reaction product of HEC-TLL.

The peaks at m/z 905-915 correspond to the $[M+Na]^+$ adducts. Analyzing these peaks, it is apparent how the shape and isotope distribution of the peak in the crude reaction products (Figure 47B and C) is different from that of pure triolein (Figure 47A).

The most intense peak in the spectra is the one corresponding to $[M+Na]^+$. Analyzing this peak, it is apparent how the shape and isotope distribution of the peak in the crude reaction product is different from that of pure triolein. In particular, a series of intense peaks at m/z = 908-910 can be observed; these peaks cannot be due to the presence of residual tristearin ($[M+Na]^+$ m/z = 913), nor can be isotope peaks of triolein due to their intensity vastly different from the isotope peaks of pure triolein (Figure 47A). Therefore, these peaks can be attributed to the presence of interesterification products, which display m/z values 2 or 4 units higher than those of triolein.

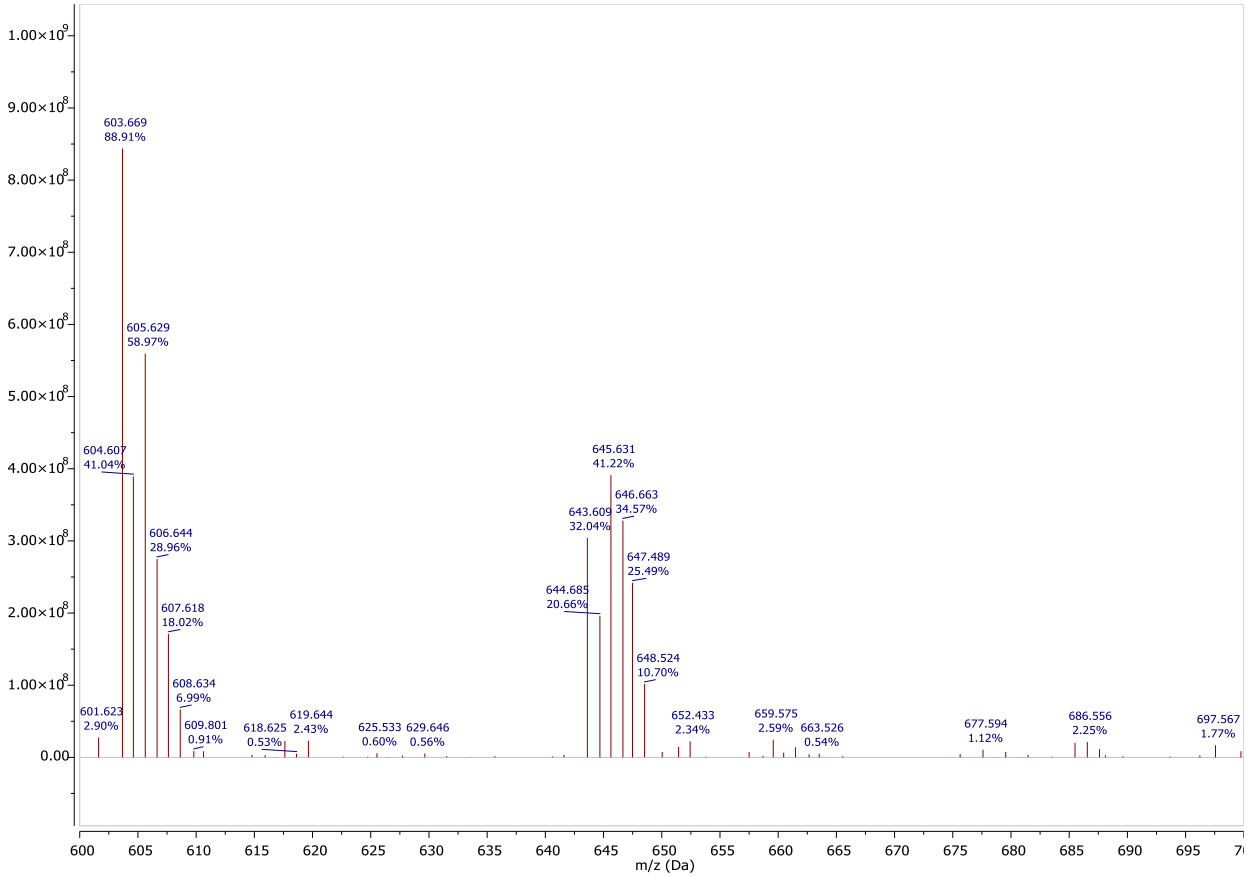

Figure 48: ESI-MS spectrum of the crude of the interesterification catalyzed by PVP-TLL – Enlargement of the interval m/z = 600-700

Another series of interesting peaks can be found in the interval m/z = 600-700. In the case of PVP-TLL (Figure 48) there are two clusters of peaks, one at m/z = 603-609 and the other at m/z = 643-648. The cluster at m/z = 643-648 was attributed to the $[M+Na]^+$ adduct of diolein (OOX); this indicates the potential presence of a concurrent hydrolysis reaction together with the interesterification reaction. The cluster at m/z = 603-609 was initially attributed to the $[3M+K]^+$ adduct of oleic acid (m/z = 603.4); however, this hypothesis was discarded for two main reasons: (1) the pattern of the peaks is far too complex to be the normal isotopic pattern of oleic acid (see theoretical isotopic pattern in the Annex section) and (2) the peak at m/z=603 was also present in the reference spectrum of pure triolein. A literature research revealed that, in the ESI-MS analysis of triglycerides, despite the *soft ionization* technique there can be fragmentation of the triglyceride adducts; in particular, the fragmentation of $[M+Na]^+$ or $[M+2Na]^+$ adducts can lead to the loss of neutral-charge fatty acid chains, in the form of RCOOH or RCOONa salt.[213] In the case of triolein, the peak at m/z = 603.7 can be attributed to the adduct $[M+Na–RCOONa]^+$. Therefore, the peak at m/z = 605.6 can be attributed to the corresponding adduct for the interesterification product SOO/OSO/OSS. This further indicates that the interesterification reaction was successful. The attributed ESI-MS peaks are summarized in the following table.

Table 21: Identified peaks in the ESI-MS spectrum of the interesterification with PVP-TLL

m/z	Compound	Ion
603.7	OOO	$[M+Na-RCOONa]^+$
605.6	OSO / OOS / SOO	$[M+Na-RCOONa]^+$
643.6	OOX	$[M+Na]^+$
645.6	SOX	$[M+Na]^+$
908.0	OOO	$[M+Na]^+$
909.8	OSO / OOS / SOO	$[M+Na]^+$

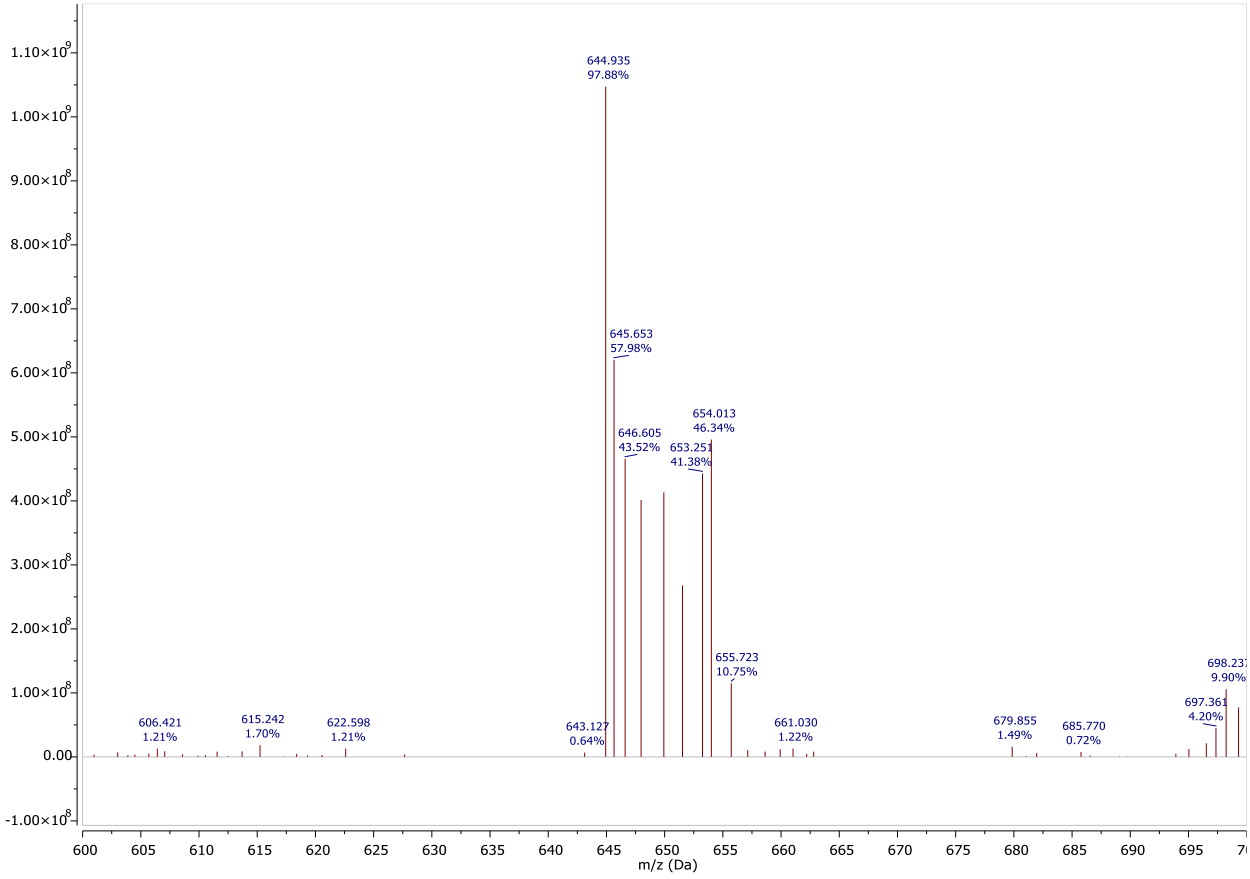

Figure 49: ESI-MS spectrum of the crude of the interesterification catalyzed by HEC-TLL – Enlargement of the interval m/z = 600-700

Interestingly, in the case of the reaction catalyzed by HEC-TLL (Figure 49) the cluster of peaks at m/z = 603-610 (corresponding to OOS or OSO) is completely absent; it is however present, with high intensity, the cluster of peaks at m/z = 643-655, corresponding to the mono-hydrolyzed product OOX. However, no distinct signals corresponding to free carboxylic acids are not evident, in accordance with NMR data. The identified m/z peaks are summarized in the following table.

Table 22: Identified peaks in the ESI-MS spectrum of the interesterification with HEC-TLL

m/z	Compound	Ion
644.9	OOX	$[M+Na]^+$
646.6	SOX / OSX	$[M+Na]^+$
908.6	OOO	$[M+Na]^+$
910.2	SOO / OSO / OOS	$[M+Na]^+$

4.3.3 Recyclability of the physically immobilized TLL for the interesterification of tristearin and triolein

The recyclability of the physically immobilized TLL formulations was tested in the interesterification of triolein and tristearin with the same procedure detailed before, with two batch reaction cycles. Between the two cycles, the crude reaction product was removed, and new reagents were added to the reaction flask without washing the enzyme. The reaction was monitored by taking samples of the crude product at different time intervals and analyzing them *via* DSC analysis. The final crude reaction products were also analyzed by ESI-MS. The results are displayed in the following paragraphs.

4.3.3.1 PVP-TLL

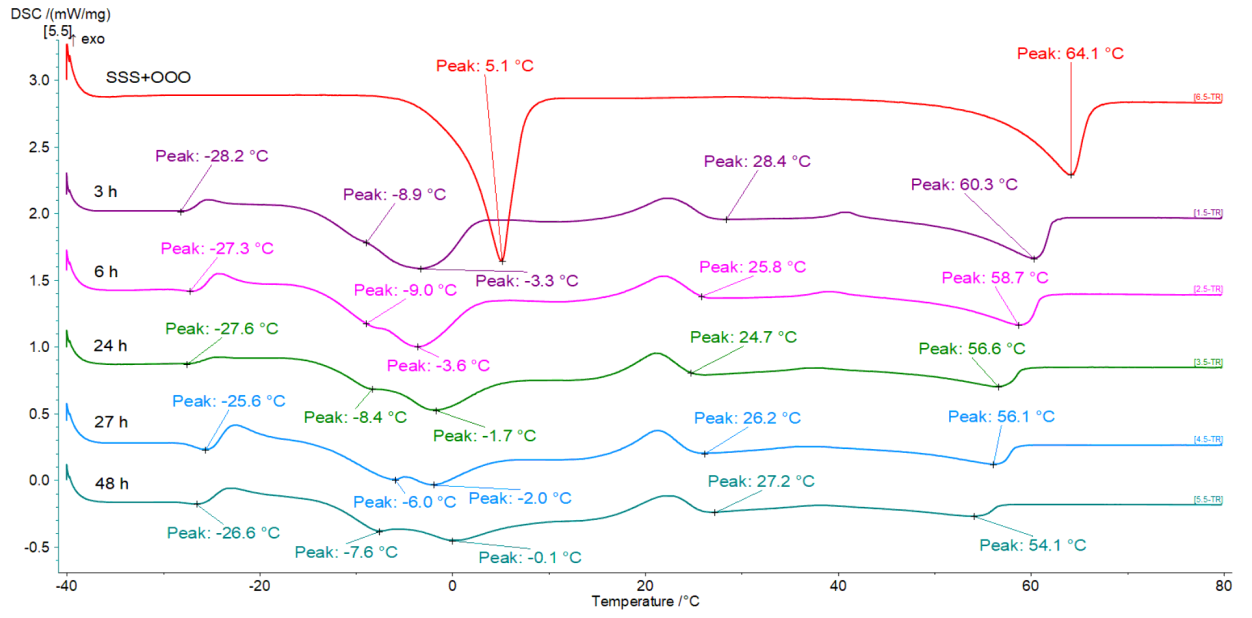

*Figure 50: DSC Analysis of the **first** interesterification cycle of tristearin and triolein with TLL-PVP*

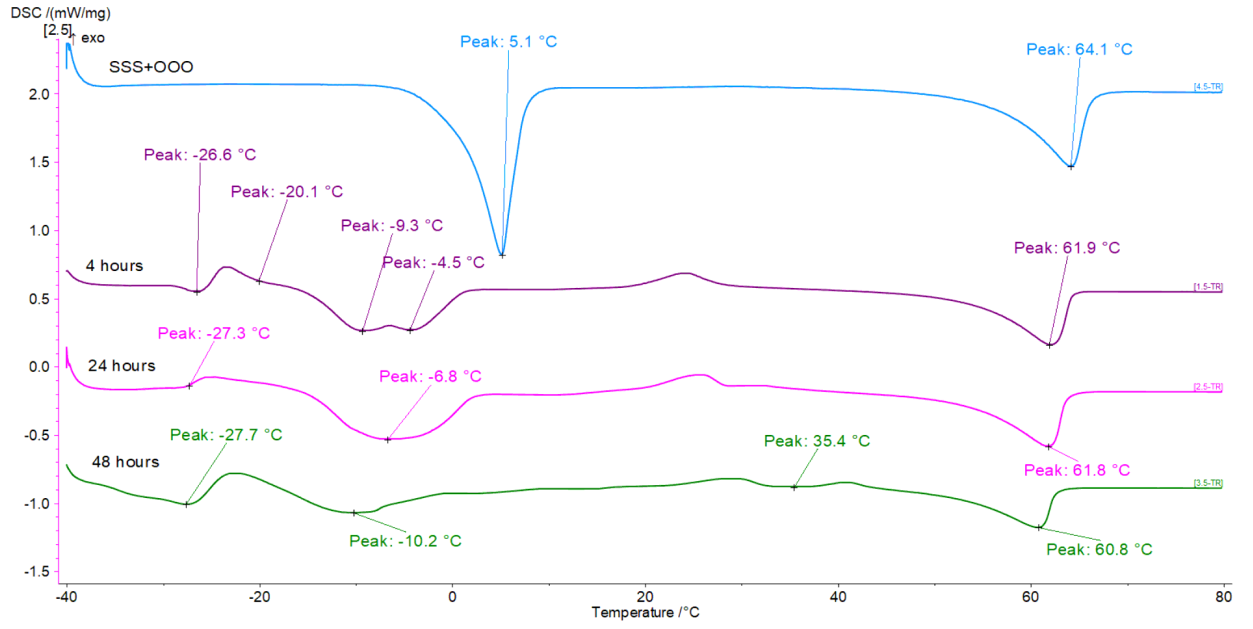

*Figure 51: DSC Analysis of the **second** interesterification cycle of tristearin and triolein with TLL-PVP*

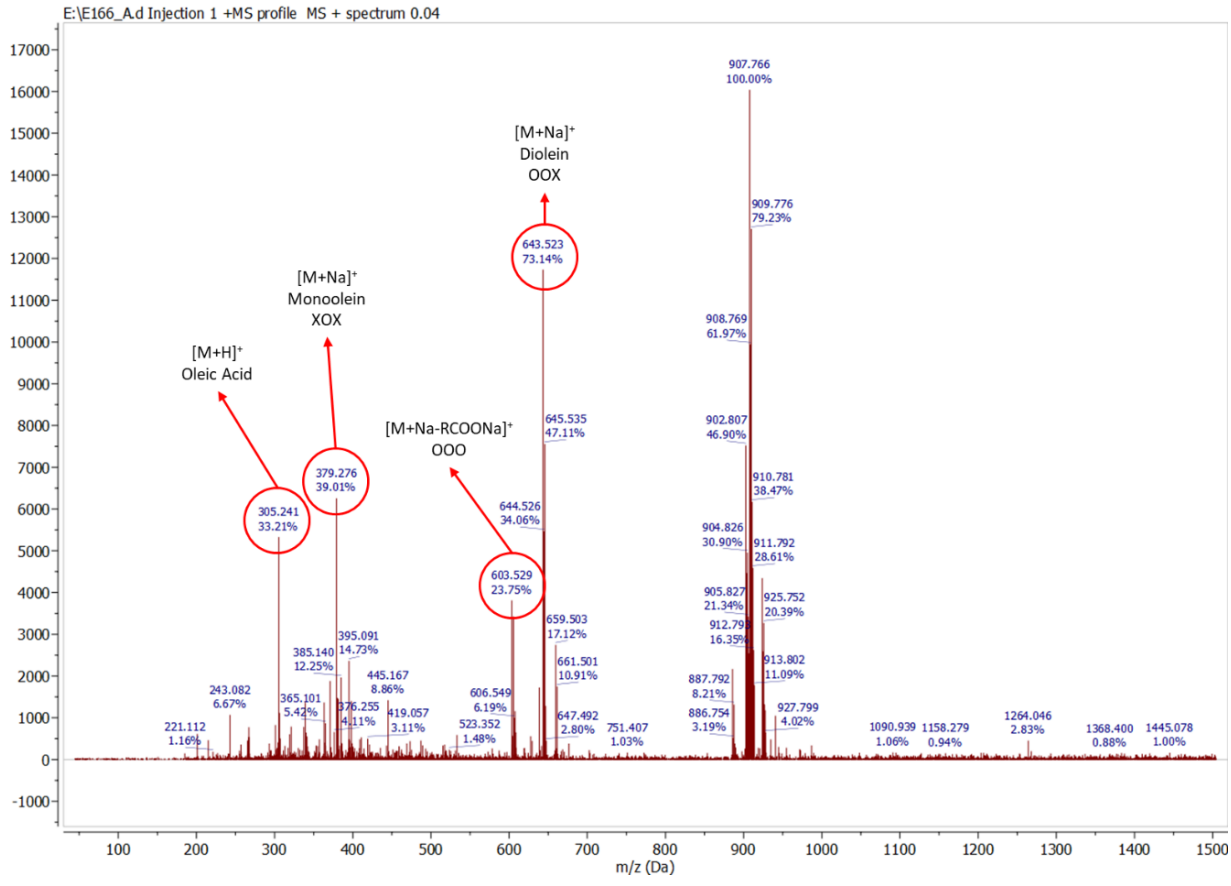

*Figure 52: ESI-MS Analysis of the raw product of the **first** cycle of interesterification with TLL-PVP*

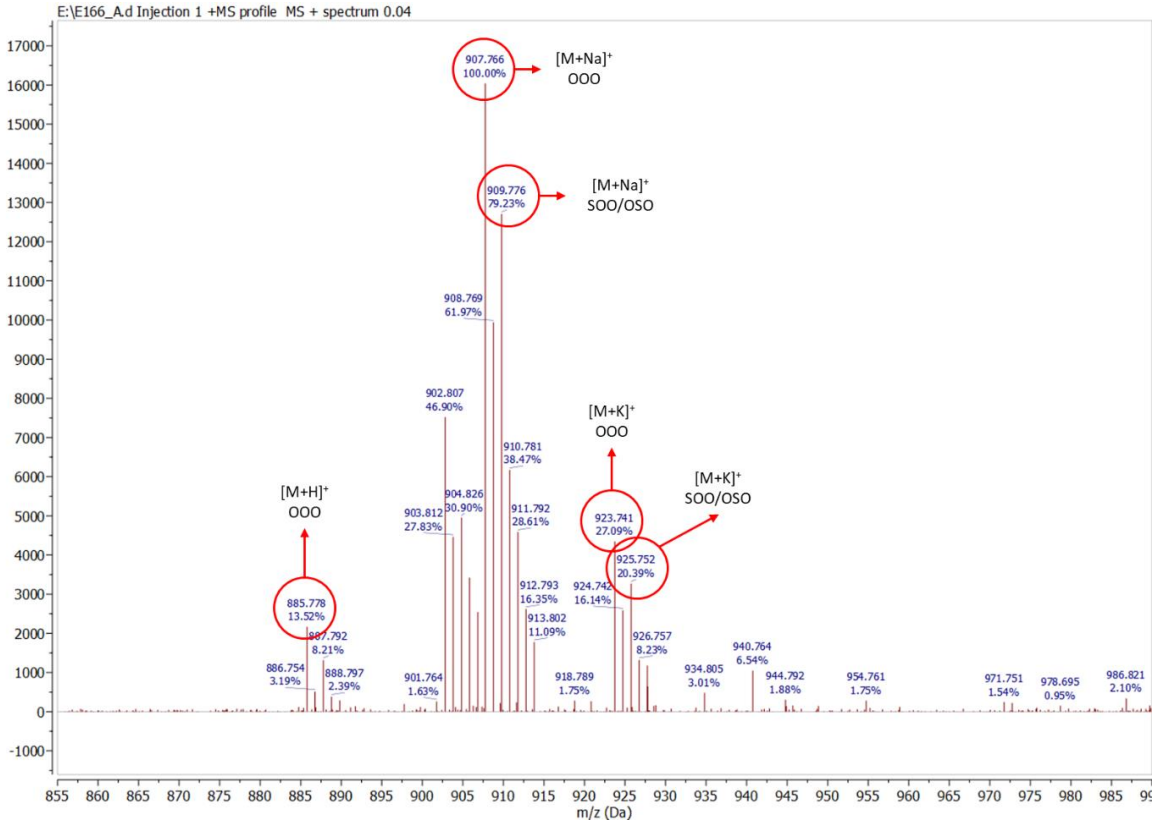

*Figure 53: ESI-MS Analysis of the raw product of the **first** cycle of interesterification with TLL-PVP – Enlargement of the area 855-990 m/z*

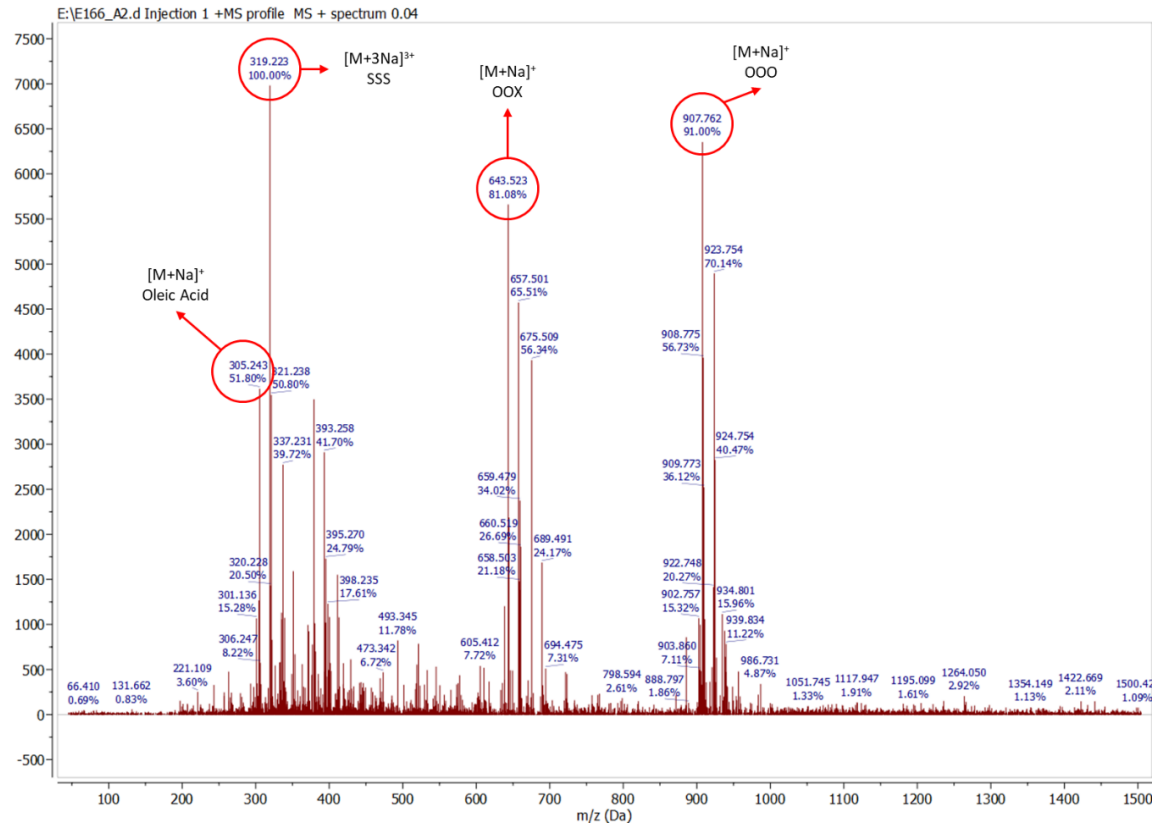

*Figure 54: ESI-MS Analysis of the raw product of the **second** cycle of interesterification with TLL-PVP*

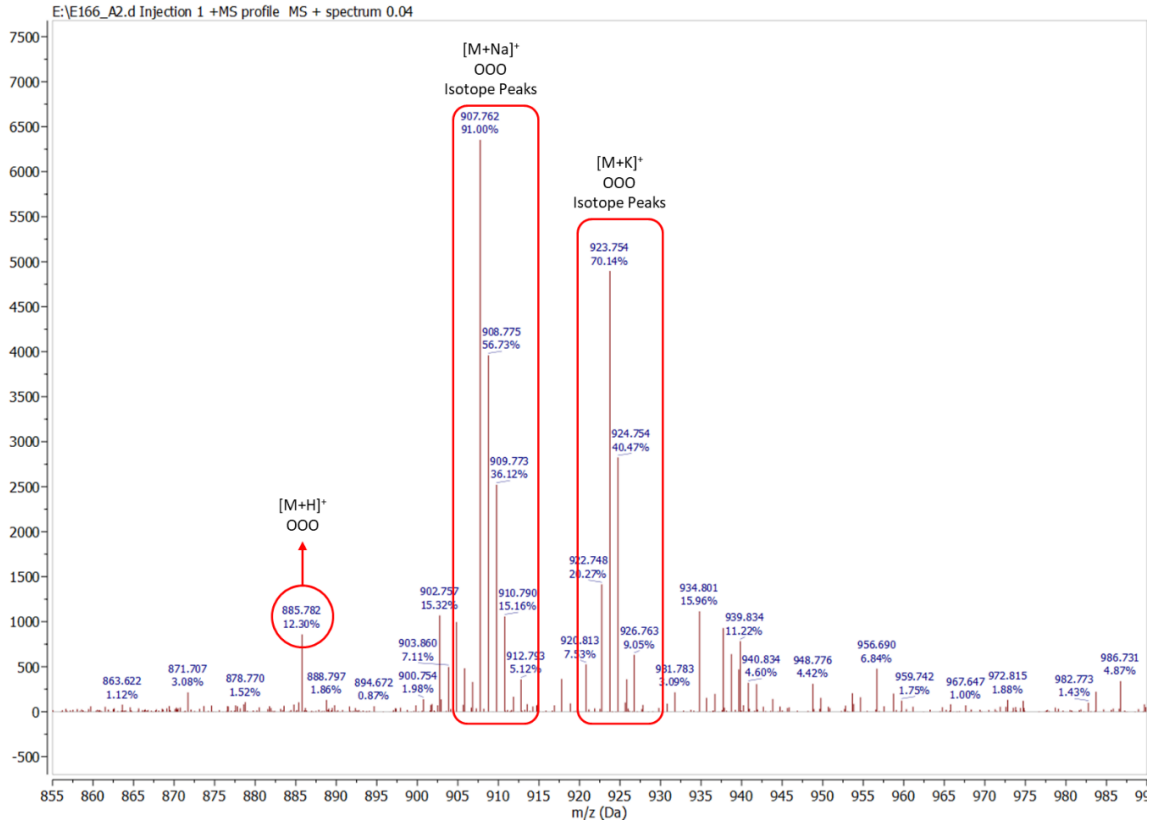

*Figure 55: ESI-MS Analysis of the raw product of the **second** cycle of interesterification with TLL-PVP – Enlargement of the area 855-990 m/z*

In the case of the first interesterification conducted with PVP-TLL, the reaction was not complete after 24 hours, as can be noted from the presence of a melting peak at 56.1°C, corresponding to the melting of tristearin in the mixture (Figure 50). For this reason, the reaction was let to continue up to a total time of 48 hours.

As can be seen from the last thermogram in Figure 50, the tristearin melting peak had not completely disappeared after 48 hours; however, the reaction was stopped.

The ESI-MS analysis, reported in Figure 52 and Figure 53, evidences the presence of products of hydrolysis of triolein. The most abundant peak in the MS spectrum corresponds to unreacted triolein (m/z 907.766, $[M+Na]^+$). The presence of interesterification products is confirmed by the peak at m/z 909.776 (corresponding to the interesterified product SOO/OSO, with one stearic acid chain and two oleic acid chains bound to the glycerol); this peak is too intense to be an isotopic peak of triolein, showing that the interesterification reaction took indeed place. The attributed MS peaks are summarized in the table below.

*Table 23: Identified peaks in the ESI-MS spectrum of the **first** cycle of the interesterification with TLL-PVP*

m/z	Compound	Ion
305.241	Oleic acid	$[M+Na]^+$
379.276	XOX	$[M+Na]^+$
603.529	OOO	$[M+Na-RCOONa]^+$
603.536	SOO/OSO	$[M+Na-RCOONa]^+$
643.523	OOX	$[M+Na]^+$
885.778	OOO	$[M+H]^+$
907.766	OOO	$[M+Na]^+$
909.776	SOO/OSO	$[M+Na]^+$
923.741	OOO	$[M+K]^+$
925.752	SOO/OSO	$[M+K]^+$

The enzyme, separated from the raw reaction product, was recycled for a second interesterification reaction. The thermograms from the recycle reaction are displayed in Figure 51. As can be seen from the figure, the interesterification reaction barely took place: the peak corresponding to the melting of tristearin does not disappear even after 48 hours of reaction.

This observation is confirmed also from the ESI-MS analysis. In Figure 54, it can be seen that the most intense ESI-MS peak corresponds to unreacted tristearin (m/z 319.223, ion $[M+3Na]^{3+}$). In Figure 55, it is shown that the peaks corresponding to triolein adducts display the typical pattern of triolein isotope peaks, evidencing that the formation of interesterified products did not occur. The attributed MS peaks are summarized in the table below.

*Table 24: Identified peaks in the ESI-MS spectrum of the **second** cycle of the interesterification with TLL-PVP*

m/z	Compound	Ion
305.243	Oleic acid	$[M+Na]^+$
319.223	SSS	$[M+3Na]^{3+}$
643.523	OOX	$[M+Na]^+$
885.782	OOO	$[M+H]^+$
907.762	OOO	$[M+Na]^+$
908.775		
909.773		
923.754	OOO	$[M+K]^+$
924.754		

It is clear that the PVP-TLL preparation cannot withstand the high temperature conditions of the reaction for long times. The first interesterification attempt (described in Section 4.2) was conducted for 72 hours, but no recycles were made; this interesterification recycle experiment evidenced that, after already 48 hours of reaction, the PVP-TLL had inactivated. On the other hand, after 24 hours of reaction the interesterification reaction had not yet reached completion. Therefore, different TLL preparations need to be developed for the interesterification of triolein to tristearin, as PVP-TLL is not sufficiently fast in catalyzing the reaction, nor it has the necessary stability to be reused in different reaction batches.

4.3.3.2 HEC-TLL

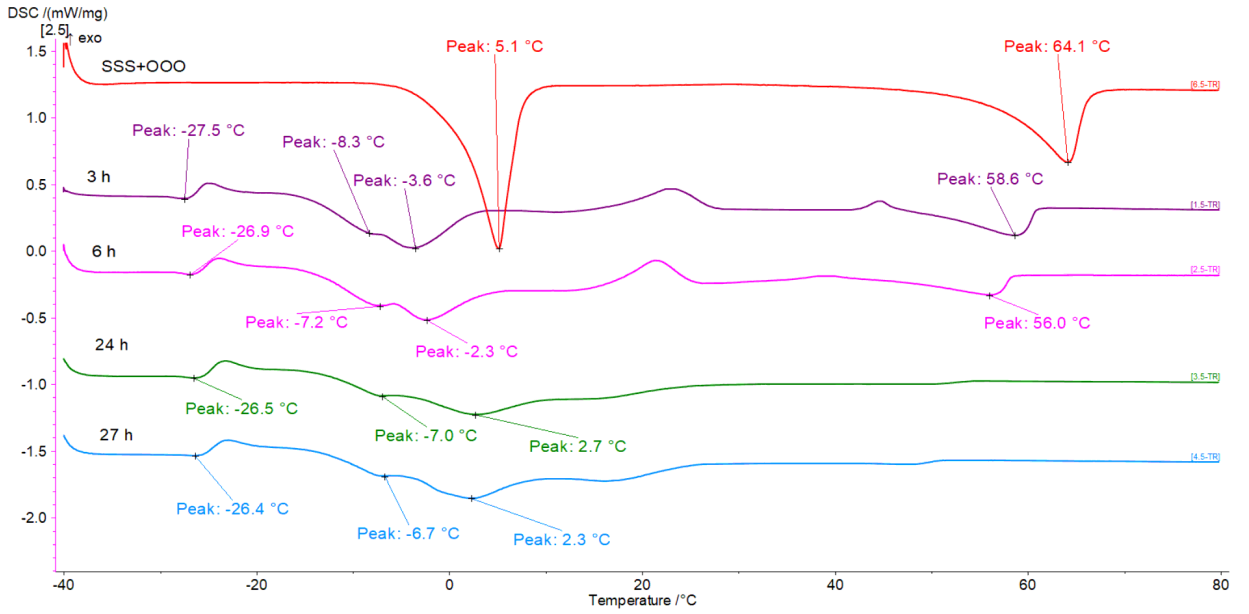

*Figure 56: DSC Analysis of the **first** interesterification cycle of tristearin and triolein with TLL-HEC*

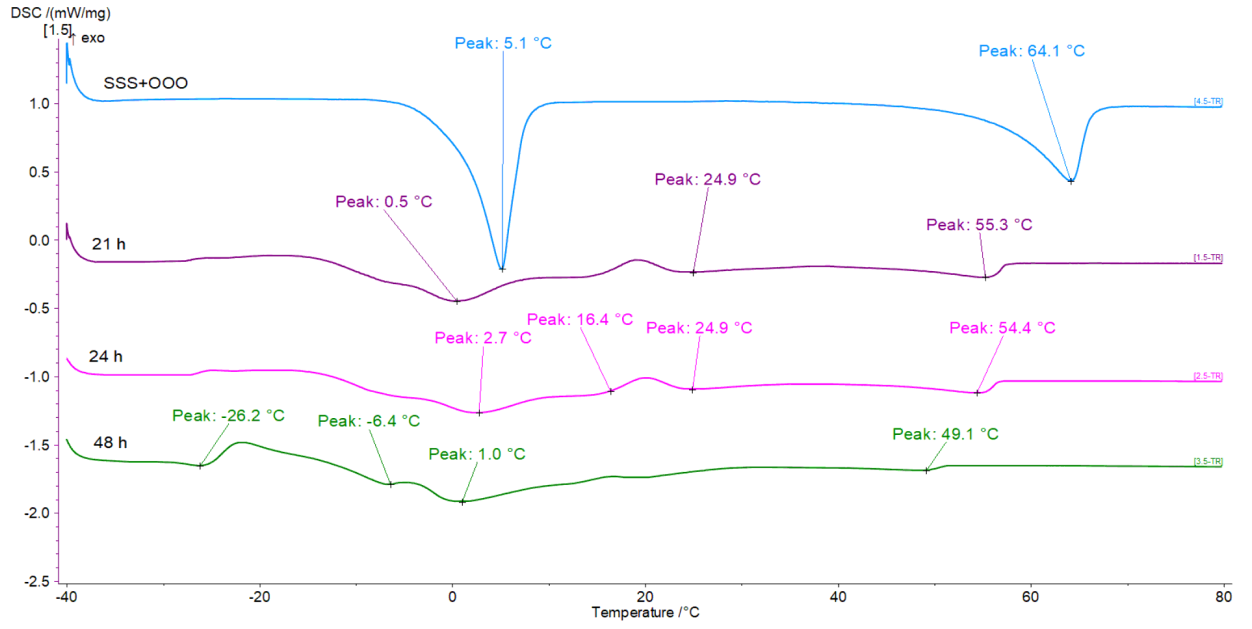

*Figure 57: DSC Analysis of the **second** interesterification cycle of tristearin and triolein with TLL-HEC*

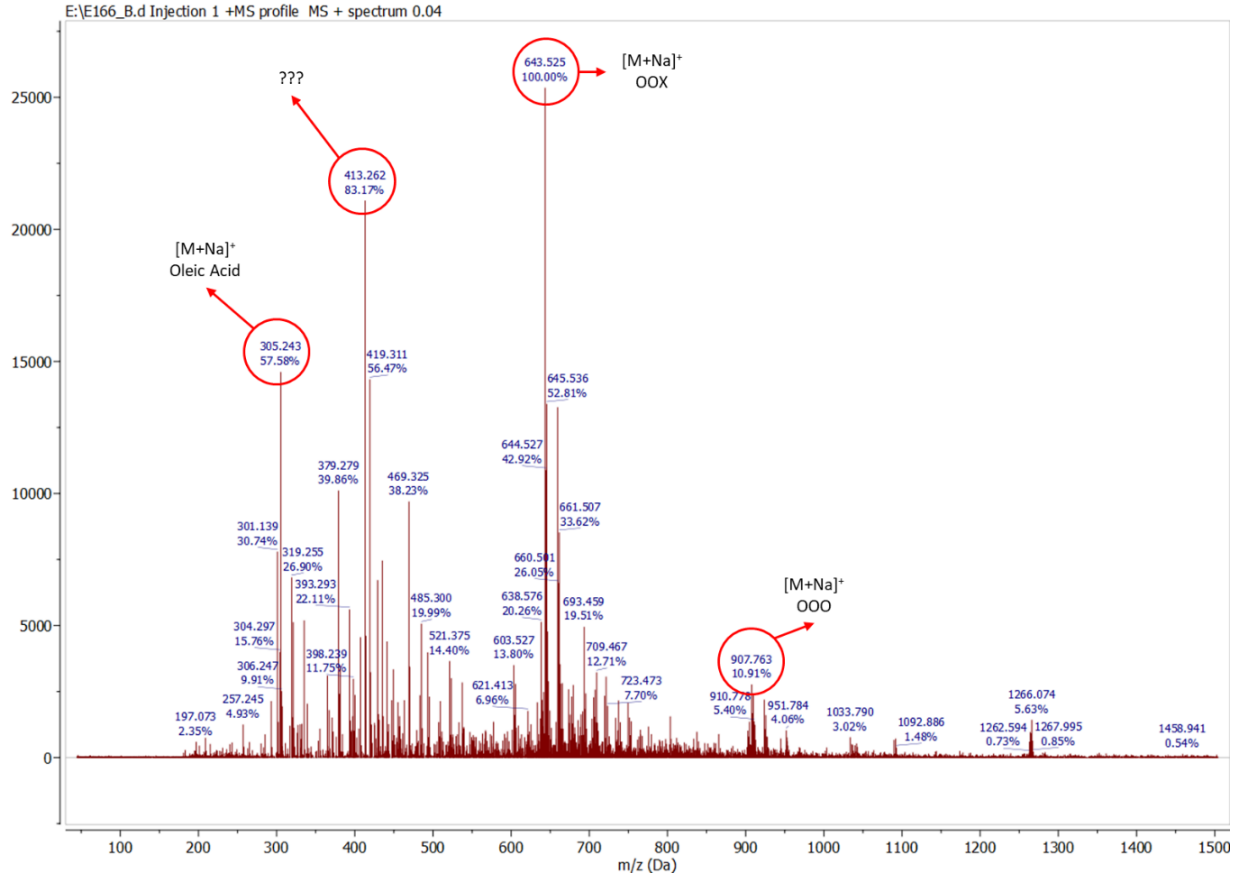

*Figure 58: ESI-MS Analysis of the raw product of the **first** cycle of interesterification with TLL-HEC*

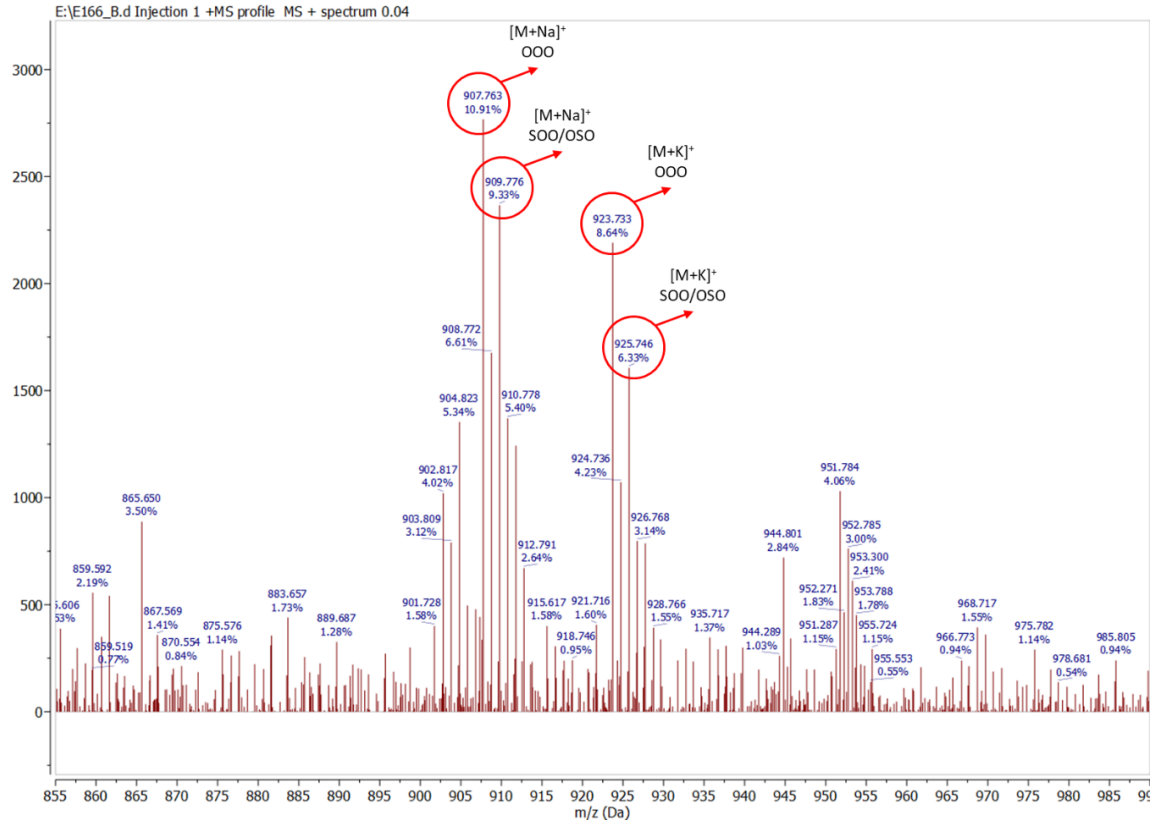

*Figure 59: ESI-MS Analysis of the raw product of the **first** cycle of interesterification with TLL-HEC – Enlargement of the area 855-990 m/z*

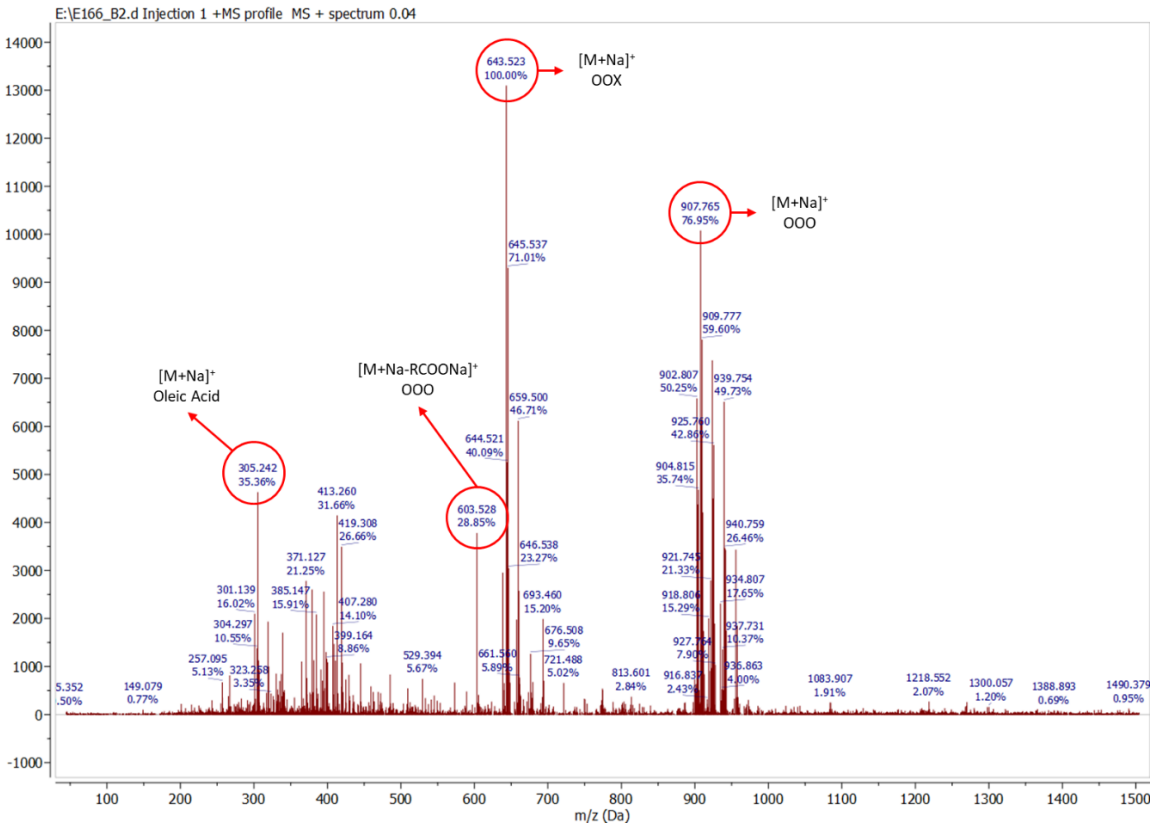

*Figure 60: ESI-MS Analysis of the raw product of the **second** cycle of interesterification with TLL-HEC*

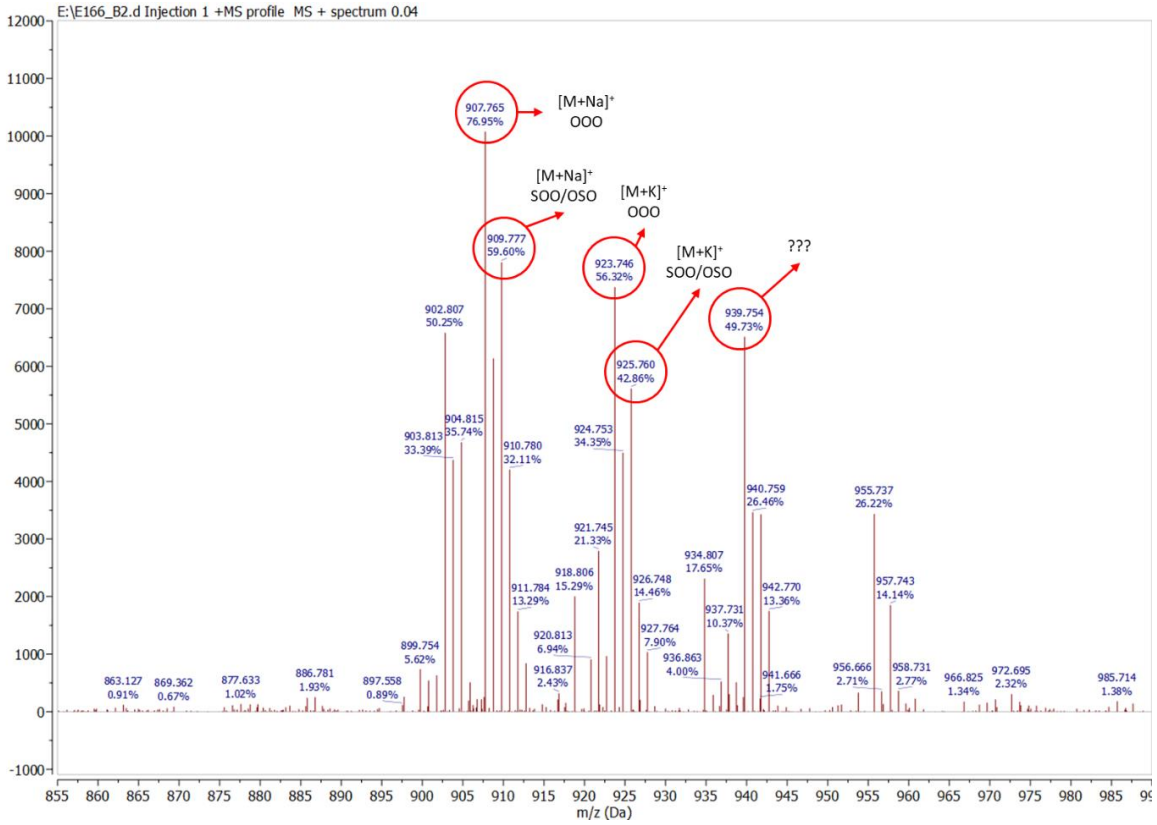

*Figure 61: ESI-MS Analysis of the raw product of the **second** cycle of interesterification with TLL-HEC– Enlargement of the area 855-990 m/z*

As can be seen in Figure 56, the interesterification with HEC-TLL had been completed already after 24 hours of reaction: the peak corresponding to the melting of tristearin had disappeared from the thermogram.

The enzyme was reused for a second reaction cycle. In this case, the reaction proceeded more slowly, as there was still the melting peak of tristearin after 24 hours of reaction (Figure 57); the recycling reaction was let proceed for 48 hours.

Figure 58 and Figure 59 report the ESI-MS spectrum obtained from the raw product of the first reaction cycle. The main peak in the mass spectrum is that corresponding to diolein, a hydrolysis product (m/z 643.525). There is also a peak corresponding to oleic acid (m/z 305.243), as well as an unidentified peak at m/z 413.262. The signals corresponding to unreacted triolein (m/z 907.763) and to the interesterification products SOO/OSO (m/z 909.776) are evident. The following table summarizes the identified ESI-MS peaks.

*Table 25: Identified peaks in the ESI-MS spectrum of the **first** cycle of the interesterification with TLL-HEC*

m/z	Compound	Ion
305.243	Oleic acid	$[M+Na]^+$
413.262	???	???
643.525	OOX	$[M+Na]^+$
907.763	OOO	$[M+Na]^+$
909.776	SOO/OSO	$[M+Na]^+$
923.733	OOO	$[M+K]^+$
925.746	SOO/OSO	$[M+K]^+$

Figure 60 and Figure 61 report the ESI-MS spectra of the raw product of the second reaction cycle obtained from TLL-HEC. In this case, it is evident that some competing hydrolytic reactions occurred, suggesting that the biocatalyst and/or the reagents need to be dehydrated. Notably, they were used without any pre-treatment. The following table summarizes the identified ESI-MS peaks.

*Table 26: Identified peaks in the ESI-MS spectrum of the **second** cycle of the interesterification with TLL-HEC*

m/z	Compound	Ion
305.242	Oleic acid	$[M+Na]^+$
643.523	OOX	$[M+Na]^+$
907.765	OOO	$[M+Na]^+$
909.777	SOO/OSO	$[M+Na]^+$
923.746	OOO	$[M+K]^+$
925.760	SOO/OSO	$[M+K]^+$

Contrary to PVP-TLL, HEC-TLL was faster in catalyzing the disappearance of tristearin from the reaction mixture, despite its hydrolytic activity being lower than PVP-TLL. However, as observed previously, there is a higher amount of hydrolysis product (diolein OOX) in the final crude product, suggesting that the hydrolysis of triglycerides is much more pronounced than in the case of PVP-TLL. In any case, the first interesterification cycle was deemed to be complete after 24 hours. No comparison regarding the stability of the preparations can be made, as PVP-TLL was maintained in operation for 24 hours more than HEC-TLL before the enzyme recycling.

4.3.4 Interesterification after DFF crosslinking

The interesterification of triolein and tristearin was also attempted using PVP-TLLc and HEC-TLLc, namely after crosslinking with DFF, with the procedures described in Section 4.3.1. As previously described, the reaction substrate was a mixture of tristearin and triolein (27:73 w/w), with an enzyme dosage of 10 wt.%, and no solvent. The mixture was heated to 70°C for 24 hours, and samples were taken after 4 and 24 hours and analyzed *via* ESI-MS spectrometry.

This preliminary set of experiments had the aim to verify whether the crosslinking with DFF would impact the synthetic activity of the enzyme in the interesterification process, since the overall crosslinking process causes a decrease in the measured hydrolytic activity of the preparations. The enzyme samples used for the reaction were PVP-TLLc or HEC TLLc crosslinked in (a) KPi, 0.1 M, pH 7; (b) NaCl 3 M; (c) CH_2Cl_3, with a crosslinking reaction time of 4 hours. The enzyme amounts used for the assay interesterification reaction are reported in the following table.

Table 27: Enzyme loading for the interesterification assay with PVP-TLLc and HEC-TLLc

Reaction	Enzyme	Crosslinking conditions	Enzyme amount (U)	Enzyme amount ($U/g_{substrate}$)
3	PVP-TLLc	KPi, 0.1 M, pH 7	6.15	12.3
4	HEC-TLLc	KPi, 0.1 M, pH 7	9.55	19.1
5	PVP-TLLc	NaCl 3 M	12.55	25.1
6	HEC-TLLc	NaCl 3 M	10.35	20.7
7	PVP-TLLc	CH_2Cl_2, 4h	100.75	201.5
8	HEC-TLLc	CH_2Cl_2, 4h	132.8	265.6

In general, the ESI-MS spectra obtained from the raw reaction product were all similar, and they indicated the presence of interesterification products, more specifically SOO/OSO. Comparing the spectra obtained after 4 hours with those obtained after 24 hours, it was evident the increase in intensity of the peaks corresponding to this interesterification product, as expected. The identified ESI-MS peaks in the various spectra are reported in the following table, while enlargements of the most significant peak clusters are reported in Figure 62 and Figure 63.

Table 28: Identified peaks in the ESI-MS spectra of the raw products obtained from the interesterification of triolein and tristearin with crosslinked PVP-TLLc and HEC-TLLc

m/z	Compound	Ion	Peak Label in Figures	Identified in spectrum from reaction					
				3	4	5	6	7	8
445.2	SSO / SOS	$[M+2H]^+$	–	–	Yes	Yes	Yes	Yes	Yes
603.7	OOO or SOO / OSO	$[M+Na–RCOONa]^*$	a	Yes	Yes	Yes	Yes	Yes	Yes
605.7	OSO / SOO or SSO / SOS	$[M+Na–RCOONa]^*$	b	Yes	Yes	Yes	Yes	Yes	Yes
621.5	OOX	$[M+H]^+$	–	Yes*	Yes*	Yes	Yes	Yes	Yes
885.9	OOO	$[M+H]^+$	c	Yes	Yes	Yes	Yes	Yes	Yes
887.9	OSO / SOO	$[M+H]^+$	d	Yes	Yes	Yes	Yes	Yes	Yes
902.8	OOO	$[M+NH_4]^+$	e	Yes	Yes	Yes	Yes	Yes	Yes
904.8	OSO / SOO	$[M+NH_4]^+$	f	Yes	Yes	Yes	Yes	Yes	Yes

* The peak is present with a very low intensity

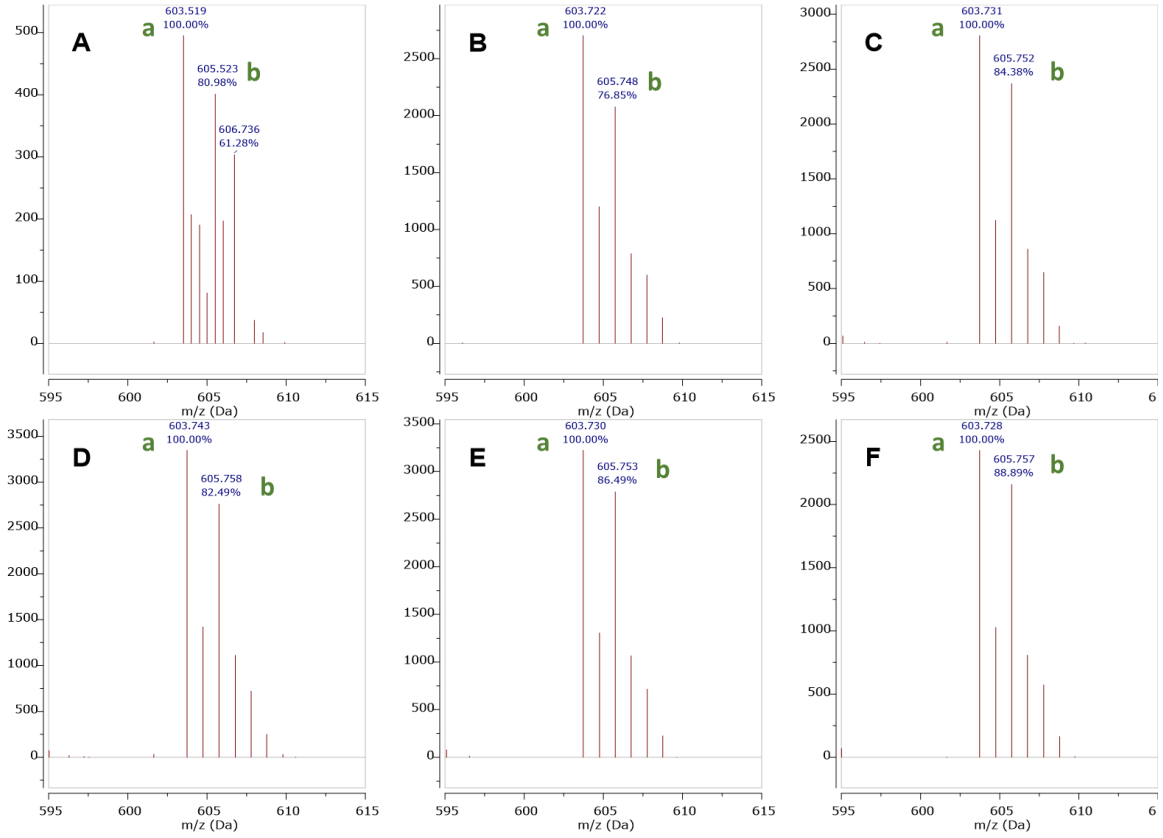

Figure 62: Enlargement of the area m/z 595-615 of the ESI-MS spectra of the interesterification products. Enzymes used for the reaction are (A) PVP-TLL crosslinked in KPi, 0.1 M, pH 7; (B) HEC-TLL crosslinked in KPi, 0.1 M, pH 7; (C) PVP-TLL crosslinked in NaCl 3 M; (D) HEC-TLL crosslinked in NaCl 3 M; (E) PVP-TLL crosslinked in CH_2Cl_2; (F) HEC-TLL crosslinked in CH_2Cl_2.

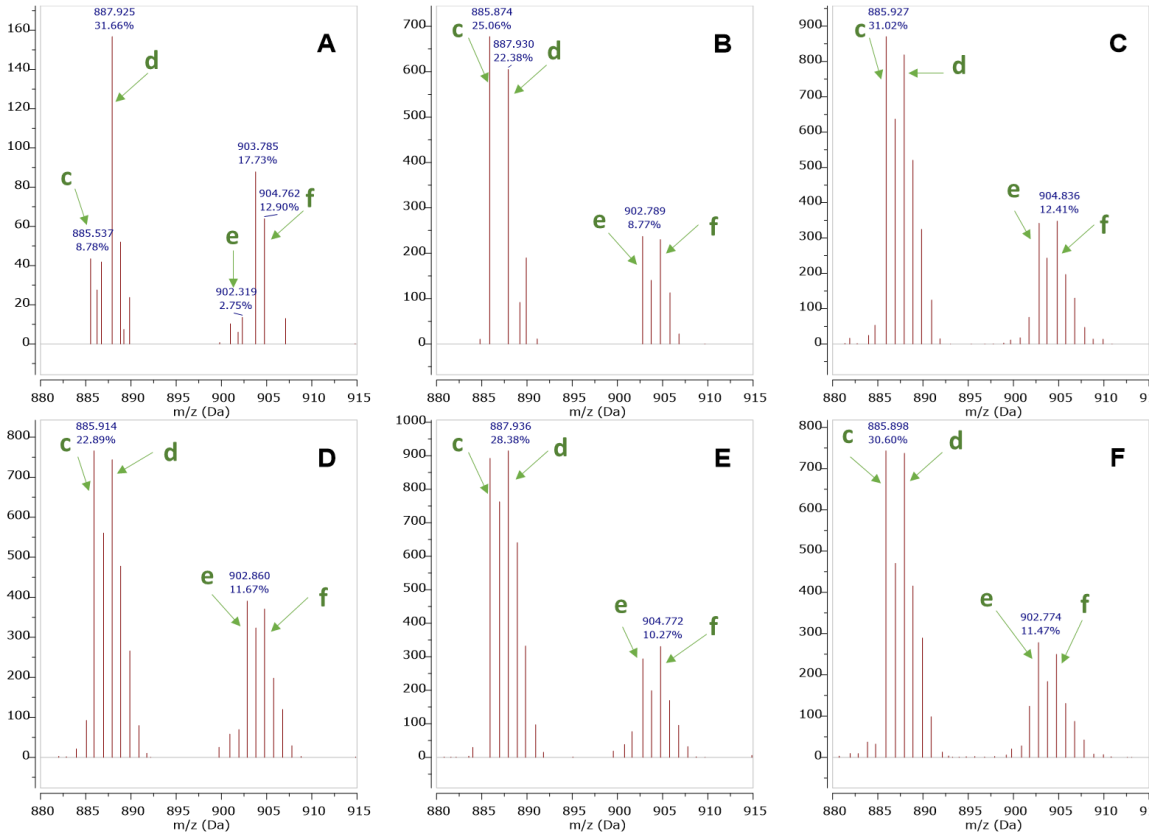

Figure 63: Enlargement of the area m/z 880-915 of the ESI-MS spectra of the interesterification products. Enzymes used for the reaction are (A) PVP-TLL crosslinked in KPi, 0.1 M, pH 7; (B) HEC-TLL crosslinked in KPi, 0.1 M, pH 7; (C) PVP-TLL crosslinked in NaCl 3 M; (D) HEC-TLL crosslinked in NaCl 3 M; (E) PVP-TLL crosslinked in CH_2Cl_2; (F) HEC-TLL crosslinked in CH_2Cl_2.

In all cases, the most intense cluster of peaks is that between 600-610 m/z. As previously discussed for the reaction with non-crosslinked enzyme preparations, these peaks can be attributed to the $[M+Na\text{-}RCOONa]^+$ fragmentation adducts of triolein (OOO) and its interesterification derivatives. In particular, the peak at m/z = 603.7 can be due to the $[M+Na–OlCOONa]^+$ adduct of triolein or to the $[M+Na–StCOONa]^+$ adduct of the interesterification product SOO/OSO. The peak at m/z = 605.7 can be attributed to the $[M+Na–OlCOONa]^+$ adduct of SOO/OSO or to the $[M+Na–StCOONa]^+$ adduct of SSO/SOS.

No peak cluster was observed between m/z 640-650, unlike what was observed in the case of the reactions catalyzed by non-crosslinked physically immobilized TLL. These peaks could be attributed to the $[M+Na]^+$ adduct of diolein, a hydrolysis product of triolein; the absence of this cluster of peaks suggests that the contribution of concurrent hydrolysis reactions catalyzed by the lipase is minimal. This observation is consistent with the fact that the peak at 621.5 m/z, corresponding to the $[M+H]^+$ adduct of OOX, has very low intensity in all the spectra.

The other peak clusters identified for all of the samples are at m/z 885-895, corresponding to the $[M+H]^+$ adducts of the triglycerides (in particular of triolein and SOO/OSO), and at m/z 900-910, corresponding to the $[M+NH_4]^+$ peaks of the same triglycerides. No significative peak signaling the presence of unreacted tristearin was identified ($[M+H]^+$ at 891.8, $[M+NH_4]^+$ at 908.8 or $[M+Na]^+$ at 913.8). A list of the more

common adducts of the reactant, the interesterification products and the hydrolysis products can be found in the Annex section, together with their monoisotopic molecular mass.

Finally, all samples (except for those obtained with PVP-TLL crosslinked in KPi 0.1 M, pH 8) present a series of mass peaks at m/z 970-990. These peaks could not be identified.

In conclusion, the formulations that underwent to the crosslinking treatment showed better performances, leading to complete conversion of tristearin within 24 and without significant production of hydrolytic products. Most probably that was a consequence of the washing and drying steps applied at the end of the crosslinking protocols that removed the residual water more efficiently. Further perspectives in the study of these crosslinked enzyme preparations can be the performance of recycling studies analogous to what was previously done for the non-crosslinked formulations, together with DSC analysis to have insight on the kinetic of the reaction.

4.4 Conclusions

Two TLL formulations obtained from physical immobilization on rice husk were investigated as potential replacer of the commercial product Lipozyme TL IM in industrial processes addressing vegetal oil transformations.

Looking for some covalent modifications able to confer higher stability to the rice-husk formulations, crosslinking experiments were conducted on PVP-TLL and HEC-TLL but without reaching the intended purpose, since the enzyme preparations maintained low stability in aqueous environment, undergoing enzyme leaching. Since the crosslinker used (DFF) was proven to be effective for reaction with proteins and enzyme immobilization in the previous chapter, it is unlikely that the failure of the crosslinking experiment is not due to poor reactivity of the crosslinker. It can be hypothesized that, in this case, the single enzyme molecules were too far apart from each other on the rice husk to allow an effective crosslinking between the enzyme molecules.

Nevertheless, when used in low-water and solvent-free media, both the original TLL formulations and the "crosslinked" formulations were effective in synthetic applications, namely the interesterification of triolein and tristearin. The interesterification of triglycerides is a process employed at >10,000 ton per year for the production of cocoa butter analogues. The rice husk formulations were employed at 70°C and monitored by Differential Scanning Calorimetry (DSC), observing the disappearance of the melting peak of tristearin (defective reagent) within 24h. The recyclability of the immobilized enzyme was demonstrated and the formation of the products was confirmed by ESI-MS. The formulations pre-treated according to the crosslinking protocols showed a better performance, leading to complete conversion of tristearin within 24h without formation of significant amounts of hydrolytic products. Most probably, that was ascribable to a more accurate removal of the residual water during the pre-treatment of the formulations. Recyclability studies will be done in the future for confirming the stability of the biocatalysts.

The low cost and sustainability of the rice-husk make these formulations of potential relevance for the food industry applications, since the large volumes and low costs of the products set stringent economic and environmental constraints. Notably, a potential advantage of the rice husk TLL preparations compared to the commercial Lipozyme TL IM is the easier disposal of the spent immobilized enzyme after use.

4.5 Materials and Methods

4.5.1 Chemicals

All chemicals were purchased from Sigma Aldrich (now Merck) and were of the highest grade available. Deuterated solvents for NMR analyses were purchased from Sigma Aldrich.

4.5.2 Biocatalysts

HEC-TLL and **PVP-TLL** were in-house enzyme preparations.

4.5.3 Other Equipment

DSC analyses were performed with a NETZSCH DSC300 Select calorimeter. **Titrations and pH measurements** were performed with an automatic titrator Mettler-Toledo Graphic DL50. **NMR spectra** were acquired with a Varian 400 (400 MHz) spectrometer. **Mass spectra** were obtained with an LTQ XL spectrometer (ThermoFischer Scientific, USA) equipped with an ESI ion source.

4.5.4 Crosslinking in aqueous environment

4.5.4.1 Protocol 1

600 mg of PVP-TLL or HEC-TLL immobilized enzyme were introduced in a 20 mL glass vial. The immobilized enzyme was suspended in 1.5 mL of isopropanol + 1.5 mL of potassium phosphate buffer (0.1 M, pH 7). Then, 5.4 mg (72.5 µmol/g) of DFF were added to the mixture. The mixture was kept shaking on the orbital shaker for 2 hours at 25°C. At the end of the shaking, the mixture was dried on the air at room temperature for 2 days.

The immobilized enzyme was then resuspended in about 3 mL of H_2O, then it was filtered on a Buchner filter under vacuum. The preparation was then washed with 2×3 mL of CH_2Cl_2, then dried on the filter. The sample was stored in the fridge at 4°C.

4.5.4.2 Protocol 2

400 mg of PVP-TLL or HEC-TLL immobilized enzyme were introduced in a 20 mL glass vial. The immobilized enzyme was suspended in 2.5 mL of NaCl 3M. Then, 37 mg (800 µmol/g) of DFF were added to the mixture. The mixture was kept shaking on the orbital shaker at 25°C for 4 hours.

At the end of the shaking, the sample was filtered on a Buchner filter under vacuum. The sample was rinsed with 2×3 mL of CH_2Cl_2, then dried on the filter. The sample was stored in the fridge at 4°C.

4.5.4.3 Protocol 3

400 mg of PVP-TLL or HEC-TLL immobilized enzyme were introduced in a 20 mL glass vial. The immobilized enzyme was suspended in 2.5 mL of KPi 0.1 M, pH 7. Then, 37 mg (800 µmol/g) of DFF were added to the mixture. The mixture was kept shaking on the orbital shaker at 25°C for 4 hours.

At the end of the shaking, the sample was filtered on a Buchner filter under vacuum. The sample was rinsed with 2×3 mL of CH_2Cl_2, then dried on the filter. The sample was stored in the fridge at 4°C.

4.5.5 Crosslinking in organic solvent

4.5.5.1 Protocol 4

400 mg of PVP-TLL or HEC-TLL immobilized enzyme were introduced in a 20 mL glass vial. The immobilized enzyme was suspended in 2.5 mL of CH_2Cl_2. Then, 10 mg of DFF were added to the mixture. The mixture was kept shaking on the orbital shaker at 25°C for 4 hours.

At the end of the shaking, the sample was filtered on a Buchner filter under vacuum. The sample was rinsed with 2×3 mL of CH_2Cl_2, then dried on the filter. The sample was stored in the fridge at 4°C.

4.5.5.2 Protocol 5

400 mg of PVP-TLL or HEC-TLL immobilized enzyme were introduced in a 20 mL glass vial. The immobilized enzyme was suspended in 2.5 mL of CH_2Cl_2. Then, 10 mg of DFF were added to the mixture. The mixture was kept shaking on the orbital shaker at 25°C for 24 hours.

At the end of the shaking, the sample was filtered on a Buchner filter under vacuum. The sample was rinsed with 2×3 mL of CH_2Cl_2, then dried on the filter. The sample was stored in the fridge at 4°C.

4.5.6 Tributyrin assay for the determination of lipase activity

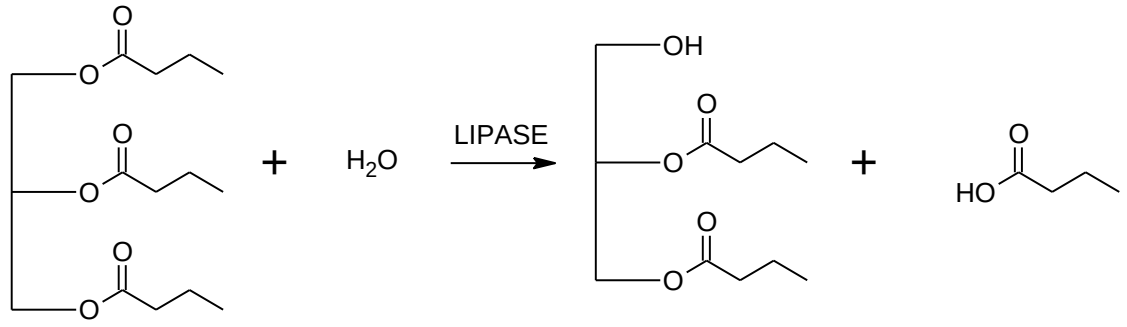

Scheme 15:. Tributyrin hydrolysis reaction

4.5.6.1 Emulsifier solution preparation – A

- Prepare a solution of 0.6 g of gum arabic in 6 mL of milli-Q water in a beaker with magnetic stirring (gum arabic solution).
- Prepare a solution consisting of 1.79 g of NaCl and 0.041 g of KH_2PO_4 in 30 mL of milli-Q water in a beaker. Add 54 mL of glycerol and 6 ml of gum arabic (emulsifier) solution.
- Adjust pH of emulsifier solution at 4.5 ± 0.05 using NaOH or HCl 0.1 M.
- Dilute the solution up to 100 mL by adding milli-Q water.

4.5.6.2 Substrate emulsion preparation – B

- 5 mL of tributyrin, 17 mL of emulsifier solution and 78 ml of milli-Q water are poured in a 100 mL flask.
- The solution is stirred for 30 minutes and the pH is adjusted at 4.75 ± 0.05 using NaOH or HCl 0.1 M.

- The substrate emulsion is stirred for at least 30 minutes before use.

4.5.6.3 Tributyrin hydrolysis assay

- 30 mL of substrate emulsion and 2 mL of KPi 0.1 M pH 7.0 are added in a plastic beaker for titration.
- The emulsion is thermostatted at 30°C the pH is measured and its value set as end point.
- 30 mg of enzymatic preparation are added to the thermostatted substrate solution and the automatic titrator is started (titration solution is NaOH 0.1 M).
- Perform a pH-stat titration of the assay mixture. The volume of titration solution used for the assay is used to calculate the amount of butyric acid generated in the hydrolysis, and subsequently the activity of the enzyme.

$$Activity\ \left(\frac{U}{g}\right) = \frac{V_{NaOH}(mL) \times [NaOH](mM)}{t_{Assay}\ (min) \times g_{enzyme}}$$

4.5.7 Determination of water content of TLL physically immobilized on rice husk

50 mg of PVP-TLL or HEC-TLL were weighed in a vial. The samples were dried in the vacuum oven at 100°C for 24 hours. The weight of the samples after drying was measured. Water content was calculated as follows:

$$Water\ content\ (\%) = \frac{weight_{RH,i}(g) - weight_{RF,f}(g)}{weight_{RH,i}(g)} \times 100$$

4.5.8 Interesterification of triolein and tristearin with TLL physically immobilized on rice husk

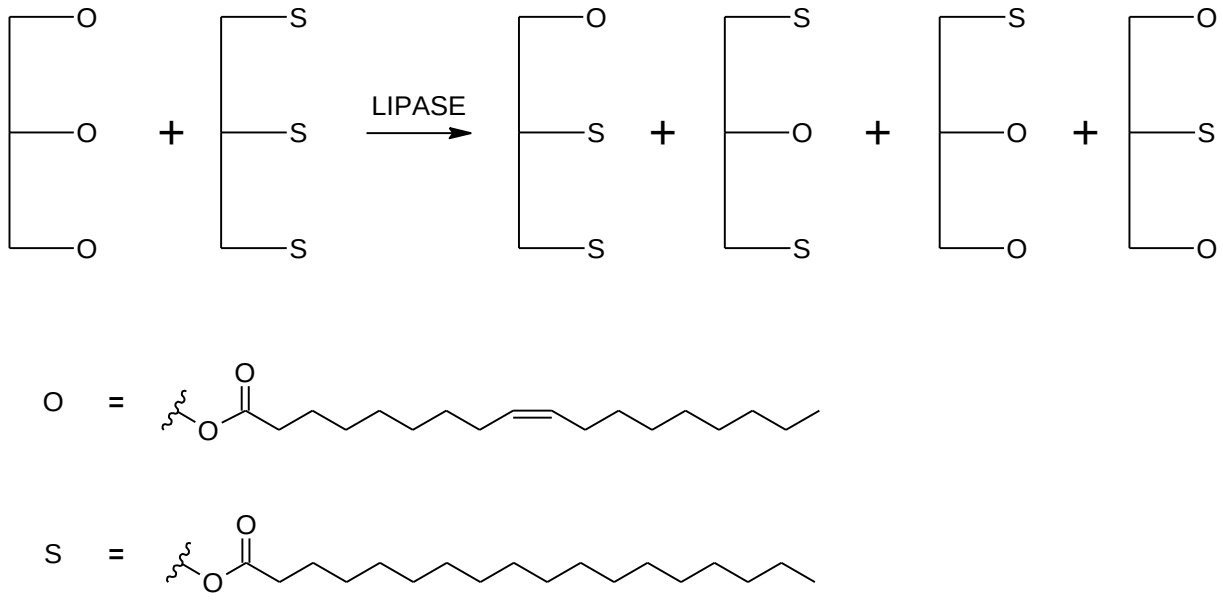

Scheme 16: Enzymatic interesterification of triolein and tristearin

0.135 g of tristearin and 0.365 g of triolein were introduced in a 4 mL vial; the total weight of the substrates is 0.5 g. Then, 0.05 g of PVP-TLL or HEC-TLL (10% w/w) were added to the mixture. The mixture was stirred at 70°C for 3 days. Samples were collected every day and analyzed *via* TLC (eluent: hexane/diethyl ether 80:20).

The reaction crude was also analyzed *via* ^{1}H NMR (after dissolution in $CDCl_3$) and ESI-MS (after dissolution in $CHCl_3$).

4.5.9 DSC analysis of the product of interesterification between triolein and tristearin[214]

5 to 10 mg of reaction sample was introduced in an aluminum pan, which was then sealed; an empty, sealed aluminum pan was used as reference. The sample then underwent the following heating/cooling cycle:

1. Heating from 20°C to 80°C, 10°C/min
2. Holding temperature of 80°C for 10 minutes
3. Cooling from 80°C to –40°C at 10°C/min
4. Holding temperature of –40°C for 30 minutes
5. Heating from –40°C to 80°C at 5°C/min

The final heating profile was defined from the last heating cycle.

4.6 Annex

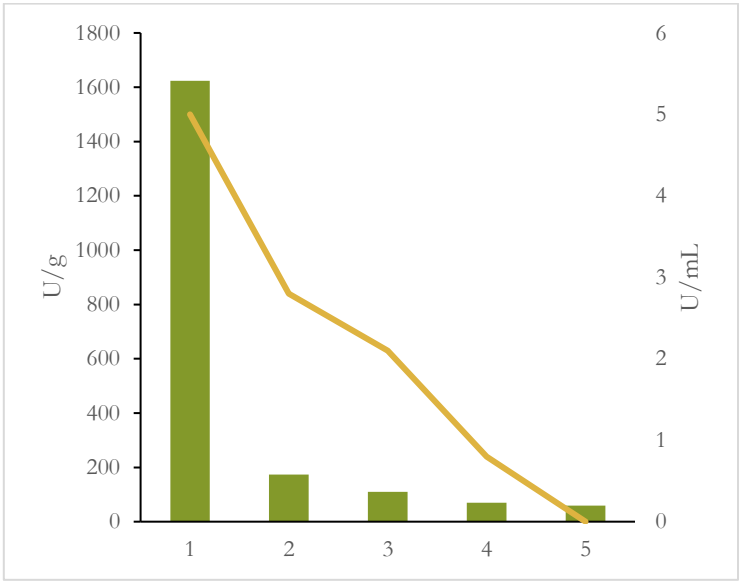

Figure 64: Recovered activity (columns) and leaching (line) in the experiment of crosslinking of PVP-TLL in dichloromethane for 4 hours

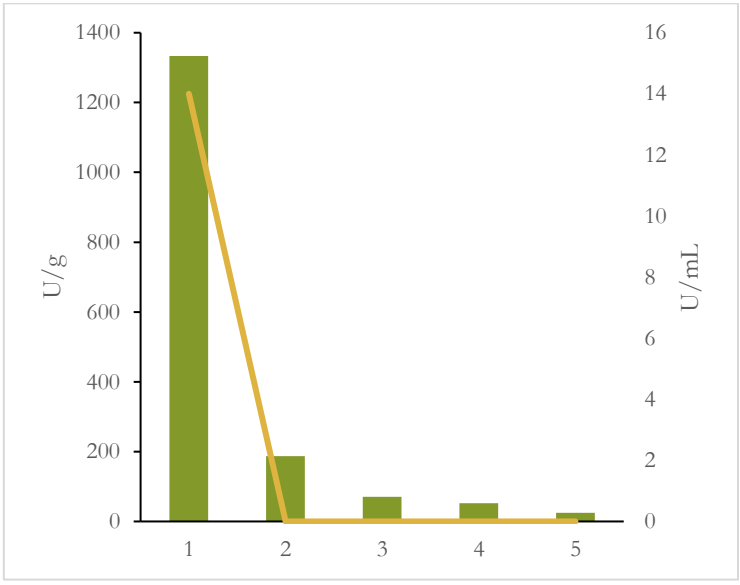

Figure 65: Recovered activity (columns) and leaching (line) in the experiment of crosslinking of PVP-TLL in dichloromethane for 24 hours

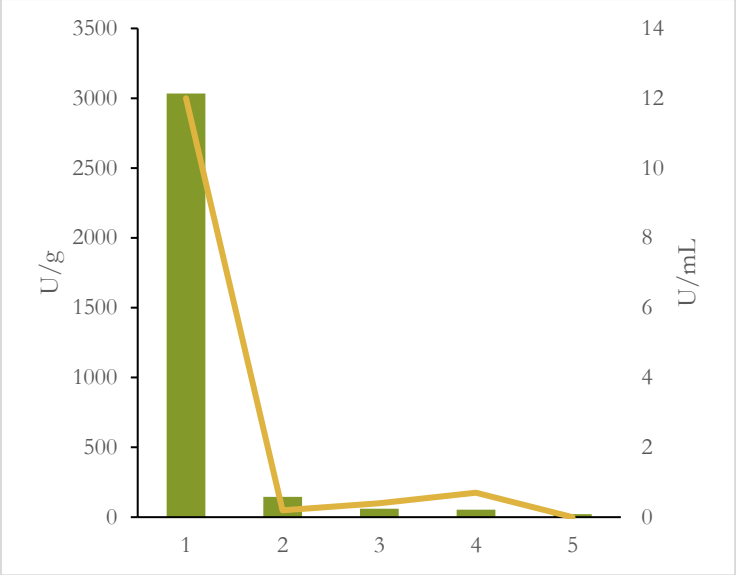

Figure 66: Recovered activity (columns) and leaching (line) in the experiment of crosslinking of HEC-TLL in dichloromethane for 4 hours

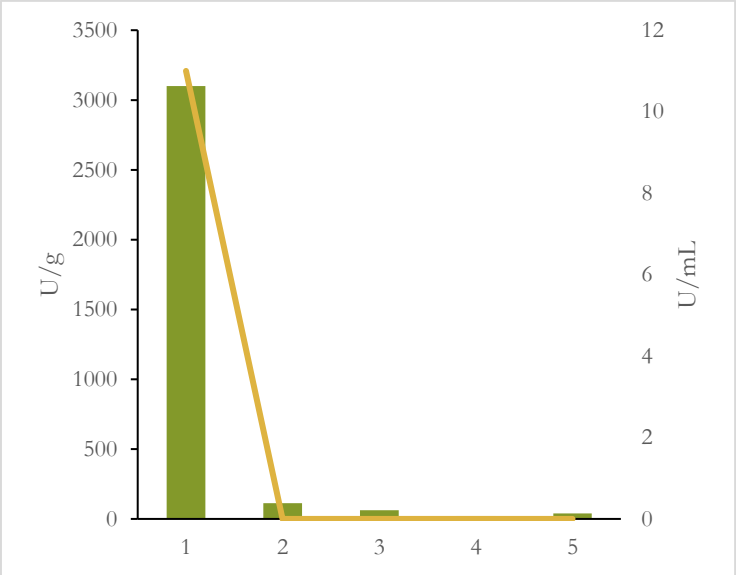

Figure 67: Recovered activity (columns) and leaching (line) in the experiment of crosslinking of HEC-TLL in dichloromethane for 24 hours

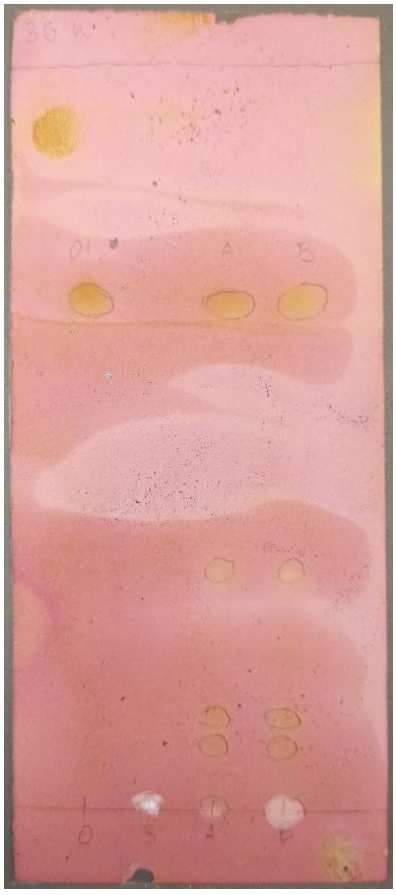

Figure 68: TLC (hexane/ diethyl ether 80:20) of the interesterification reaction between triolein and tristearin. From left to right: reference triolein (O); reference tristearin (S), reaction mixture A (PVP-TLL), reaction mixture B (HEC-TLL).

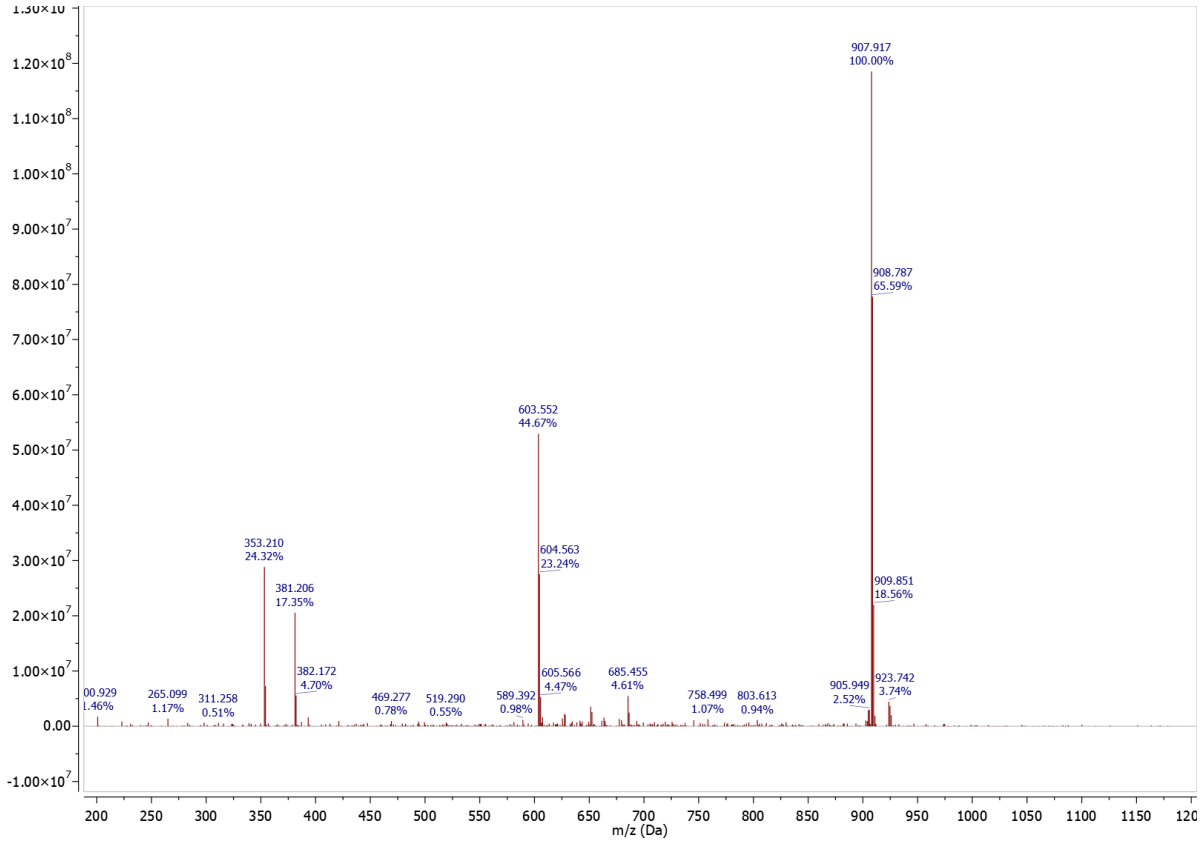

Figure 69: ESI-MS spectrum of reference triolein (99% purity)

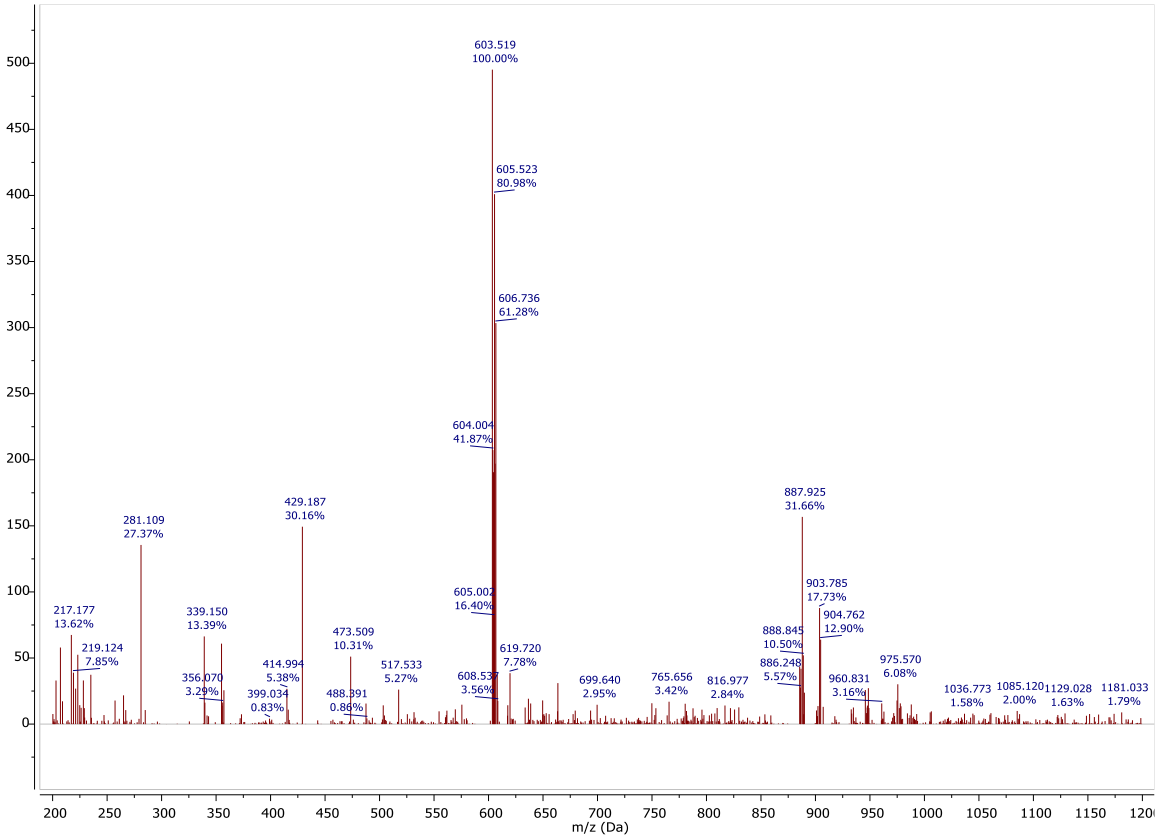

Figure 70: ESI-MS spectrum of the raw interesterification product obtained with PVP-TLL crosslinked with DFF in KPi, 0.1 M, pH 7

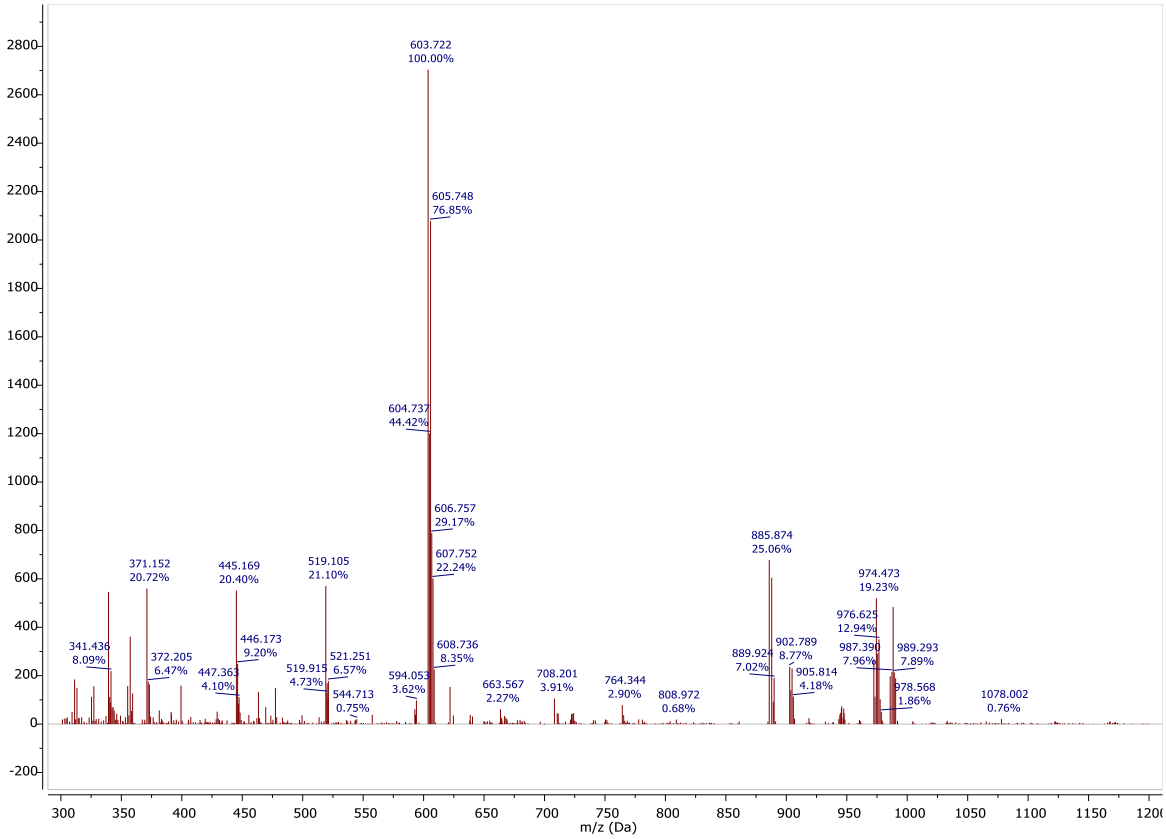

Figure 71: ESI-MS spectrum of the raw interesterification product obtained with HEC-TLL crosslinked with DFF in KPi, 0.1 M, pH 7

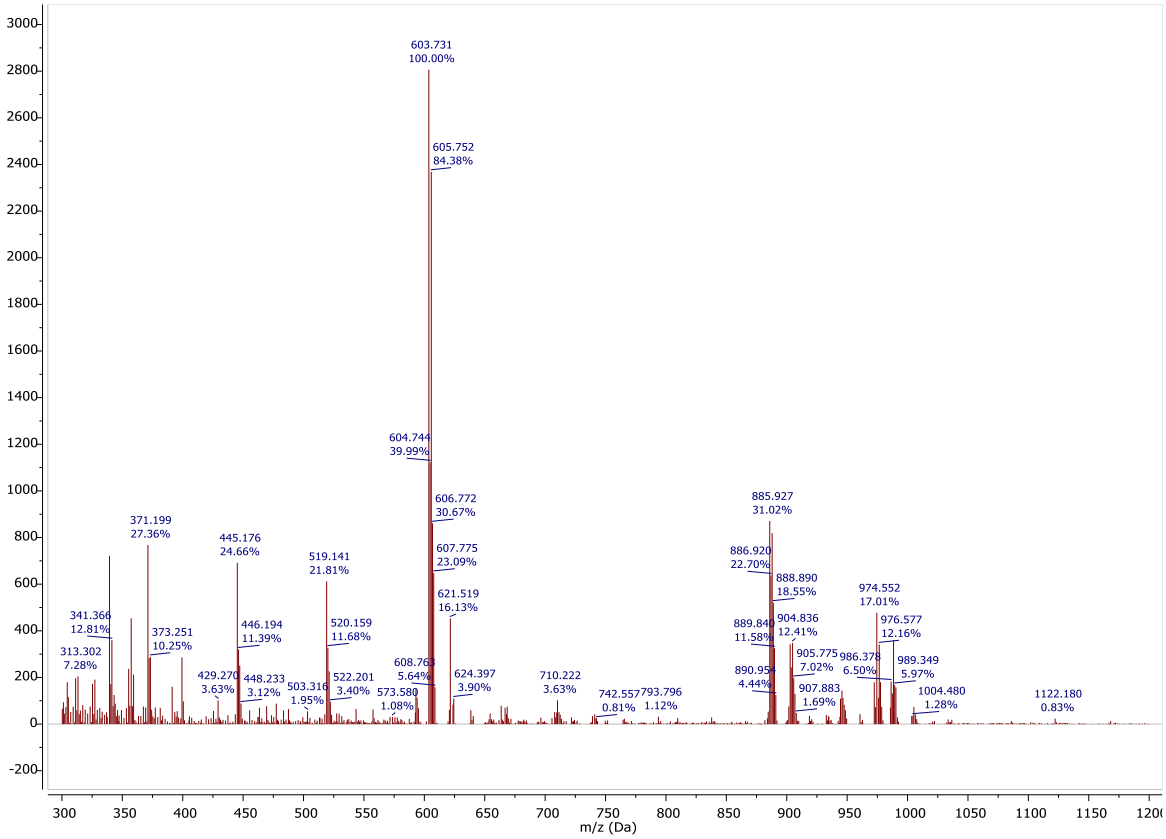

Figure 72: ESI-MS spectrum of the raw interesterification product obtained with PVP-TLL crosslinked with DFF in NaCl 3 M

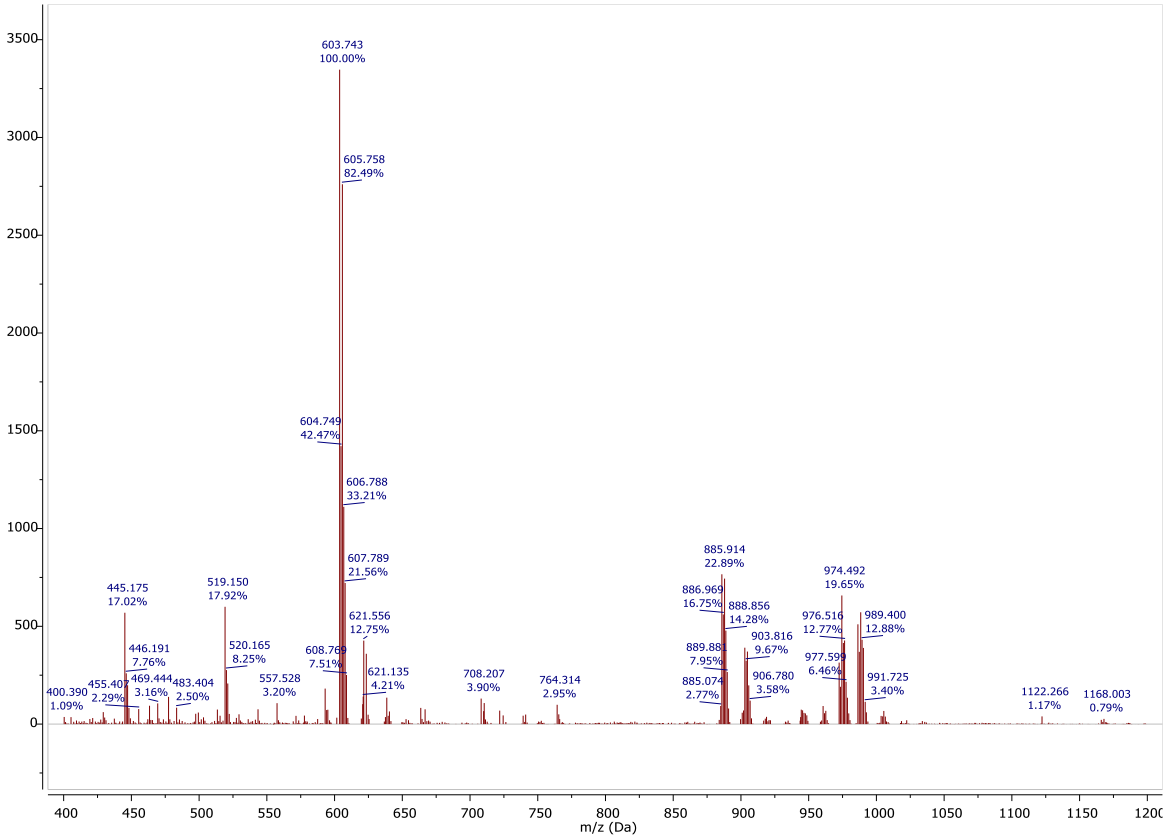

Figure 73: ESI-MS spectrum of the raw interesterification product obtained with HEC-TLL crosslinked with DFF in NaCl 3 M

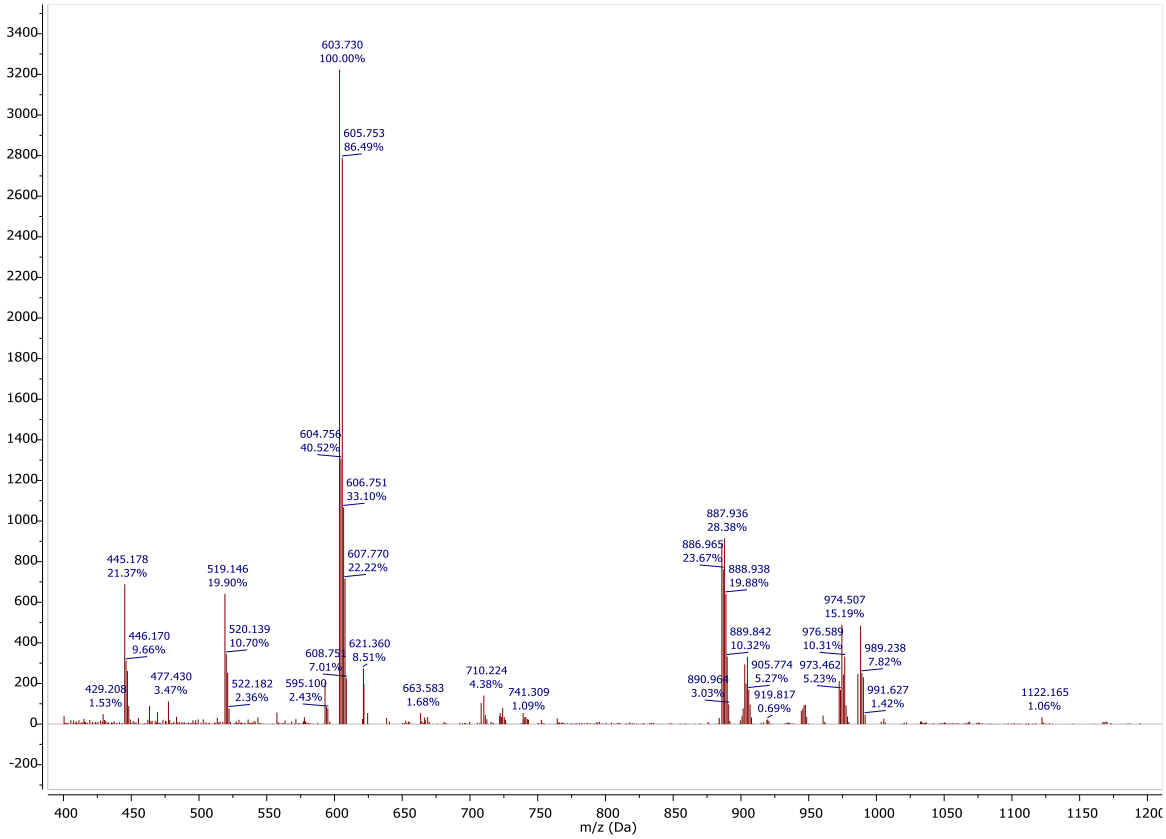

Figure 74: ESI-MS spectrum of the raw interesterification product obtained with PVP-TLL crosslinked with DFF in CH_2Cl_2

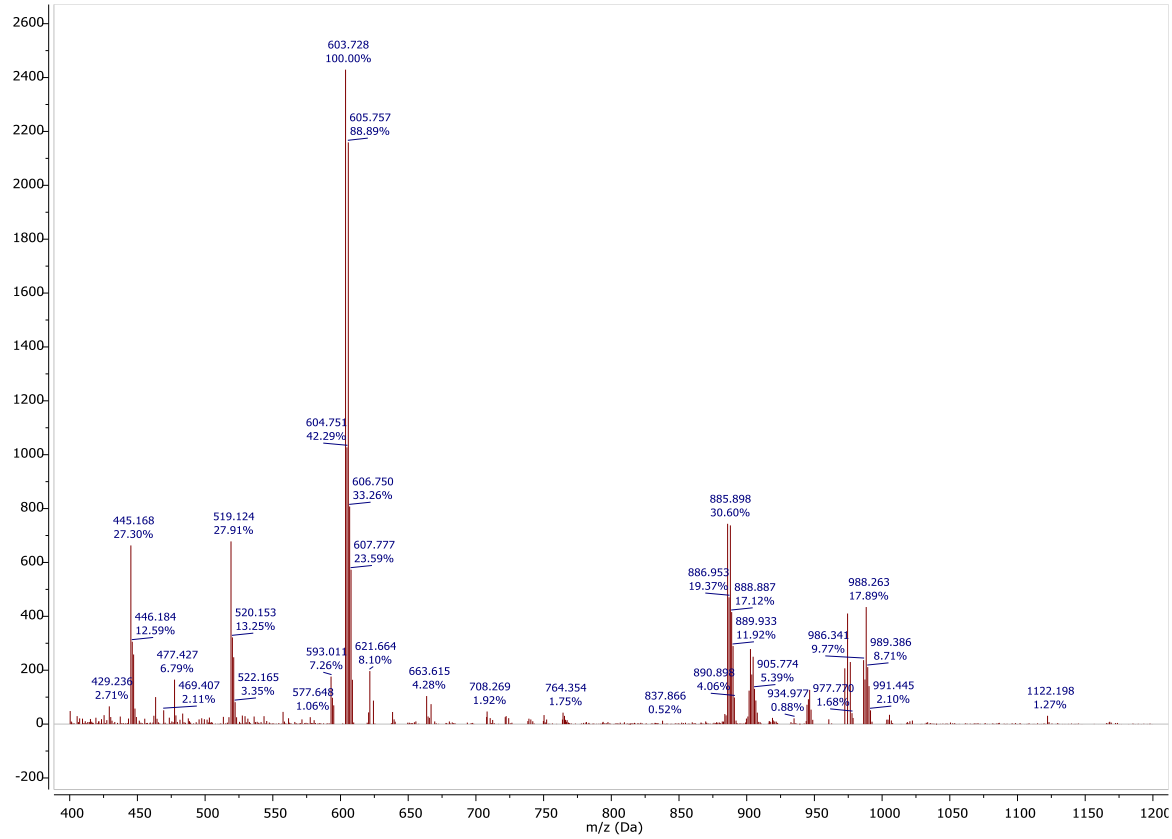

Figure 75: ESI-MS spectrum of the raw interesterification product obtained with HEC-TLL crosslinked with DFF in CH_2Cl_2

Table 29: Possible reaction products and relative monoisotopic mass in the interesterification between triolein and tristearin

Structure	Name / Abbreviation	Monoisotopic Mass
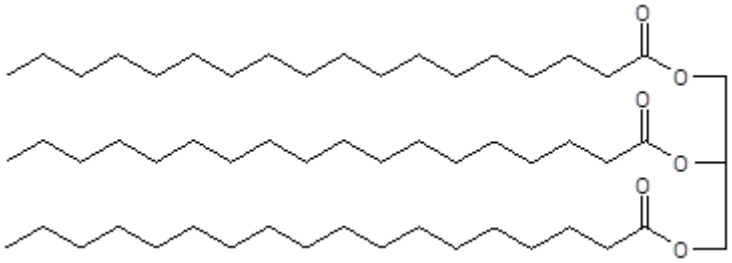	Tristearin SSS	890.830
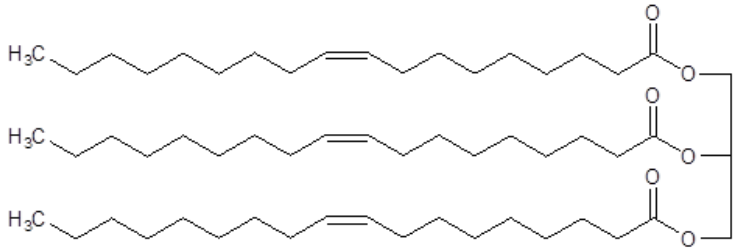	Triolein OOO	884.783
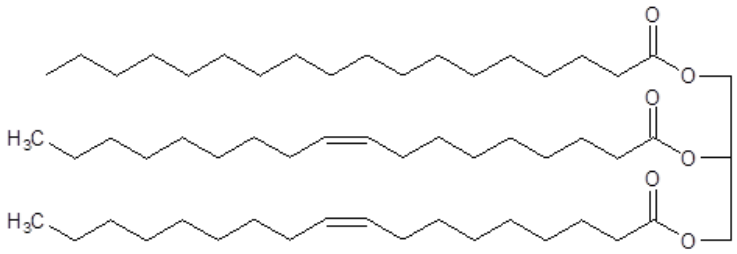	SOO/OOS	886.799
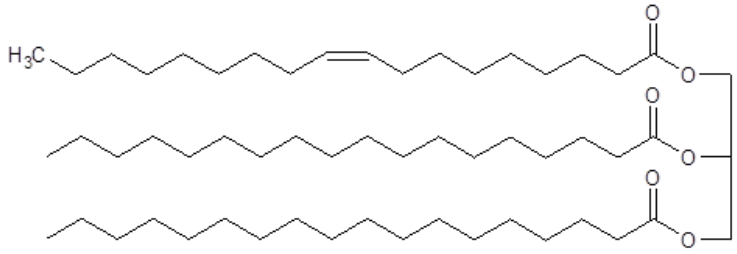	OSS/SSO	888.815
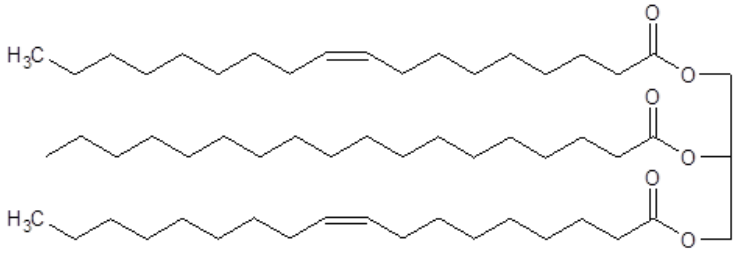	OSO	886.799
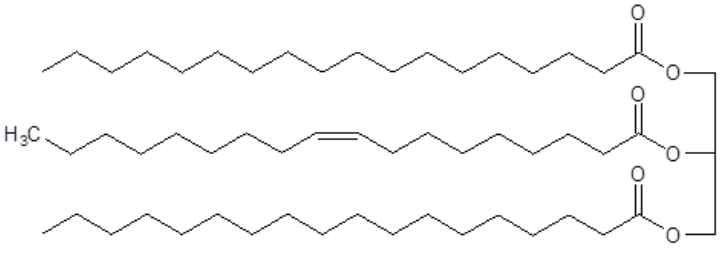	SOS	888.815

Structure	Name / Abbreviation	Monoisotopic Mass
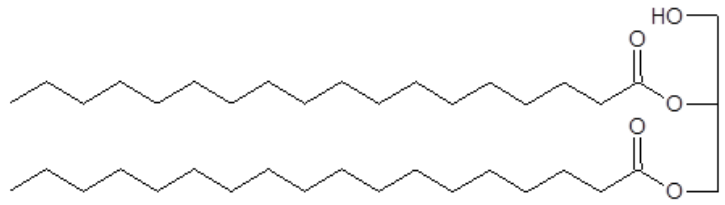	Product 7 SSX	624.569
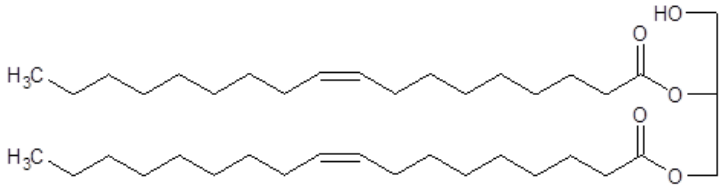	Product 8 OOX	620.538
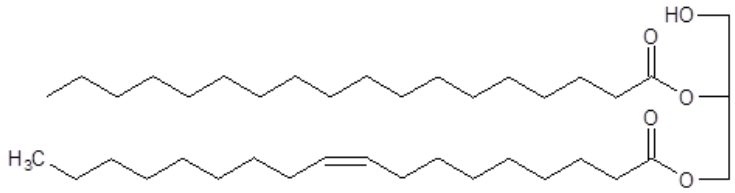	Product 9 SOX	622.554
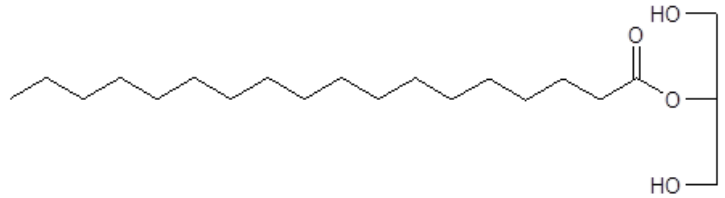	Product 10 XSX	358.308
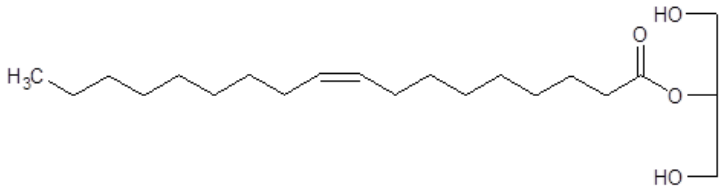	Product 10 XOX	356.293
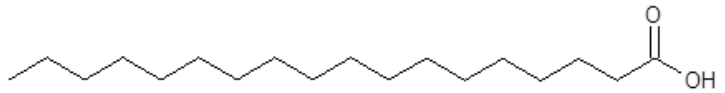	Stearic acid	284.272
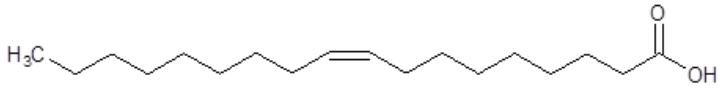	Oleic acid	282.256

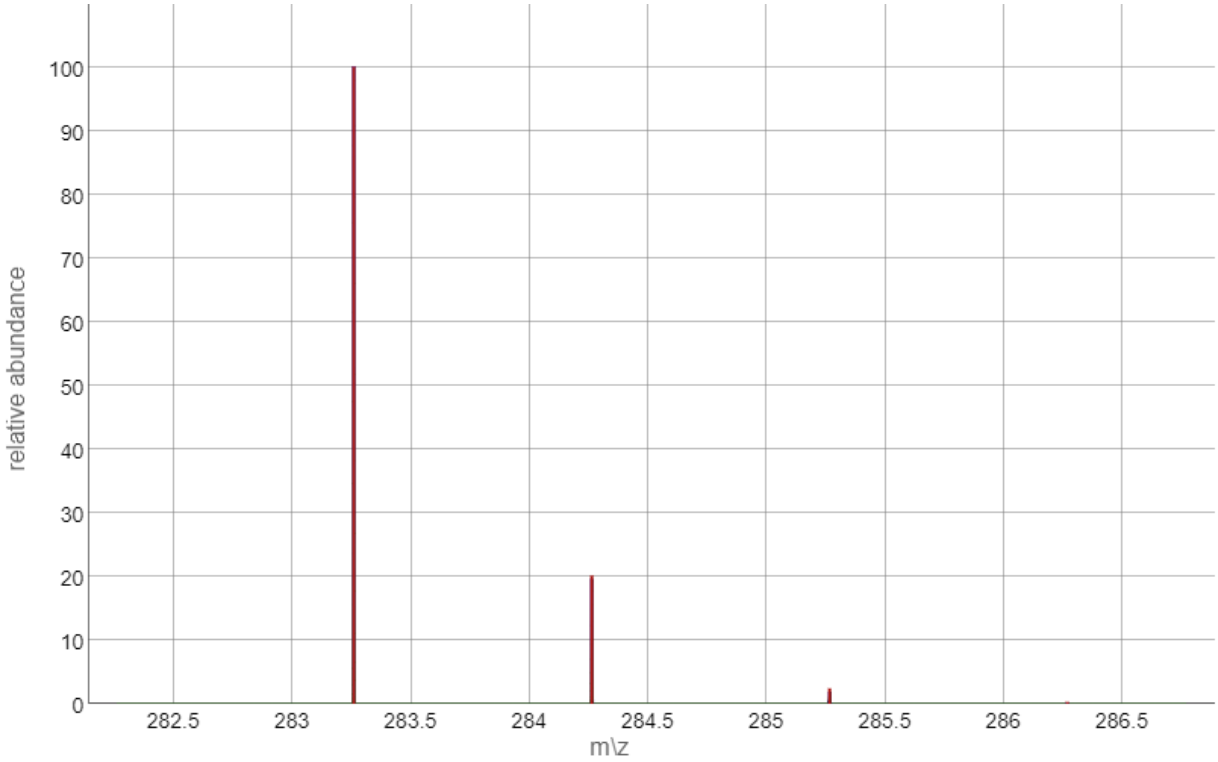

Figure 76: Isotopic pattern for the $[M+H]^+$ ESI-MS peak of oleic acid

Table 30: Theoretical ESI-MS peaks for the possible reaction products of the interesterification of triolein and tristearin

	SSS	OOO	SOO-OSO	SSO-SOS	SSX	OOX	SOX	XSX	XOX	Stearic	Oleic
Monoisotopic Mass	**890.830**	**884.783**	**886.799**	**888.815**	**624.569**	**620.538**	**622.554**	**358.308**	**356.293**	**284.272**	**282.256**
$[M+3H]^{3+}$	297.951	295.935	296.607	297.279	209.197	207.853	208.525	120.443	119.771	95.764	95.093
$[M+2H+Na]^{3+}$	305.278	303.262	303.934	304.606	216.524	215.181	215.852	127.771	127.099	103.092	102.420
$[M+H+2Na]^{3+}$	312.606	310.590	311.262	311.934	223.852	222.508	223.180	135.099	134.427	110.420	109.748
$[M+3Na]^{3+}$	319.933	317.917	318.589	319.261	231.179	229.835	230.507	142.425	141.753	117.746	117.075
$[M+2H]^{2+}$	446.422	443.399	444.407	445.415	313.292	311.276	312.284	180.161	179.154	143.143	142.135
$[M+H+Na]^{2+}$	457.413	454.390	455.398	456.406	324.283	322.267	323.275	191.152	190.145	154.134	153.126
$[M+H+K]^{2+}$	465.400	462.377	463.385	464.393	332.270	330.254	331.262	199.139	198.132	162.121	161.113
$[M+2Na]^{2+}$	468.404	465.381	466.389	467.397	335.274	333.258	334.266	202.143	201.136	165.125	164.117
$[M+Na\text{-}StCOONa]^{+}$	607.567	N/D	603.536	605.552	341.306	N/D	339.291	75.045	N/D	N/D	N/D
$[M+Na\text{-}OlCOONa]^{+}$	N/D	603.535	605.551	607.567	N/D	339.290	341.306	N/D	75.045	N/D	N/D
$[M+H]^{+}$	891.838	885.791	887.806	889.822	625.577	621.545	623.561	359.316	357.300	285.279	283.263
$[M+NH_4]^{+}$	908.864	902.817	904.833	906.848	642.603	638.572	640.587	376.342	379.282	302.305	300.290
$[M+Na]^{+}$	913.819	907.773	909.788	911.804	647.558	643.527	645.543	381.298	379.282	307.261	305.245
$[M+K]^{+}$	929.793	923.746	925.762	927.778	663.532	659.501	661.517	397.271	395.256	323.235	321.219
$[M+2Na\text{-}H]^{+}$	935.801	929.754	931.770	933.786	669.540	665.509	667.525	403.279	401.264	329.243	327.227
$[M+2K\text{-}H]^{+}$	967.749	961.702	963.718	965.734	701.488	697.457	699.473	435.227	433.212	361.191	359.175
$[2M+H]^{+}$	1782.668	1770.574	1774.605	1778.636	1250.146	1242.083	1246.115	717.624	713.593	569.550	565.519
$[2M+Na]^{+}$	1804.650	1792.556	1796.587	1800.618	1272.128	1264.065	1268.096	739.606	735.575	591.532	587.501
$[2M+K]^{+}$	1820.624	1808.530	1812.561	1816.592	1288.102	1280.039	1284.070	755.580	751.548	607.506	603.475

OlCOONa = Sodium oleate

StCOONa = Sodium stearate

5 Immobilization of enzymes by covalent binding on functionalized rice husk

5.1 Background

5.1.1 Rice husk

As previously discussed in th[215]e introduction of this thesis, one of the main hindrances to the use of immobilized enzymes at an industrial scale is the overall cost of the immobilization process, which is mostly affected by the high cost of the carriers, especially the commercial fossil-based resins.[34] On top of their cost, polymeric carriers also present other problems such as poor performance under chemical and mechanical stress,[62] as well as their contribution to the overall greenhouse gas emissions of the biocatalytic process.[33]

Previous studies by prof. Gardossi's group explored the potential of milled rice husk as an enzyme carrier.[15,53,62] Rice husk is a lignocellulosic material obtained as a by-product of rice production. It accounts for a production of 120 Mt per year, of which only 20 Mt find an application. Rice husk is a robust composite material mainly formed by SiO_2, lignin, cellulose and hemicellulose.[15] From a morphological point of view, it presents two markedly different surfaces: the external surface is rich in silica, which forms linear ripples and confers mechanical stability to the material, while the internal surface is smoother and much richer in cellulose.[53] Inside the material there are linear, fibrous tubular structures, named tracheids, which serve as canals for water and nutrients in the plant cell wall.[53]

The milling of the rice husk before enzyme immobilization serves several purposes: it is used to achieve fragments of comparable size to polymeric enzyme carriers, but more importantly it increases the exposure of the internal, cellulose-rich portions of the material, favouring the attack by chemical and enzymatic agents and the functionalization procedures.

Indeed, the cellulose component of rice husk can be exploited for enzyme immobilization *via* functionalization. The oxidation of cellulose, obtained by chemical[15,53] or enzymatic[62] means, introduces aldehyde groups on the rice husk matrix. These aldehyde groups can then react with difunctional agents such as glutaraldehyde[15,53] or directly with lysine residues on the enzyme surface[62] to achieve enzyme immobilization. It is important to note that the two oxidation methodologies have different effects on the overall morphology of rice husk: the enzymatic oxidation left the tridimensional structure mostly intact, while the more aggressive, less specific chemical oxidation had a corrosive effect on the rice husk surface opening the access to deeper layers of the material.[62]

The immobilization on rice husk proved effective for enzymes such as lipases[15,45,53,62] and cutinases[216], which are active on hydrophobic substrates. The immobilization of invertase was also achieved, both covalently on oxidized rice husk[15] or by adsorption-crosslinking.[15,217] Notably, the adsorption of invertase was effective only by pre-coating the rice husk matrix with poly(ethyleneimine), which increases the hydrophilicity of the carrier.

5.2 Summary and objectives

In this chapter, rice husk was thoroughly characterized as a renewable enzyme carrier. The milled rice husk was analyzed as-is and after being subjected to alkaline delignification, in order to remove the hydrophobic component of the material (i.e. lignin) and improve its affinity for more hydrophilic enzymes such as glucoamylase. The study reported in chapter 3 indicated that glucoamylase from *Aspergillus niger* is highly glycosylated and hydrophilic, and as such it is very different from the enzymes previously immobilized on rice husk.

Rice husk, both raw and delignified, was oxidized and used for enzyme immobilization, comparing the performance of both materials. The enzymes selected for the immobilization were (1) glucoamylase from *Aspergillus niger* and (2) lipase from *Thermomyces lanuginosus*. The first enzyme was tested in the hydrolysis of starch whereas the lipase was assayed in the hydrolysis of tributyrin. In both cases the attention was focused on the efficiency of the new immobilization protocols to form stable covalent bonds able to prevent the leaching of the proteins when exposed to aqueous media.

Glucoamylase from *Aspergillus niger* was covalently immobilized on an amino-functionalized methacrylic carrier (Chapter 3) using DFF as a carrier-activating agent. It is highly glycosylated and hydrophilic, and as such is very different from the enzymes previously immobilized on rice husk. In the present chapter we will investigate whether it can be immobilized on rice husk *via* pre-established protocols and whether the use of delignified rice husk, more hydrophilic, is beneficial to the immobilization of this enzyme.

Lipase from *Thermomyces lanuginosus* has been previously successfully immobilized on rice husk. In this chapter, we will investigate whether the use of delignified rice husk for the immobilization process changes the efficiency of the immobilization method.

5.3 Results and Discussion

5.3.1 Delignification process

As stated in the introduction, rice husk is mainly composed of silica, lignin, cellulose and hemicellulose. Of these components, lignin confers hydrophobicity to the material: it is a complex organic polymer formed mainly by phenolic monomers. In order to increase the hydrophilic character of rice husk, the milled material was subjected to delignification.

Delignification is the process of removing lignin from a lignocellulosic biomass; it is used for example in the pre-treatment of the lignocellulosic biomass for the production of bioethanol.[218,219] Lignin removal can be achieved by various means, including the use of enzymes such as lignin peroxidase,[220] or by employing chemicals such as NaOH.[221,222]

In this case, it was employed an alkaline delignification process, using NaOH and with the aid of hydrogen peroxide as an oxidant. The rice husk was suspended in hydrogen peroxide, and the reaction mixture was heated up to 70°C; then, NaOH was added in portions to the mixture, and the mixture was kept at 70°C for 5 hours. After the delignification procedure, rice husk appears of a pale yellow color, in contrast with the light brown color of the non-delignified material. The milled, delignified rice husk was then analyzed with different methods and further used for enzyme immobilization.

5.3.2 Characterization of rice husk as a renewable carrier

5.3.2.1 Stereoscopic microscopy

A) **B)**

Figure 77: Stereoscopic microscopy images of raw (A) and delignified (B) milled rice husk, particle size 200-400 µm.

Figure 77A and Figure 77B show the stereoscopic microscopy images of, respectively, raw and delignified milled rice husk. Delignified rice husk appears lighter in color compared to non-delignified rice husk, due to the removal of the lignin fraction. It can also be noticed that the morphological structure of the cuticle is preserved during the delignification process.

5.3.2.2 SEM Microscopy

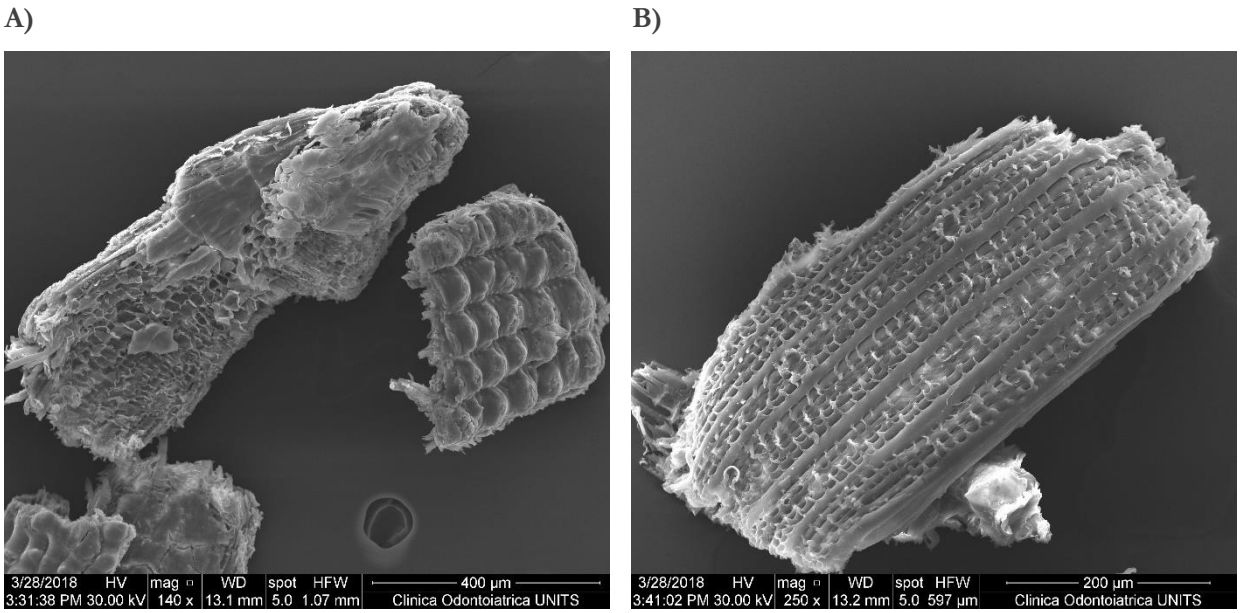

Figure 78: SEM microscopy images of milled rice husk before (A) and after (B) the alkaline delignification process

Figure 78A and Figure 78B report scanning electron microscope (SEM) images of milled rice husk, respectively before and after the delignification process. These images confirm what was previously observed with stereoscopic microscopy: the delignification process did not impact the overall morphology of the rice husk fragments.

5.3.2.3 Bulk Density

Bulk density of milled RH (particle size 200-400 µm), both raw and delignified, was determined using the procedure described in the Materials and Methods section. The results are presented in Table 31. The bulk density of rice husk has decreased after the delignification process, coherently with the fact that lignin has been removed from the matrix, while the overall structure was not damaged by the delignification process.

Table 31: Bulk density of raw and pre-treated milled rice husk (particle size 200-400 µm).

	Density (g/mL)
Raw rice husk (200-400 µm)	0.437
Delignified rice husk (200-400 µm)	0.354

5.3.2.4 Porosity analysis

Table 32 reports the results from the porosimetry analysis of raw and delignified rice husk. From a morphological point of view, the two samples are equivalent. The two samples have both a macroporosity of about 0.1 µm, as evidenced by the average pore diameter. Moreover, both samples have a good degree of porosity (around 40%) and a very similar total pore area.

The similarity of the two samples and the equivalence of the morphological structure evidences the resistance of the rice husk matrix to chemical treatments, such as the delignification procedure. This robustness makes it a good candidate as carrier for biocatalytic applications.

Table 32: Comparison of porosity of milled rice husk (particle size 200-400 μm) before and after delignification. Data were obtained with mercury porosimetry.

	Total Intrusion Volume (mL/g)	Total pore area (m^2/g)	Average pore diameter (μm)	Porosity (%)
Raw rice husk (200-400 μm)	0.4162	18.740	0.0888	41.3
Delignified rice husk (200-400 μm)	0.3811	15.783	0.0966	39.3

5.3.2.5 Water retention

Water retention capacity of RH was measured with an established procedure,[15] using a series of soaking treatments with increasing H_2O/EtOH ratios to promote the full wettability of the matrix and the retention of water in the tunnels of the material. This treatment is necessary as raw rice husk has a high content in lignin (31% of the organic components of rice husk[15]), which is hydrophobic. The results were compared with control samples of RH that did not undergo the soaking treatment.

The analysis results shows that the water retained in the matrix after the soaking treatments is about the same between raw and delignified rice husk; this is coherent with the fact that the morphological structures and the structure of the pores do not change in the delignification process.

However, the humidity in the control sample of delignified rice husk is higher than that in the control sample of raw rice husk. This can be explained as delignified rice husk has a reduced content in lignin, which is hydrophobic. Therefore, it tends to retain a higher amount of humidity in the matrix compared to the non-delignified rice husk.

Table 33: Water retention capability of raw and pre-treated milled rice husk (particle size 200-400 μm)

		Water retention
Raw rice husk (200-400 μm)	With soaking treatment	42.6%
	Control	9.6%
Delignified rice husk (200-400 μm)	With soaking treatment	43.6%
	Control	14.2%

The results obtained for the water adsorption capacity of rice husk were in line with those obtained in previous studies.[15] Moreover, Corici et al. pointed out that the water adsorption capacity of rice husk particles is much lower than that of epoxy-functionalized methacrylic resins (water retention 63%); the authors attributed this to the presence of less structured pores in the biomaterial compared to the synthetic resin.[15]

5.3.2.6 Contact angle measures

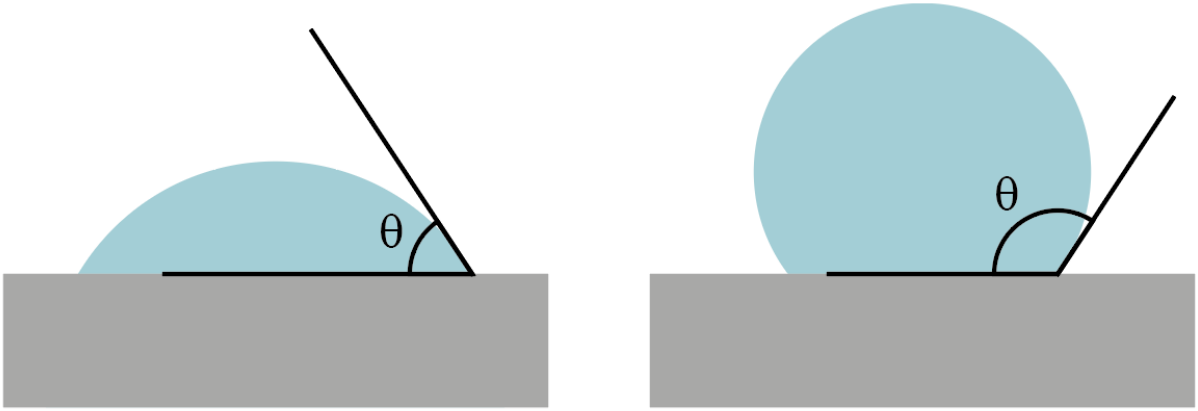

Figure 79: Contact angle for an object with high wettability (left) and low wettability (right)

To complete the study of rice husk wettability, contact angle measures were performed. The contact angle indicates the degree of wetting of a solid during its interaction with a liquid, in this case water. A small contact angle (<90°) indicates high wettability, while a high contact angle (>90°) indicates low wettability.[15] The results of measures on milled rice husk, both raw and delignified, are reported in Table 34.

Table 34: Average measured contact angles of raw and delignified rice husk

	Contact Angle (°)
Raw rice husk (200-400 μm)	79.3 ± 3.6
Delignified rice husk (200-400 μm)	40.6 ± 2.5

The measure for milled, non-delignified rice husk is in disagreement with what measured previously by Corici et al. (58.10 ± 11.59); the rice husk analyzed for this thesis is less prone to aqueous wetting than the one analyzed in that work. This can be explained by the fact that the rice husk samples came from different batches.

From the measured values, it is evident that delignified rice husk is much more prone to wetting than non-delignified rice husk. This is coherent with the fact that lignin, the most hydrophobic component of rice husk, has been removed from the material during the delignification process.

5.3.2.7 ATR-IR measures

Figure 80 shows a comparison between the ATR-IR spectra of raw (in blue) and delignified (in orange) rice husk, between 1800 and 600 cm^{-1}. The main components of rice husk (lignin, cellulose and silica[15]) give characteristic signals, which are evidenced in the figure and reported in the table below.

Table 35: Signals of interest in the ATR-IR spectra of raw and delignified milled rice husk.

Functional group	**cm^{-1}**
Carbonyl group (stretching)	1730
Lignin aromatic groups	1600-1650
Total carbohydrates (cellulose)	1030
SiO_2	785

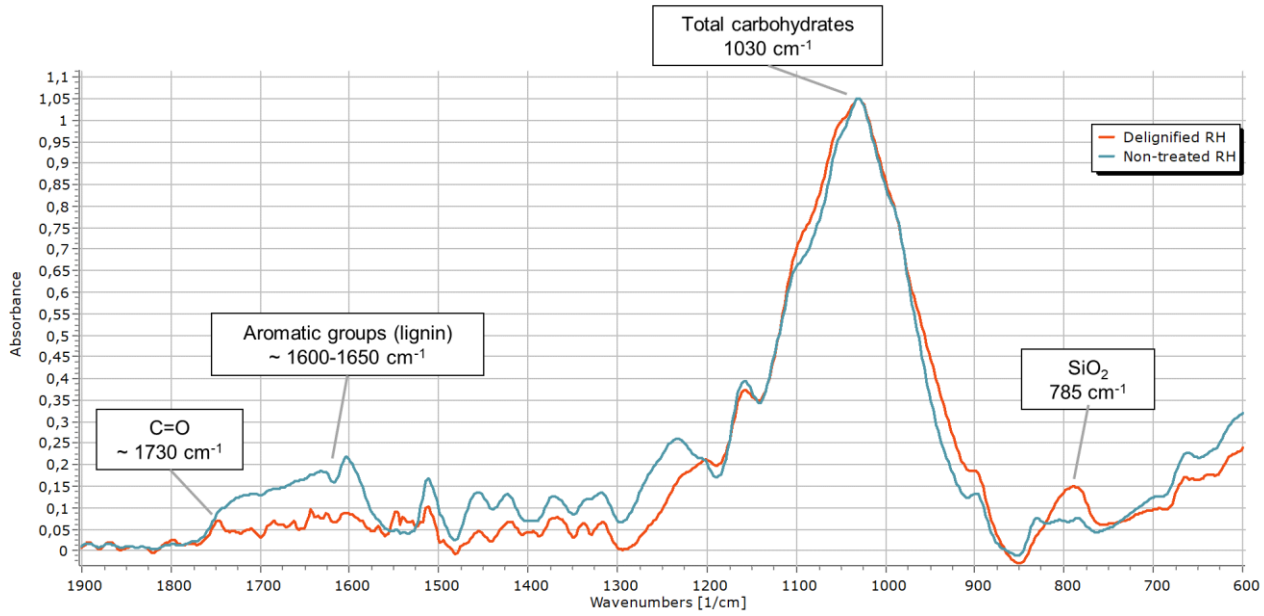

Figure 80: ATR-IR analysis of milled rice husk (particle size 200-400 µm). In black: raw rice husk; in yellow: delignified rice husk

From a qualitative analysis, it is evident how the intensity of the signals of lignin (between 1600 and 1650 cm^{-1}) decreases in delignified rice husk compared to raw rice husk. This confirms the effectiveness of the delignification pretreatment.

5.3.3 Marine biodegradability of rice husk

The marine biodegradability of raw and delignified milled rice husk (particle size 200-400 µm) was tested in accordance with ISO 17556:2019, using the procedure as reported in literature.[223] The test involves the use of OxiTop® devices, equipped with sensor in order to measure the biochemical oxygen demand (BOD) required to biodegrade the introduced material in the assay environment. The liquid culture used for the assay was prepared by following the procedure reported in the Materials and Methods section, and using water collected from the Adriatic Sea (Trieste) in the period February-March 2023 as inoculum. The two rice husk samples were compared with a sample of amino-functionalized PMMA carrier, as used in the first part of the project for the immobilization of glucoamylase. The results after 5, 10 and 20 days of incubation are presented in the following table.

Table 36: Results of the biodegradability assay for rice husk, delignified rice husk and an amino-functionalized PMMA carrier in marine environment. The results are expressed in mg/L.

Sample	BOD_5	BOD_{10}	BOD_{20}
Rice husk	0.00 ± 0.00	-0.01 ± 0.49	0.02 ± 1.34
Delignified Rice Husk	0.01 ± 1.06	0.02 ± 2.83	-0.01 ± 1.13
PMMA carrier	0.01 ± 0.71	-0.01 ± 0.49	0.02 ± 0.71

As evident from the table, none of the sample resulted to be biodegradable in the selected conditions. It is important to note, however, that the assay employed is usually applied to organic molecules, and could not be the best choice for testing the biodegradability of composite solids such as rice husk or the polymeric enzyme carrier. Further studies are needed to determine the biodegradability of these enzymatic carriers, also in media other than the marine system studied.

It is important to note that other studies proved the degradability of rice husk composite materials in soil,[224–226] further suggesting that the biodegradation of raw and delignified rice husk needs to be examined with different culture media.

5.3.4 Rice husk functionalization

The oxidation of rice husk targets the cellulose component of the lignocellulosic matrix; the process causes the introduction of aldehyde groups. Aldehyde groups can then be exploited for covalent immobilization of enzymes, which react with the aldehyde groups through the amine functionality of lysine side chains. Two different oxidation methods have been used on both raw and delignified rice husk.

5.3.4.1 Chemical oxidation of rice husk with $NaIO_4$

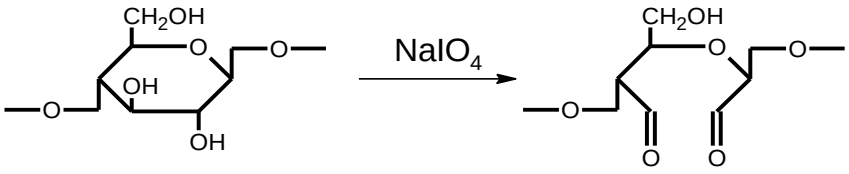

Scheme 17: Oxidation of cellulose with $NaIO_4$

Milled rice husk (particle size 200-400 μm) was washed with a 1:1 EtOH/H_2O solution, dried in the oven at 120°C and then oxidized with $NaIO_4$ following an established procedure.[15] The reaction targets the cellulose component of rice husk, cleaving the C2-C3 bond in the glucose units and replacing the hydroxyl groups with aldehyde groups (Scheme 17).

5.3.4.2 Enzymatic oxidation of rice husk with a laccase-mediator system

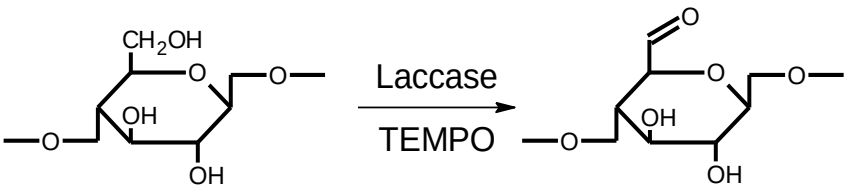

Scheme 18: Enzymatic oxidation of cellulose with a laccase-mediator system

Milled rice husk (particle size 200-400 μm) was washed with a 1:1 EtOH/H_2O solution, dried in the oven at 120°C and then oxidized with a laccase-mediator system. Rice husk was incubated with Laccase from *Trametes sp.* at 70°C for 48 hours in the presence of TEMPO. In this case, the reaction targets the primary hydroxyl groups at the C6 of the glucose units of cellulose, converting them into aldehyde groups (Scheme 18).[3]

5.3.4.3 Morphology of rice husk after oxidation

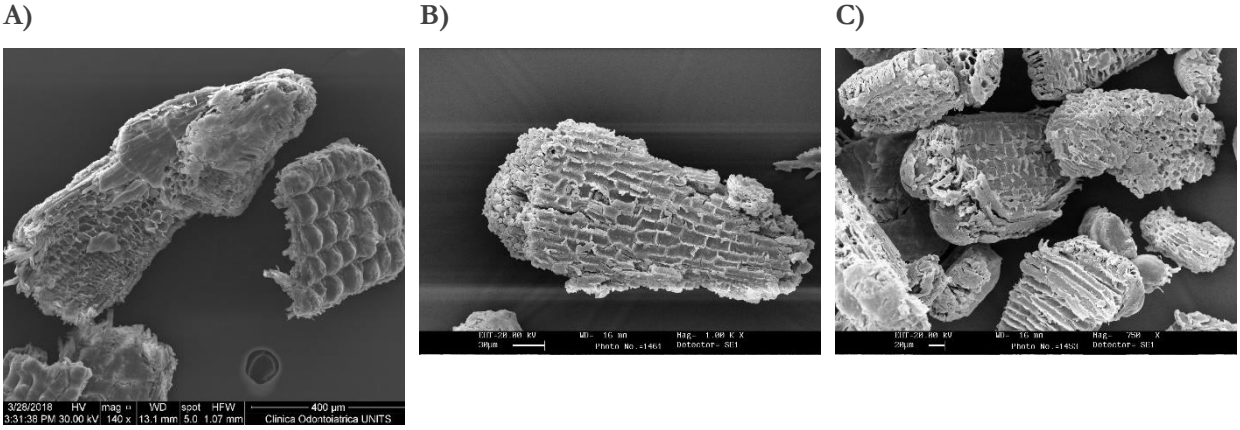

Figure 81: SEM microscopy images of non-oxidized milled rice husk (A), milled rice husk oxidized with $NaIO_4$ (B) and milled rice husk oxidized with LMS (C)

The morphology of the rice husk samples after oxidation was examined by SEM microscopy imaging (Figure 81). As it was observed in previous studies,[62] the treatment with $NaIO_4$ has a corrosive effect on the surface of rice husk, due to its poor selectivity towards the various components of the lignocellulosic matrix. On the contrary, the laccase-mediator system was shown to cause negligible modifications to the morphology of the external surface of rice husk.

5.3.4.4 Carbonyl group determination

The oxidized rice husk samples have been analyzed in order to determine the concentration of carbonyl groups introduced in the matrix. The concentration of carbonyl groups on oxidized rice husk was determined using an established protocol reported in literature.[15] The assay is based on the reaction of carbonyl groups with hydroxylamine hydrochloride, which generates HCl (Scheme 19). Titration of the HCl formed in the reaction allows to determine the concentration of carbonyl groups on the oxidized material.

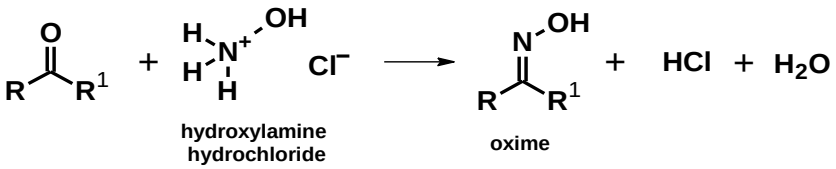

Scheme 19: Reaction of carbonyl groups with hydroxylamine hydrochloride

The results were compared to a reference measure of non-oxidized rice husk. As shown in Table 37 and Figure 82, enzymatic oxidation introduces about the same amount of carbonyl groups on both raw and delignified rice husk; compared to non-oxidized rice husk, the carbonyl group content has triplicated. In the case of chemical oxidation, the carbonyl group concentration on delignified rice husk is 43% higher to that on non-delignified rice husk; this can be explained with the fact that the removal of lignin has increased accessibility of $NaIO_4$ to the cellulose component of the material. In fact, previous studies indicated that $NaIO_4$ has an inherent corrosive ability that increases the roughness of the rice husk surface.[62]

Table 37: Carbonyl group content in oxidized rice husk, both raw and delignified.

Rice Husk	Oxidation	Average [C=O] (mmol/g)
Raw	$NaIO_4$	1.618 ± 0.013
	Lac C + TEMPO	0.179 ± 0.060
Delignified	$NaIO_4$	2.320 ± 0.195
	Lac C + TEMPO	0.150 ± 0.019
Reference	Non oxidized	0.049

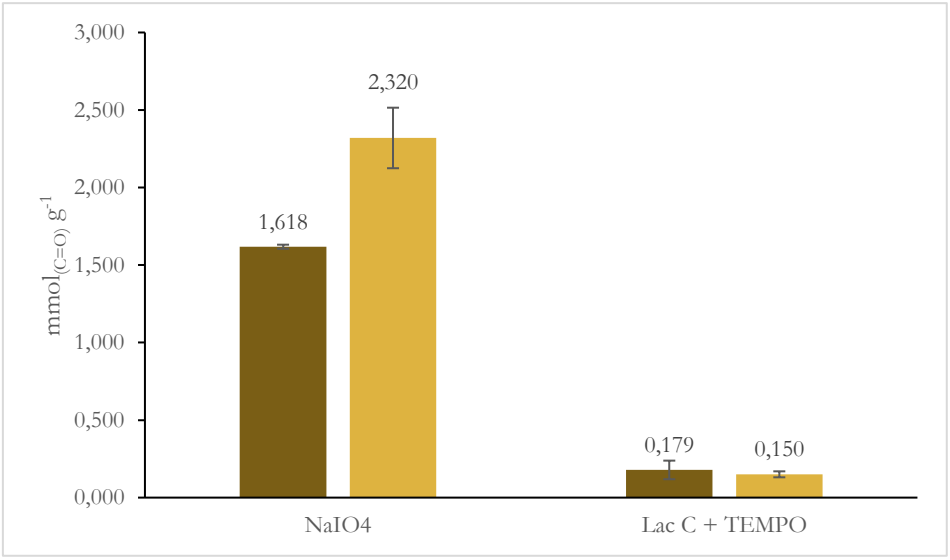

Figure 82: Carbonyl group content comparison for raw (in brown) and delignified (in yellow) rice husk, with two different oxidation methods.

5.3.5 Immobilization of glucoamylase on functionalized rice husk

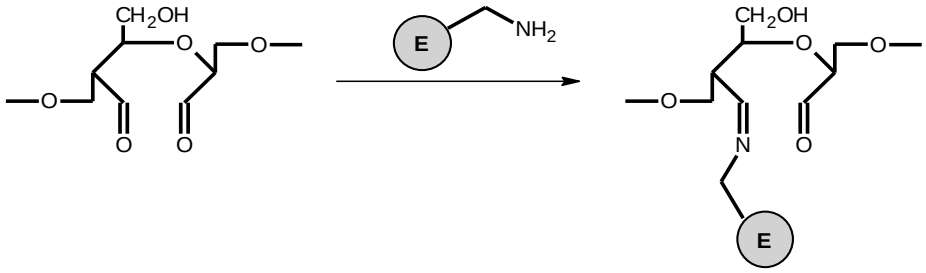

Figure 83: Immobilization of an enzyme on chemically oxidized rice husk

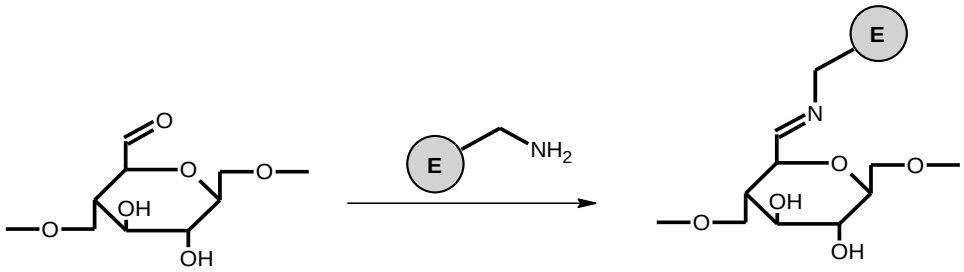

Figure 84: Immobilization of an enzyme on enzymatically oxidized rice husk

Glucoamylase from *Aspergillus niger* was incubated with chemically oxidized rice husk and with enzymatically oxidized rice husk to achieve enzyme immobilization. Several immobilization conditions were then tested to identify the better immobilization condition for glucoamylase, an enzyme that had not been previously immobilized on the biobased carrier.

The first set of immobilization experiments involved the incubation of glucoamylase with oxidized rice husk (both chemically and enzymatically oxidized) in 25 mM KPi, the same buffer used for the immobilization of glucoamylase on the methacrylic carrier. The buffer choice was done in order to compare the data obtained for the methacrylic carrier with those for glucoamylase on rice husk. Two different buffer pH were chosen: (a) pH 7, the same used for the immobilization of glucoamylase on the methacrylic carrier and (b) pH 8, in order to facilitate the formation of the imine bond between the enzyme and the oxidized cellulose component of the rice husk. The chosen incubation time, 24 hours, was also selected as it was the same incubation time used for the immobilization on the PMMA carrier.

After the incubation, the supernatant mixture for each immobilization was analyzed in a Bradford assay of protein content; the disappearance of protein from the supernatant solution would indicate the immobilization of the protein itself on the carrier. Only samples which showed disappearance of the protein from the supernatant solution were then analyzed in a hydrolytic activity assay. Procedures for the assays can be found in the Materials and Methods section.

Table 38: Results of the first batch of experiments for the immobilization of glucoamylase on rice husk. Immobilization conditions: 25 mM KPi, 25°C, 24 h. Loading: 365 U/g.

Experiment	Rice husk oxidation	Immobilization pH	Initial protein concentration (mg/mL)	Final protein concentration (mg/mL)	Immobilization yield (%)[a]
1	$NaIO_4$	7	18.46 ± 0.04	19.69 ± 0.10	–
2	$NaIO_4$	8	18.46 ± 0.04	16.67 ± 0.17	9.7
3	LMS	7	18.46 ± 0.04	19.91 ± 0.07	–
4	LMS	8	18.46 ± 0.04	20.00 ± 0.09	–

[a] Calculated as $\frac{Initial\ protein\ concentration - Final\ protein\ concentration}{Initial\ protein\ concentration} \times 100$

As can be seen in the previous table, only one of the four immobilization experiments showed the disappearance of protein from the supernatant solution. For this reason, only that sample was analyzed in a batch hydrolytic assay. The measure was performed in duplicate, and the results are displayed in the following table.

Table 39: Results of the activity assay on the immobilized glucoamylase sample from experiment 2.

Experiment	Measure	Activity (U/g)
2	1	0
	2	0

Unfortunately, the immobilized enzyme sample did not display any activity. For this reason, different immobilization conditions were explored. The second set of experiments was conducted on chemically oxidized rice husk, using a higher concentration of buffer: KPi, 0.1 M, pH 7. The higher concentration was chosen hypothesizing that a higher ionic strength of the solution would favor the partition of the protein on rice husk. Two different experiments were conducted, using two different reaction volumes, to verify whether the dilution of the enzyme during the incubation influenced the final immobilization yield. A detailed procedure can be found in the Materials and Methods section.

Table 40: Results of the second batch of experiments for the immobilization of glucoamylase on rice husk. Immobilization conditions: KPi 0.1 M pH 7, 25°C, 24 h. Loading: 365 U/g.

Experiment	Rice husk oxidation	Total reaction volume (mL)	Initial protein concentration (mg/mL)	Final protein concentration (mg/mL)	Immobilization yield (%)[a]
5	$NaIO_4$	2.00	13.31 ± 0.16	11.89 ± 0.20	10.6
6	$NaIO_4$	1.26	17.76 ± 0.09	22.80 ± 0.52	–

[a] Calculated as $\frac{Initial\ protein\ concentration - Final\ protein\ concentration}{Initial\ protein\ concentration} \times 100$

Only one of the two samples showed the disappearance of protein from the supernatant solution; for this reason, only that sample was analyzed in a batch hydrolysis assay. The results are shown in the following table.

Table 41: Results of the activity assay on the immobilized glucoamylase sample from experiment 5. Loading: 365 U/g_{dry}.

Experiment	Activity (U/g_{wet})	Activity (U/g_{dry})	Recovered activity (%)[a]
5	0.37	0.49	0.13

[a] Calculated as: $\frac{Activity\left(\frac{U}{g_{dry}}\right)}{Loading\left(\frac{U}{g_{dry}}\right)} \times 100$

In this case, there was recovered activity in the final enzyme preparation; however, this displayed activity was extremely low, especially when compared to the initial enzyme loading of 365 U/g carrier.

A new set of experiments was planned, with a different enzyme loading. The loading was increased based on what reported on the paper from Spennato et al.[62]; that paper concerned the immobilization of lipases, therefore using the same loading in terms of enzymatic units per gram of carrier was not viable. For this reason, the new loading was calculated maintaining the same protein amount (in mg/$g_{carrier}$) of the protocol by Spennato. The buffer and reaction times used in the experiments were also extrapolated from the same paper. All experiments from this batch were performed on chemically oxidized rice husk.

Table 42: Results of the second batch of experiments for the immobilization of glucoamylase on chemically oxidized rice husk. Enzyme loading: 632 U/g.

Experiment	Immobilization buffer	Reaction time (h)	Initial protein concentration (mg/mL)	Final protein concentration (mg/mL)	Immobilization yield (%)[a]
7	KPi, 0.1 M, pH 7	48	25.29 ± 0.22	27.10 ± 0.12	–
8	KPi, 0.5 M, pH 8	48	27.70 ± 0.20	28.56 ± 0.17	–
9	KPi, 0.5 M, pH 8	72	27.70 ± 0.20	27.04 ± 0.14	2.0

[a] Calculated as $\frac{Initial\ protein\ concentration - Final\ protein\ concentration}{Initial\ protein\ concentration} \times 100$

As was the case in the previous sets of experiments, the immobilization yield was very low, and two of the experiments were not successful. Since the yield was so low even for the experiment which showed a decrease in protein concentration in the supernatant, no activity assay was performed on any of the samples.

Until this point, the approach employed the direct immobilization of the enzyme on the aldehyde groups introduced on oxidized rice husk, without further functionalization. The failure of this approach, however, suggested that the direct covalent bond between glutaraldehyde and rice husk does not form; for this reason, a different approach was tested, introducing a diamine spacer between the carrier and the enzyme in the immobilization process. The immobilization protocol is displayed in the following scheme, and was first reported by Corici et al.[15]

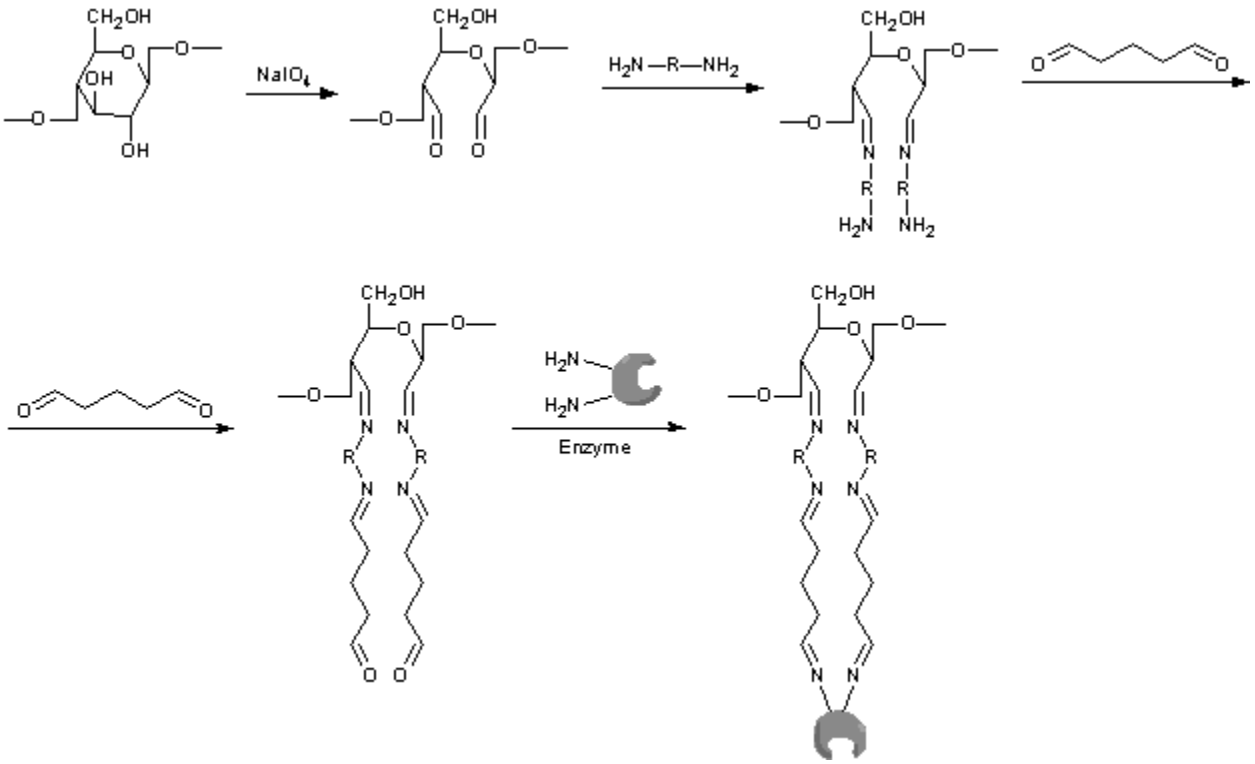

Scheme 20: Covalent immobilization of an enzyme on oxidized rice husk with the aid of a diamine spacer, hexamethylenediamine, during the immobilization process.[15]

In this case, chemically oxidized rice husk was first incubated in a 0.9 M solution of hexamethylenediamine (HMDA); then, the resulting amino-functionalized rice husk was activated by incubation in a 1.25% solution of glutaraldehyde in KPi (0.5 M, pH 8). The final activated rice husk sample was then incubated with glucoamylase for enzyme immobilization. However, hydrolytic activity batch assays performed on the final enzymatic preparation showed no recovered enzymatic activity: again, the immobilization of glucoamylase on oxidized rice husk was not successful.

Table 43: Results of the activity assay on the immobilized glucoamylase sample from experiment 10.

Experiment	Activity (U/g)
10	0

Given the negative results for the immobilization of glucoamylase on raw rice husk, a final batch of experiments was planned using oxidized, delignified rice husk as a support. This was based on the consideration that glucoamylase is a hydrophilic, highly glycosylated enzyme, therefore the partition of the enzyme on a hydrophobic, lignin-based matrix such as raw rice husk might be unfavorable. On the other hand, delignified rice husk is much more hydrophilic, so the immobilization of glucoamylase on this matrix could be more favorable. The buffer chosen for this batch of experiments was KPi, 0.025 M, pH 7, which is the same buffer used for the covalent immobilization of glucoamylase on activated PMMA carrier. A detailed immobilization procedure can be found in the Materials and Methods section.

Table 44: Results of the experiments for the immobilization of glucoamylase on oxidized, delignified rice husk.

Experiment	Rice husk oxidation	Initial protein concentration (mg/mL)	Final protein concentration (mg/mL)	Immobilization yield (%)[a]
11	$NaIO_4$	31.94 ± 2.36	29.87 ± 1.23	6
12	LMS	31.94 ± 2.36	30.06 ± 5.44	6

[a] Calculated as $\frac{Initial\ protein\ concentration - Final\ protein\ concentration}{Initial\ protein\ concentration} \times 100$

In this case, there is a higher immobilization yield than what observed for all the experiments on non-delignified rice husk. This further points towards the fact that delignified rice husk, being more hydrophilic, has a higher affinity for glucoamylase compared to the raw material. However, batch hydrolytic activity assays performed on the obtained samples displayed no recovered activity, as was the case with the previous samples.

In conclusion, there is the necessity to develop new, innovative immobilization protocols to obtain a fully renewable immobilized glucoamylase preparation, since the pre-existing protocols for the immobilization of enzymes on rice husk did not show the hoped results.

5.3.6 Immobilization of TLL on oxidized rice husk

A second enzyme for immobilization on rice husk was selected. The enzyme of choice was lipase from *Thermomyces lanuginosus* (TLL). This enzyme was selected since it is largely used in the food industry, has many possible industrial applications, and since as of the time of writing, there are no covalently immobilized formulations of this specific lipase on the market, despite its extensive use.

For TLL immobilization, the enzyme was incubated with raw or delignified rice husk, particle size 200-400 μm. In particular: (1) rice husk (raw or delignified) was oxidized by (a) chemical oxidation with sodium periodate ($NaIO_4$) or (b) enzymatic oxidation with a laccase-mediator system (LMS); then (2) each of the rice husk samples was incubated with TLL in the following conditions: potassium phosphate buffer, 0.5 M, pH 8, in the presence of 2 mg/mL PEG-3000. The results of the experiments are reported in the following table.

Table 45: Results of the experiments for the covalent immobilization of TLL on oxidized rice husk.

Experiment	RH	RH oxidation	Initial protein concentration (mg/mL)	Final protein concentration (mg/mL)	Yield[a] (%)
13	Raw	Chemical	9.20 ± 0.21	7.55 ± 0.43	18
14	Raw	Enzymatic	9.20 ± 0.21	9.33 ± 0.26	ND
15	Delignified	Chemical	9.20 ± 0.21	7.04 ± 0.27	23
16	Delignified	Enzymatic	9.20 ± 0.21	9.48 ± 0.45	ND

[a] Calculated as $\frac{Initial\ protein\ concentration - Final\ protein\ concentration}{Initial\ protein\ concentration} \times 100$

The Bradford assay for the supernatants of the enzymatically oxidized samples gave inconclusive results, showing an increase in protein concentration of the solution after incubation with the rice husk. Despite this, the final rice husk sample displayed hydrolytic activity, albeit small. A possible cause of the Bradford assay results could be the laccase used for the oxidation process; the laccase, despite extensive washing of the rice husk, could have still been adsorbed on the biomatrix, and could have solubilized during the 48-hour incubation period for TLL immobilization, thus contributing to the total protein concentration in the supernatant. Another possible explanation of the inconclusive results from the Bradford assay is the fact that the composition of the commercial TLL solution used for the immobilization is unknown, as the manufacturer did not release the nature and amount of additives present in the solution. Certain additives have been proven to interfere with Bradford assay.[227] Therefore, the presence of additives in the commercial enzyme solution may have influenced the results of the assay itself.

Observing the results for the chemically oxidized support, it is interesting to note that the adsorbed protein for the delignified rice husk is slightly more than that for the non-delignified rice husk. This suggests that there is a higher affinity of the protein for the less hydrophobic carrier, although the difference is small.

Table 46: Results of the activity assays on the samples of TLL on oxidized rice husk.

Experiment	RH	RH oxidation	Enzyme loading (U/g_{dry})	Recovered activity (U/g)[a]	Yield[b] (%)
13	Raw	Chemical	5081	41.3	0.81
14	Raw	Enzymatic	5081	39.6	0.78
15	Delignified	Chemical	5081	27.3	0.54
16	Delignified	Enzymatic	5081	16.8	0.33

[a] Activity determined with the hydrolysis of tributyrin. 1 tributyrin unit is the amount of enzyme that produces 1 μmol of butyric acid per minute at 31°C. Assay performed by M. Spennato.

[b] Calculated as $\frac{Recovered\ activity\ \left(\frac{U}{g}\right)}{Enzyme\ loading\ \left(\frac{U}{g}\right)} \times 100$

All samples underwent hydrolytic activity determination *via* hydrolysis of tributyrin. As can be seen in Table 46, all samples displayed an extremely low activity. The samples that displayed the higher activity were those of TLL immobilized on non-delignified rice husk, suggesting that the lipase has a higher affinity for the more hydrophobic carrier. This is in contrast with what observed from the results of the Bradford assay, which pointed towards a slightly higher affinity of TLL for the delignified rice husk. However, the activity values are so low that no definitive conclusion can be made for the analyzed enzymes.

5.4 Conclusions

In order to explore the possibility of improving the hydrophilicity of rice husk and increase its affinity for the heavily glycosylated glucoamylase, lignin and hemicellulose were removed in basic conditions. The delignification of rice husk was successful, as proven by the ATR-IR measurements, which clearly showed the decrease in lignin content in the material after the alkaline treatment. The delignified rice husk displayed a lower bulk density than the non-delignified rice husk, while maintaining the same morphological structure as evidenced by the SEM images. The hydrophilicity of the material was increased, as shown by the contact angle measurements.

Chemical and enzymatic oxidation of the cellulose component were conducted on both raw and delignified rice husk. The rice husk was oxidized both chemically and enzymatically, using laccase enzymes in the presence of TEMPO mediator. The insertion of diamine spacers was explored in the attempt to promote the formation of stable bonds between the enzyme and the functionalized carrier. Based on the carbonyl group content measures, the chemical oxidation procedure was much more effective on delignified rice husk; on the other hand, the enzymatic oxidation procedure gave similar results for the two rice husk samples.

Unfortunately, none of the immobilization attempts done with glucoamylase was successful. Even when protein loading on the carrier was detected, the final preparation displayed no enzymatic activity. The experiments on delignified rice husk were also unsuccessful, suggesting that, in the case of glucoamylase, there are other factors influencing the success of the immobilization, not related to the hydrophilic/hydrophobic nature of the carrier. It is worth noting that several immobilization conditions were tested.

Finally, the covalent immobilization of TLL on rice husk gave also poor results, in contrast with what was observed by previous studies,[62] probably ascribable to the use of a different batch of native enzyme. One interesting observation, though, is that the use of delignified rice husk did not cause an improvement in the final enzyme activity. This is consistent with the fact that lipases, which present a large lipophilic surface, do not benefit from the use of a more hydrophilic carrier such as delignified rice husk.

In conclusion, the functionalization of rice husk for the covalent immobilization of different enzymes appears a difficult route for developing generally applicable protocols. Despite the positive results previously reported with lipases CaLB and TLL,[62] similar protocols resulted unsuccessful when the very hydrophilic and glycosylated glucoamylase was employed. Moreover, also in the case of TLL the simple change of batch for the native enzyme led to much lower yields. These variations in the observed results might be also ascribable to stabilizers (e.g. glycerol, salts, etc.) present in different percentage in the commercial native enzymes.

5.5 Materials and Methods

5.5.1 Chemicals

All chemicals were purchased from Sigma Aldrich (now Merck) and were of the highest grade available.

5.5.2 Enzymes

Glucoamylase from *Aspergillus niger*, liquid solution (Dextrozyme GA, activity: 240 U/g, protein content: 83 mg/mL) was from Novozymes (Denmark). **Lipase from *Thermomyces lanuginosus*** (Lipolase 100L, expressed in *Aspergillus oryzae*, activity: 1613 U/g) was from Novozymes (Denmark) and was purchased from Sigma Aldrich. **Laccase C from *Trametes versicolor*** (powder, activity: 2176 U/g) was from ASA Spezialenzyme GmbH (Germany).

5.5.3 Carriers

Rice husk was donated by Riseria Cusaro (Binasco, Milano, Italy). It was milled with a blade mill (VERDER SCIENTIFIC S.r.l., Bergamo) and sieved to obtain a fraction with dimension 200-400 μm).

5.5.4 Other equipment

UV-Vis measurements were performed with a Shimadzu UV-2450 spectrometer (Shimadzu Corporation, Kyoto, Japan). **ATR-IR** spectra were recorded in attenuated total reflectance (ATR) mode with a Shimadzu IRAffinity-1S spectrophotometer equipped with a QATR 10 accessory. **Titrations and pH measurements** were performed with an automatic titrator Graphic DL50 (Mettler Toledo, USA).

5.5.5 Pretreatment of rice husk: washing procedure

10 g of milled rice husk (particle size 200-400 μm) are suspended in 30 mL of a 50:50 EtOH/H_2O mixture. The suspension is stirred on a magnetic stirring plate for 1 hour, after which the liquid phase is removed by decanting. The procedure is repeated 2 more times.

After washing, rice husk is filtered under vacuum, then dried in the oven at 120 °C for 3 hours.

5.5.6 Rice husk bulk density measures

Before density measures, the rice husk (raw or delignified) was dried in the vacuum oven (80°C, overnight) in order to make it anhydrous.

A 100 mL graduated cylinder was filled with anhydrous rice husk up to the 100 mL mark. The material was pressed to make it even and compact. The rice husk was then weighed, and the density was determined by:

$$density\ (g\ mL^{-1}) = \frac{weight_{rice\ husk}(g)}{Volume_{rice\ husk}(mL)} = \frac{weight_{rice\ husk}(g)}{100\ mL}$$

Measures were conducted in triplicate.

5.5.7 Rice husk water retention measures[15]

The water retention capacity of rice husk was determined with a series of soaking treatments, using increasing H_2O/EtOH ratios in order to promote the full wettability of the matrix and the absorption of water in the pores.

0.45 g of milled rice husk (raw or delignified, particle size 200-400 µm) were suspended in 2 mL of EtOH; the sample was shaken on the blood rotator (200 rpm) at 25°C for 10 minutes. After the soaking treatment, the particles were filtered. This soaking treatment was repeated 6 more times, by suspending rice husk in H_2O/EtOH solutions (2 mL) with increasing water contents (respectively, 10%, 30%, 50%, 70%, 90% and 100%).

After the last soaking treatment, the particles were rinsed 3 times with 10 mL of water, to completely remove the ethanol, and then filtered under reduced pressure. The wet particles were weighed and then dried in the oven at 100°C for 6 hours. The resulting anhydrous particles were weighed again. The water retention capacity was determined by:

$$water\ retention\ (\%) = \frac{weight_{wet}(g) - weight_{anhydrous}(g)}{weight_{wet}(g)} \times 100$$

As a control, a sample of RH was weighted before and after drying in the oven (100°C, 6 h) without applying the soaking treatments.

Measures were conducted in triplicate.

5.5.8 Stereoscopic measures

The materials were characterized by using a stereomicroscope (Leica MZ 16, Leica Microsystems, Wetzlar, Germany), equipped with a Nikon E4500 camera (Nikon, Japan). The images were acquired by S. Kaleb.

5.5.9 SEM microscopy imaging

Samples were metallized using a S150A Sputter Coater instrument (Edwards High Vacuum, Crawley, West Sussex, UK). Metallized samples were observed with a Leica Stereoscan 430i scanning electron microscope (Leica Cambridge Ltd., Cambridge, UK).

5.5.10 Contact angle measurements

Contact angle measurements were performed by prof. D. Voinovich. Before analysis, rice husk was pressed into disks using a manual press (Perkin Elmer) and imparting a force of 5 tons for 1 minute. The flat tablets were analysed with a Drop Shape Analysis System Krüss DSA 30 (A. Krüss Optronic GmbH, Germany), using as wetting solution 5 mL of purified water. The contact angle measurements were performed after 10 seconds. All measures were performed in triplicate.

5.5.11 Porosity analysis

Porosity was determined by prof. J. Kaspar using a mercury porosimeter.

5.5.12 ATR-IR measures

To have a qualitative assessment of the composition of the two rice husk samples, ATR-IR analyses (ATR = Attenuated Total Reflectance) were performed. ATR-IR spectra were acquired with a IRAffinity-1S (Shimadzu) spectrometer.

5.5.13 Oxidation of rice husk with $NaIO_4$[15]

2 g of dry rice husk (particle size 200-400 µm) are suspended in 50 mL of a 0.2 M solution of $NaIO_4$. The reaction mixture is shaken on the blood rotator for 22 hours at 25°C in the dark. At the end of the reaction, oxidized rice husk is filtered under vacuum and washed with deionized water (4 × 15 mL).

5.5.14 Oxidation of rice husk with LMS[62]

In a round bottomed flask are introduced 10 mL of 0.1 M sodium citrate buffer at pH 5, 39 mg of TEMPO and 20 U/mL of Laccase C (ASA, activity 2176 U/mL). Then 500 mg of dry rice husk (particle size 200-400 µm) are added to the reaction mixture, and the volume is brought up to 25 mL by addition of 0.1 M sodium citrate buffer at pH 5. The final concentrations of TEMPO and Laccase C are, respectively, 10 mM and 8 U/mL.

The mixture is allowed to react under magnetic stirring for 48 hours at 70°C. During the course of the reaction, compressed air is introduced a total of 5 times in the reaction vessel to increase exposure of the laccase to atmospheric oxygen; each compressed air treatment is 2 minutes long.

At the end of the reaction, the rice husk is filtered under vacuum and rinsed with deionized water (4×15 mL).

5.5.15 Determination of the content of carbonyl groups with the method of hydroxylamine hydrochloride[15]

The pH of 25 mL of a 0.25 M solution of hydroxylamine hydrochloride is adjusted to 3.20±0.05 by addition of HCl 0.1M. Then, 50 mg of oxidized rice husk are suspended in the solution, and the mixture is allowed to react on the blood rotator for 2 hours at 20-25 °C. At the end of the reaction, the mixture is titrated with 0.01 M NaOH to adjust the pH back to 3.20. Each measure was performed three times.

A blank, consisting of 50 mL of washed, dry, non-oxidized rice husk, was analyzed with the same method.

The concentration of carbonyl groups, in mmoles per gram of oxidized rice husk, is obtained with the following formula:

$$mmol_{C=O}\ g_{carrier}^{-1} = \frac{[NaOH]\ (M) \times V_{NaOH}(mL)}{m_{sample,dry}\ (g)}$$

Where $[NaOH]\ (M)$ is the concentration of the NaOH solution used for the titration, $V_{NaOH}(mL)$ is the volume of NaOH consumed in the titration, and $m_{sample,dry}\ (g)$ is the weight of dry rice husk used for the assay.

5.5.16 Delignification of rice husk

50 g of rice husk were introduced in a 5 L beaker and suspended in 200 mL of H_2O_2; the mixture was stirred for 10 minutes to fully soak the rice husk, and heated up to 70°C. Then, 1 g of milled NaOH powder was added to the mixture; the formation of a great volume of foam is observed. Subsequent 1 g aliquots of NaOH were added to the mixture after 45 and 90 minutes from the first. The mixture was kept under magnetic stirring, at 70°C, for a total time of 5 hours. The resulting material is light yellow in color. The rice husk was filtered under reduced pressure and washed with 6 × 50 mL of H_2O. The final product was dried in the oven at 100°C for 2 hours.

5.5.17 Biodegradation studies[223]

Biodegradation studies of rice husk were carried out in accordance with ISO 17556:2019. The procedure involves the use of the OxiTop® Control S6 system (Xylem Analytics, Weilheim, Germany), which uses a respirometric method to measure the oxygen demand released during the aerobic biodegradation of organic materials. The OxiTop® Control S6 system was equipped with six measuring units (amber glass bottles, volume 510 mL, and self-check measuring units), an inductive stirring platform, and magnetic stirring bars. The following components were added in each unit: 327.5 mL of salt solution (prepared as described below), 1 mL of demineralized water, 36.5 mg of rice husk sample (to a final sample concentration of 100 mg/L), and 36.5 mL of seawater (inoculum). The bottles were closed with the measuring cap and were placed in an incubator with a controlled temperature of 21 ± 1 °C.

The salt solution was prepared by diluting 1 mL of each of the following solutions (1 to 4) with distilled water to reach a final volume of 1 L. *Solution 1* was prepared by dissolving 8.5 g of KH_2PO_4, 21.75 g of K_2HPO_4, 33.4 g of $Na_2HPO_4 \cdot 7\ H_2O$ and 1.7 g of NH_4Cl in distilled water to a final volume of 1 L. *Solution 2* was prepared by dissolving 22.5 g of $MgSO_4 \cdot 7\ H_2O$ in distilled water to a final volume of 1 L. *Solution 3* was prepared by dissolving 27.5 g of anhydrous $CaCl_2$ (or an equivalent amount if the hydrate is used) in distilled water to a final volume of 1 L. *Solution 4* was prepared by dissolving 0.25 g of $FeCl_3 \cdot 6\ H_2O$ in distilled water to a final volume of 1 L.

The biochemical oxygen demand (BDO) for each sample is calculated as follows:

$$BOD_S = \frac{BOD_x - BOD_g}{c}$$

Where S is the number of measurement days, BOD_S is the biochemical oxygen demand of the analyzed sample within S days (in mg/L), BOD_x is the biochemical oxygen demand of the measuring system (bottle with sample and water, in mg/L), BOD_g is the biochemical oxygen demand of water without the sample (blank bottle, in mg/L) and c is the sample concentration in the tested system (in mg/L).

5.5.18 Bradford assay of protein content

5.5.18.1 BSA calibration curve

10.0 mg of albumin from bovine serum (BSA) are dissolved in 10 mL of milliQ water, or in the medium of the protein sample of unknown concentration (e.g. KPi, 0.1 M, pH 7). The actual concentration of the stock BSA solution is calculated by measuring the UV-Vis absorbance of the solution at 280 nm and dividing the value for the extinction coefficient of BSA ($\varepsilon_{280} = 0.67\ mL\ mg^{-1}\ mL^{-1}$).

Samples for the calibration curve are then prepared by diluting the stock solution with the same liquid medium, to obtain samples with protein concentration in the range 0.1-1 mg/mL. The samples are analyzed as described below in the *Protein content assay* section, and the results are plotted in an absorbance vs concentration graph.

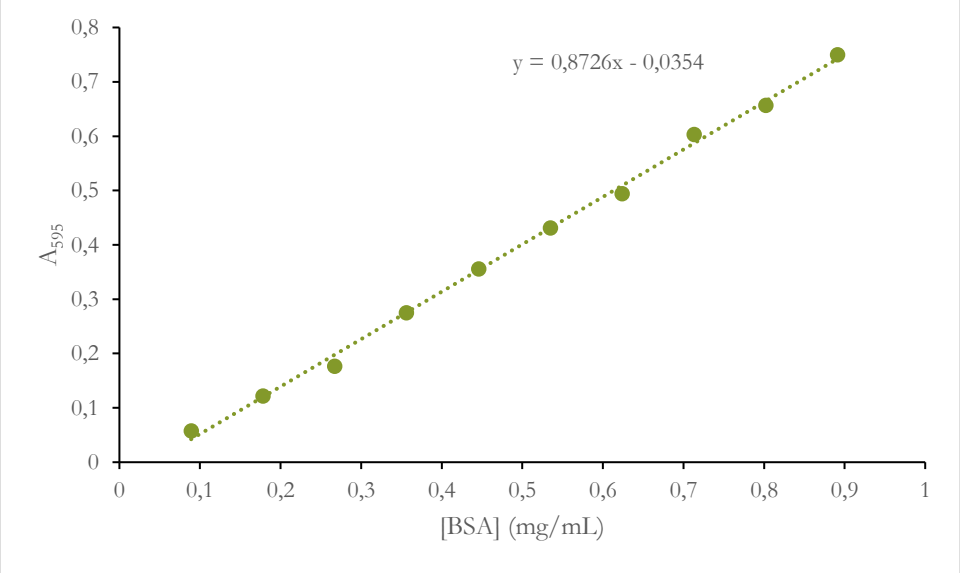

Figure 85: Example of BSA calibration curve for the Bradford assay of protein content

5.5.18.2 Sample preparation

Samples of the unknown solution are prepared by diluting the original solution in the same medium, in order to obtain a protein concentration in the range of 0.1-1.0 mg/mL. If the approximate protein concentration of the sample is unknown, different dilutions are prepared, taking note of the dilution factor.

5.5.18.3 Protein content assay

1.5 mL of Bradford reagent and 50 µL of diluted unknown sample or standard sample are introduced in an UV-Vis cuvette. The cuvette is mixed by inversion, then it is incubated at 25°C for at least 5 minutes. Samples prepared this way can be analyzed up to 1 hour from the sample preparation. The absorbance at 595 nm is then acquired, preferably in triplicate; the absorbance of a blank solution, prepared by mixing 1.5 mL of Bradford reagent with 50 µL of the dilution medium (water or buffer), is also acquired.

The concentration of the unknown protein samples can be calculated in the following way:

$$protein\ concentration\ \left(\frac{mg}{mL}\right) = \frac{\left(A_{595,S} - A_{595,B}\right) - intercept}{slope} \times df$$

Where $A_{595,S}$ is the measured absorbance of the unknown sample at 595 nm; $A_{595,B}$ is the measured absorbance of the blank sample at 595 nm; $intercept$ is the intercept of the calibration curve equation; $slope$ is the slope of the calibration curve equation; df is the dilution factor of the unknown sample.

5.5.19 Immobilization of glucoamylase on oxidized rice husk

5.5.19.1 Protocol 1

0.200 g of chemically oxidized rice husk were suspended in 1 mL of KPi buffer (25 mM, pH 7). Then, 0.26 mL of commercial glucoamylase solution (Dextrozyme GA) were added to the reaction mixture. The final volume is 1.26 mL, and the enzyme loading is 365 $U/g_{rice\ husk}$. The mixture was shaken on the blood rotator at 25°C for 24 hours.

The immobilization supernatant was removed by decanting and analyzed in a protein content assay (Bradford). The enzyme preparation was then rinsed with 4 × 2 mL of KPi (25 mM, pH 7), decanting the liquid after each rinsing step. The enzyme preparation was finally stored in the fridge at 4°C in 4 mL of KPi (25 mM, pH 7).

5.5.19.2 Protocol 2

0.200 g of chemically oxidized rice husk were suspended in 1 mL of KPi buffer (25 mM, pH 8). Then, 0.26 mL of commercial glucoamylase solution (Dextrozyme GA) were added to the reaction mixture. The final volume is 1.26 mL, and the enzyme loading is 365 $U/g_{rice\ husk}$. The mixture was shaken on the blood rotator at 25°C for 24 hours.

The immobilization supernatant was removed by decanting and analyzed in a protein content assay (Bradford). The enzyme preparation was then rinsed with 4 × 2 mL of KPi (25 mM, pH 8), decanting the liquid after each rinsing step. The enzyme preparation was finally stored in the fridge at 4°C in 4 mL of KPi (25 mM, pH 8).

5.5.19.3 Protocol 3

0.200 g of enzymatically oxidized rice husk were suspended in 1 mL of KPi buffer (25 mM, pH 7). Then, 0.26 mL of commercial glucoamylase solution (Dextrozyme GA) were added to the reaction mixture. The final volume is 1.26 mL, and the enzyme loading is 365 $U/g_{rice\ husk}$. The mixture was shaken on the blood rotator at 25°C for 24 hours.

The immobilization supernatant was removed by decanting and analyzed in a protein content assay (Bradford). The enzyme preparation was then rinsed with 4 × 2 mL of KPi (25 mM, pH 7), decanting the liquid after each rinsing step. The enzyme preparation was finally stored in the fridge at 4°C in 4 mL of KPi (25 mM, pH 7).

5.5.19.4 Protocol 4

0.200 g of enzymatically oxidized rice husk were suspended in 1 mL of KPi buffer (25 mM, pH 8). Then, 0.26 mL of commercial glucoamylase solution (Dextrozyme GA) were added to the reaction mixture. The final volume is 1.26 mL, and the enzyme loading is 365 $U/g_{rice\ husk}$. The mixture was shaken on the blood rotator at 25°C for 24 hours.

The immobilization supernatant was removed by decanting and analyzed in a protein content assay (Bradford). The enzyme preparation was then rinsed with 4 × 2 mL of KPi (25 mM, pH 8), decanting the liquid after each rinsing step. The enzyme preparation was finally stored in the fridge at 4°C in 4 mL of KPi (25 mM, pH 8).

Table 47: Summary of the conditions of the first batch of experiments for the covalent immobilization of glucoamylase on oxidized rice husk

Protocol	RH oxidation	Buffer	pH	Reaction time (h)	Loading (U/g_{dry})	Loading ($mg_{protein}/g_{dry}$)
1	$NaIO_4$	KPi, 25 mM	7	24	365	108
2	$NaIO_4$	KPi, 25 mM	8	24	365	108
3	LMS	KPi, 25 mM	7	24	365	108
4	LMS	KPi, 25 mM	8	24	365	108

5.5.19.5 Protocol 5

200 mg of chemically oxidized rice husk were suspended in 1.74 mL of KPi (0.1 M, pH 7). Then, 0.26 mL of commercial glucoamylase solution (Dextrozyme GA) were added to the reaction mixture. The final volume is 2 mL, while the enzyme loading is 365 U/g. The mixture was kept stirring on the blood rotator for 24 hours at 25°C.

The immobilization supernatant was removed by decanting and analyzed in a protein content assay (Bradford). The enzyme preparation was then rinsed with 4 × 2 mL of KPi (0.1 m, pH 7), decanting the liquid after each rinsing step. The enzyme preparation was finally stored in the fridge at 4°C in 4 mL of KPi (0.1 M, pH 7).

5.5.19.6 Protocol 6

200 mg of chemically oxidized rice husk were suspended in 1.00 mL of KPi (0.1 M, pH 7). Then, 0.26 mL of commercial glucoamylase solution (Dextrozyme GA) were added to the reaction mixture. The final volume is 1.26 mL, while the enzyme loading is 365 U/g. The mixture was kept stirring on the blood rotator for 24 hours at 25°C.

The immobilization supernatant was removed by decanting and analyzed in a protein content assay (Bradford). The enzyme preparation was then rinsed with 4 × 2 mL of KPi (0.1 m, pH 7), decanting the liquid after each rinsing step. The enzyme preparation was finally stored in the fridge at 4°C in 4 mL of KPi (0.1 M, pH 7).

Table 48: Summary of the conditions of the second batch of experiments for the covalent immobilization of glucoamylase on oxidized rice husk

Protocol	RH oxidation	Buffer	V_{enzyme} (mL)	V_{buffer} (mL)	Reaction time (h)	Loading (U/g_{dry})	Loading ($mg_{protein}/g_{dry}$)
5	$NaIO_4$	KPi, 0.1 M, pH 7	0.26	1.00	24	365	108
6	$NaIO_4$	KPi, 0.1 M, pH 7	0.26	1.74	24	365	108

5.5.19.7 Protocol 7

3 mL of glucoamylase commercial solution (Dextrozyme GA) were diluted to 10 mL with KPi, 0.1 M, pH 7. 200 mg of chemically oxidized rice husk were suspended in 1.5 mL of diluted glucoamylase solution; the final enzyme loading is 632 U/g (37.17 $mg_{protein}/g$). The mixture was kept shaking on the blood rotator at 25°C for 48 hours.

The immobilization supernatant was removed by decanting and analyzed in a protein content assay (Bradford). The enzyme preparation was then rinsed with 4 × 2 mL of KPi (0.1 m, pH 7), decanting the liquid after each rinsing step. The enzyme preparation was finally stored in the fridge at 4°C in 4 mL of KPi (0.1 M, pH 7).

5.5.19.8 Protocol 8

3 mL of glucoamylase commercial solution (Dextrozyme GA) were diluted to 10 mL with KPi, 0.5 M, pH 8. 200 mg of chemically oxidized rice husk were suspended in 1.5 mL of the diluted glucoamylase solution; the final enzyme loading is 362 U/g. The mixture was kept shaking on the blood rotator at 25°C for 48 hours.

The immobilization supernatant was removed by decanting and analyzed in a protein content assay (Bradford). The enzyme preparation was then rinsed with 4 × 2 mL of KPi (0.5 M, pH 8), decanting the liquid after each rinsing step. The enzyme preparation was finally stored in the fridge at 4°C in 4 mL of KPi (0.5 M, pH 8).

5.5.19.9 Protocol 9

3 mL of glucoamylase commercial solution (Dextrozyme GA) were diluted to 10 mL with KPi, 0.5 M, pH 8. 200 mg of chemically oxidized rice husk were suspended in 1.5 mL of the diluted glucoamylase solution; the final enzyme loading is 362 U/g. The mixture was kept shaking on the blood rotator at 25°C for 72 hours.

The immobilization supernatant was removed by decanting and analyzed in a protein content assay (Bradford). The enzyme preparation was then rinsed with 4 × 2 mL of KPi (0.5 M, pH 8), decanting the liquid after each rinsing step. The enzyme preparation was finally stored in the fridge at 4°C in 4 mL of KPi (0.5 M, pH 8).

Table 49: Summary of the conditions of the third batch of experiments for the covalent immobilization of glucoamylase on oxidized rice husk

Protocol	RH oxidation	Buffer	Reaction time (h)	Loading (U/g_{dry})	Loading ($mg_{protein}/g_{dry}$)
7	$NaIO_4$	KPi, 0.1 M, pH 7	48	632	187
8	$NaIO_4$	KPi, 0.5 M, pH 8	48	632	187
9	$NaIO_4$	KPi, 0.5 M, pH 8	72	632	187

5.5.19.10 Protocol 10

Functionalization with HMDA

8.36 g of hexamethylenediamine (HMDA) were dissolved in 80 mL of methanol, to a concentration of 0.9 M. Then, 400 mg of chemically oxidized rice husk were suspended in the solution. The mixture was kept shaking on the blood rotator for 72 hours at 25°C. The oxidized and functionalized rice husk was then filtered under reduced pressure and rinsed with 3 × 30 mL of demineralized water. The rice husk was then dried on the filter.

Activation with glutaraldehyde

300 mg of amino-functionalized rice husk were suspended in 4.5 mL of a 1.25% solution of glutaraldehyde in KPi (0.05 M, pH 8). The mixture was kept shaking on the blood rotator for 5 hours at 25°C. The rice husk was filtered under reduced pressure and rinsed with 3 × 20 mL of demineralized water, then dried on the filter.

Enzyme solution

3 mL of commercial glucoamylase solution (Dextrozyme GA) were diluted up to a volume of 10 mL with KPi (0.5 M, pH 8).

Enzyme immobilization

200 mg of rice husk (amino functionalized with HDMA and then activated with glutaraldehyde) were suspended in 1.5 mL of the diluted glucoamylase solution. The mixture was kept shaking on the blood rotator for 48 at 25°C. The supernatant solution was then decanted, and the sample was rinsed with 3 × 5 mL of H_2O, decanting the liquid after each wash. The immobilized enzyme sample was finally stored in the fridge in 3 mL of KPi buffer (0.1 M, pH 7).

Table 50: Summary of the conditions of the fourth batch of experiments for the covalent immobilization of glucoamylase on oxidized rice husk

Protocol	RH sample	Buffer	Reaction time (h)	Loading (U/g_{dry})	Loading ($mg_{protein}/g_{dry}$)
10	Oxidized with $NaIO_4$, functionalized with HDMA + glutaraldehyde	KPi, 0.5 M, pH 8	48	632	187

5.5.19.11 Protocol 11

3 mL of commercial glucoamylase solution (Dextrozyme GA) were diluted to 10 mL with KPi (0.025 M, pH 7). 200 mg of chemically oxidized, delignified rice husk were suspended in 1.5 mL of diluted enzyme solution. The mixture was kept shaking on the orbital shaker at 25°C for 48 hours. The supernatant was then removed by decanting, and analyzed for residual protein concentration (Bradford assay). The rice husk was then washed with 3 × 5 mL of H_2O, decanting the liquid after each wash. The final enzyme preparation was stored in the fridge at 4°C in 3 mL of KPi (0.025 M, pH 7).

5.5.19.12 Protocol 12

3 mL of commercial glucoamylase solution (Dextrozyme GA) were diluted to 10 mL with KPi (0.025 M, pH 7). 200 mg of enzymatically oxidized, delignified rice husk were suspended in 1.5 mL of diluted enzyme solution. The mixture was kept shaking on the orbital shaker at 25°C for 48 hours. The supernatant was then removed by decanting, and analyzed for residual protein concentration (Bradford assay). The rice husk was then washed with 3 × 5 mL of H_2O, decanting the liquid after each wash. The final enzyme preparation was stored in the fridge at 4°C in 3 mL of KPi (0.025 M, pH 7).

Table 51: Summary of the reaction conditions for the experiments of covalent immobilization of glucoamylase on oxidized, delignified rice husk.

Protocol	RH oxidation	Buffer	Reaction time (h)	Loading (U/g_{dry})	Loading ($mg_{protein}/g_{dry}$)
11	$NaIO_4$	KPi, 25 mM, pH 7	48	632	187
12	LMS	KPi, 25 mM, pH 7	48	632	187

5.5.20 Immobilization of TLL on oxidized rice husk[62]

5.5.20.1 Protocol 13

3.15 mL of the commercial TLL solution (activity: 1613 U/g, protein concentration: 24.1 U/mL) were diluted with 5 mL of a 2 mg/mL PEG-3000 solution in KPi (0.5 M, pH 8), to a total volume of 8.15 mL.

200 mg of chemically oxidized, milled rice husk (particle size 200-400 µm) were suspended in 1.63 mL of the enzyme immobilization solution. The enzyme loading is 5081 U/g_{dry}. The mixture was kept shaking on the blood rotator at 25°C for 48 hours. After immobilization, the rice husk was filtered under reduced pressure, and washed 4 times with 10 mL H_2O. The solid was dried on the filter and stored in the fridge at 4°C.

5.5.20.2 Protocol 14

3.15 mL of the commercial TLL solution (activity: 1613 U/g, protein concentration: 24.1 U/mL) were diluted with 5 mL of a 2 mg/mL PEG-3000 solution in KPi (0.5 M, pH 8), to a total volume of 8.15 mL.

200 mg of enzymatically oxidized, milled rice husk (particle size 200-400 µm) were suspended in 1.63 mL of the enzyme immobilization solution. The enzyme loading is 5081 U/g_{dry}. The mixture was kept shaking on the

blood rotator at 25°C for 48 hours. After immobilization, the rice husk was filtered under reduced pressure, and washed 4 times with 10 mL H_2O. The solid was dried on the filter and stored in the fridge at 4°C.

5.5.20.3 Protocol 15

3.15 mL of the commercial TLL solution (activity: 1613 U/g, protein concentration: 24.1 U/mL) were diluted with 5 mL of a 2 mg/mL PEG-3000 solution in KPi (0.5 M, pH 8), to a total volume of 8.15 mL.

200 mg of chemically oxidized, milled delignified rice husk (particle size 200-400 µm) were suspended in 1.63 mL of the enzyme immobilization solution. The enzyme loading is 5081 U/g_{dry}. The mixture was kept shaking on the blood rotator at 25°C for 48 hours. After immobilization, the rice husk was filtered under reduced pressure, and washed 4 times with 10 mL H_2O. The solid was dried on the filter and stored in the fridge at 4°C.

5.5.20.4 Protocol 16

3.15 mL of the commercial TLL solution (activity: 1613 U/g, protein concentration: 24.1 U/mL) were diluted with 5 mL of a 2 mg/mL PEG-3000 solution in KPi (0.5 M, pH 8), to a total volume of 8.15 mL.

200 mg of enzymatically oxidized, milled delignified rice husk (particle size 200-400 µm) were suspended in 1.63 mL of the enzyme immobilization solution. The enzyme loading is 5081 U/g_{dry}. The mixture was kept shaking on the blood rotator at 25°C for 48 hours. After immobilization, the rice husk was filtered under reduced pressure, and washed 4 times with 10 mL H_2O. The solid was dried on the filter and stored in the fridge at 4°C.

Table 52: Summary of the conditions for the covalent immobilization of TLL on oxidized rice husk

Protocol	RH	RH oxidation	Buffer	pH	[buffer] (M)	Incubation time (h)	Enzyme loading (U/g_{dry})
13	Raw	Chemical	KPi	8	0.5	48	5081
14	Raw	Enzymatic	KPi	8	0.5	48	5081
15	Delignified	Chemical	KPi	8	0.5	48	5081
16	Delignified	Enzymatic	KPi	8	0.5	48	5081

5.6 Annex

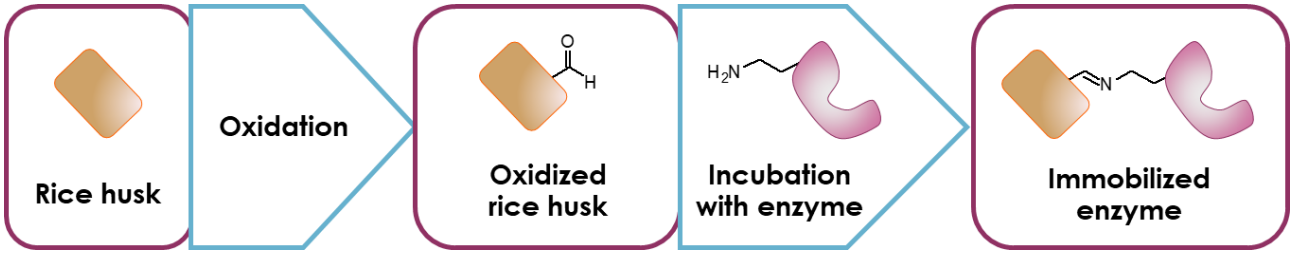

Figure 86: Schematic representation of the experiments of immobilization of glucoamylase on oxidized rice husk

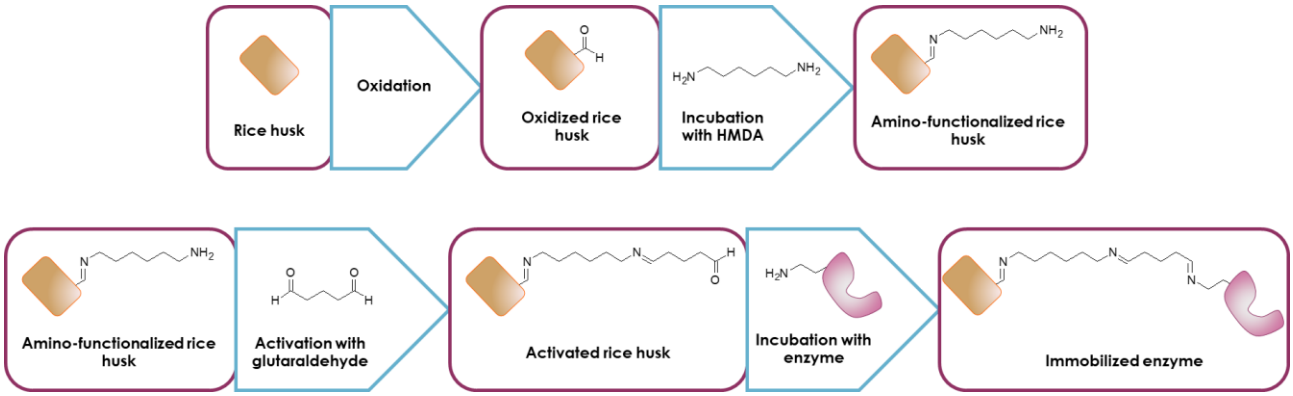

Figure 87: Schematic representation of the experiments of immobilization of glucoamylase on oxidized rice husk functionalized with hexamethylenediamine

6 Immobilization of enzymes on rice husk by adsorption and crosslinking

6.1 Summary and objectives

Following the scarce results obtained in the study of the covalent immobilization of enzymes on functionalized rice husk, an alternative, simpler method was tested, involving crosslinking agents. Glucoamylase, as well as TLL and CaLB, were immobilized on rice husk *via* adsorption followed by crosslinking.

The immobilization attempts will be made both on non-delignified and on delignified milled rice husk, using several procedures derived from literature. In the case of glucoamylase, adsorption will be attempted both from diluted buffer solution and in the presence of PEG-3000, which has been shown to have a stabilizing effect on some enzyme during immobilization. The crosslinking of glucoamylase will be performed with glutaraldehyde.

In the case of TLL and CaLB, the immobilization will be performed both from diluted aqueous buffer and in a biphasic system with *n*-hexane, to verify if the presence of the organic solvent will improve the recovered activity after immobilization. TLL and CaLB will be crosslinked using DFF, which previously demonstrated to be effective for the covalent immobilization of enzymes on polymeric supports (Chapter 3).

6.2 Results and Discussion

Enzyme immobilization on rice husk via adsorption and crosslinking was attempted for both TLL and glucoamylase. Firstly, the enzyme was incubated with the carrier for 24 hours; then, the adsorbed enzyme was crosslinked by addition of glutaraldehyde. Adsorption and crosslinking were attempted on (a) raw, milled rice husk (particle size 200-400 μm) and (b) delignified rice husk (particle size 200-400 μm).

6.2.1.1 Glucoamylase on delignified rice husk

The first set of experiments for the immobilization of glucoamylase on rice husk was performed in two different buffers: (a) KPi, 0.5 M, pH 8, selected based on the previously reported lipase immobilization protocols by M. Spennato[62] and (b) KPi, 0.1 M, pH 7, which was selected based on the previous experiments for the immobilization of glucoamylase on PMMA carriers.

Initially, the delignified rice husk was suspended in an enzyme solution in the appropriate buffer, and incubated in this solution for 72 hours. At the end of the incubation period, the supernatant was analyzed in a Bradford assay of protein content in order to determine whether there was a decrease in protein concentration during the incubation. Then, the protein was crosslinked by incubation with a 3% solution of glutaraldehyde. Detailed procedures can be found in the Materials and Methods section of this chapter.

Table 53: Results of the first set of experiments for the adsorption and crosslinking of glucoamylase on delignified rice husk.

Protocol	Buffer	Initial protein concentration (mg/mL)	Final protein concentration (mg/mL)	Immobilization (%)[a]
1	KPi, 0.5 M, pH 8	31.11 ± 0.70	33.14 ± 0.94	–
2	KPi, 0.1 M, pH 7	31.07 ± 0.93	32.10 ± 0.35	–

[a] Calculated as $\frac{Initial\ protein\ concentration - Final\ protein\ concentration}{Initial\ protein\ concentration} \times 100$

Delignified rice husk, which was used in this experiment, has a higher hydrophilicity compared to its non-delignified precursor; for this reason, it was considered more suitable for the immobilization of glucoamylase, a hydrophilic and highly glycosylated enzyme. Despite this, both experiments did not display the adsorption on the carrier.

A final set of experiments was performed for the adsorption and crosslinking of glucoamylase on rice husk. In this case, both raw and delignified milled rice husk were used. Two different buffer solutions were also used, namely KPi (0.5 M, pH 8) and KPi (0.1 M, pH 7). Finally, the incubation of glucoamylase on rice husk was performed in the presence of 2 mg/mL of PEG-3000, as reported in a literature protocol for lipases.[15] The crosslinking was performed by incubation in a 3% glutaraldehyde solution. Detailed procedures can be found in the Materials and Methods section.

Table 54: Results of the second set of experiments for the adsorption and crosslinking of glucoamylase on rice husk, in the presence of 2 mg/mL PEG-3000.

Protocol	Rice husk	Buffer	Initial protein concentration (mg/mL)	Final protein concentration (mg/mL)	Immobilization (%)[a]
3	Raw	KPi, 0.5 M, pH 8	27.56 ± 0.71	27.05 ± 2.86	1.9
4	Delignified	KPi, 0.5 M, pH 8	27.56 ± 0.71	30.02 ± 0.41	–
5	Raw	KPi, 0.1 M, pH 7	27.76 ± 0.69	27.39 ± 2.03	1.3
6	Delignified	KPi, 0.1 M, pH 7	27.76 ± 0.69	29.31 ± 0.85	–

[a] Calculated as $\frac{Initial\ protein\ concentration - Final\ protein\ concentration}{Initial\ protein\ concentration} \times 100$

In this case, a minimal adsorption of protein on the support was observed for the samples immobilized on raw rice husk. However, there was no recovered activity in any of the samples, as was the case for the previous batch of experiments.

The failure of all the immobilization experiments for glucoamylase on rice husk can be attributed to the high hydrophilicity of the protein, that does not have a sufficient partition onto the solid lignocellulosic matrix in order to obtain an appreciable recovered activity. Therefore, different methodologies have to be developed in order to obtain the immobilization of glucoamylase on this renewable carrier.

6.2.2 Lipases

On the basis of the discouraging results obtained in the study of the covalent immobilization of lipases on oxidized rice husk, new protocols were developed for immobilizing lipases TLL and CaLB, through adsorption on the carrier and subsequent crosslinking with DFF.

For the immobilization, different conditions were tested for each enzyme. Two different solutions were used for the incubation of each lipase with the support: (1) TRIS-HCl buffer, 0.1 M, pH 7, following conditions previously reported in literature for the immobilization of a cutinase;[216] (2) NaCl 3M, to promote the partition of the protein on rice husk, following a protocol reported in literature for CaLB.[15]

Moreover, two different crosslinking procedures were employed for the samples adsorbed in NaCl 3M solution: (a) incubation of the adsorbed enzyme preparation with a 160 mM solution of DFF; (b) addition of hexane to the immobilization mixture,[228] followed by incubation with a 160 mM solution of DFF. A scheme of the experiments can be found in the Annex for this chapter, and detailed procedures can be found in the Materials and Methods section. The use of hexane was motivated by previous evidence of the positive effects deriving from the exposure of some lipases to organic solvents during the immobilization procedure. Lipases have been evolved for transforming insoluble hydrophobic substrates and they have large hydrophobic regions surrounding the opening of their active site. Previous molecular dynamics studies carried out in our group

demonstrated that TLL, when exposed to water, achieve a close conformation, hampering the substrate access to active site.[139]

Therefore, diluted aqueous solutions are unfavorable media for immobilizing covalently lipases, since the newly formed covalent bonds "freeze" the enzyme in the close conformation.[229] It was experimentally demonstrated that the covalent immobilization of lipases from *Bulchorderia cepacia* and from *Ryzopus oryzae* is by far more efficient when carried out in the presence of a hydrophobic liquid phase that promotes their activation during the immobilization process.[228]

The resulting enzyme preparations were characterized by measuring the recovered activity in the hydrolysis of tributyrin. The results are reported in the following table.

Table 55: Recovered activity for the samples of TLL and CaLB immobilized on rice husk by adsorption and crosslinking under different conditions.

	Immobilization	Loading ($mg_{protein}/g$)	Loading (U/g_{dry})	Recovered activity (U/g_{dry})	Recovered activity (%)[a]
TLL	Protocol 1	15	2775	118	4.2
	Protocol 2	15	2775	236	8.5
	Protocol 3	15	2775	427	15.4
CaLB	Protocol 1	15	4125	98	2.7
	Protocol 2	15	4125	73	2.0
	Protocol 3	15	4125	102	2.8

[a] Calculated as $\frac{Recovered\ activity\left(\frac{U}{g_{dry}}\right)}{Loading\left(\frac{U}{g_{dry}}\right)} \times 100$

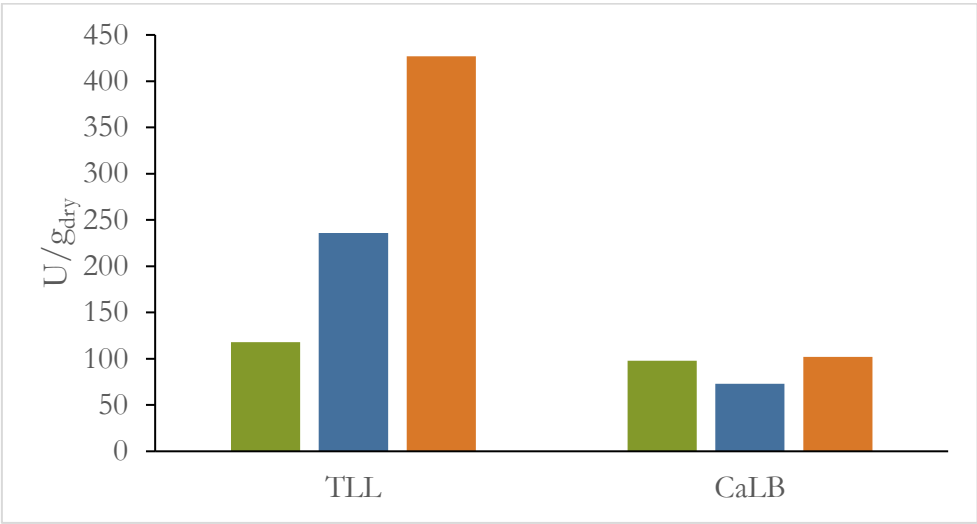

Figure 88: Results of the experiments for the adsorption and crosslinking of TLL and CaLB on rice husk. Immobilization conditions: in green, protocol 1; in blue, protocol 2; in orange, protocol 3.

As evident from the recovered activity values, the immobilization method is more effective in the case of TLL. Notably, for TLL the highest recovered activity (2 and 3 folds higher respectively) was obtained with immobilization condition 3, also employing hexane. In this case, the enzyme was preliminarily incubated with rice husk for 24 hours; then, before adding the crosslinker, hexane was added to the reaction mixture. The crosslinker was then added to the solution, and the mixture was incubated again for 4 hours before washing the immobilized enzyme preparation. The result confirms that the presence of a hydrophobic surface is crucial for promoting the immobilization of the open active conformation of those lipases that undergo interfacial activation. As a matter of fact, CaLB is not significantly affected by the presence of the hydrophobic solvent, since its conformation does not change passing from hydrophilic to hydrophobic environments.[139]

6.3 Conclusions

The immobilization of glucoamylase on rice husk by adsorption and crosslinking was unsuccessful, confirming the low affinity of the enzyme for rice husk, also observed in the case of the immobilization on the oxidized material.

In the case of lipases, the immobilizations were successfully achieved using the bio-based dialdehyde DFF (see Chapter 3). TLL displayed the most interesting behaviour: when immobilized from diluted buffer solution, the recovered activity is about 4.2% of the loaded enzyme units; when using a concentrated salt solution (NaCl 3M), the partition of the enzyme on the carrier is favored due to a salting out effect, and the recovered activity doubles compared to the previous immobilization conditions. Finally, in the presence of a hydrophobic phase such as *n*-hexane, the activity further increases, up to 15.4% of the initial loaded units. This can be explained considering the mechanism of interfacial activation of TLL: in the presence of the hydrophobic solvent, there is a conformational change in the lipase, which make the active site more accessible by lifting a domain called "*lid*". As a result, the protein immobilized on rice husk is in a more active conformation than the corresponding protein immobilized in the absence of *n*-hexane.

On the other hand, the immobilization of CaLB in all three tested conditions gave comparable results. The lack of activation of CaLB in the presence of the organic solvent can be explained by the fact that CaLB does not have a *lid*, and therefore is not further activated in the presence of an organic phase, in contrast with what observed for TLL.

In conclusion, a new immobilization method was developed, which employs a renewable biomass (rice husk) and a bio-based crosslinker. A 15.4% of activity was recovered in the case of lipase TLL, which represent a very promising result for a lipase. Future studies will address the stability of the different formulations under industrially relevant conditions.

6.4 Materials and Methods

6.4.1 Chemicals

All chemicals were purchased by Sigma Aldrich and are of the highest available quality.

6.4.2 Enzymes

Glucoamylase from *Aspergillus niger*, liquid solution (Dextrozyme GA, activity: 240 U/g, protein content: 83 mg/mL) was from Novozymes (Denmark). **Lipase from *Thermomyces lanuginosus*** (Lipolase 100L, expressed in *Aspergillus oryzae*, activity: 3639 U/g, protein content 24.1 mg/mL) was from Novozymes (Denmark) and was purchased from Sigma Aldrich. ***Lipase B from Candida antarctica*** (liquid solution, activity: 3639 U/g, protein content: 5.3 mg/mL) was from Novozymes (Denmark).

6.4.3 Carriers

Rice husk was donated by Riseria Cusaro (Binasco, Milano, Italy). It was milled with a blade mill (VERDER SCIENTIFIC S.r.l., Bergamo) and sieved to obtain a fraction with dimension 200-400 μm).

6.4.4 Immobilization of glucoamylase on delignified rice husk by adsorption and crosslinking

6.4.4.1 Protocol 1

3 mL of commercial glucoamylase solution (Dextrozyme GA) were diluted up to 10 mL with KPi (0.5 M, pH 8). 0.2 g of milled, delignified rice husk (particle size 200-400 μm) were suspended in 1.5 mL of the diluted enzyme solution. The mixture was shaken on the blood rotator at 25°C for 72 hours. The supernatant was then removed by decanting, and the rice husk was resuspended in 1.5 mL of a 3% glutaraldehyde solution in KPi (0.5 M, pH 8). The mixture was kept shaking at 25°C for 4 hours. The crosslinking supernatant solution was decanted. The rice husk was rinsed with 3 × 5 mL of demineralized water, decanting the liquid after each wash. The enzyme preparation was stored in the fridge in 4 mL of KPi (0.5 M, pH 8).

6.4.4.2 Protocol 2

3 mL of commercial glucoamylase solution (Dextrozyme GA) were diluted up to 10 mL with KPi (0.1 M, pH 7). 0.2 g of milled, delignified rice husk (particle size 200-400 μm) were suspended in 1.5 mL of the diluted enzyme solution. The mixture was shaken on the blood rotator at 25°C for 72 hours. The supernatant was then removed by decanting, and the rice husk was resuspended in 1.5 mL of a 3% glutaraldehyde solution in KPi (0.1 M, pH 7). The mixture was kept shaking at 25°C for 4 hours. The crosslinking supernatant solution was decanted. The rice husk was rinsed with 3 × 5 mL of demineralized water, decanting the liquid after each wash. The enzyme preparation was stored in the fridge in 4 mL of KPi (0.1 M, pH 7).

Table 56: Summary of the immobilization conditions for the adsorption and crosslinking of glucoamylase on delignified rice husk.

Protocol	Buffer	Buffer concentration (M)	pH	Reaction time (h)	Loading (U/g_{dry})	Loading ($mg_{protein}/g_{dry}$)
1	KPi	0.5	8	72	632	187
2	KPi	0.1	7	72	632	187

6.4.4.3 Protocol 3

20 mg of PEG-3000 were dissolved in KPi (0.5 M, pH 8) to a final volume of 10 mL (final PEG concentration: 2 mg/mL). 3 mL of commercial glucoamylase solution were diluted with the PEG-3000 solution to a final volume of 10 mL.

200 mg of raw, milled rice husk (particle size 200-400 µm) were suspended in 1.5 mL of the enzyme solution. The mixture was shaken on the orbital shaker at 25°C for 24 hours. The supernatant was then decanted and analyzed in a protein concentration (Bradford) assay. The rice husk was resuspended in 1.5 mL of a 3% glutaraldehyde solution in KPi (0.5 M, pH 8); the solution was shaken on the blood rotator at 25°C for 4 hours. The glutaraldehyde solution was removed by decanting. The immobilized enzyme preparation was washed with 3 × 5 mL of H_2O, decanting the liquid after each wash. The immobilized enzyme was stored in the fridge at 4°C in 3 mL of KPi (0.05 M, pH 7).

6.4.4.4 Protocol 4

20 mg of PEG-3000 were dissolved in KPi (0.5 M, pH 8) to a final volume of 10 mL (final PEG concentration: 2 mg/mL). 3 mL of commercial glucoamylase solution were diluted with the PEG-3000 solution to a final volume of 10 mL.

200 mg of delignified, milled rice husk (particle size 200-400 µm) were suspended in 1.5 mL of the enzyme solution. The mixture was shaken on the orbital shaker at 25°C for 24 hours. The supernatant was then decanted and analyzed in a protein concentration (Bradford) assay. The rice husk was resuspended in 1.5 mL of a 3% glutaraldehyde solution in KPi (0.5 M, pH 8); the solution was shaken on the blood rotator at 25°C for 4 hours. The glutaraldehyde solution was removed by decanting. The immobilized enzyme preparation was washed with 3 × 5 mL of H_2O, decanting the liquid after each wash. The immobilized enzyme was stored in the fridge at 4°C in 3 mL of KPi (0.05 M, pH 7).

6.4.4.5 Protocol 5

20 mg of PEG-3000 were dissolved in KPi (0.1 M, pH 7) to a final volume of 10 mL (final PEG concentration: 2 mg/mL). 3 mL of commercial glucoamylase solution were diluted with the PEG-3000 solution to a final volume of 10 mL.

200 mg of raw, milled rice husk (particle size 200-400 µm) were suspended in 1.5 mL of the enzyme solution. The mixture was shaken on the orbital shaker at 25°C for 24 hours. The supernatant was then decanted and analyzed in a protein concentration (Bradford) assay. The rice husk was resuspended in 1.5 mL of a 3%

glutaraldehyde solution in KPi (0.1 M, pH 8); the solution was shaken on the blood rotator at 25°C for 4 hours. The glutaraldehyde solution was removed by decanting. The immobilized enzyme preparation was washed with 3 × 5 mL of H_2O, decanting the liquid after each wash. The immobilized enzyme was stored in the fridge at 4°C in 3 mL of KPi (0.05 M, pH 7).

6.4.4.6 Protocol 6

20 mg of PEG-3000 were dissolved in KPi (0.1 M, pH 7) to a final volume of 10 mL (final PEG concentration: 2 mg/mL). 3 mL of commercial glucoamylase solution were diluted with the PEG-3000 solution to a final volume of 10 mL.

200 mg of delignified, milled rice husk (particle size 200-400 μm) were suspended in 1.5 mL of the enzyme solution. The mixture was shaken on the orbital shaker at 25°C for 24 hours. The supernatant was then decanted and analyzed in a protein concentration (Bradford) assay. The rice husk was resuspended in 1.5 mL of a 3% glutaraldehyde solution in KPi (0.1 M, pH 7); the solution was shaken on the blood rotator at 25°C for 4 hours. The glutaraldehyde solution was removed by decanting. The immobilized enzyme preparation was washed with 3 × 5 mL of H_2O, decanting the liquid after each wash. The immobilized enzyme was stored in the fridge at 4°C in 3 mL of KPi (0.05 M, pH 7).

Table 57: Summary of the reaction conditions for the second batch of experiments for the adsorption and crosslinking of glucoamylase on rice husk

Protocol	Rice husk	Buffer	Buffer concentration (M)	pH	PEG-3000 (mg/mL)	Loading (U/g_{dry})	Loading ($mg_{protein}/g_{dry}$)
3	Raw	KPi	0.5	8	2	632	187
4	Delignified	KPi	0.5	8	2	632	187
5	Raw	KPi	0.1	7	2	632	187
6	Delignified	KPi	0.1	7	2	632	187

6.4.5 Immobilization of TLL on rice husk by adsorption and crosslinking

6.4.5.1 Protocol 1

400 mg of milled, washed rice husk (particle size 200-400 μm) were suspended in 3.75 mL of TRIS-HCl buffer (pH 7, 0.1 M). Then, 0.25 mL of commercial TLL solution (Lipolase 100L, 3639 U/g, 24.1 $mg_{protein}$/mL) were added to the reaction mixture. The final volume is 4 mL; the protein loading is 15 mg/$g_{carrier}$. The mixture was shaken on the orbital shaker at 25°C for 24 hours.

The supernatant was removed by decanting. The RH was resuspended in 2 mL of a 160 mM aqueous solution of DFF. The mixture was shaken on the orbital shaker for 4 hours at 25°C. The supernatant was removed by decanting, and the enzyme preparation was rinsed 4 times with 10 mL of TRIS-HCl buffer (pH 7, 0.1 M).

6.4.5.2 Protocol 2

400 mg of milled, washed rice husk (particle size 200-400 μm) were suspended in 3.75 mL of NaCl 3M. Then, 0.25 mL of commercial TLL solution (Lipolase 100L, 3639 U/g, 24.1 $mg_{protein}$/mL) were added to the reaction mixture. The final volume is 4 mL; the protein loading is 15 mg/$g_{carrier}$. The mixture was shaken on the orbital shaker at 25°C for 24 hours.

The supernatant was removed by decanting. The RH was resuspended in 2 mL of a 160 mM aqueous solution of DFF. The mixture was shaken on the orbital shaker for 4 hours at 25°C. The supernatant was removed by decanting, and the enzyme preparation was rinsed 4 times with 10 mL of TRIS-HCl buffer (pH 7, 0.1 M).

6.4.5.3 Protocol 3

400 mg of milled, washed rice husk (particle size 200-400 μm) were suspended in 3.75 mL of NaCl 3M. Then, 0.25 mL of commercial TLL solution (Lipolase 100L, 3639 U/g, 24.1 $mg_{protein}$/mL) were added to the reaction mixture. The final volume is 4 mL; the protein loading is 15 mg/$g_{carrier}$. The mixture was shaken on the orbital shaker at 25°C for 24 hours.

After incubation, 1 mL of hexane was added to the reaction mixture; the mixture was shaken on the vortex to promote the formation of an emulsion. Then, 39.4 mg of DFF (0.318 mmol) were added to the reaction mixture. The mixture was again shaken on the vortex to promote the formation of an emulsion, and then shaken on the orbital shaker for 4 hours.

The supernatant was then removed by decanting. The enzyme preparation was rinsed 4 times with 10 mL of TRIS-HCl buffer (pH 7, 0.1 M).

6.4.6 Immobilization of CaLB on rice husk by adsorption and crosslinking

6.4.6.1 Protocol 1

400 mg of milled, washed rice husk (particle size 200-400 µm) were suspended in 2.87 mL of TRIS-HCl buffer (pH 7, 0.1 M). Then, 1.13 mL of commercial CaLB solution (1460 U/g, 5.3 $mg_{protein}$/mL) were added to the reaction mixture. The final volume is 4 mL; the protein loading is 15 mg/$g_{carrier}$. The mixture was shaken on the orbital shaker at 25°C for 24 hours.

The supernatant was removed by decanting. The RH was resuspended in 2 mL of a 160 mM aqueous solution of DFF. The mixture was shaken on the orbital shaker for 4 hours at 25°C. The supernatant was removed by decanting, and the enzyme preparation was rinsed 4 times with 10 mL of TRIS-HCl buffer (pH 7, 0.1 M).

6.4.6.2 Protocol 2

400 mg of milled, washed rice husk (particle size 200-400 µm) were suspended in 2.87 mL of NaCl 3M. Then, 1.13 mL of commercial CaLB solution (1460 U/g, 5.3 $mg_{protein}$/mL) were added to the reaction mixture. The final volume is 4 mL; the protein loading is 15 mg/$g_{carrier}$. The mixture was shaken on the orbital shaker at 25°C for 24 hours.

The supernatant was removed by decanting. The RH was resuspended in 2 mL of a 160 mM aqueous solution of DFF. The mixture was shaken on the orbital shaker for 4 hours at 25°C. The supernatant was removed by decanting, and the enzyme preparation was rinsed 4 times with 10 mL of TRIS-HCl buffer (pH 7, 0.1 M).

6.4.6.3 Protocol 3

400 mg of milled, washed rice husk (particle size 200-400 µm) were suspended in 2.87 mL of NaCl 3M. Then, 1.13 mL of commercial CaLB solution (1460 U/g, 5.3 $mg_{protein}$/mL) were added to the reaction mixture. The final volume is 4 mL; the protein loading is 15 mg/$g_{carrier}$. The mixture was shaken on the orbital shaker at 25°C for 24 hours.

After incubation, 1 mL of hexane was added to the reaction mixture; the mixture was shaken on the vortex to promote the formation of an emulsion. Then, 39.4 mg of DFF (0.318 mmol) were added to the reaction mixture. The mixture was again shaken on the vortex to promote the formation of an emulsion, and then shaken on the orbital shaker for 4 hours.

The supernatant was then removed by decanting. The enzyme preparation was rinsed 4 times with 10 mL of TRIS-HCl buffer (pH 7, 0.1 M).

Table 58: Immobilization conditions for the adsorption and crosslinking of TLL and CaLB on rice husk

Incubation solution	**Crosslinking step**	
	Incubation with 160 mM DFF	**Addition of hexane + Incubation with 160 mM DFF**
TRIS-HCl buffer (0.1 M, pH 7)	Condition 1	–
NaCl 3 M	Condition 2	Condition 3

6.5 Annex

Figure 89: Schematic representation of the procedure for the adsorption and crosslinking of enzymes on rice husk

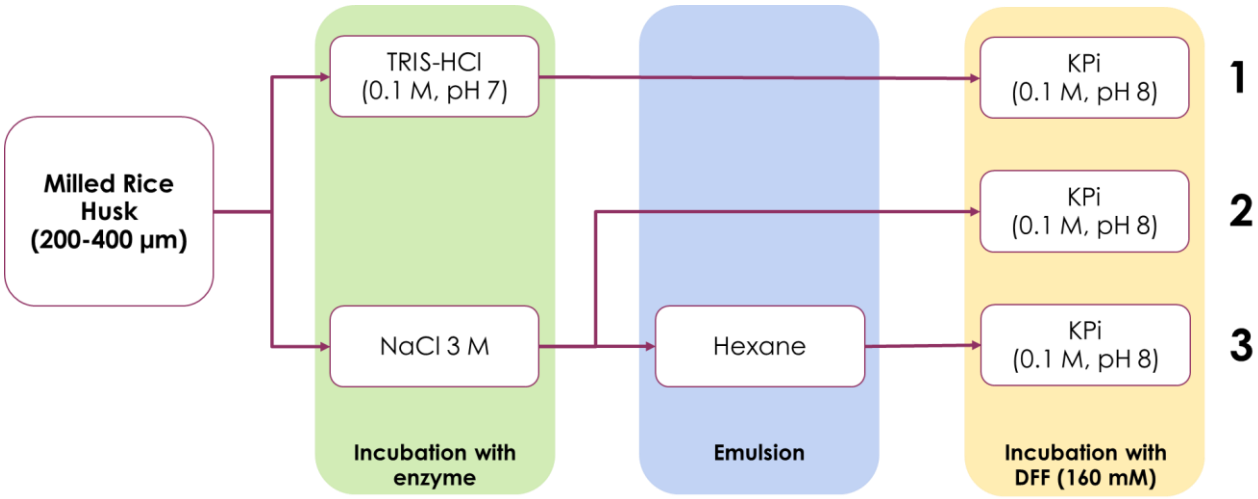

Figure 90: Summary of the conditions for the adsorption and crosslinking of TLL and CaLB on rice husk.

Conclusions: advances beyond the state of the art and expected potential impact

The first objective of this thesis was to find a bio-based, greener alternative for glutaraldehyde for enzyme immobilization. DFF was demonstrated to be a suitable replacer for glutaraldehyde, since (1) it displays a very similar efficiency in enzyme binding, (2) the enzyme immobilized with DFF is very robust, displaying activity in a continuous flow setting over at least 13 days of operation, without showing significant leaching of the enzyme from the carrier, (3) DFF and glutaraldehyde display similar marine toxicity in the employed assay, (4) DFF is non-volatile, therefore the occupational toxicity related to potential inhalation of the chemical during enzyme immobilization is minimized. To employ DFF on an industrial scale, it is still necessary to reduce its production costs and optimize a large-scale synthesis of this molecule. This thesis presents some initial screening for the use of isolated enzymes, as well as whole cells, in the biotransformation of HMF to DFF. However, optimization of the procedure was beyond the scope of this thesis.

TLL physically immobilized on rice husk demonstrated to be effective in the interesterification of tristearin and triolein. Interesterification of triglycerides is important in industry as it is, for example, used for the production of cocoa butter equivalents. The new TLL formulations are robust and inexpensive, and proved effective in viscous, solvent-free conditions. Compared to existing commercial formulations, the cost factor is certainly appealing: cocoa butter is one of the most expensive edible fats in the world, and the effective production of cheap analogues is key for the food industry. Moreover, these TLL formulations present another advantage in the ease of the disposal of spent enzyme: while commercial preparations are immobilized on inorganic carriers (silica) or on polymeric carriers, these formulations are immobilized on rice husk, which is proven to be degradable in soil.

Delignification of rice husk proved to be an interesting tool to modify the surface properties of this composite material. ATR-IR analysis showed a clear decrease in the amount of lignin present in the material, and the contact angle measures confirmed how, after the treatment, the material becomes more hydrophilic. Simultaneously, the microscopy and porosimetry analyses showed how the overall tridimensional structure of rice husk is unchanged after delignification. Therefore, it is possible to change the surface properties of rice husk without damaging its interesting tridimensional morphology.

The immobilization of glucoamylase on rice husk did not yield the expected results. Both in the case of the covalent immobilization on oxidized rice husk and in the case of adsorption and crosslinking, the final preparations displayed no recovered activity. This was attributed initially to a low affinity of the hydrophilic glucoamylase to the mainly hydrophobic rice husk; however, even in the case of delignified rice husk (more hydrophilic), glucoamylase did not immobilize. This suggests that the immobilization of this protein to the carrier is determined by mechanisms more complex than the surface interactions. However, the immobilization of glucoamylase on a very inexpensive material is certainly an attractive opportunity, and for this reason further

investigation will be conducted to develop a new immobilization protocol for glucoamylase on rice husk. Similar conclusions were drawn from the immobilization of lipases on oxidized rice husk.

The covalent immobilization of lipases on rice husk has been previously reported in literature, and it is certainly an interesting possibility, but the cost of the rice husk oxidation procedure certainly needs to be taken into account when calculating the final economic impact of the immobilized enzyme. For this reason, the adsorption and crosslinking methodology for the adsorption of TLL and CaLB was explored, since this methodology does not require a modification of the support material. Several protocols were tested for both lipases, and they were all successful. An interesting observation emerged from these experiments: in the case of CaLB, the recovered activity stayed mostly the same regardless of the medium used for the immobilization. In the case of TLL, on the contrary, the recovered activity increased dramatically in the presence of hexane, an apolar solvent. This is attributed to the fact that TLL, unlike CaLB, presents a lid covering the active site when in aqueous environment; in the presence of an interface with an apolar solvent, the protein conformation changes and the lid opens, facilitating the access to the active site. Therefore, the enzyme immobilized in the presence of hexane is in a more active conformation than the enzyme immobilized in aqueous buffer.

Bibliography

1 INTERfaces Website, www.h2020interfaces.eu/, (accessed 15 October 2023).

2 R. A. Sheldon, *Green Chem.*, 2017, **19**, 18–43. doi: 10.1039/C6GC02157C.

3 R. A. Sheldon and J. M. Woodley, *Chem. Rev.*, 2018, **118**, 801–838. doi: 10.1021/acs.chemrev.7b00203.

4 F. López-Gallego, E. Jackson and L. Betancor, *Chem. – A Eur. J.*, 2017, **23**, 17841–17849. doi: 10.1002/chem.201703593.

5 M. L. Granados, D. M. Alonso and N. Gatherhood, Eds., *Furfural - An Entry Point of Lignocellulose in Biorefineries to Produce Renewable Chemicals, Polymers, and Biofuels*, WORLD SCIENTIFIC (EUROPE), 2018, vol. 02. doi: 10.1142/q0142.

6 P. Domínguez de María, Ed., *Industrial Biorenewables: A Practical Viewpoint*, Wiley, 2016. doi: 10.1002/9781118843796.

7 T. Narancic, R. Davis, J. Nikodinovic-Runic and K. E. O' Connor, *Biotechnol. Lett.*, 2015, **37**, 943–954. doi: 10.1007/s10529-014-1762-4.

8 O. Kirk, T. V. Borchert and C. C. Fuglsang, *Curr. Opin. Biotechnol.*, 2002, **13**, 345–351. doi: 10.1016/S0958-1669(02)00328-2.

9 A. L. Mokale Kognou, S. Shrestha, Z. Jiang, C. (Charles) Xu, F. Sun and W. Qin, *J. Bioresour. Bioprod.*, 2022, **7**, 148–160. doi: 10.1016/j.jobab.2022.03.004.

10 F. Hasan, A. A. Shah and A. Hameed, *Enzyme Microb. Technol.*, 2006, **39**, 235–251. doi: 10.1016/j.enzmictec.2005.10.016.

11 U. Hanefeld, L. Gardossi and E. Magner, *Chem. Soc. Rev.*, 2009, **38**, 453–468. doi: 10.1039/b711564b.

12 M. C. R. Franssen, P. Steunenberg, E. L. Scott, H. Zuilhof and J. P. M. Sanders, *Chem. Soc. Rev.*, 2013, **42**, 6491–6533. doi: 10.1039/c3cs00004d.

13 R. Di Cosimo, J. Mc Auliffe, A. J. Poulose and G. Bohlmann, *Chem. Soc. Rev.*, 2013, **42**, 6437–6474. doi: 10.1039/c3cs35506c.

14 S. Cantone, V. Ferrario, L. Corici, C. Ebert, D. Fattor, P. Spizzo and L. Gardossi, *Chem. Soc. Rev.*, 2013, **42**, 6262–6276. doi: 10.1039/c3cs35464d.

15 L. Corici, V. Ferrario, A. Pellis, C. Ebert, S. Lotteria, S. Cantone, D. Voinovich and L. Gardossi, *RSC Adv.*, 2016, **6**, 63256–63270. doi: 10.1039/c6ra12065b.

16 K. Bachosz, J. Zdarta, M. Bilal, A. S. Meyer and T. Jesionowski, *Sci. Total Environ.*, 2023, **868**, 161630. doi: 10.1016/j.scitotenv.2023.161630.

17 M. Vanhanen, T. Tuomi, U. Tiikkainen, O. Tupasela, R. Vuotilainen and H. Nordman, *Occup. Environ. Med.*, 2000, **57**, 121–125. doi: 10.1136/oem.57.2.121.

18 D. A. Basketter, F. H. Kruszewski, S. Mathieu, D. B. Kirchner, A. Panepinto, M. Fieldsend, V. Siegert, F. Barnes, R. Bookstaff, M. Simonsen and B. Concoby, *J. Occup. Environ. Hyg.*, 2015, **12**, 431–437. doi: 10.1080/15459624.2015.1011741.

19 J. M. Woodley, *ChemSusChem*, , DOI:10.1002/cssc.202102683. doi: 10.1002/cssc.202102683.

20 R. A. Sheldon, *Adv. Synth. Catal.*, 2007, **349**, 1289–1307. doi: 10.1002/adsc.200700082.

21 I. Petry, A. Ganesan, A. Pitt, B. D. Moore and P. J. Halling, *Biotechnol. Bioeng.*, 2006, **95**, 984–991. doi: 10.1002/bit.21074.

22 L. Betancor and H. R. Luckarift, *Trends Biotechnol.*, 2008, **26**, 566–572. doi: 10.1016/j.tibtech.2008.06.009.

23 P. Nikolova and O. P. Ward, *J. Ind. Microbiol.*, 1993, **12**, 76–86. doi: 10.1007/BF01569905.

24 N. W. J. T. Heinsman, C. G. P. H. Schroën, A. van der Padt, M. C. R. Franssen, R. M. Boom and K. van't Riet, *Tetrahedron: Asymmetry*, 2003, **14**, 2699–2704. doi: 10.1016/S0957-4166(03)00577-9.

25 L. B. Barnett and H. B. Bull, *Biochim. Biophys. Acta*, 1959, **36**, 244–246. doi: 10.1016/0006-3002(59)90090-3.

26 K. E. Cassimjee, M. Trummer, C. Branneby and P. Berglund, *Biotechnol. Bioeng.*, 2008, **99**, 712–716. doi: 10.1002/bit.21587.

27 L. Cao, L. van Langen and R. A. Sheldon, *Curr. Opin. Biotechnol.*, 2003, **14**, 387–394. doi: 10.1016/S0958-1669(03)00096-X.

28 N. L. St. Clair and M. A. Navia, *J. Am. Chem. Soc.*, 1992, **114**, 7314–7316. doi: 10.1021/ja00044a064.

29 L. Cao, F. van Rantwijk and R. A. Sheldon, *Org. Lett.*, 2000, **2**, 1361–1364. doi: 10.1021/ol005593x.

30 L. Cao, L. M. van Langen, F. van Rantwijk and R. A. Sheldon, *J. Mol. Catal. B Enzym.*, 2001, **11**, 665–670. doi: 10.1016/S1381-1177(00)00078-3.

31 S. Velasco-Lozano, F. López-Gallego, J. C. Mateos-Díaz and E. Favela-Torres, *Biocatalysis*, , DOI:10.1515/boca-2015-0012. doi: 10.1515/boca-2015-0012.

32 C. Garcia-Galan, Á. Berenguer-Murcia, R. Fernandez-Lafuente and R. C. Rodrigues, *Adv. Synth. Catal.*, 2011, **353**, 2885–2904. doi: 10.1002/adsc.201100534.

33 S. Kim, C. Jiménez-González and B. E. Dale, *Int. J. Life Cycle Assess.*, 2009, **14**, 392–400. doi: 10.1007/s11367-009-0081-9.

34 P. Tufvesson, J. Lima-Ramos, M. Nordblad and J. M. Woodley, *Org. Process Res. Dev.*, 2011, **15**, 266–274. doi: 10.1021/op1002165.

35 U.S. Congress, Biomass Research and Development Act of 2000, https://energy.gov/eere/bioenergy/downloads/biomass-research-and-development-act-2000, (accessed 15 October 2023).

36 N. Dahmen, I. Lewandowski, S. Zibek and A. Weidtmann, *GCB Bioenergy*, 2019, **11**, 107–117. doi: 10.1111/gcbb.12586.

37 K. S. Baig, *Bioresour. Bioprocess.*, 2020, **7**, 21. doi: 10.1186/s40643-020-00310-0.

38 R. Ravindran, S. Hassan, G. Williams and A. Jaiswal, *Bioengineering*, 2018, **5**, 93. doi: 10.3390/bioengineering5040093.

39 V. Sharma, M.-L. Tsai, P. Nargotra, C.-W. Chen, C.-H. Kuo, P.-P. Sun and C.-D. Dong, *Catalysts*, 2022, **12**, 1373. doi: 10.3390/catal12111373.

40 J. S. Hero, C. M. Romero, J. H. Pisa, N. I. Perotti, C. Olivaro and M. A. Martinez, *Int. J. Biol. Macromol.*, 2018, **111**, 229–236. doi: 10.1016/j.ijbiomac.2017.12.166.

41 D. Sud, G. Mahajan and M. Kaur, *Bioresour. Technol.*, 2008, **99**, 6017–6027. doi: 10.1016/j.biortech.2007.11.064.

42 A. A. Chavan, J. Pinto, I. Liakos, I. S. Bayer, S. Lauciello, A. Athanassiou and D. Fragouli, *ACS Sustain. Chem. Eng.*, 2016, **4**, 5495–5502. doi: 10.1021/acssuschemeng.6b01098.

43 M. Bilal, Z. Wang, J. Cui, L. F. R. Ferreira, R. N. Bharagava and H. M. N. Iqbal, *Sci. Total Environ.*, 2020, **722**, 137903. doi: 10.1016/j.scitotenv.2020.137903.

44 S. Budžaki, N. Velić, M. Ostojčić, M. Stjepanović, B. B. Rajs, Z. Šereš, N. Maravić, J. Stanojev, V. Hessel and I. Strelec, *Foods*, 2022, **11**, 409. doi: 10.3390/foods11030409.

45 A. M. Girelli, M. L. Astolfi and F. R. Scuto, *Chemosphere*, , DOI:10.1016/j.chemosphere.2019.125368. doi: 10.1016/j.chemosphere.2019.125368.

46 A. M. Girelli and V. Chiappini, *J. Biotechnol.*, 2023, **365**, 29–47. doi: 10.1016/j.jbiotec.2023.02.003.

47 T. A. Costa-Silva, A. K. F. Carvalho, C. R. F. Souza, L. Freitas, H. F. De Castro and W. P. Oliveira, *Chem. Eng. Res. Des.*, 2022, **183**, 41–55. doi: 10.1016/j.cherd.2022.04.026.

48 R. K. de S. Lira, R. T. Zardini, M. C. C. de Carvalho, R. Wojcieszak, S. G. F. Leite and I. Itabaiana, *Biomolecules*, 2021, **11**, 445. doi: 10.3390/biom11030445.

49 T. A. Costa-Silva, R. C. Cognette, C. R. F. Souza, S. Said and W. P. Oliveira, *Dry. Technol.*, 2013, **31**, 1756–1763. doi: 10.1080/07373937.2013.810637.

50 J. A. Torres, F. G. E. Nogueira, M. C. Silva, J. H. Lopes, T. S. Tavares, T. C. Ramalho and A. D. Corrêa, *RSC Adv.*, 2017, **7**, 16460–16466. doi: 10.1039/C7RA01309D.

51 K.-I. Chen, Y.-C. Lo, C.-W. Liu, R.-C. Yu, C.-C. Chou and K.-C. Cheng, *Food Chem.*, 2013, **139**, 79–85. doi: 10.1016/j.foodchem.2013.01.093.

52 B. G. Palma, R. A. C. Leão, R. O. M.A. de Souza and O. G. Pandoli, *Catal. Today*, 2021, **381**, 280–287. doi: 10.1016/j.cattod.2020.04.041.

53 M. Cespugli, S. Lotteria, L. Navarini, V. Lonzarich, L. Del Terra, F. Vita, M. Zweyer, G. Baldini, V. Ferrario, C. Ebert and L. Gardossi, *Catalysts*, , DOI:10.3390/catal8100471. doi: 10.3390/catal8100471.

54 T. A. Costa Silva, C. R. F. Souza, S. Said and W. P. Oliveira, *African J. Biotechnol.*, 2015, **14**, 3019–3026. doi: 10.5897/AJB2015.14830.

55 L. F. S. Santos, M. R. L. Silva, E. E. A. Ferreira, R. S. Gama, A. K. F. Carvalho, J. C. S. Barboza, J. H. H. Luiz, A. A. Mendes and D. B. Hirata, *Biocatal. Agric. Biotechnol.*, 2021, **36**, 102142. doi: 10.1016/j.bcab.2021.102142.

56 R. Abdulla, S. A. Sanny and E. Derman, *IOP Conf. Ser. Mater. Sci. Eng.*, 2017, **206**, 012032. doi: 10.1088/1757-899X/206/1/012032.

57 C. Ulker, N. Gokalp and Y. Guvenilir, *Biocatal. Biotransformation*, 2016, **34**, 172–180. doi: 10.1080/10242422.2016.1247818.

58 T. A. Costa-Silva, A. K. F. Carvalho, C. R. F. Souza, L. De Freitas, H. F. Castro and W. P. Oliveira, in *Proceedings of 21th International Drying Symposium*, Universitat Politècnica València, Valencia, 2018. doi: 10.4995/IDS2018.2018.7544.

59 T. A. Costa-Silva, A. K. F. Carvalho, C. R. F. Souza, H. F. De Castro, L. Bachmann, S. Said and W. P. Oliveira, *J. Clean. Prod.*, 2021, **284**, 124728. doi: 10.1016/j.jclepro.2020.124728.

60 T. A. Costa-Silva, A. K. F. Carvalho, C. R. F. Souza, H. F. De Castro, S. Said and W. P. Oliveira, *Energy & Fuels*, 2016, **30**, 4820–4824. doi: 10.1021/acs.energyfuels.6b00208.

61 L. C. D. Lima, D. G. C. Peres and A. A. Mendes, *Bioprocess Biosyst. Eng.*, 2018, **41**, 991–1002. doi: 10.1007/s00449-018-1929-9.

62 M. Spennato, A. Todea, L. Corici, F. Asaro, N. Cefarin, G. Savonitto, C. Deganutti and L. Gardossi, *EFB Bioeconomy J.*, 2021, **1**, 100008. doi: 10.1016/j.bioeco.2021.100008.

63 R. A. Wahab, N. Elias, F. Abdullah and S. K. Ghoshal, *React. Funct. Polym.*, 2020, **152**, 104613. doi: 10.1016/j.reactfunctpolym.2020.104613.

64 P. Gemeiner, P. Halák and K. Poláková, *J. Solid-Phase Biochem.*, 1980, **5**, 197–209. doi:

10.1007/BF03000656.

65 J. Spadavecchia, J. Moreau, J. Hottin and M. Canva, *Sensors Actuators B Chem.*, 2009, **143**, 139–143. doi: 10.1016/j.snb.2009.09.007.

66 B. J. Abbott and D. S. Fukuda, *Antimicrob. Agents Chemother.*, 1975, **8**, 282–288. doi: 10.1128/AAC.8.3.282.

67 G. Spagna, R. N. Barbagallo, D. Casarini and P. G. Pifferi, *Enzyme Microb. Technol.*, 2001, **28**, 427–438. doi: 10.1016/S0141-0229(00)00340-9.

68 D. I. Rozkiewicz, B. J. Ravoo and D. N. Reinhoudt, *Langmuir*, 2005, **21**, 6337–6343. doi: 10.1021/la050438i.

69 H. H. J. Persson, W. R. Caseri and U. W. Suter, *Langmuir*, 2001, **17**, 3643–3650. doi: 10.1021/la001265u.

70 A. Wang, H. Wang, S. Zhu, C. Zhou, Z. Du and S. Shen, *Bioprocess Biosyst. Eng.*, 2008, **31**, 509–517. doi: 10.1007/s00449-007-0189-x.

71 R. Schoevaart, A. Siebum, F. van Rantwijk, R. Sheldon and T. Kieboom, *Starch - Stärke*, 2005, **57**, 161–165. doi: 10.1002/star.200400357.

72 C. Mateo, J. M. Palomo, L. M. van Langen, F. van Rantwijk and R. A. Sheldon, *Biotechnol. Bioeng.*, 2004, **86**, 273–276. doi: 10.1002/bit.20033.

73 O. Barbosa, C. Ortiz, Á. Berenguer-Murcia, R. Torres, R. C. Rodrigues and R. Fernandez-Lafuente, *RSC Adv.*, 2014, **4**, 1583–1600. doi: 10.1039/C3RA45991H.

74 Glutaraldehyde Market Overview, https://www.futuremarketinsights.com/reports/glutaraldehyde-market, (accessed 12 October 2023).

75 Glutaraldehyde Solution Safety Data Sheet, https://www.carlroth.com/medias/SDB-3778-IE-EN.pdf?context=bWFzdGVyfHNlY3VyaXR5RGF0YXNoZWV0c3w0MzA4NDd8YXBwbGljYXRpb24vcGRmfHNlY3VyaXR5RGF0YXNoZWV0cy9oYzgvaDkzLzkwNDM2NDc5NTQ5NzQucGRmfGFhNzY1MDJjMDA4MmY2Zjc5ZDg2YzA5NWExMzBiY2UxZWMzZTgzODJkZTM0NWM2YzMwNmQy, (accessed 12 October 2023).

76 National Industrial Chemicals Notification and Assessment Scheme (Australia), *Priority Existing Chemical no. 3 - Glutaraldehyde*, 1994.

77 T. Takigawa and Y. Endo, *J. Occup. Health*, 2006, **48**, 75–87. doi: 10.1539/joh.48.75.

78 Toxicological Profile for Glutaraldehyde, https://www.atsdr.cdc.gov/sites/peer_review/tox_profile_glutaraldehyde.html, (accessed 12 October 2023).

79 Glutaraldehyde Infocard, https://echa.europa.eu/it/substance-information/-/substanceinfo/100.003.506, (accessed 12 October 2023).

80 I. Migneault, C. Dartiguenave, M. J. Bertrand and K. C. Waldron, *Biotechniques*, 2004, **37**, 790–802. doi: 10.2144/04375RV01.

81 A. Dibenedetto, M. Aresta, L. di Bitonto and C. Pastore, *ChemSusChem*, 2016, **9**, 118–125. doi: 10.1002/cssc.201501181.

82 S. P. Teong, G. Yi and Y. Zhang, *Green Chem.*, 2014, **16**, 2015. doi: 10.1039/c3gc42018c.

83 M. Ventura, A. Dibenedetto and M. Aresta, *Inorganica Chim. Acta*, 2018, **470**, 11–21. doi: 10.1016/j.ica.2017.06.074.

84 A. A. Rosatella, S. P. Simeonov, R. F. M. Frade and C. A. M. Afonso, *Green Chem.*, 2011, **13**, 754. doi: 10.1039/c0gc00401d.

85 U.S. Department of Energy, *Top Value Added Chemicals from Biomass - Volume I: Results of Screening for Potential Candidates from Sugars and Synthesis Gas*, 2004.

86 C. A. Sutton, A. Polykarpov, K. Jan van den Berg, A. Yahkind, L. J. Lea, D. C. Webster and M. P. Sibi, *ACS Sustain. Chem. Eng.*, 2020, **8**, 18824–18829. doi: 10.1021/acssuschemeng.0c08207.

87 L. Lalanne, G. S. Nyanhongo, G. M. Guebitz and A. Pellis, *Biotechnol. Adv.*, 2021, **48**, 107707. doi: 10.1016/j.biotechadv.2021.107707.

88 J. Carro, P. Ferreira, L. Rodríguez, A. Prieto, A. Serrano, B. Balcells, A. Ardá, J. Jiménez-Barbero, A. Gutiérrez, R. Ullrich, M. Hofrichter and A. T. Martínez, *FEBS J.*, 2015, **282**, 3218–3229. doi: 10.1111/febs.13177.

89 D. W. Boykin, A. Kumar, J. Spychala, M. Zhou, R. J. Lombardy, W. D. Wilson, C. C. Dykstra, S. K. Jones and J. E. Hall, *J. Med. Chem.*, 1995, **38**, 912–916. doi: 10.1021/jm00006a009.

90 M. Del Poeta, W. A. Schell, C. C. Dykstra, S. Jones, R. R. Tidwell, A. Czarny, M. Bajic, M. Bajic, A. Kumar, D. Boykin and J. R. Perfect, *Antimicrob. Agents Chemother.*, 1998, **42**, 2495–2502. doi: 10.1128/AAC.42.10.2495.

91 K. T. Hopkins, W. D. Wilson, B. C. Bender, D. R. McCurdy, J. E. Hall, R. R. Tidwell, A. Kumar, M. Bajic and D. W. Boykin, *J. Med. Chem.*, 1998, **41**, 3872–3878. doi: 10.1021/jm980230c.

92 D. T. Richter and T. D. Lash, *Tetrahedron Lett.*, 1999, **40**, 6735–6738. doi: 10.1016/S0040-4039(99)01352-0.

93 J. Ma, M. Wang, Z. Du, C. Chen, J. Gao and J. Xu, *Polym. Chem.*, 2012, **3**, 2346. doi: 10.1039/c2py20367g.

94 A. S. Amarasekara, D. Green and L. D. Williams, *Eur. Polym. J.*, 2009, **45**, 595–598. doi:

10.1016/j.eurpolymj.2008.11.012.

95 J. Ma, Z. Du, J. Xu, Q. Chu and Y. Pang, *ChemSusChem*, 2011, **4**, 51–54. doi: 10.1002/cssc.201000273.

96 T. Heinks, L. M. Merz, J. Liedtke, M. Höhne, L. M. van Langen, U. T. Bornscheuer, G. Fischer von Mollard and P. Berglund, *Catalysts*, 2023, **13**, 875. doi: 10.3390/catal13050875.

97 B. Karimi, H. M. Mirzaei and E. Farhangi, *ChemCatChem*, 2014, **6**, 758–762. doi: 10.1002/cctc.201301081.

98 Y. Zhu, M. Shen, Y. Xia and M. Lu, *Catal. Commun.*, 2015, **64**, 37–43. doi: 10.1016/j.catcom.2015.01.031.

99 F. Neaţu, R. S. Marin, M. Florea, N. Petrea, O. D. Pavel and V. I. Pârvulescu, *Appl. Catal. B Environ.*, 2016, **180**, 751–757. doi: 10.1016/j.apcatb.2015.07.043.

100 J. Nie, J. Xie and H. Liu, *J. Catal.*, 2013, **301**, 83–91. doi: 10.1016/j.jcat.2013.01.007.

101 C. A. Antonyraj, J. Jeong, B. Kim, S. Shin, S. Kim, K.-Y. Lee and J. K. Cho, *J. Ind. Eng. Chem.*, 2013, **19**, 1056–1059. doi: 10.1016/j.jiec.2012.12.002.

102 T. Ståhlberg, E. Eyjólfsdóttir, Y. Y. Gorbanev, I. Sádaba and A. Riisager, *Catal. Letters*, 2012, **142**, 1089–1097. doi: 10.1007/s10562-012-0858-5.

103 Y. Yan, K. Li, J. Zhao, W. Cai, Y. Yang and J.-M. Lee, *Appl. Catal. B Environ.*, 2017, **207**, 358–365. doi: 10.1016/j.apcatb.2017.02.035.

104 X. Liu, H. Ding, Q. Xu, W. Zhong, D. Yin and S. Su, *J. Energy Chem.*, 2016, **25**, 117–121. doi: 10.1016/j.jechem.2015.08.012.

105 C. Laugel, B. Estrine, J. Le Bras, N. Hoffmann, S. Marinkovic and J. Muzart, *ChemCatChem*, 2014, **6**, 1195–1198. doi: 10.1002/cctc.201400023.

106 M. M. Cajnko, U. Novak, M. Grilc and B. Likozar, *Biotechnol. Biofuels*, 2020, **13**, 1–12.

107 M. M. Cajnko, M. Grilc and B. Likozar, *Chem. Eng. Sci.*, , DOI:10.1016/j.ces.2021.116982. doi: 10.1016/j.ces.2021.116982.

108 Y.-Z. Qin, Y.-M. Li, M.-H. Zong, H. Wu and N. Li, *Green Chem.*, 2015, **17**, 3718–3722. doi: 10.1039/C5GC00788G.

109 A. Millán Acosta, C. Cuesta Turull, D. Cosovanu, N. Sala Martí and R. Canela-Garayoa, *ACS Sustain. Chem. Eng.*, 2021, **9**, 14550–14558. doi: 10.1021/acssuschemeng.1c05308.

110 R. F. M. Frade, J. A. S. Coelho, S. P. Simeonov and C. A. M. Afonso, *Toxicol. Res. (Camb).*, 2014, **3**, 311–314. doi: 10.1039/c4tx00019f.

111 S. P. M. Ventura, P. De Morais, J. A. S. Coelho, T. Sintra, J. A. P. Coutinho and C. A. M. Afonso, *Green*

Chem., 2016, **18**, 4733–4742. doi: 10.1039/c6gc01211f.

112 C. Martins, D. O. Hartmann, A. Varela, J. A. S. Coelho, P. Lamosa, C. A. M. Afonso and C. Silva Pereira, *Microb. Biotechnol.*, 2020, **13**, 1983–1996. doi: 10.1111/1751-7915.13649.

113 J. Lee and M. Paetzel, *Acta Crystallogr. Sect. F Struct. Biol. Cryst. Commun.*, 2011, **67**, 188–192. doi: 10.1107/S1744309110049390.

114 C. Roth, O. V. Moroz, A. Ariza, L. K. Skov, K. Ayabe, G. J. Davies and K. S. Wilson, *Acta Crystallogr. Sect. D Struct. Biol.*, 2018, **74**, 463–470. doi: 10.1107/S2059798318004989.

115 D. Norouzian, A. Akbarzadeh, J. M. Scharer and M. Moo Young, *Biotechnol. Adv.*, 2006, **24**, 80–85. doi: 10.1016/j.biotechadv.2005.06.003.

116 J. Sauer, B. W. Sigurskjold, U. Christensen, T. P. Frandsen, E. Mirgorodskaya, M. Harrison, P. Roepstorff and B. Svensson, *Biochim. Biophys. Acta - Protein Struct. Mol. Enzymol.*, 2000, **1543**, 275–293. doi: 10.1016/S0167-4838(00)00232-6.

117 S. Chiba, *Biosci. Biotechnol. Biochem.*, 1997, **61**, 1233–1239. doi: 10.1271/bbb.61.1233.

118 T. Christensen, B. B. Stopper, B. Svensson and U. Christensen, *Eur. J. Biochem.*, 1997, **250**, 638–645. doi: 10.1111/j.1432-1033.1997.00638.x.

119 Chimera Software Page, https://www.cgl.ucsf.edu/chimera/, (accessed 13 October 2023).

120 A. Basso, P. Braiuca, S. Cantone, C. Ebert, P. Linda, P. Spizzo, P. Caimi, U. Hanefeld, G. Degrassi and L. Gardossi, *Adv. Synth. Catal.*, 2007, **349**, 877–886. doi: 10.1002/adsc.200600337.

121 NetNGlyc, http://www.cbs.dtu.dk/services/NetNGlyc/, (accessed 15 October 2023).

122 NetOGlyc, http://www.cbs.dtu.dk/services/NetOGlyc/, (accessed 15 October 2023).

123 K. Obleser, H. Kalaus, B. Seidl, M. Kozich, C. Stanetty and M. D. Mihovilovic, *ChemBioChem*, , DOI:10.1002/cbic.202200411. doi: 10.1002/cbic.202200411.

124 A. Dijksman, I. W. C. E. Arends and R. A. Sheldon, *Platin. Met. Rev.*, 2001, **45**, 15.

125 J. E. Nutting, M. Rafiee and S. S. Stahl, *Chem. Rev.*, 2018, **118**, 4834–4885. doi: 10.1021/acs.chemrev.7b00763.

126 A. C. Cardiel, B. J. Taitt and K.-S. Choi, *ACS Sustain. Chem. Eng.*, 2019, **7**, 11138–11149. doi: 10.1021/acssuschemeng.9b00203.

127 S. J. B. Duff and W. D. Murray, *Biotechnol. Bioeng.*, 1988, **31**, 44–49. doi: 10.1002/bit.260310108.

128 W. D. Murray, S. J. B. Duff and P. H. Lanthier, *Appl. Microbiol. Biotechnol.*, 1989, **32**, 95–100. doi: 10.1007/BF00164829.

129 M. Rennig, K. Bach Falkenberg, C. Hernandez Rollan, A. B. Bertelsen and M. Norholm, 2020, 1–6.

130 S. J. B. Duff and W. D. Murray, *Biotechnol. Bioeng.*, 1988, **31**, 790–795. doi: 10.1002/bit.260310805.

131 S. J. B. Duff and W. D. Murray, *Biotechnol. Bioeng.*, 1989, **34**, 153–159. doi: 10.1002/bit.260340203.

132 W. D. Murray and S. J. B. Duff, *Biotechnol. Bioeng.*, 1990, 202–205.

133 K. Kawakami and T. Nakahara, *Biotechnol. Bioeng.*, 1994, **43**, 918–924. doi: 10.1002/bit.260431004.

134 M. C. Fragnelli, P. Hoyos, D. Romano, R. Gandolfi, A. R. Alcántara and F. Molinari, *Tetrahedron*, 2012, **68**, 523–528. doi: 10.1016/j.tet.2011.11.014.

135 F. Molinari, E. G. Occhiato, F. Aragozzini and A. Guarna, *Tetrahedron Asymmetry*, 1998, **9**, 1389–1394. doi: 10.1016/S0957-4166(98)00096-2.

136 S. Bruzzone, C. Chiappe, S. E. Focardi, C. Pretti and M. Renzi, *Chem. Eng. J.*, 2011, **175**, 17–23. doi: 10.1016/j.cej.2011.08.073.

137 C. Pretti, M. Renzi, S. Ettore Focardi, A. Giovani, G. Monni, B. Melai, S. Rajamani and C. Chiappe, *Ecotoxicol. Environ. Saf.*, 2011, **74**, 748–753. doi: 10.1016/j.ecoenv.2010.10.032.

138 D. Hopwood, *Histochem. J.*, 1972, **4**, 267–303. doi: 10.1007/BF01005005.

139 R. D. Schmid and R. Verger, *Angew. Chemie Int. Ed.*, 1998, **37**, 1608–1633. doi: 10.1002/(SICI)1521-3773(19980703)37:12<1608::AID-ANIE1608>3.0.CO;2-V.

140 V. Ferrario, C. Ebert, L. Knapic, D. Fattor, A. Basso, P. Spizzo and L. Gardossi, *Adv. Synth. Catal.*, 2011, **353**, 2466–2480. doi: 10.1002/adsc.201100397.

141 L. Casas-Godoy, F. Gasteazoro, S. Duquesne, F. Bordes, A. Marty and G. Sandoval, in *Lipases and Phospholipases*, ed. G. Sandoval, Springer, 2018, pp. 3–38. doi: 10.1007/978-1-4939-8672-9_1.

142 P. Desnuelle, L. Sarda and G. Ailhaud, *Biochim. Biophys. Acta*, 1960, **37**, 570–571. doi: 10.1016/0006-3002(60)90532-1.

143 G. Borrelli and D. Trono, *Int. J. Mol. Sci.*, 2015, **16**, 20774–20840. doi: 10.3390/ijms160920774.

144 N. B. Melani, E. B. Tambourgi and E. Silveira, *Sep. Purif. Rev.*, 2020, **49**, 143–158. doi: 10.1080/15422119.2018.1564328.

145 Y. Wang, R. Ma, S. Li, M. Gong, B. Yao, Y. Bai and J. Gu, *AMB Express*, 2018, **8**, 95. doi: 10.1186/s13568-018-0618-z.

146 US 6017866A, *Lipases with improved surfactant resistance*, 1995.

147 A. I. Adetunji and A. O. Olaniran, *Brazilian J. Microbiol.*, 2021, **52**, 1257–1269. doi: 10.1007/s42770-021-00503-5.

148 T. Fujii, T. Tatara and M. Minagawa, *J. Am. Oil Chem. Soc.*, 1986, **63**, 796–799. doi: 10.1007/BF02541967.

149 JPH0277498A, *Detergent composition for use in automatic dishwasher*, 1998.

150 EP0346136A1, *Enzymatic dishwashing and rinsing composition*, 1988.

151 JPH038401A, *Removing method of dirt from dry cleaning solvent by using lipase*, 1989.

152 EP0140669A1, *Microbial enzymatic contact lens cleaner and methods of use*, 1984.

153 WO2009106575A1, *Lipases with high specificity towards short chain fatty acids and uses thereof*, 2009.

154 Palatase product page, https://www.novozymes.com/en/products/dairy/cheese/palatase, (accessed 19 October 2023).

155 O. B. Karaca and M. Güven, *Foods*, 2018, **7**, 125. doi: 10.3390/foods7080125.

156 US3973042A, *Flavor development by microbial lipases in pasteurized milk blue cheese*, 1974.

157 S. M. Farahat, A. M. Rabie and A. A. Farag, *Food Chem.*, 1990, **36**, 169–180. doi: 10.1016/0308-8146(90)90052-6.

158 WO2008010543A1, *Process for production of hard butter suitable for chocolate product*, 2007.

159 J. Ray, Z. K. Nagy, K. W. Smith, K. Bhaggan and A. G. F. Stapley, *Biochem. Eng. J.*, 2013, **73**, 17–28. doi: 10.1016/j.bej.2012.12.018.

160 S. Raveendran, B. Parameswaran, S. B. Ummalyma, A. Abraham, A. K. Mathew, A. Madhavan, S. Rebello and A. Pandey, *Food Technol. Biotechnol.*, , DOI:10.17113/ftb.56.01.18.5491. doi: 10.17113/ftb.56.01.18.5491.

161 A. Larios, H. S. García, R. M. Oliart and G. Valerio-Alfaro, *Appl. Microbiol. Biotechnol.*, 2004, **65**, 373–376. doi: 10.1007/s00253-004-1602-x.

162 Lipopan 50 product page, https://www.novozymes.com/en/products/baking/dough-strengthening/lipopan-50, (accessed 19 October 2023).

163 Sensea Wrap product page, https://www.novozymes.com/en/products/baking/freshness/sensea-wrap, (accessed 19 October 2023).

164 A. Mehta, S. Guleria, R. Sharma and R. Gupta, in *Microbial Biotechnology in Food and Health*, Elsevier, 2021, pp. 143–164. doi: 10.1016/B978-0-12-819813-1.00006-2.

165 R. J. Kazlauskas and U. T. Bornscheuer, in *Biotechnology*, Wiley, 1998, pp. 36–191. doi: 10.1002/9783527620906.ch3.

166 Noopazyme product page, https://www.novozymes.com/en/products/baking/dough-strengthening/noopazyme, (accessed 19 October 2023).

167 WO2004024930A2, *Process for the production of transesterified oils/fats or triglycerides*.

168 L. Zu-Yi and O. P. Ward, *Biotechnol. Lett.*, 1993, **15**, 185–188. doi: 10.1007/BF00133021.

169 C. Tecelão, M. Guillén, F. Valero and S. Ferreira-Dias, *Biochem. Eng. J.*, 2012, **67**, 104–110. doi: 10.1016/j.bej.2012.06.001.

170 S. Ramarethinam, K. Lahta and N. Rajalakshmi, *Food Sci. Technol. Res.*, 2002, **8**, 328–332. doi: 10.3136/fstr.8.328.

171 P. Bajpai, *Biotechnol. Prog.*, 1999, **15**, 147–157. doi: 10.1021/bp990013k.

172 A. Gutiérrez, J. C. del Río and A. T. Martínez, *Appl. Microbiol. Biotechnol.*, 2009, **82**, 1005–1018. doi: 10.1007/s00253-009-1905-z.

173 EP1364089A2, *Neutral deinking with a deinking composition comprising a lipase and a fatty acid ester*, 2002.

174 JPH02229290A, *Ink removal promoter of old paper*, 1989.

175 H. Y. Zhang, X. Wang, C. B. Ching and J. C. Wu, *Biotechnol. Appl. Biochem.*, 2005, **42**, 67–71. doi: 10.1042/BA20040163.

176 R. V Muralidhar, R. R. Chirumamilla, V. N. Ramachandran, R. Marchant and P. Nigam, *Meded. Rijksuniv. Gent. Fak. Landbouwkd. Toegep. Biol. Wet.*, 2001, **66**, 227–32.

177 Sustine 110 IM product page, https://www.novozymes.com/en/products/fine-chemicals/biocatalysis/sustine-110-im, (accessed 19 October 2023).

178 Sustine 120 IM product page, https://www.novozymes.com/en/products/fine-chemicals/biocatalysis/sustine-120-im, (accessed 19 October 2023).

179 Sustine 130 IM product page, https://www.novozymes.com/en/products/fine-chemicals/biocatalysis/sustine-130-im, (accessed 19 October 2023).

180 Sustine 111 product page, https://www.novozymes.com/en/products/fine-chemicals/biocatalysis/sustine-111, (accessed 19 October 2023).

181 Sustine 121 product page, https://www.novozymes.com/en/products/fine-chemicals/biocatalysis/sustine-121, (accessed 19 October 2023).

182 JPH01186820A, *Therapeutic agent for malignant tumor*, 1988.

183 Creonipe Product Page (in Italian), https://www.codifa.it/farmaci/c/creonipe-pancrelipasi-enzimi-pancreatici, (accessed 18 October 2023).

184 IT1232776B, *Reagent for analysis of triglycerides and analysis that use the same*, 1989.

185 J. A. Lott and C. J. Lu, *Clin. Chem.*, 1991, **37**, 361–368. doi: 10.1093/clinchem/37.3.361.

186 M. B. Ansorge-Schumacher and O. Thum, *Chem. Soc. Rev.*, 2013, **42**, 6475. doi: 10.1039/c3cs35484a.

187 T. Maugard, B. Rejasse and M. D. Legoy, *Biotechnol. Prog.*, 2002, **18**, 424–428. doi: 10.1021/bp025508f.

188 DE1242794B, *Process for making permanent waves*, 1964.

189 H. Noureddini, X. Gao and R. S. Philkana, *Bioresour. Technol.*, 2005, **96**, 769–777. doi: 10.1016/j.biortech.2004.05.029.

190 D. de Oliveira, M. Di Luccio, C. Faccio, C. D. Rosa, J. P. Bender, N. Lipke, S. Menoncin, C. Amroginski and J. V. de Oliveira, in *Proceedings of the Twenty-Fifth Symposium on Biotechnology for Fuels and Chemicals Held May 4–7, 2003, in Breckenridge, CO*, Humana Press, Totowa, NJ, 2004, pp. 771–780. doi: 10.1007/978-1-59259-837-3_62.

191 Y. Chen, B. Xiao, J. Chang, Y. Fu, P. Lv and X. Wang, *Energy Convers. Manag.*, 2009, **50**, 668–673. doi: 10.1016/j.enconman.2008.10.011.

192 WO1992017613A1, *Hide liming and drenching process using enzyme*, 1992.

193 Greasex Ultra product page, https://www.novozymes.com/en/products/leather/degreasing/greasex-ultra, (accessed 19 October 2023).

194 KR20050029996A, *A wastewater treatment device for fat and oil rich wastewaters*, 2003.

195 S. Dharmsthiti and B. Kuhasuntisuk, *J. Ind. Microbiol. Biotechnol.*, 1998, **21**, 75–80. doi: 10.1038/sj.jim.2900563.

196 S. Danthine, S. Closset, J. Maes, S. Mascrez, C. Blecker, G. Purcaro and V. Gibon, *OCL*, 2022, **29**, 36. doi: 10.1051/ocl/2022029.

197 V. Gibon and M. Kellens, in *Trans Fats Replacement Solutions*, Elsevier, 2014, pp. 153–185. doi: 10.1016/B978-0-9830791-5-6.50013-7.

198 Z. Zhang, W. J. Lee and Y. Wang, *Crit. Rev. Food Sci. Nutr.*, 2021, **61**, 3145–3159. doi: 10.1080/10408398.2020.1793725.

199 R. C. da Silva, D. F. Soares, M. B. Lourenço, F. A. S. M. Soares, K. G. da Silva, M. I. A. Gonçalves and L. A. Gioielli, *LWT - Food Sci. Technol.*, 2010, **43**, 752–758. doi: 10.1016/j.lwt.2009.12.010.

200 Y. Jiang, in *Rice Bran and Rice Bran Oil*, Elsevier, 2019, pp. 97–123. doi: 10.1016/B978-0-12-812828-2.00004-4.

201 J. H. Lee, J. M. Son, C. C. Akoh, M. R. Kim and K.-T. Lee, *N. Biotechnol.*, 2010, **27**, 38–45. doi: 10.1016/j.nbt.2009.10.006.

202 T. Yang, X. Xu, C. He and L. Li, *Food Chem.*, 2003, **80**, 473–481. doi: 10.1016/S0308-8146(02)00315-1.

203 K. Bhandari, S. P. Chaurasia, A. K. Dalai and A. Gupta, *J. Am. Oil Chem. Soc.*, 2013, **90**, 1637–1644. doi: 10.1007/s11746-013-2322-0.

204 M. M. Soumanou, U. T. Bornscheuer, U. Schmid and R. D. Schmid, *Lipid - Fett*, 1998, **100**, 156–160. doi: 10.1002/(SICI)1521-4133(19985)100:4/5<156::AID-LIPI156>3.0.CO;2-9.

205 A. Huyghebaert, D. Verhaeghe and H. De Moor, in *Fats in Food Products*, Springer US, Boston, MA, 1994, pp. 319–345. doi: 10.1007/978-1-4615-2121-1_9.

206 S. M. Ghazani and A. G. Marangoni, *Sci. Rep.*, 2018, **8**, 15271. doi: 10.1038/s41598-018-33600-x.

207 M. W. Christensen, L. Andersen, T. L. Husum and O. Kirk, *Eur. J. Lipid Sci. Technol.*, 2003, **105**, 318–321. doi: 10.1002/ejlt.200390062.

208 T. H. Rønne, T. Yang, H. Mu, C. Jacobsen and X. Xu, *J. Agric. Food Chem.*, 2005, **53**, 5617–5624. doi: 10.1021/jf050646g.

209 H. Zhang, X. Xu, J. Nilsson, H. Mu, J. Adler-Nissen and C. Høy, *J. Am. Oil Chem. Soc.*, 2001, **78**, 57–64. doi: 10.1007/s11746-001-0220-4.

210 H. Yang, Y. Mu, H. Chen, C. Su, T. Yang and Z. Xiu, *Chinese J. Chem. Eng.*, 2014, **22**, 1016–1020. doi: 10.1016/j.cjche.2014.06.027.

211 N. M. Osório, M. M. R. da Fonseca and S. Ferreira-Dias, *Eur. J. Lipid Sci. Technol.*, 2006, **108**, 545–553. doi: 10.1002/ejlt.200600029.

212 R. Fernandez-Lafuente, *J. Mol. Catal. B Enzym.*, 2010, **62**, 197–212. doi: 10.1016/j.molcatb.2009.11.010.

213 S. D. Segall, W. E. Artz, D. S. Raslan, V. P. Ferraz and J. A. Takahashi, *J. Sci. Food Agric.*, 2006, **86**, 445–452. doi: 10.1002/jsfa.2349.

214 V. Seriburi and C. C. Akoh, *JAOCS, J. Am. Oil Chem. Soc.*, 1998, **75**, 711–716. doi: 10.1007/s11746-998-0210-9.

215 S. Shackley, S. Carter, T. Knowles, E. Middelink, S. Haefele, S. Sohi, A. Cross and S. Haszeldine, *Energy Policy*, 2012, **42**, 49–58. doi: 10.1016/j.enpol.2011.11.026.

216 A. Pellis, V. Ferrario, M. Cespugli, L. Corici, A. Guarneri, B. Zartl, E. Herrero Acero, C. Ebert, G. M. Guebitz and L. Gardossi, *Green Chem.*, 2017, **19**, 490–502. doi: 10.1039/c6gc02142e.

217 S. F. D'Souza and S. S. Godbole, *J. Biochem. Biophys. Methods*, 2002, **52**, 59–62. doi: 10.1016/S0165-022X(02)00032-5.

218 R. Singh, A. Shukla, S. Tiwari and M. Srivastava, *Renew. Sustain. Energy Rev.*, 2014, **32**, 713–728. doi: 10.1016/j.rser.2014.01.051.

219 J. Lee, *J. Biotechnol.*, 1997, **56**, 1–24. doi: 10.1016/S0168-1656(97)00073-4.

220 O. Sanchez, R. Sierra and C. J., in *Alternative Fuel*, InTech, 2011. doi: 10.5772/22381.

221 U. Ashgar, M. Nadeem, M. Irfan, Q. Syed, R. Nelofer and M. Iram, *Environ. Prog. Sustain. Energy*, 2016, **35**, 284–288. doi: 10.1002/ep.12211.

222 J. M. Gould, *Biotechnol. Bioeng.*, 1985, **27**, 225–231. doi: 10.1002/bit.260270303.

223 F. Zappaterra, M. Renzi, M. Piccardo, M. Spennato, F. Asaro, M. Di Serio, R. Vitiello, R. Turco, A. Todea and L. Gardossi, *Polymers (Basel).*, 2023, **15**, 1536. doi: 10.3390/polym15061536.

224 C. C. Costa, G. R. S. Andrade and L. E. Almeida, *Matéria (Rio Janeiro)*, , DOI:10.1590/s1517-707620180004.0598. doi: 10.1590/s1517-707620180004.0598.

225 S. Y. Yap, S. Sreekantan, M. Hassan, K. Sudesh and M. T. Ong, *Polymers (Basel).*, 2020, **13**, 104. doi: 10.3390/polym13010104.

226 Q. Zhao, J. Tao, R. C. M. Yam, A. C. K. Mok, R. K. Y. Li and C. Song, *Polym. Degrad. Stab.*, 2008, **93**, 1571–1576. doi: 10.1016/j.polymdegradstab.2008.05.002.

227 Sigma Aldrich (Merck), Bradford Reagent - Technical Bulletin, https://www.sigmaaldrich.com/deepweb/assets/sigmaaldrich/product/documents/358/973/b6916bul-mk.pdf, (accessed 15 October 2023).

228 WO2012085206 (A1), EP2655611 (A1), *Method for covalent immobiization of enzymes on functionalized solid polymeric support*, 2011.

229 V. Ferrario, H. Veny, E. De Angelis, L. Navarini, C. Ebert and L. Gardossi, *Biomolecules*, 2013, **3**, 514–534. doi: 10.3390/biom3030514.

Acknowledgements

This project has received funding from the European Union's Horizon 2020 research and innovation programme under the Marie Skłodowska-Curie grant agreement No 860414

At the end of my PhD, I would also like to extend my thanks to everyone that supported me during these three years.

First and foremost, I would like to thank my supervisors, prof. Lucia Gardossi and Dr. Luuk van Langen, for welcoming me in their respective groups, and for their guidance in this entire project. We had many fruitful discussions and they constantly helped me solving my doubts and seeing the best in my research project.

I also acknowledge the help and support of prof. Fioretta Asaro, an invaluable source of knowledge in prof. Gardossi's group, and Dr. Anamaria Todea, whose patience, support and expertise was priceless during many uncertainties. I also thank all the members of prof. Gardossi's group that I had the pleasure to work with during the years: Dr. Caterina Deganutti, Dr. Federico Zappaterra, Demi Vattovaz, Pasquale Ditalia, Simone Sedran, Marco Giannetto, Marco Mercadante and Ioan Bîtcan.

I also thank prof. Dario Voinovich, for his help in the characterization of rice husk and for fruitful discussions on many topics; prof. Jan Kaspar, for his contribution with the porosimetry analysis; dr. Sara Kaleb, for the acquisition of the optical microscopy images of rice husk; prof. Monia Renzi and her group, who performed the ecotoxicology assays; and prof. Patrizia Nitti, for the many fruitful discussions. Moreover, I would like to acknowledge Dr. Fabio Hollan and Dr. Sara Drioli, for most of the NMR and MS spectra acquisitions, and for the endless patience and kindness when I needed their help.

Regarding the INTERfaces project, I would like to thank Prof. Selin Kara, for her fundamental guidance in the project, Dr. Laura-Carlota Paz, for all her coordination efforts, and all the PIs that supported us ESRs sharing their knowledge and research experiences.

I would also like to thank Luisa Merz, for being the best friend and sidekick I could ask for when moving to a new research group in a totally different country. I could not have made it without our science talks, chats, shared complaint sessions, and without all the shared tea, especially in rather dark moments.

I would like to thank Iulia Rădoi, my lab partner in Italy, for more shared complaint sessions, science discussions, and for sharing with me many adventurous travels to conference locations. And her cats; never forget the cats.

Of course, a big thank you goes to all the other INTERfaces ESRs, who shared with me learning time and fun time during our numerous Workshops. Nicoletta, Karishma, Nicolette, Philipp, Jakub, Antía, Kamela, Sara, Nadiya Lucija and Milica, thank you for your company.

A big thank you to all my students, present and past: Deborah Boes, Valentina Puppi and Alice Suergiu, it has been the most rewarding experience to teach them and learn from them, and I am very proud of all they accomplished.

On a more personal note, I have of course to thank my family: my mother, my father, my sister and my grandfather, who were the most supportive when I decided to move to another country for a doctorate during a pandemic. It certainly has not been the easiest time, but I've never felt anything but love and support from them.

A huge thank you to Giovanni, who has known me for ten years and has been nothing but supportive and caring for this whole time, through the highs and the (very) lows. I can't imagine how it would have been to go through some really challenging periods of my life without him.

Thank you to all of my friends, that were close to me in these three years: Claudia, Giulia Z., Giulia E., Pier, Damiano, Johanna, and many, many others. You know who you are, and I'm proud to call you my friends.

And finally, thank you to FdN, Z, BvZ, G, R and GM for the unending and unwavering (even if a bit destructive) emotional support.